

**Identification and characterisation of bacterial TIR domains,
with particular focus on *Yersinia pestis***

Abigail Mary Spear, MBiochem

**This thesis is submitted for examination for the degree of Doctor of Philosophy to the
London School of Hygiene and Tropical Medicine**

Biomedical Sciences Department, Dstl Porton Down

December 2010

© Crown copyright 2010. Published with the permission of the Defence Science and
Technology Laboratory on behalf of the Controller of HMSO

Declaration

I have read and understood the School's definition of plagiarism and cheating given in the Research Degrees Handbook. I declare that this thesis is my own work, and that I have acknowledged all results and quotations from the published or unpublished work of other people. I have read and understood the School's definition and policy on the use of third parties (either paid or unpaid) who have contributed to the preparation of this thesis by providing copy editing and, or, proof reading services. I declare that no changes to the intellectual content or substance of this thesis were made as a result of this advice, and, that I have fully acknowledged all such contributions.

Signed:  Date: 13.12.10

Full name: ABIGAIL M. SPEAR(please print clearly)

Abstract

The Toll/IL-1 Receptor (TIR) domain is an essential signalling module in eukaryotic innate immune signalling pathways. Homotypic interaction between TIR domains allows the formation of a signalling platform in which molecules are able to interact and activate each other to initiate an immune signalling cascade. Proteins containing TIR domains have also been discovered in bacteria. Studies have subsequently shown that these proteins are able to modulate mammalian immune signalling pathways dependent on TIR interactions and that this forms an evasion strategy for bacterial pathogens.

In this study a bioinformatic search for proteins containing TIR domains was carried out across unicellular organisms, including bacteria. TIR domain proteins (Tdps) from highly pathogenic bacteria were down-selected for investigation. After an initial screen of their activity, a Tdp from *Yersinia pestis*, the causative agent of plague, was down-selected for further investigation.

The bioinformatic analysis found a high representation of Tdps in bacteria generally classified as non-pathogens, and that TIR domains are promiscuous in their co-occurrence with other domains. This analysis also showed that they are not necessarily conserved between strains and species. These findings question the universal role of Tdps in the pathogenic evasion of a host immune response and suggest they may have other functions. Initial screening of down-selected Tdps showed that they were able to modulate immune signalling pathways *in vitro*, but studies with a Tdp-deficient mutant of *Y. pestis* did not demonstrate a role for this protein in the virulence of *Y. pestis* in a mouse model. However, this Tdp-deficient mutant did display two characteristics *in vitro*: an increased auto-aggregation phenotype when compared to wild-type *Y. pestis* and an inability to survive as well as wild-type bacteria in conditions of high salinity. These findings indicate that TIR domain proteins may have other roles in bacterial physiology unrelated to immune evasion.

Acknowledgements

I should like to thank my two PhD supervisors, Dr. Helen Atkins and Dr. Greg Bancroft for their support throughout this PhD. Thank you to Helen for giving me the opportunity to study for a PhD with this project, for her support and encouragement throughout, and for her thorough and very speedy reading of my thesis drafts. Thank you to Greg for allowing me to study at the London School of Hygiene and Tropical Medicine and for his boundless optimism.

I should like to thank a variety of other people for their academic support. Even though I didn't feel it at the time (!) I would like to thank Professor Mark Pallen for a challenging transfer viva and for the wonderful opportunity to spend time at the University of Birmingham while carrying out the PSI-BLAST searches. I thoroughly enjoyed working with you and am grateful for the way in which you stretched me. Thank you also to Dr. Nick Loman at the University of Birmingham for helping me to collate my bioinformatic searches. I also enjoyed our conversations about food! Thank you to Professor Andrew Bowie and all his lab members at Trinity College, Dublin for their advice and reagents when setting up the luciferase reporter assays and for allowing me to spend time in their lab learning how to do co-IPs (in particularly Dr. Julianne Stack, co-IP Goddess!). I hugely enjoyed my time in the Bowie lab and I am grateful for your help and hospitality. I should also like to thank Dr. Bernadette Byrne and Dr. Rohini Rana at Imperial College, London for supplying me with YpTIR protein and for their helpful discussions and insight into the behaviour of the *Y. pestis* YpTdp protein! Thank you also to Rohini for her positivity and support as a fellow PhD student. I should also like to thank Professor Petra Oyston at Dstl for her intellectual discussions and encouragement and for containment level 3 training, Dr. Di Williamson for her technical input and all the animal checking staff at Dstl for their help with the animal studies.

There are many people at Dstl who have helped to make the last four years enjoyable and I am grateful to them all. I would particularly like to thank Donna for her company and input through many hours in the containment suite, Karleigh for the distraction of Italian lessons (I miss the cake!), Claire for her unbelievable knowledge about *everything*, Richard for introducing me to House and lending me all the DVDs and for being my TLR buddy, Jon

for some fabulous intellectual discussions, Matt for many a car-related chat and Natalie for being a great person to sit next to! Thank you all for your friendship.

Outside of work I would like to thank all my friends and family, particularly Tom for being a very supportive brother, Hel and Rosie who have been there throughout, and to all the Jeanne girls for their unfailing interest and enthusiasm.

I owe a lot to three very inspirational women; Grandma Sea, Grandma Coal and Great Auntie Floss.

I don't have the words to express my love and gratitude to my parents whose support has always been over-whelming.

Finally to my lovely husband Nick who has barely known me when I haven't been studying for something! You have borne the brunt of this process and your love and support make every day that much brighter.

My doctorate is for Daddy

Publications

Data in this thesis has been presented as follows:

Articles:

Spear, A.M., Loman, N.J., Atkins, H.S., Pallen, M.J. (2009) Microbial TIR domains: not necessarily agents of subversion? *Trends Microbiol.* 17, 393-398

Spear, A.M., Rana, R.R., Oyston, P.C.F., Simpson, P., Matthews, S.J., Bancroft, G.J., Byrne, B., Atkins, H.S. (2010) A TIR domain protein from *Yersinia pestis* interacts with mammalian IL-1/TLR pathways but does not play a central role in the virulence of *Y. pestis* in a mouse model of bubonic plague. **Awaiting submission**

Oral presentations:

Spear, A.M. Identification and characterisation of Toll/Interleukine-1 Receptor family proteins in a range of pathogenic bacteria. *Innate Immunity: Signalling Mechanisms.*

Keystone Symposia, Colorado, USA. February 2008

Spear, A.M. Identification and characterisation of putative Toll/Interleukin-1 Receptor family proteins in pathogenic bacteria. **Innate Immunity and Endotoxin Society Annual Meeting**, Edinburgh, UK. August 2008

Posters:

Spear, A.M., Lingard, B., Bowie, A., Bancroft, G., Atkins, H.S. Identification and characterisation of Toll/Interleukine-1 Receptor family proteins in a range of pathogenic bacteria. *Innate Immunity: Signalling Mechanisms.* **Keystone Symposia**, Colorado, February 2008

Spear, A.M., Lingard B., Bowie A., Bancroft G., Atkins H.S. Identification and characterisation of putative Toll/Interleukin-1 Receptor family proteins in pathogenic bacteria. **Innate Immunity and Endotoxin Society Annual Meeting**, Edinburgh, UK. August 2008

Spear, A.M., Loman, N.J., Bowie, A., Pallen, M.J., Atkins, H.S. The role of TIR domains in bacteria. **SET for Britain competition**, House of Commons, UK.

Table of Contents

Declaration.....	2
Abstract.....	3
Acknowledgements.....	4
Publications	7
Table of Contents	8
List of Figures.....	13
List of Tables	17
Chapter 1: General Introduction	21
1.1. The innate immune response and pattern recognition.....	21
1.2. Toll and Toll-like receptor signalling.....	22
1.2.1. TLR ligands and ligand binding	24
1.2.2. TLR location and expression	29
1.2.3. TLR signalling: transduction through the TIR domain.....	30
1.3. The TIR domain	45
1.3.1. The BB loop.....	47
1.3.2. The DD loop	49
1.3.3. Other loops	49
1.3.4. α helices and β sheets.....	49
1.3.5. Receptor-adaptor interactions	50
1.4. The pivotal role of TLR/IL-1R signalling in innate immunity.....	51
1.4.1. Activation of transcription factors	51
1.4.2. Production of immune effector molecules.....	52
1.4.3. TLRs and DCs	54
1.4.4. TLRs in B cell activation and antibody production	55
1.4.5. TLRs and T cells.....	55
1.4.6. TLR signalling and direct anti-microbial activity.....	56

1.4.7.	Cell death.....	57
1.4.8.	Phagocytosis	59
1.5.	Pathogenic modulation of TLR/IL-1R signalling.....	60
1.5.1.	Modification and concealment of TLR ligands	60
1.5.2.	Using TLR pathway activation	62
1.5.3.	Immunomodulatory proteins.....	62
1.6.	Bacteria as potential bio-terrorism agents	65
1.6.1.	Bacillus anthracis.....	65
1.6.2.	Yersinia pestis.....	67
1.6.3.	Burkholderia pseudomallei.....	69
1.6.4.	Brucella melitensis.....	71
1.7.	Aims of this research	74

Chapter 2: General Methods75

2.1.	Bioinformatic methods	75
2.1.1.	Saturated BLAST.....	75
2.1.2.	PSI-BLAST	76
2.1.3.	FUGUE.....	77
2.1.4.	3D Jury	77
2.1.5.	The GOLD database	77
2.1.6.	Pfam.....	77
2.1.7.	Multiple sequence alignments	78
2.2.	Buffers and Media	78
2.3.	Animals.....	81
2.3.1.	Methods of inoculation.....	81
2.3.2.	Analysis of bacterial colonisation.....	84
2.4.	Bacteria.....	84
2.4.1.	Production of electrocompetent cells.....	84
2.4.2.	Growth curves.....	85
2.4.3.	Surface hydrophobicity assay	85
2.4.4.	Autoaggregation assay.....	85
2.4.5.	Minimum inhibitory concentration (MIC) assay	85
2.4.6.	Salt shock assay	86
2.4.7.	Preparation of inoculum for animal dosing	86
2.4.8.	Infection of macrophage cell line with bacteria.....	87

2.5.	DNA	87
2.5.1.	Vectors.....	87
2.5.2.	Genomic DNA.....	90
2.5.3.	Polymerase chain reaction (PCR).....	90
2.5.4.	Agarose gel electrophoresis.....	92
2.5.5.	PCR product purification.....	92
2.5.6.	DNA ligation.....	93
2.5.7.	Transformation of DNA into chemically competent bacteria.....	93
2.5.8.	Transformation of DNA into electrocompetent bacteria.....	93
2.5.9.	DNA extraction.....	93
2.5.10.	Quantification of DNA.....	93
2.5.11.	DNA sequencing.....	94
2.6.	Cell culture.....	94
2.6.1.	Routine maintenance of cell lines.....	94
2.6.2.	Seeding of cells for confocal microscopy.....	94
2.6.3.	Transient transfection.....	94
2.6.4.	Stimulation of cells.....	95
2.6.5.	Preparation of cell lysates.....	95
2.6.6.	Measurement of luciferase activity.....	96
2.6.7.	Measurement of alkaline phosphatase activity.....	96
2.6.8.	Cell viability assays.....	98
2.6.9.	Staining of cells for confocal microscopy.....	98
2.7.	Protein methods.....	98
2.7.1.	Antibodies.....	98
2.7.2.	Western blot.....	99
2.7.3.	Co-immunoprecipitation.....	100
2.7.4.	Enzyme-linked immunosorbant assay (ELISA).....	100
2.8.	Statistics.....	101

Chapter 3: Identification of TIR domain proteins in bacteria.....102

3.1.	Introduction.....	102
3.2.	Aims and objectives.....	104
3.2.1.	Nomenclature.....	105
3.3.	Results.....	106
3.3.1.	Bacterial TIR domain protein results from Saturated BLAST.....	106
3.3.2.	TIR domain protein results from PSI-BLAST.....	109

3.4.	Conclusions	129
------	-------------------	-----

Chapter 4: The effect of bacterial TIR domain proteins on mammalian immune signalling.....134

4.1.	Introduction	134
4.2.	Aims and objectives	135
4.3.	Results	139
4.3.1.	Cloning of the genes encoding selected bacterial TIR domain proteins	139
4.3.2.	Expression of bacterial TIR domain proteins in HEK293 cells	139
4.3.3.	Setting up the NFκB luciferase reporter assay.....	141
4.3.4.	The effect of Tdps on IL-1β signalling to NFκB.	143
4.3.5.	The effect of Tdps on basal NFκB activity.....	148
4.3.6.	The effect of Tdps on TNFα signalling to NFκB.....	148
4.3.7.	Specificity of the effect of YpTdp and BthTdp on IL-1β signalling to NFκB.....	148
4.3.8.	The effect of Tdps on LPS signalling to NFκB.	151
4.4.	Conclusions	158

Chapter 5: Further *in vitro* investigation of YpTdp and its effects on mammalian immune signalling.....162

5.1.	Introduction	162
5.2.	Aims and objectives	163
5.3.	Results	164
5.3.1.	Cloning and expression of the YpTdp TIR domain (YpTIR).....	164
5.3.2.	The effect of YpTIR on IL-1β, TNFα and LPS signalling to NFκB.....	164
5.3.3.	IL-8 production.....	167
5.3.4.	IκBα degradation	167
5.3.5.	Interaction studies.....	169
5.3.6.	TIR adaptor-induced signalling to NFκB	174
5.4.	Conclusions	177

Chapter 6: Assessment of the contribution to the virulence of *Yersinia pestis* from YpTdp.....183

6.1.	Introduction	183
------	--------------------	-----

6.2.	Aims and objectives	185
6.3.	Results	186
6.3.1.	Production and confirmation of <i>Yersinia pestis</i> $\Delta YpTdp$	186
6.3.2.	Growth of <i>Yersinia pestis</i> $\Delta YpTdp$ in vitro.....	188
6.3.3.	Uptake and replication of <i>Yersinia pestis</i> $\Delta YpTdp$ in a macrophage cell line.....	194
6.3.4.	Virulence of <i>Yersinia pestis</i> $\Delta YpTdp$ in a murine model.....	194
6.3.5.	Other characteristics of the <i>Y. pestis</i> $\Delta YpTdp$	202
6.4.	Conclusions	205
Chapter 7: General discussion.....		208
7.1.	Osmoregulation-related function.....	211
7.2.	Phage-related function.....	212
7.3.	Biofilm formation.....	213
7.4.	Methylglyoxyl synthase.....	215
7.5.	Further work.....	216
7.6.	Concluding remarks.....	219
References.....		221
Appendix A: Amino acid sequences of bacterial TIR domain proteins investigated in this work.....		256
Appendix B: Full list of PSI-BLAST protein results		258
Appendix C: DNA sequences of bacterial TIR domain proteins cloned in this work		259
Appendix D: Publications		260

List of Figures

Figure 1-1:	A schematic representation of data from crystallographic studies on ligand bound to TLR-ECD	27
Figure 1-2:	Domain organisation of five TIR domain-containing adaptor proteins	32
Figure 1-3:	MyD88-dependent signalling pathways	33
Figure 1-4:	The role of MyD88 in Interleukin signalling	35
Figure 1-5:	The cycle of Mal in TLR4 signalling	38
Figure 1-6:	TRIF-dependent signalling	41
Figure 1-7:	The cycle of TRAM in TLR4 signalling	44
Figure 1-8:	Multiple sequence alignment of eukaryotic TIR domains	46
Figure 2-1:	Clustal colourscheme for Jalview alignments	79
Figure 2-2:	Schematic representation of commercially available vectors used in this work	88
Figure 3-1:	Screen shot of the first page of the web-based PSI-BLAST search	110
Figure 3-2:	Screen shots of PSI-BLAST results	111
Figure 3-3:	Screen shot of the second iteration of a PSI-BLAST search	112
Figure 3-4:	Multiple sequence alignment of y2426 from <i>Y. pestis</i> KIM with eukaryotic TIR domain proteins	121
Figure 3-5:	Multiple sequence alignment of BaTdp with homologous TIR domain proteins	123

Figure 3-6:	Multiple sequence alignment of BMEI1674 with homologous TIR domain proteins	125
Figure 3-7:	Multiple sequence alignment of BMEI1216 with homologous TIR domain proteins	127
Figure 3-8:	Diverse domain architectures of bacterial proteins containing TIR domains	132
Figure 4-1:	Flow diagram explaining the link between the bioinformatic searches and subsequent experimental work	137
Figure 4-2:	Expression of bacterial TIR domain proteins in HEK293H cells.	140
Figure 4-3:	The catalysis of luciferin into oxyluciferin with the concurrent emission of light as catalysed by firefly luciferase.	142
Figure 4-4:	The effect of chloramphenicol acetyltransferase on NF κ B activity downstream of IL-1 β stimulation.	144
Figure 4-5:	Results from representative IL-1 β signalling experiments	146
Figure 4-6:	The effect of selected bacterial Tdps on IL-1 β -induced NF κ B activity.	147
Figure 4-7:	The effect of selected bacterial Tdps on the basal activity of NF κ B (in the absence of any exogenous immune stimulation).	149
Figure 4-8:	The effect of selected bacterial Tdps on NF κ B activity downstream of TNF α stimulation	150
Figure 4-9:	The dose-dependent affect of YpTdp and BthTdp on IL-1 β signalling to NF κ B.	152
Figure 4-10:	Results from representative LPS signalling experiments	154

Figure 4-11:	The effect of selected Tdps on NFκB activity downstream of LPS stimulation	155
Figure 4-12:	The effect of selected bacterial Tdps on basal NFκB activity (absence of any exogenous immune stimulation) in HEK-Blue™ hTLR4 cells	156
Figure 4-13:	Percentage viability of HEK-Blue™ hTLR4 cells 24 h after transfection with Tdp constructs	157
Figure 5-1:	Confirmation of the expression of YpTIR-V5 in HEK293 cells by Western blotting	165
Figure 5-2:	The effect of YpTIR on NFκB activity after IL-1β, TNFα or LPS stimulation.	166
Figure 5-3:	Effect of YpTdp/YpTIR on IL-8 production downstream of IL-1β, TNFα or LPS stimulation.	168
Figure 5-4:	The effect of YpTdp and YpTIR on IκBα levels after IL-1β stimulation.	170
Figure 5-5:	Intracellular pattern of expression of MyD88 over-expressed in HEK293H cells.	172
Figure 5-6:	The intracellular expression pattern of YpTdp and MyD88 when over-expressed together in HEK293H cells.	173
Figure 5-7:	Co-immunoprecipitation of YpTdp and MyD88	175
Figure 5-8:	The effect of YpTdp and YpTIR on MyD88-, Mal-, or TRIF-induced signalling to NFκB.	176
Figure 5-9:	Hypotheses for the different experimental observations between YpTdp and YpTIR	179
Figure 6-1:	Schematic representation of the steps carried out in the creation of a <i>Y. pestis</i> <i>YpTdp</i> gene knockout.	187

Figure 6-2:	Growth of <i>Y. pestis</i> GB and <i>Y. pestis</i> $\Delta YpTdp$ in BAB broth.	189
Figure 6-3:	Enumeration of <i>Y. pestis</i> GB and <i>Y. pestis</i> $\Delta YpTdp$ at timepoints during broth culture	190
Figure 6-4:	Sedimentation of <i>Y. pestis</i> GB and <i>Y. pestis</i> $\Delta YpTdp$ in culture	192
Figure 6-5:	Hydrophobicity of <i>Y. pestis</i> GB and $\Delta YpTdp$	193
Figure 6-6:	The intracellular growth of <i>Yersinia pestis</i> GB and <i>Yersinia pestis</i> $\Delta YpTdp$ in J774 murine macrophages	195
Figure 6-7:	Survival curves for the three comparable doses of <i>Y. pestis</i> GB and <i>Y. pestis</i> $\Delta YpTdp$ given during the MLD study.	199
Figure 6-8:	Reed-Meunch calculation for MLD of <i>Y. pestis</i> $\Delta YpTdp$.	201
Figure 6-9:	Survival of <i>Y. pestis</i> GB and $\Delta YpTdp$ in different concentrations of polymixin B	203
Figure 6-10:	The survival of <i>Y. pestis</i> GB and $\Delta YpTdp$ in sodium chloride	204
Figure 7-1:	Screen shot from a Conserved Domains Database (CDD) search using YpTIR	214
Figure 7-2:	Proposed metabolic pathways for polyglucose use by <i>Desulfovibrio gigas</i>	217

List of Tables

Table 1-1:	A list of current ligands for each human TLR	25
Table 2-1:	TIR domain proteins used as seeds for Saturated BLAST searches	75
Table 2-2:	TIR domain proteins used as seeds for PSI-BLAST searches	76
Table 2-3:	Study timetable for the assessment of the competitive index of <i>Y. pestis</i> $\Delta YpTdp$ in competition with wild-type <i>Y. pestis</i> GB	82
Table 2-4:	Study timetable for assessment of median lethal dose of <i>Y. pestis</i> $\Delta YpTdp$.	83
Table 2-5:	Details of vectors used in this study given as gifts	89
Table 2-6:	Oligonucleotide PCR primers used in this study	91
Table 2-7:	Example normalisation of NF κ B activity in the presence and absence of stimulation.	97
Table 3-1:	TIR domain proteins in CDC Category A and B agents (Saturated BLAST search strategy)	107
Table 3-2:	Summary table of TIR domain proteins in bacterial and archaeal species.	114
Table 3-3:	Summary table of TIR domain proteins in bacterial and archaeal species.	117
Table 3-4:	TIR domain proteins in CDC Category A and B agents (PSI-BLAST search strategy)	119
Table 3-5:	Summary table of the bioinformatic characteristics of TIR domain proteins from CDC category A and B bacteria	128

Table 4-1:	Bacterial TIR domain proteins down-selected for initial <i>in vitro</i> signalling assays	138
Table 4-2:	A summary of the effect of selected bacterial TIR domain proteins on TIR -dependent (IL-1/LPS) and -independent (basal, TNF α) signalling to NF κ B	161
Table 6-1:	Bacterial numbers per spleen from the <i>in vivo</i> competitive index study	197
Table 6-2:	A summary of the number of surviving mice in each dose group in the MLD study and their median time to death	200

Abbreviations

AP-1	Activator protein-1
CI	Competitive index
DC	Dendritic cell
dsRNA	Double-stranded RNA
Dstl	Defence science and technology laboratory
ECD	Ectodomain
ER	Endoplasmic reticulum
h	Hour(s)
HEK293	Human embryonic kidney 293
HSP	Heat shock protein
IFN	Interferon
IKK	I κ B kinase
IL-	Interleukin-
IRAK	Interleukin-1 receptor-associated kinase
IRF	Interferon regulatory factor
Jnk	Jun N-terminal kinase
L-agar	Luria agar
L-broth	Luria broth
LPS	Lipopolysaccharide
LTA	Lipoteicoic acid
Mal	MyD88 adaptor like
MAPK	Mitogen-activated protein kinase
MDA5	Melanoma differentiation-associated gene 5
mDC	Myeloid derived dendritic cell
MHC	Major histocompatibility complex
MOI	Multiplicity of infection
MyD88	Myeloid differentiation primary response protein 88
NF κ B	Nuclear factor kappa B
NK	Natural killer (cell)
NLR	NOD-like receptor
PAMP	Pathogen-associated molecular pattern
PBS	Phosphate buffered saline

PCR	Polymerase chain reaction
pDC	Plasmacytoid dendritic cell
PIP2	Phosphatidylinositol (4,5)-bisphosphate
PRR	Pattern recognition receptor
rpm	Revolutions per minute
RIG-I	Retinoic acid-induced gene-1
RIP	Receptor interacting protein
RLR	RIG-I-like receptor
RLU	Relative luciferase units
RNS	Reactive nitrogen species
ROS	Reactive oxygen species
s	Second(s)
SARM	sterile α - and armadillo-motif-containing protein
SDS-PAGE	Sodium dodecyl sulphate-polyacrylamide gel electrophoresis
SEM	Standard error of the mean
SIGIRR	Single immunoglobulin Il-1R-related molecule
SOCS	Suppressor of cytokine signalling
ssRNA	Single-stranded RNA
STAT	Signal transducer and activator of transcription
TAB1	TAK-1 binding protein-1
TAK1	Transforming growth factor β -activated kinase-1
TANK	TRAF-family member-associated NF κ B activator
TBK1	TANK-binding kinase-1
TICAM	TIR-containing adaptor molecule
TIR	Toll-like/Interleukin-1 receptor (domain)
TIRAP	TIR domain-containing adaptor protein (=Mal)
TLR	Toll-like receptor
TNFR	Tumour necrosis factor receptor
TRAF	TNFR-associated factor
TRAM	TRIF-related adaptor molecule (=TICAM2)
TRIF	TIR domain-containing adaptor protein inducing interferon- β (=TICAM1)
TTSS	Type three (III) secretion system
Yop(s)	<i>Yersinia</i> outer protein(s)

Chapter 1: General Introduction

1.1. The innate immune response and pattern recognition

Multi-cellular organisms must defend themselves against invasion by the wide variety of micro-organisms that populate their environment. For this reason a complex and highly conserved suite of immune defences has evolved. Elimination of harmful microbes depends both on the ability to quickly mount defences and to effectively maintain a response. For the majority of its research life, the field of immunology has paid great attention to the study of the specific and lasting response we now call “adaptive” immunity. The study of adaptive immunity began as early as 1796 when Edward Jenner inoculated an eight-year old boy with pus from a cowpox blister, thus generating lasting immunity in that boy to smallpox¹. The adaptive immune system is incredibly specific, potent and potentially long-lasting. However, the response takes time and does not account for the initial rapid detection of invasion. This arm of the immune system, termed “innate” immunity was also first described over a century ago and precedes the adaptive response to provide an initial suite of effects to try and contain and eliminate an invading organism, subsequently activating the adaptive response if necessary. The innate immune system acts at the earliest phase of infection and is mediated by phagocytes such as macrophages and dendritic cells². The adaptive response acts later in infection, if it has not been dealt with by the innate system, and achieves complete specificity by clonal selection of lymphocytes bearing the correct antigen-specific receptor. These receptors arise in an almost infinite selection via a gene rearrangement mechanism^{3,4}.

In general the innate immune system was the less well appreciated arm of the immune response but this changed after the question of how the host so rapidly first detects microbial invasion began to be solved. This broad detection of an invasion event referred to as “pattern recognition” has now been studied intensely over its short ten-year history. In 1989, during his lecture to open the annual Cold Spring Harbor symposium of quantitative biology, Dr. Charles Janeway proposed the existence of receptors on immune cells that were able to detect microbes and trigger the host’s response to infection⁵. These receptors, now called “pattern recognition receptors (PRRs)” rapidly recognise conserved molecular patterns that distinguish foreign organisms from host cells⁶. Recently it has also been discovered that these receptors can also recognise host proteins out of their normal context,

thus signalling tissue damage to the immune system⁷⁻⁹. PRRs now include Toll-like receptors (TLRs), lectins, NOD-like receptors (NLRs) and retinoic acid-induced gene-1 (RIG-I)-like receptors (RLRs), amongst others⁶. All PRRs possess the following general characteristics: they recognise microbial patterns that are disadvantageous for a microbe to alter; they are expressed constitutively in a host and are therefore able to act immediately and independently of life-cycle stage; they are encoded by the germline and are preferentially expressed on cell types that will be the first to encounter a pathogen and have no immunological memory. The only specificity shown by PRRs is that they each have a specific set of ligands (which can be incredibly disparate) and that they activate specific signalling pathways. Different PRRs act in concert to co-ordinate a host of effects aimed at the elimination of potentially harmful organisms. However, pathogenic microbes are involved in a dynamic race with their hosts to overcome such defences and the most pathogenic of organisms are often successful.

1.2. Toll and Toll-like receptor signalling

Despite Dr. Janeway's insightful lecture in 1989 it took another seven years for the first class of PRRs to be identified. In 1996 Lemaitre et al. showed that the "Toll" receptor in *Drosophila melanogaster* was involved in the detection of fungi¹⁰. This led the way for the identification of "Toll-like" receptors (TLRs) in vertebrates. The gene *toll* in *Drosophila* had originally been identified by a group in Germany during a routine genetic screen¹¹. *Toll* is the German word for "weird" or "far out" and this mutant was so-named because parts of the fly which should have been present on its bottom half were present on its top half, and *vice versa*. They concluded that the gene had a role in dorso-ventral patterning of the fly during embryogenesis. Lemaitre's group discovered that mutant flies with non-functioning *toll* succumbed to over-whelming fungal infection¹⁰ and therefore showed that Toll also had a role to play in the detection and elimination of invading micro-organisms.

Toll is a type I transmembrane receptor consisting of an extracellular leucine rich repeat domain, a transmembrane helix, and a conserved intracellular domain denoted TIR (Toll/Interleukin 1 Receptor) domain after it was discovered that this domain is also present within the interleukin-1 receptor (IL-1R)^{12,13}. A homologous human receptor was identified (initially termed hToll, then TLR4) as the long-sought-for receptor for LPS, and, subsequently, TLRs were identified across vertebrate species. Variants of this system are

now known to be present in all multicellular organisms, and have even been found to have a role in the lifestyle of the multicellular form of the amoeba *Dictyostelium discoideum* which, in many respects, forms a bridge between the uni- and multi-cellular world¹⁴. TLRs belong to a wider family of proteins, the Toll/Interleukin-1 superfamily, characterised by the presence of a TIR domain. Also present within the family are the IL-1, IL-18 and IL-33 receptors and TIR domain-containing cytoplasmic adaptor molecules which transduce ligand binding at the receptor level into an intracellular immune signalling cascade. To date thirteen mammalian TLRs have been identified (ten in humans and twelve in mice)¹⁵.

All TLRs are involved in the detection of microbial patterns, such as the CpG DNA of bacteria, or the ssRNA of an RNA virus. On recognition of ligand by TLRs or the Interleukin receptors, signal transduction pathways are initiated by the interaction of TIR domains between receptors, and also between receptors and TIR-containing adaptor molecules. These signalling cascades involve the activation of a variety of kinases via phosphorylation and ubiquitination events, finally leading to the activation of transcription factors that control the expression of a variety of pro- and anti-inflammatory molecules, chemokines and pathway molecules. These effector molecules aid in the containment and elimination, or tolerance towards, an invading microbe by activating and directing cells of the immune system, and also initiate the development of an acquired, memory immune response. The wider effects of TLR signalling are discussed in Section 1.4.

Although traditionally PRRs have been considered to discriminate self from non-self, it is now known that some PRRs, including some TLRs, can recognise endogenous ligands, but only out of their normal context. For example, TLR9 recognises host DNA, which would only be detected by the receptor during uncontrolled cell death characteristic of tissue damage or infection¹⁶. Some of these “danger” signals may also be actively secreted during infection^{8,17}. TLRs, together with other PRRs, form an alarm system critical to the activation of macrophages and dendritic cells (DCs) that phagocytose and degrade pathogens, migrate to secondary lymphoid tissue and present antigen to T cells. PRRs also signal invasion in stromal and other somatic cells.

1.2.1. TLR ligands and ligand binding

TLRs have a wide range of ligands which vary greatly in their structure. A current list of subjected ligands for each TLR is shown in Table 1-1. To date, no ligands for TLR10 have been confirmed. Experiments to elucidate the ligands of each receptor are difficult, since contamination with other potential stimulants, principally endotoxin (a TLR4 ligand), provides an ever-present problem¹⁸. Sometimes susceptible animal models have given an indication as to a likely TLR ligand. Two strains of mice, C3H/HeJ and C57BL10/ScCr, were known for a long time to be hypo-responsive to lipopolysaccharide (LPS) and when two independent groups identified that they both had mutations in their *Tlr4* gene this gave a useful indication that TLR4 was the receptor for LPS^{19,20}. Similarly a role in LPS signalling for TLR2 is suggested by the use of a cell lines derived from Chinese Hamster cells which carry a point mutation in the *tlr2* gene which encodes for a premature STOP codon and therefore a non-functional protein²¹.

TLRs recognise ligand through their extracellular region, composed of 19-25 tandem copies of the leucine rich repeat (LRR) motif. About 500 LRR-containing proteins with diverse, and often unknown, functions have been identified in the human genome. Generally, in nature, LRRs are widely used as building blocks to make scaffolds of protein interfaces primarily designed for specific protein-protein interactions.

The particulars of ligand binding are beginning to be elucidated with the completion of crystallographic studies with receptor ectodomain (ECD) bound to ligand, in addition to modelling studies^{22,23}. The LRR domains in all ten human TLRs are N-glycosylated with the un-glycosylated surfaces corresponding to the areas of ligand binding. The first published structure of a TLR-ECD was that of murine TLR3 (mTLR3) derived simultaneously by two groups^{24,25}. Three years later the structure of mTLR3-ECD bound to dsRNA was solved²⁶. It shows that mTLR3-ECD interacts with the sugar-phosphate backbone of the RNA but not with individual bases, which explains why TLR3 lacks specificity for any particular nucleotide sequence^{27,28}. This is in contrast to TLR7 and TLR8 which have been implicated in the sequence dependent detection of RNA oligonucleotides²⁹⁻³¹, although there are conflicting reports over the relative stimulatory properties of single-stranded (ss) and double-stranded (ds) RNA³²⁻³⁶. The dsRNA makes

Toll-like receptor	Ligand
TLR1/2	Triacylated lipoprotein Soluble factors & Porin PorB (Neisseria meningitides) OspA (Borrelia burgdorferi)
TLR2	Lipoprotein/lipopeptides Diacylated lipoprotein Lipoteichoic acid Peptidoglycan Zymosan Lipoarabinomannan (Mycobacteria) Phenol-soluble modulins (Staphylococcus epidermidis) Glycoinositolphospholipids (Trypanosma cruzi) Glycolipids (Treponema maltophilum) Porins (Neisseria meningitides) Atypical LPS (Leptospira interrogans & Pophyromonas gingivalis) Hyaluronan
TLR2/6	Diacylated lipoprotein Hemagglutinin (measles) HSP-60, -70, -96
TLR3	dsRNA mRNA
TLR4	Lipopolysaccharide F-protein (RSV) HSP-22, -60, -70 Fibronectin Flavolipin (Flavobacterium meningosepticum) ER-112022, E5564, E5531 Taxol Envelope proteins (mouse mammary tumour virus) Oligosaccharides of hyaluronic acid Polysaccharide fragments of heparin sulphate Fibrinogen α A crystallin and HSPB8
TLR5	Flagellin
TLR7	ssRNA Imidazoquinolines (imiquimod, R848) Bropirimine Guanosine analogues
TLR8	ssRNA R848
TLR9	Unmethylated CpG DNA DNA Chromatin-IgG complexes

Table 1-1: A list of current ligands for each human TLR

Blue text denotes bacterial ligands, purple text for viral ligands, green text for host-derived (endogenous) ligands, orange text for fungal ligands, red text for plant ligands, brown text for synthetic ligands and black for protist ligands. Table adapted from Table 1 in Gay et. al. 2007³⁷

contact with the TLR3-ECD at two points 120Å apart which accounts for why a minimum of 40-50 base pairs are required for binding of dsRNA to TLR3²⁸. Two other crystal structures of TLR-ECD with bound ligand have also been solved; that of TLR1 and TLR2 ECDs bridged by the ligand Pam₃CSK₄³⁸ and TLR4 bound to its accessory protein myeloid differentiation protein-2 (MD-2) and Eritoran, a synthetic analogue of lipid A³⁸⁻⁴⁰ (Figure 1-1).

These three structures show both similarities and differences: with regards to the position of ligand binding, in the TLR1/2 structure two lipid chains of Pam₃CSK₄ bind to a pocket in TLR2 and the third chain binds to a channel located a similar region on TLR1 so the binding pocket is at the boundary of the central and C-terminal part of the TLRs (Figure 1-1B). The TLR3 binding sites, however, are at regions near the N- and C- termini (Figure 1-1A). In the TLR4 structure MD-2 (it is the accessory protein that contacts TLR4, rather than the ligand) binds to the “inside” of the horseshoe shape in each ECD and Eritoran binds to the hydrophobic pocket of MD-2 (Figure 1-1C). With regards to interaction forces, in the TLR1/2 structure it is hydrophobic interactions which play the crucial role in ligand binding, whereas in TLR3 and TLR4 the interaction with ligand (dsRNA or MD-2) involves mainly electrostatic and hydrogen (H-) bond interactions. Despite these differences the ligand-induced dimers of all these structures form the same general structure of an “M” shaped dimer with a two-fold symmetry axis when viewed from above, and the ligand bridges the two ECDs by a similar area of glycan-free surface. It is interesting to note, however, that although the structure has not been solved by x-ray crystallography, detailed structural investigation and modelling studies on the Toll ECD bound to its ligand Spatzle do not demonstrate an “M” shaped dimer structure⁴¹.

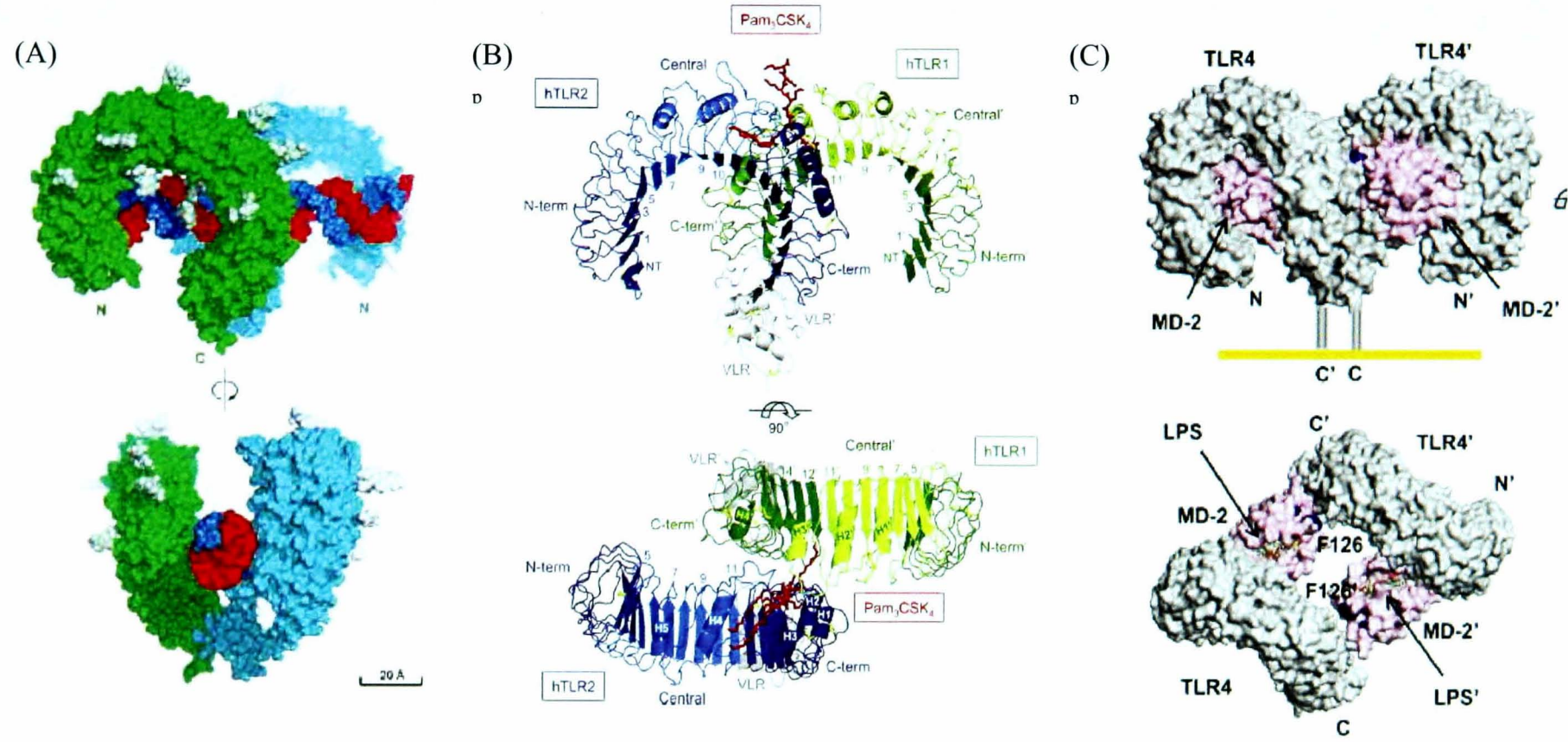


Figure 1-1: A schematic representation of data from crystallographic studies on ligand bound to TLR-ECD
 (A) dsRNA:TLR3 signalling complex. Mouse TLR3 ECDs (green and cyan) form a dimer on the dsRNA (blue and red). The N-glycans are shown (light green and light blue). The top picture shows the N- and C-terminal binding sites. The bottom picture shows how the two C-terminal domains are brought together in the complex. (B) Structure of the TLR1/TLR2-ECD dimer with bound Pam₃CSK₄ ligand (red). The TLR1-ECD is shown in green, the TLR2-ECD is shown in blue. The top picture shows a side view and the bottom picture shows a top view. (C) Three dimensional representation of TLR4-ECD/MD-2/Eritotan structure. Surfaces of TLR4 and MD-2 are grey and magenta, respectively. Figure adapted from Refs^{26,38,40}

1.2.1.1. The diversity in ligand binding

As can be seen from Table 1-1, TLRs recognise a vast array of ligands and this ability is thought to be partly due to the fact that TLR-ECDs often have insertions in some of their LRR units. For example, the TLR3-ECD has insertions at LRR12 and LRR20²⁵ and these are completely conserved in TLR3 from other species, suggesting that they play an important role in ligand binding^{42,43}. Further diversity is achieved by the use of accessory proteins for ligand binding and the homo- and hetero- oligomerisation of receptors. For example, the LPS response requires the sequential interaction and transfer of LPS to LPS-binding protein, the glycosylphosphatidylinositol-anchored protein CD14 and MD-2 which binds to the TLR4-ECD (Section 1.2.1)^{44,45}. CD14 is also required for signalling induced by TLR2 ligands⁴⁶ and it is believed that CD36 is involved in the recognition of diacylated lipopeptides by TLR2/6 dimers⁴⁷.

In addition, like other type-I transmembrane receptors it is thought that most, if not all, TLRs signal either as homo- or hetero-dimers, or higher oligomers^{24,25,48,49}. It is known that TLR2 forms heterodimers with TLR1 or TLR6 while TLR4 homodimerises like dToll^{48,49}. Certain ligands, including mycobacterial lipoarabinomannan, appear to be recognised by TLR2 independent of TLR1 or TLR6, suggesting homodimerisation of TLR2, or its heterodimerisation with another molecule⁴⁶. It has been the subject of some debate as to whether TLRs exist as non-functional dimers/oligomers in the absence of ligand and that ligand binding induces conformational rearrangement of the intracellular TIR domains creating a scaffold onto which TIR-containing adaptors can bind^{37,41,50}, or whether ligand binding brings two or more TLRs together in the membrane, thus bringing their TIR domains into close proximity, thereby forming the same signalling platform⁵¹. In a study that examined the interaction of dToll with its ligand Spätzle, it was concluded that Spätzle binds directly to the Toll ECD, thereby cross-linking two receptors, and that this dimerisation was necessary for signalling to occur⁴⁹. A similar suggestion was made of the binding of dsRNA to TLR3^{24,25,28}. The fact that the overall structure of the TLR3 ECD was unchanged upon dsRNA binding supports a signalling mechanism in which receptor dimerisation is ligand-induced. However, other evidence suggests a mechanism comprising elements of both hypotheses in which receptors are loosely dimerised within the membrane, with ligand binding inducing conformational changes that allow stable receptor association

and bring the TIR domains into the correct conformation for a signalling platform to be formed^{28,49}. This is supported by a study of ligand binding onto TLR9 which demonstrated that TLR9 exists as “inactive” homodimers in the membrane and that stimulatory, but not unstimulatory, DNA led to conformational changes in the TLR9 ECDs which resulted in close apposition of the TIR domains⁵⁰. This coming together, and potential re-orientation, is considered likely to be required for TIR-adaptor recruitment and similar models have been suggested for receptors other than TLRs⁵². In the case of CpG DNA binding to TLR9 it also seems that the sequence of the CpG may alter the quantity and quality of the conformational change which would explain how subtle sequence variations in DNA ligands can lead to quantitatively different responses or even TLR9 inhibition⁵³.

1.2.2. TLR location and expression

TLRs are differentially expressed on a wide range of cell types including immune cells such as DCs and macrophages as well as non-immune epithelial and fibroblast cells. Monocytes and macrophages seem to express all TLRs to some extent, except TLR3 (and Hornung *et. al* found barely detectable levels of TLR7 or TLR10)^{54,55}. Expression of TLRs in DCs is dependent on their subset and maturation state⁵⁶⁻⁶¹.

TLR1 and TLR6 seem to be ubiquitously expressed across cell types. In comparison, TLR10 is expressed most highly in B cells, whereas monocytes are characterised by a high expression of TLR2. Plasmacytoid DCs (pDCs) and B cells mainly express TLR7 and TLR9 but TLR7 is absent from NK cells and T cells and possibly monocytes. In some studies TLR7 expression was detected on both pDCs and mDCs^{56,57} whereas others have found TLR7 only on pDCs^{60,61}. TLR8 is mainly expressed in monocytes and myeloid DCs (mDCs) and at lower levels in pDCs⁵⁴.

TLR expression also appears to be differentially regulated by stimulation on different cells types. For example, stimulation of B cells with CpGs leads to a reduction in TLR7 and TLR9 expression but stimulation of pDCs with CpG leads to an increase in TLR7 but a decrease in TLR9 expression^{54,62}. TLR2 and TLR4 have also shown to be regulated in response to LPS stimulation^{63,64}. TLR3 is unique in that it is preferentially expressed in mature DCs⁵⁸. Overall, most tissues express at least one TLR, and phagocytes show an

abundant expression of all known TLRs despite some preferential expression in certain cell types⁶⁵.

In general, the TLRs that are mainly responsible for the detection of bacterial products (TLRs 1, 2, 4, 5, and 6) are expressed on the cell surface, while the subset of TLRs that sense viral components (TLRs 3, 7, 8, and 9) are located intracellularly on endosomal membranes. In some instances, TLRs 2, 4 and 5 have been found intracellularly and TLR9 on the cell surface⁶⁶⁻⁶⁹. The endosomal TLRs, along with the RIG-like receptors RIG-I and MDA5, induce anti-viral immunity by activating the transcription of type I interferons (IFNs) and IFN-regulatory genes via the interferon regulator factor (IRF) transcription factors^{70,71}. TLR3, however, has distinct properties that allow recognition of extracellular virus-derived dsRNA and the subsequent induction of type I IFN, cytokine production and DC maturation that results in the activation of natural killer (NK) cells and cytotoxic T lymphocytes (CTLs)^{27,72-74}. In comparison, the TLRs on the plasma membrane are unable to induce IFNs, with the exception of TLR4. This suggests that TLR4 must be translocated to the endosome to activate its IFN pathway (mediated by the adaptor TRIF, see Section 1.2.3.3) and this is indeed the case. The reason for this segregation of signalling between membranes is the absence of the signalling factor TRAF3 in the plasma membrane. TRAF3 is required for IFN production and mutations in TRAF3 that allow it to bind the plasma membrane result in Pam3Cys-induced IFN β production by TLR1/2 thus demonstrating the ability of plasma membrane TLRs to produce IFNs but only if TRAF3 is available to them in this artificial way⁷⁵.

1.2.3. TLR signalling: transduction through the TIR domain

After ligand binding, cytoplasmic adaptor molecules are recruited to activated TLRs. There are five known mammalian TIR domain-containing adaptors: myeloid differentiation factor 88 (MyD88), MyD88 adaptor like (Mal; also known as TIR domain-containing adaptor protein, TIRAP), TIR domain-containing adaptor protein inducing interferon- β (TRIF; also known as TIR-containing adaptor molecule 1, TICAM1), TRIF-associated molecule (TRAM; also known as TICAM2) and sterile α - and armadillo-motif containing protein (SARM). MyD88, Mal, TRIF and TRAM recruit down-stream signalling molecules which lead to the activation of NF κ B and members of the IRF family of transcription factors. while it is believed SARM may act as a negative regulator.

The signalling pathways activated downstream of each TLR are largely dependent on the differential usage of these adaptor molecules. The adaptors exhibit different molecular dynamics in response to stimulation by different TLRs, providing specificity to TLR signalling. For this reason the TLR pathways are usually defined by adaptor usage (“MyD88-dependent pathway,” for example). Figure 1-2 shows the domain architecture for each of the five TIR adaptor molecules.

1.2.3.1. MyD88 and MyD88-dependent signalling

MyD88 is 296 amino acids long and comprises a C-terminal TIR domain and an N-terminal death domain (DD), separated by a small intermediate domain (ID)⁷⁶ (Figure 1-2). MyD88 was first shown to be an adaptor molecule in IL-1 signalling, serving to link the IL-1R to signalling intermediates^{77,78}. It was then shown that MyD88 served an equivalent function downstream of TLR4⁷⁹. MyD88 is required for signalling through all TLRs, except TLR3. It has also recently been shown that the IL-1R can signal independently of MyD88 in anterior hypothalamic neurons and potentially in other cell types⁸⁰. For TLR2 and TLR4 signalling only, MyD88 requires another TIR domain adaptor protein, Mal, to bridge it to the receptor (Section 1.2.3.2). MyD88 has shown the ability to homo-dimerise via its DD and TIR domain and to hetero-dimerise with Mal via its TIR domain⁸¹. The crucial role that MyD88 plays in TLR signalling is demonstrated by the fact that MyD88-deficient mice lose the ability to produce pro-inflammatory cytokines in response to a wide variety of TLR ligands⁸²⁻⁸⁶.

TLR/IL-1R signalling to NF κ B via MyD88 follows this general sequence of events (Figure 1-3): MyD88 is recruited to the TLR/IL-1R TIR domain either alone or via its bridging adaptor Mal, in the case of TLR2 and TLR4 signalling, and interacts with the Interleukin-1 receptor associated kinase IRAK4 via its intermediate domain⁸⁷. Initial studies indicated that IRAK4 then interacted with IRAK1 via homophilic DD interactions^{78,88} and phosphorylated, thus activating, IRAK1⁸⁹. It was postulated that IRAK1 then went on to interact with TNF α receptor associated factor-6 (TRAF6) through its DD, ID, and C-terminal TRAF6 binding sites, which was thought to cause the oligomerisation and activation of TRAF6⁹⁰. This

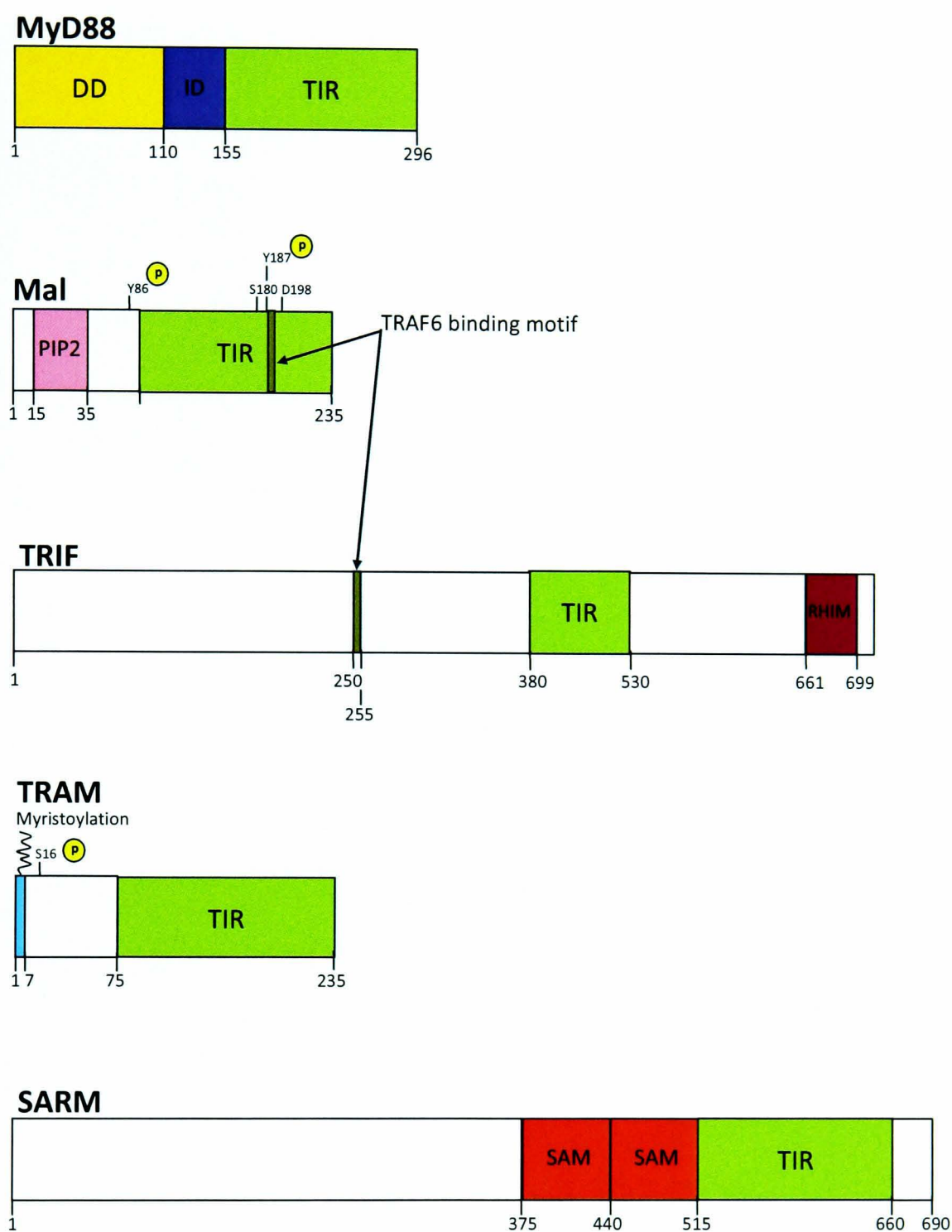


Figure 1-2: Domain organisation of five TIR domain-containing adaptor proteins

ID: intermediate domain, DD: death domain, PIP2: phosphatidylinositol-4,5-bisphosphate binding motif, RHIM: RIP1 homotypic interaction motif. Yellow circles: Phosphorylation sites. Adapted from O'Neill et. al., 2007⁹¹.

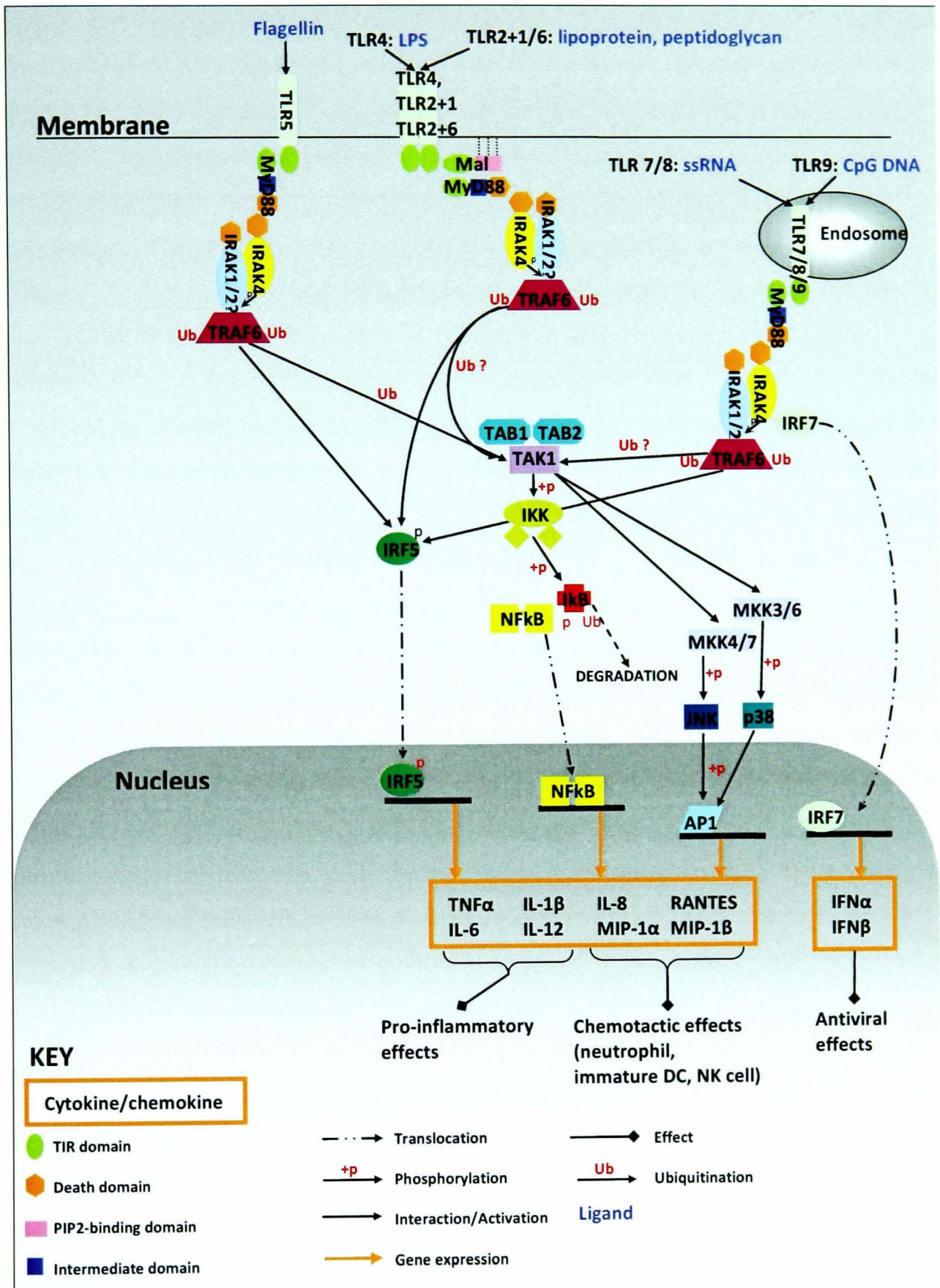


Figure 1-3: MyD88-dependent signalling pathways

view has gradually become more controversial, however⁹², and it is now thought that IRAK-2 may play a more important role in activating TRAF6 than IRAK-1^{93,94}. It has been reported that TRAF6 oligomerises and that this is important for the activation of NF κ B^{95,96}, but this has also been refuted⁹⁷. TRAF6 is a ubiquitin E3 ligase and functions with the ubiquitin-conjugating enzyme complex Ubc13-Uev1a to catalyse the synthesis of K63-linked polyubiquitin chains on target proteins including TRAF6 itself,⁹⁸ although the importance of the ubiquitin-conjugating enzyme complex in TLR/IL-1R signalling is debated^{97,99,100}. Polyubiquitinated TRAF6, in co-operation with Ubc13-Uev1a, has been shown to mediate the activation of the IKK complex via a proteasome-independent mechanism^{95,101}, although the target protein for the ubiquitin chains has yet to be identified. Ubiquitinated TRAF6 recruits the TAK-1 binding proteins, TAB1 and TAB2, along with TAK1 (transforming growth factor β -activated kinase-1). TAK1 becomes activated in this complex, potentially via ubiquitination by TRAF6⁹⁵. Phosphorylation of TAK1 and TAB2 also occurs leading to the dissociation of this complex from the membrane and IRAK degradation^{102,103}. This is a branching point in MyD88-dependent signalling for the activation of NF κ B or induction of the mitogen activated protein kinase (MAPK) pathway, leading to induction of the transcription factor activating protein-1 (AP-1). For the NF κ B pathway, activated TAK1 activates the I κ B kinase (IKK) complex which phosphorylates I κ B resulting in its ubiquitination and subsequent proteasome-mediated degradation leaving NF κ B free to translocate to the nucleus and initiate gene transcription. For the MAPK pathway, TAK1 activates MAPK kinase-6 (MKK6) which phosphorylates and activates the kinases JNK, ERK and p38, thereby mediating AP-1 activation downstream of MyD88. MyD88 also activates members of the interferon regulator factor (IRF) family of transcription factors as discussed in further detail in Section 1.4.1.

MyD88 also has a role in signalling through the IL-1Rs (Figure 1-4). Ten different IL-1Rs have been identified in human genome. Of these, IL-1RI and IL-1RAPL mediate the effects of the pro-inflammatory cytokine IL-1^{104,105} which has a variety of effects on the host response to infection and inflammation including effects on aspects of the acute phase response such as induction of fever, anorexia and non-rapid eye movement sleep^{104,106-108}. Upon binding of IL-1 to the type I IL-1R a signalling heterodimer is formed with the IL-1 receptor accessory protein IL-1RAcP¹⁰⁹. Both molecules are members of the TLR/IL-1R receptor superfamily and therefore contain a TIR domain. MyD88 associates with both the

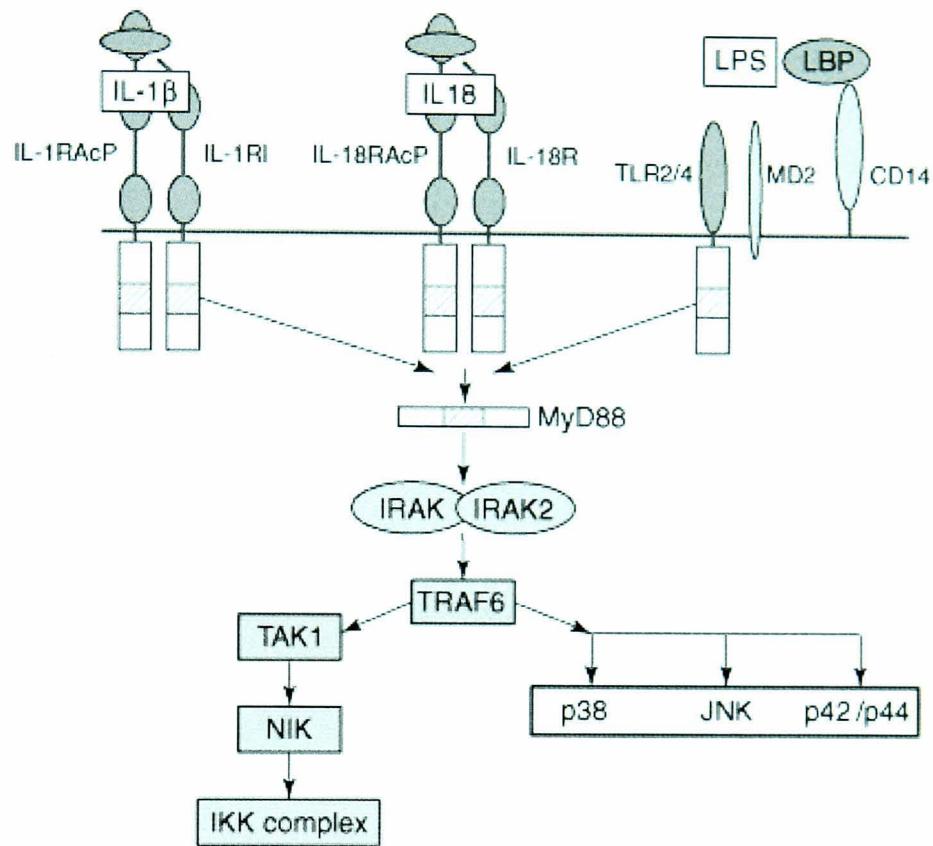


Figure 1-4: The role of MyD88 in Interleukin signalling

MyD88 is the TIR adaptor protein for IL-1 and IL-18 signalling, in addition to its role as an adaptor protein in TLR signalling. Figure reproduced from “IL-1 Receptor Family,” O’Neill and Dower¹¹⁰

IL-1RI and IL-1RacP, triggering the recruitment of Tollip^{77,111,112} and ultimately the activation of NFκB^{105,113}. The exact function of IL-1RAPL in IL-1 signalling is currently not known but its TIR domain appears to be important for its function since mutation in its TIR domain is associated with non-specific X-linked mental retardation in humans. IL-1RAPL is highly expressed in brain structures and is important for memory and learning. It is tempting to speculate that, like Toll in *Drosophila*, human TIR domain receptors may also have some role in embryogenesis or neural function. Both IL-1RAPL and its close homologue TIGIRR contain a 130-residue segment C-terminal to their TIR domain which is absent in most of the other TLRs and IL-1Rs and residues within this segment may interact with neuronal calcium sensor-1 (NCS-1). Thus, it has been postulated that IL-1RAPL may have role in regulating exocytosis of secretory and neurotransmitter substances¹¹⁴.

1.2.3.2. Mal

Mal was the second TIR domain containing adaptor molecule identified^{115,116}. It is a 25 kDa protein of 235 amino acids with a TIR domain at its C-terminus and a phosphatidylinositol (4,5)-bisphosphate (PIP2)-binding domain in its N-terminus (Figure 1-2). It acts as a bridging adaptor for MyD88 during TLR2 and TLR4 signalling^{81,117}. Mal-deficient mice have an identical phenotype to MyD88-deficient mice but only with regards to their responsiveness to TLR4 and TLR2 ligands^{116,118}. The requirement for a bridging adaptor for TLR2 and TLR4 signalling is somewhat unclear, but MyD88 and these TLRs are largely electropositive and so it is thought that the electronegative Mal is required for MyD88 to be brought to the signalling complex^{118,119}. Another explanation is that Mal is required in order to direct MyD88 to TLR2 and TLR4¹²⁰. A possible advantage of using distinct adaptors for different signalling pathways is that the responses may be modulated easily without modifying the universal adaptor MyD88, leading not only to specificity in the TLR response, but also to specific control of each pathway.

Mal is able to heterodimerise with MyD88 through its TIR domain, and to homodimerise through its TIR and N-terminal domains⁸¹. During TLR4 signalling Mal is recruited to the membrane by binding to PIP2. Mutation of the PIP2 binding site results in an inability of Mal to complement Mal-deficient macrophages for TLR4 signalling¹²¹. TLR2 and TLR4

are found in the plasma membrane where PIP2 is enriched. Membrane-bound Mal recruits MyD88 to the TLR4 signalling complex through its TIR domain, where MyD88 binds to TLR4 again through TIR-TIR interactions. If a PIP2 binding site is engineered into MyD88, this protein is able to direct MyD88 to the membrane and restores LPS signalling in MyD88, Mal and MyD88/Mal-deficient cells, suggesting that the sole function of Mal, with regards to activation of NF κ B is to recruit MyD88 to TLR4-rich regions in the plasma membrane¹²¹. The precise role that Mal plays in bringing MyD88 to TLR2 (for example whether it is PIP2 dependent) is currently not known but assumed to be very similar.

Another study has shown that Mal can bind TRAF6 through a binding site in its C-terminus (amino acids 188-193). Mutation of this site resulted in impaired NF κ B and MAPKs activation by TLR2 and TLR4. MyD88 does not contain a TRAF6 binding site and so it has been speculated that Mal binding to TRAF6 provides a MyD88-independent means of activating NF κ B and MAPKs. Mal may act in concert with MyD88 (which binds TRAF6 indirectly through IRAK-1 or IRAK-2) to increase recruitment of TRAF6 leading to increased NF κ B activation.

Mal is cleaved by caspase-1 at D198, removing around 4kDa of the protein, and this is required for activation of Mal¹²². Mal interacts with caspase-1 via its TIR domain, whereas MyD88 does not. The reason why Mal must be activated by caspase-1 is not known, although it is possible that this removal of 4kDa from the TIR domain would cause a conformational change of the TIR domain, or perhaps expose residues necessary for the interaction of Mal with TLR2, TLR4 or MyD88. The activation of Mal by caspase-1 highlights a synergy between TLRs and NLRs that activate caspase-1 (e.g. Nalp3) since these NLRs will potentiate signalling by TLR2 and TLR4 via cleavage of Mal.

It is also known that Mal undergoes covalent modifications which regulate its behaviour and phosphorylation of Mal is required for its activation. Mal is phosphorylated on specific tyrosine residues by Brutons tyrosine kinase (Btk)^{123,124}. Mutations at these residues decrease its ability to activate p38 phosphorylation, I κ B α degradation and transactivation by the NF κ B subunit p65, but enhance its ability to bind TLR4 leading to a dominant negative effect over wild type Mal (certain phosphorylation sites). The cycle of Mal in TLR4 signalling is shown in Figure 1-5.

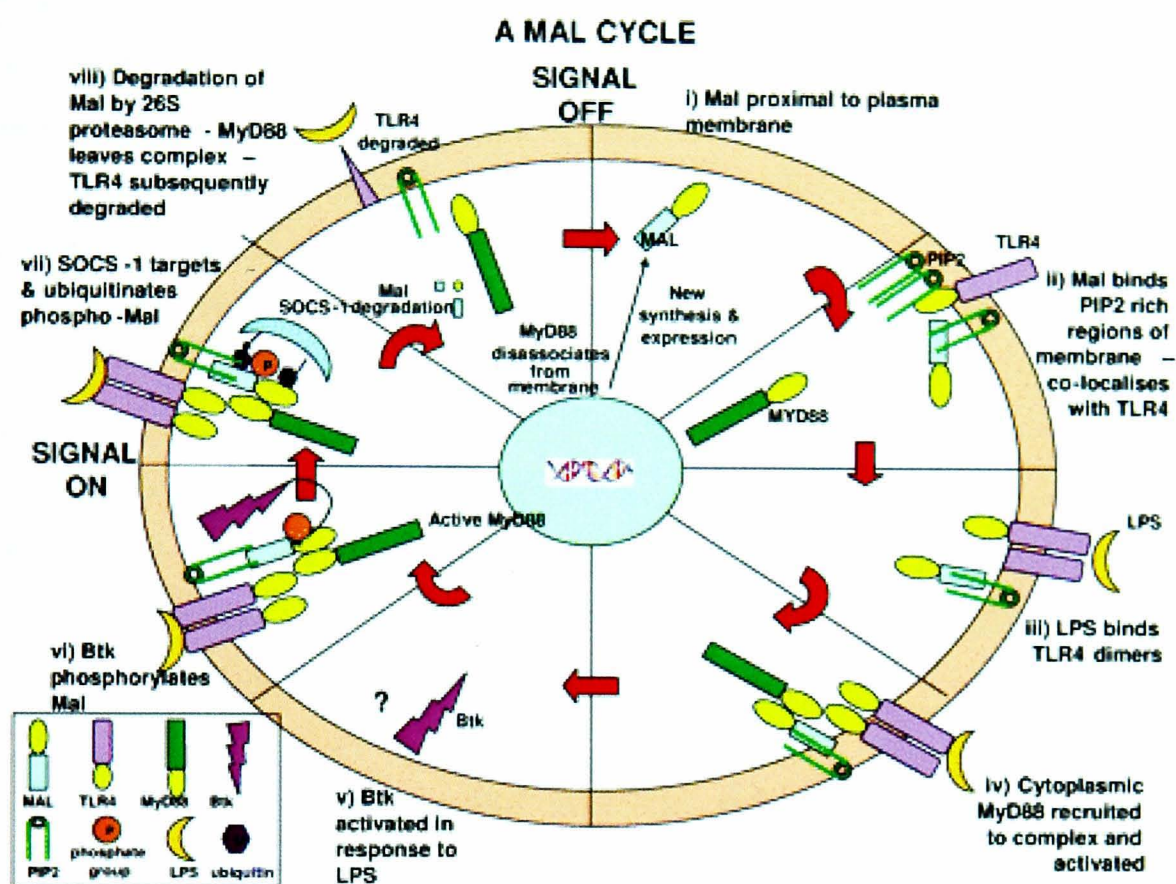


Figure 1-5: The cycle of Mal in TLR4 signalling

The TIR adaptor Mal undergoes and cycle of synthesis and degradation during signalling via TLR4 to allow regulation of signalling. Figure adapted from Sheedey *et al.* 2007¹²⁰

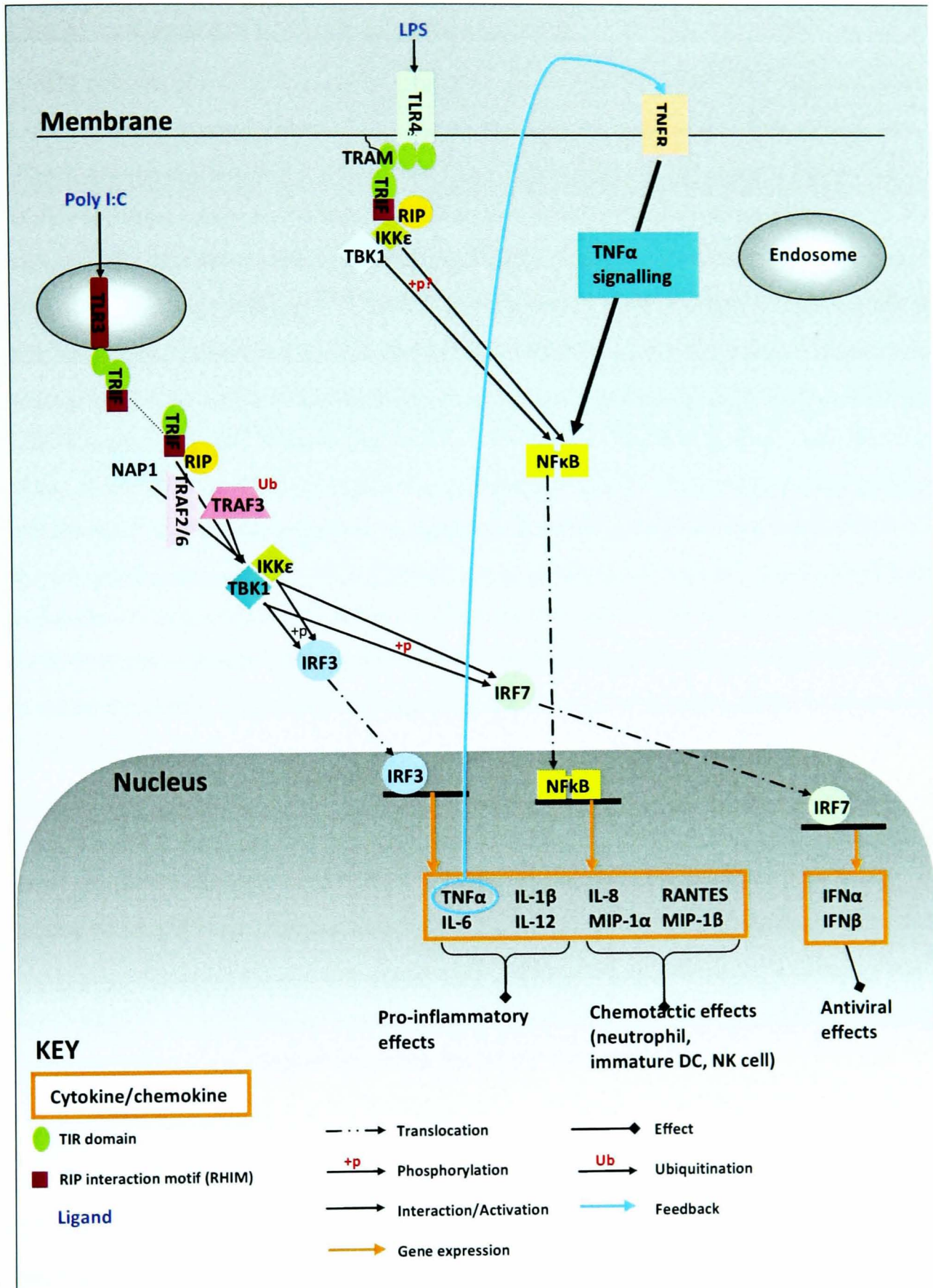
1.2.3.3. TRIF and MyD88-independent signalling

TRIF is currently the only adaptor thought to be involved in signalling from TLR3 in response to dsRNA. It also participates in TLR4 signalling but is coupled to TLR4 via the bridging adaptor TRAM (Section 1.2.3.4) in the so-called MyD88-independent pathway¹²⁵. It was noted that MyD88-deficient cells retained the ability to activate NF κ B and MAPKs in response to LPS, suggesting the presence of this TRIF-mediated MyD88-independent arm of TLR4 signalling⁸². TRIF consists of a proline-rich N-terminal region, a TIR domain and a C-terminal region containing a RIP homotypic-interacting motif (RHIM) domain (Figure 1-2). Its TIR domain is essential for binding to the TIR domain of TLR3 as well as to TRAM^{126,127}. TRIF activates transcription factors IRF3, IRF7, NF κ B and AP-1^{125,128}, and is the only adaptor known to be directly involved in the induction of apoptosis. Specifically, its C-terminal region is involved in NF κ B activation and the induction of apoptosis via binding of RIP1 to the RHIM domain^{129,130}. TRIF-deficient mice are defective in IRF3 activation, production of IFN- β downstream of TLR3 and -4, and LPS-induced inflammatory cytokine production¹²⁵.

The precise details of signalling downstream of TRIF, either alone or in collaboration with TRAM, have not been entirely elucidated, but it seems that homo-oligomerisation of TRIF is necessary for signalling which can be mediated by both its TIR and C-terminal domains (excluding RHIM)¹³¹. For signalling to IRF3 it is now thought that full activation of TRIF requires oligomerisation as well as binding of RIP1 binding to the RHIM¹³¹ even though this had previously been shown to be dispensable for IRF3 activation^{129,130,132}. For TRIF-dependent signalling to IRF3 and IRF7 downstream of TLR3 it is known that TRIF localises diffusely in the cytosol of resting cells but once TLR3 is activated, it transiently co-localises with TLR3, then dissociates from the receptor and forms structures with RIP1 and NAP1 (NAK-associated protein 1)¹³³. Oligomerisation of TRIF also seems to result in the recruitment of TRAF3, but TRAF3 does not bind to TRIF directly but potentially via TRAF2/6¹³¹. The association of TRIF with RIP1 and TRAF3 is necessary but not sufficient for signalling¹³¹. In turn, ubiquitinated TRAF3, along with NAP1, is likely to mediate recruitment of TBK1 and IKK ϵ to TRIF at its N-terminal region¹³⁴⁻¹³⁶. This N-terminal region, including the RHIM, is necessary for the recruitment of NAP1 and TBK1 and is therefore crucial for IRF activation via the recruitment of these IRF3-activating

kinases^{128,137,137-140}. The activation of TBK1 and IKK ϵ results in the phosphorylation of IRF3 and IRF7 inducing a conformational change that reveals the IRF association domain, involved in dimerisation, and the DNA binding domain. The activated IRFs translocate to the nucleus and bind to IRF motifs in relevant promoters. The downstream mechanism by which TRIF ultimately activates IRF3 may differ between TLR3 and TLR4 pathways since dsRNA induces phosphorylation of S396 in IRF3 whereas LPS stimulation does not¹⁴¹. However, both dsRNA and LPS induce phosphorylation of S386 which is considered more likely to be the crucial residue that undergoes inducible phosphorylation¹⁴².

With regards to TRIF-dependent NF κ B activation downstream of both TLR3 and TLR4, a role for TRAF6^{137,143} was ruled out, since NF κ B activation downstream of TLR3 was not affected in TRAF6-deficient mice and late NF κ B activation was still observed downstream of TLR4¹⁴⁴. However, NF κ B activation downstream of TLR3 is abolished in the absence of RIP1¹²⁹ and NF κ B activation from TLR4 is also abolished in cells deficient in both RIP1 and MyD88. These results suggest RIP1 is required for TRIF-dependent signalling to NF κ B downstream of both TLR3 and TLR4. Overexpression of both IKK ϵ and TBK1 is sufficient to activate NF κ B but this pathway is independent of the phosphorylation and degradation of I κ B α as occurs in the MyD88-dependent pathway, and is more related to the phosphorylation and increased transactivation of the NF κ B subunit p65^{145,146} although direct phosphorylation of p65 by IKK ϵ and TBK1 has yet to be demonstrated, unlike their direct phosphorylation of IRF3 and IRF7^{139,140}. There are contrasting reports as to whether the TRIF pathway is able to activate NF κ B directly¹⁴⁷⁻¹⁴⁹. It has been shown that the TRIF/TRAM pathway from TLR4 is involved in a later activation of NF κ B compared to the MyD88/Mal pathway and postulated that this is due to the production of TNF α via activation of IRF3, with TNF α subsequently acting in an autocrine manner to induce activation of NF κ B¹⁵⁰. Given that RIP1 is also critically involved in TNFR-mediated NF κ B activation it is possible that the defects in TRIF-dependent NF κ B activation observed in cells from RIP1-deficient mice are due to defective TNF signalling in these cells. TRIF signalling downstream of TLR3 and TLR4 is shown in Figure 1-6.



1.2.3.4. Regulation of TRIF signalling by SARM

SARM was the fifth TIR domain containing adaptor to be identified¹⁵¹ and appears to have a role in the down-regulation of TRIF-dependent signals. Along with a TIR domain, this protein also contains sterile α (SAM) and HEAT/artmadillo (ARM) motifs (Figure 1-2). Unlike the other adaptors, SARM does not induce NF κ B activation when over-expressed¹⁵². It is also unable to activate IRF3 and it down-regulates the TRIF-, but not MyD88-, dependent pathway^{152,153}. SARM interacts with TRIF through its TIR domain and this interaction is enhanced by LPS or dsRNA stimulation¹⁵³. SARM was also shown to be up-regulated after LPS stimulation at the protein but not mRNA level. Both the SAM and TIR domains of SARM are necessary for its inhibition of the TRIF pathway, and deletion of the N-terminus of SARM prevents its up-regulation after LPS stimulation suggesting an involvement in post-transcriptional regulation of SARM. It is not known whether the ligand-induced enhancement of the SARM-TRIF interaction is a result of increased SARM expression or conformational changes in the SARM protein. It has been suggested that SARM acts to sequester TRIF and prevent its interaction with downstream effectors¹²⁰ or that SARM interacts with TRIF via their TIR domains and recruits an, as yet unidentified, inhibitory protein¹⁵³.

SARM has also been shown to interact with MyD88 and TRAM in a recent yeast 2-hybrid study via its TIR domain⁸¹ and SARM may also have a role in the induction of stress-related cell death since neurons from SARM-deficient mice were more resistant to apoptosis induced by oxygen and glucose deprivation than neurons from wild-type mice¹⁵⁴. Since TRIF is the only adaptor considered capable of directly inducing apoptosis this may confirm SARM's involvement as a regulator of the TRIF pathway.

1.2.3.5. TRAM

TRAM is the smallest TIR adaptor at only 235 amino acids in length. It acts as a bridging adaptor between TLR4 and TRIF in the MyD88-independent pathway in response to LPS¹²⁷ leading to the activation of IRF3 and NF κ B. TLR4-, but not TLR3-mediated, TRIF-dependent IFN β production and activation of signalling cascades are abolished in TRAM-deficient cells¹⁵⁵. Furthermore, TRAM-deficient mice show defects in cytokine production,

splenocyte proliferation and up-regulation of surface molecules in response to ligands for TLR4, but not other TLRs.¹⁵⁵ As for Mal, sub-cellular localisation or surface charge complementarity may explain why TRIF should require a bridging adaptor for TLR4 signalling, while it signals alone during TLR3 activation.

Myristoylation of TRAM is required to localise it to the plasma membrane¹⁵⁶ and endosomal compartment¹²¹. The myristate group facilitates membrane binding by insertion into the hydrophobic interior of the lipid bilayer and a polybasic domain following the myristoylation site is also required for its plasma membrane localisation¹²¹. TRAM is also phosphorylated by protein kinase C ϵ (PKC ϵ) and this is required for TLR4 to signal¹⁵⁷. TLR3-dependent responses are not impaired in PKC ϵ -deficient cells, suggesting that PKC ϵ acts upstream of TRIF only in TLR4 signalling. The phosphorylation of TRAM is followed by its apparent dissociation from the plasma membrane and some have speculated that this may signify its degradation, as for Mal. The consequence of this dissociation has yet to be elucidated although it is possible that dissociation from the membrane allows TRAM to interact with and activate other down-stream molecules such as TBK-1 which would lead to IRF3 activation. Alternatively phosphorylation of TRAM may signal its depletion from the membrane perhaps as a regulatory event. The cycle of TRAM during TLR4 signalling is shown in Figure 1-7.

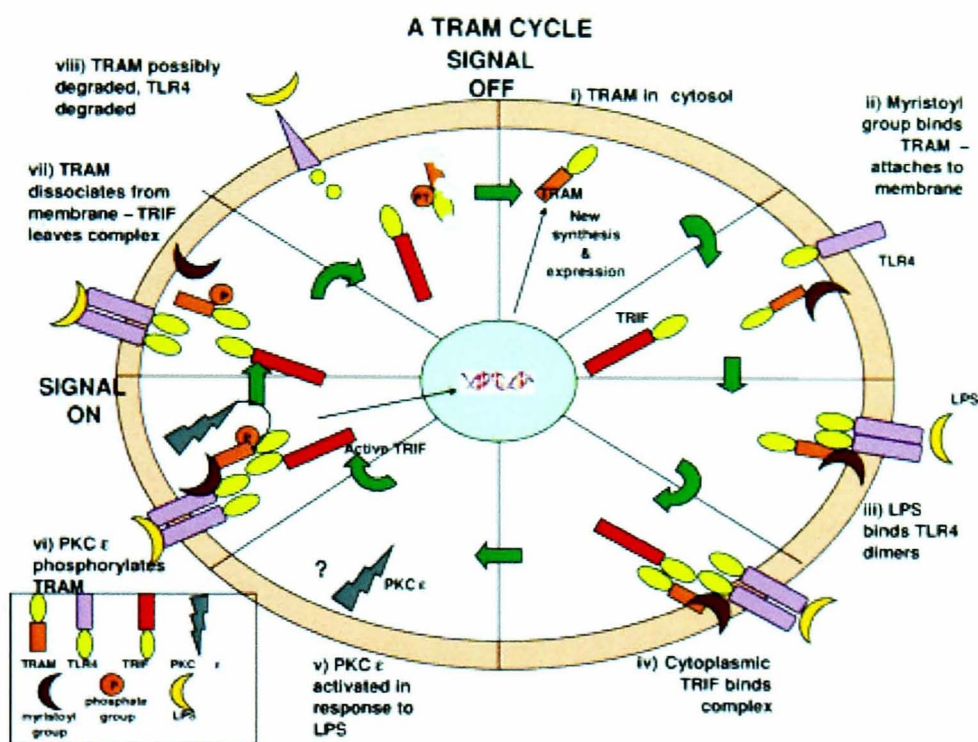


Figure 1-7: The cycle of TRAM in TLR4 signalling

The TIR adaptor TRAM cycles around the cell during TLR4 signalling, possibly undergoing degradation and resynthesis to allow regulation of signalling. Figure adapted from Sheedey *et al.* 2007¹²⁰

1.3. The TIR domain

Due to its role in the IL-1/TLR pathways and the fact that differential adaptor recruitment and ligand-dependent changes in signalling are mediated at least in part by the TIR domain, its sequence and structural features are being intensively studied. The TIR domain is approximately 160 amino acid residues in length and has been defined by three conserved regions of amino acid sequence denoted boxes 1, 2 and 3¹⁵⁸ (Figure 1-8). Mutagenesis studies on the IL-1R TIR domain showed that box 1 and box 2 were essential for signalling, while box 3 was thought to be important but its role was less clear cut¹⁵⁹⁻¹⁶¹. Structurally, the TIR domain consists of a five-stranded parallel β -sheet (β A-E) surrounded by five helices (α A- α E). The loops between these secondary structures have been named according to their connections such as the DD loop which links strand β D and helix α D¹⁶². A multiple alignment of eukaryotic TIR domains is shown in Figure 1-8. Sequence conservation between TIR domains is generally quite low (20-30%), suggesting that there are significant structural differences between TIR domains which would contribute to specificity in signal transduction¹⁶². For example, the crystal structure of IL-1RAPL shows the same overall fold as in TLR1, TLR2 and TLR10 but differs largely in particular features¹⁶³. Crystal structures of TIR domains have been difficult to obtain¹⁶⁴ and so a large body of mutagenesis and modelling data has also been amassed. It is worth noting at the outset, however, that the methods used to obtain information on specific TIR domain residues all have limitations. In structural studies, information on conformationally flexible regions can often be poor, apart from the information that they are flexible. The structural interpretation of mutagenesis data is often complicated by the fact that it is not known which specific interactions are affected by the mutations and inactivating mutants are not analysed for misfolding defects. In other studies where groups of residues have been mutated together there are also likely to be significant structural perturbations. Modelling studies obviously suffer from the fact that they are generally built around existing structures and may therefore have bias and rely on the sophistication of computer algorithms which may be limited. It is therefore important to use mutagenesis and modelling data in close collaboration with structural and functional data.

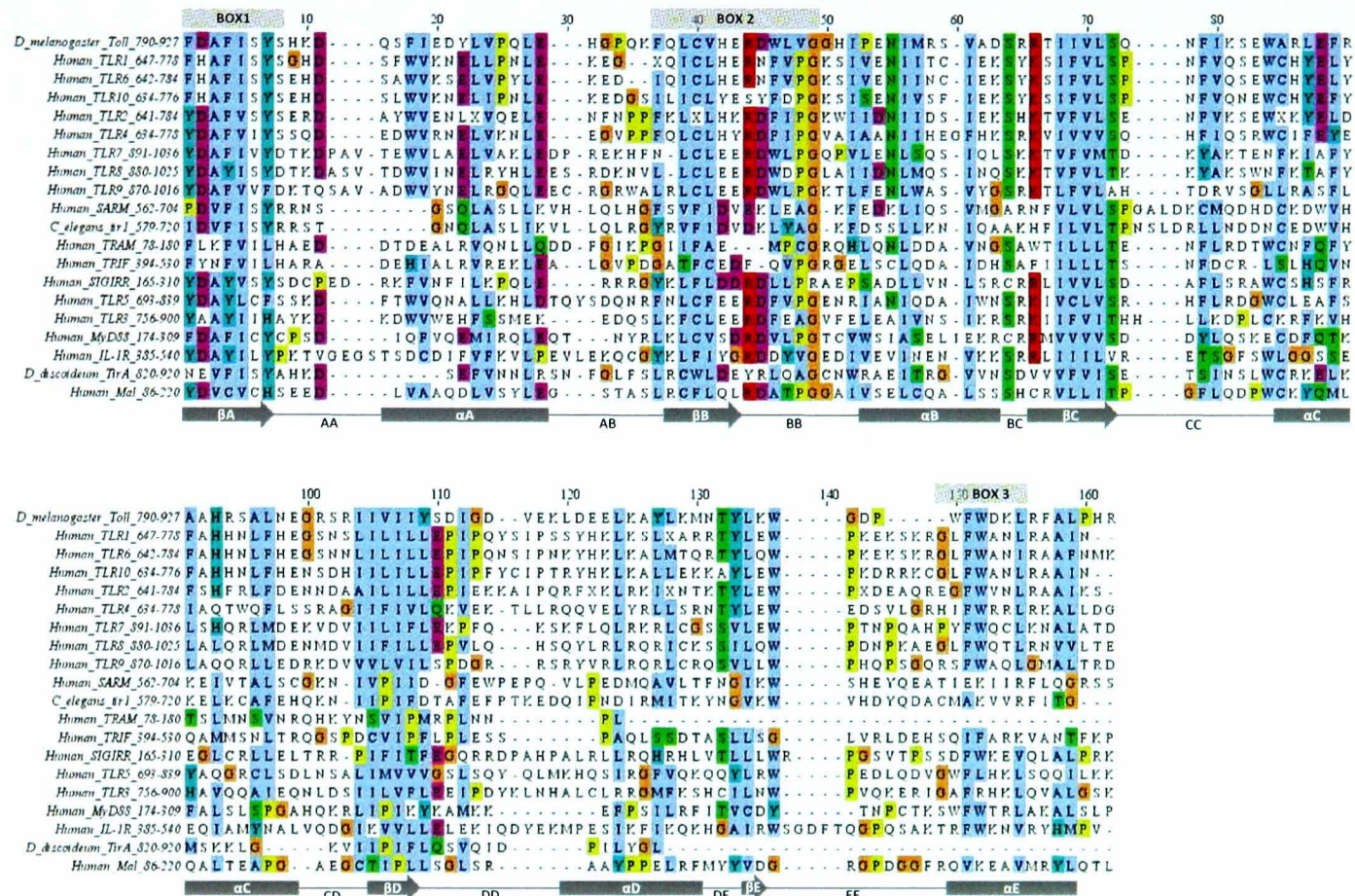


Figure 1-8: Multiple sequence alignment of eukaryotic TIR domains

Multiple sequence alignment carried out using the ClustalW2 algorithm on the EBI web server (<http://www.ebi.ac.uk/tools/clustalw2>)¹⁶⁵ and coloured according to the Clustal X colourscheme using Jalview (Section 2.1.7). TIR domain sequences taken from *Homo sapiens*, *Caenorhabditis elegans*, *Dictyostelium discoideum* and *Drosophila melanogaster*. The grey boxes correspond to areas of α -helix and the grey arrows correspond to areas of β -sheet. The lines connecting these structures correspond to the loop regions of sequence. Secondary structure predicted using 3D Jury web server¹⁶⁶ and published crystal structures^{162,163,167,168}

To date, five crystal structures of TIR domains have been solved including those of TLR1 and TLR2¹⁶², and IL-1RAPL¹⁶³ in 2000 and 2004 respectively. More recently, the crystal structure of the TIR domain from the only orphan receptor, TLR10¹⁶⁷ has been elucidated. The first structure of a bacterial TIR domain (PdTIR from *Paracoccus denitrificans*) was also solved in 2009¹⁶⁸. No TIR adaptor proteins have been crystallised, but the solution NMR structure of MyD88 has been solved¹⁶⁹.

With regards to information on the interactions that TIR domains make, the TLR10 and PdTIR structures show a physiologically relevant dimer. In comparison, the TLR2 C713S structure shows a dimer but it is considered unlikely that TLR2 is functional as a homodimer and how accurately it reflects a TLR1/2 or TLR2/6 heterodimer remains to be seen^{170,171}. In other studies TIR domain dimer structures have been proposed and correlated to mutagenesis data^{167,172}. In addition to these x-ray crystallographic studies, a number of computer-generated models of TIR domain structures and interactions have been produced¹⁷³⁻¹⁷⁵. From these studies it is clear that the loop regions of the TIR domain are the most variable in sequence and structure, often containing large insertions or deletions. Mutational analysis, combined with structural data, has highlighted areas of sequence of particular importance for receptor/adaptor function, particularly within these loop regions^{89,117,162,170,176-178}. The BB and DD loops are particularly important areas of sequence in this respect.

1.3.1. The BB loop

Most structural, mutagenesis and modelling studies conclude that the BB loop is essential for TLR signal transduction and, in the receptors, it has been suggested to be the site of adaptor recruitment⁵¹. This is supported by the fact that peptides and peptidomimetics modelled from the BB loops of MyD88 and other adaptor TIR domains have been shown to inhibit TLR¹⁷⁸⁻¹⁸¹ and IL-1R signalling¹⁸²⁻¹⁸⁴. The BB loop comprises part of box 2 (Figure 1-8). TIR domain structures from TLRs indicate that the BB loop forms an exposed protrusion from the TIR domain giving rise to an extended patch of well-preserved residues which are likely to be the site of adaptor recruitment to the receptors. These structures also indicate that it is likely to participate in the receptor dimer interface and central core of the TIR domain structure. Adaptor dimerisation is also likely to involve the BB loop since peptides derived from the BB loop prevent dimer formation¹⁸³⁻¹⁸⁵ and affect signalling¹⁸².

Interestingly, the BB loop of PdTIR does not appear to be involved in dimer interface interactions but instead is totally exposed. Of the structures solved, the PdTIR structure is most closely related to TLR1 and TLR10. However, the BB loop is the region with the highest sequence divergence between PdTIR and the other known TIR domains¹⁶⁷.

Most residues within the BB loop have been shown to be important for TIR-TIR interaction or signalling in mutagenesis, modelling or structural studies. Indeed, mutations at almost every position in the BB loop of TLR4 or dToll leads to significantly reduced signalling activity of the receptors^{162,176,186}. The BB loop also contains some of the most highly conserved residues within the TIR domain. In particular, a proline (Pro) residue within the BB loop, conserved in all TLRs except TLR3 (and dToll), and in all adaptors except SARM and TRAM, has commanded much attention. Mutation of only this residue within TLR4 renders it unresponsive to LPS, as demonstrated usefully by CH3/HeJ mice which carry this mutation¹⁹. However, whilst mutation of this residue in TLR2^{162,170}, TLR4¹⁸⁷ and TLR10¹⁸⁸ render them unable to signal, in TLR4 this proline residue is not required for binding to MyD88^{189,190} or Mal¹¹⁷. Nor did the equivalent mutations in MyD88 or Mal prevent their binding to TLR4 or their hetero- or homo-dimerisation¹¹⁷. However, the same mutation within TLR10 does affect its interaction with MyD88 as well as its signalling capacity. Somewhat surprisingly, the crystal structure of the TIR domain of the TLR2 P681H mutant did not show any significant structural changes caused by the mutation¹⁷⁰. Other highly conserved residues include the phenylalanine (Phe) at 679 in TLR2 which is conserved as a Phe or tryptophan (Trp) in all TLRs, and the isoleucine (Ile) at position 678 in TLR4 which is conserved as an aliphatic residue (Ile, leucine (Leu) or valine (Val)) in all TLRs except TLR3 (Glutamine - Glu) and TLR5 (Arginine - Arg). Modelling and crystallographic studies show the BB loop as being conformationally flexible so it is reasonable to suppose that it may undergo conformational changes upon ligand binding (as in the ligand binding model discussed in Section 1.2.1.1) or may adopt different conformations in different TIR domains^{170,176}. Interactions of TIR domains are likely to be executed in different modes for different receptors and adaptors but the high conservation of residues within the BB loop and the common use of MyD88 as an adaptor also imply the existence of common features in TIR domain signalling interactions.

1.3.2. The DD loop

The DD loop is also considered important for signalling and TIR interactions. Mutations of Arg748, Phe749 and Leu752 in TLR2 have significant effects on TLR2-TLR1 signalling, whereas most other mutations within the DD loop have little or no effect¹⁷⁶. The corresponding Arg residue in TLR10 is involved in the dimer interface but the other residues are not. The DD loop is mainly disordered in the TLR10 structure and other studies agree that it may be conformationally flexible and may undergo conformational changes upon ligand binding or may adopt different conformations in different TIR domains as for the BB loop. In the PdTIR structure the dimer interface is mediated, not by residues of the BB loop as for other TIRs, but by residues within the DD and EE loops¹⁶⁷.

1.3.3. Other loops

Molecular modelling studies with MyD88 and the TLR4 TIR domain have predicted interactions through the DD loops, AA loops and CD loops of the TLR4 TIR domain^{117,119}. The CD loop is located on the surface of the TIR domain, opposite to the BB loop where it is thought Mal binds to TLR4. In a molecular model of Mal's association with the TLR4 TIR domain it was predicted to interact through its DE loop as well as its DD loop¹¹⁹.

1.3.4. α helices and β sheets

The TLR10 structure indicates that residues from the α C helices as well as the BB loops (from each monomer) may be involved in dimer interaction. In the TLR2 structure the asymmetric dimer interface also involves interactions of the BB loop (and the α B helix) with the α C helix (and DD loop) of the contacting monomer. TLR2 may not form homodimers *in vivo* but it is possible that the asymmetric dimer of TLR2 observed in the structural studies would reflect the natural heterodimeric TLR2/TR1 or TLR2/TLR6 complexes, with the DD loop and α C helix of TLR2 contacting the BB loop and α B helix of TLR1 or TLR6^{170,176}. During a large scale mutational study of the TLR4 TIR domain mutations in the α B helix (as well as BB loop) abolished signalling activity¹⁸⁶. For TLR1, a disulfide-linked symmetric dimer was seen with the α C helix and BB loops as the central component, as in the TLR10 structure. Mutagenesis studies suggest that the cysteine (Cys) and Phe residues of the α C helices of TLR2 and TLR4 are important for receptor function^{170,172}.

The IL-1RAPL structure revealed large structural differences between its TIR domain and those of TLR1 and TLR2 particularly with respect to the helices since helix α D was found to be almost perpendicular to its position in the TLR1 and TLR2 structures. This may be important since helix α D has been said to make a significant contribution to the binding of Mal and MyD88¹¹⁹. The TIR domain of IL-1RAPL was found to be dimeric in the crystal but monomeric in solution and residues at the dimer interface were mostly unique to IL-1RAPL which likely reflects its distinct functional roles.

1.3.5. Receptor-adaptor interactions

A number of modelling studies have attempted to assess adaptor binding to TLR2 and TLR4. In one study Mal and MyD88 were predicted to bind to different regions of the TLR4 TIR domain but at the same point on TLR2^{119,178}. Monomeric receptors were used for this analysis, however, and it is now widely accepted that the receptors signal as dimers or higher oligomers⁵¹. Another study showed that MyD88 did not contact TLR4 at the TIR domain at all and would therefore be solely recruited by Mal¹⁶⁹. With regards to Mal and TRAM binding TLR4, these molecules have been modelled using the TLR1, TLR2 and TLR10 structures as templates and docking programs used to assess their interactions. Mal and TRAM were found to bind to the same region on TLR4 at the dimer interface of the receptor TIR domains¹⁷². This model did not determine whether a single activated receptor dimer can stimulate both the Mal and TRAM pathways at the same time, or whether their interactions are mutually exclusive. Mal was postulated to bind with a higher affinity to TLR4 than TRAM which may account for why Mal is the more highly regulated adaptor molecule. It is considered likely that Mal contacts MyD88 through residues that are exposed after its EE loop and α E are removed by caspase-1 cleavage. Modelling studies have predicted that the electrostatic surfaces of TIR domains are quite distinct suggesting that electrostatic complementarity may play a role in TIR-TIR binding, as is suggested by the need for Mal to bridge the interaction between MyD88 and TLR2 or TLR4. In TLR4 signalling Mal (and TRAM) are thought to contact the receptor via their BB loops, but this may not be the case for the way that they contact TLR2¹⁷⁸.

Less is known about TRIF/TRAM interactions with each other or with TLRs, but blocking peptides corresponding to their BB loops disrupt activation-signalling pathways

downstream of TLR4, although the molecular basis for this has not been determined¹⁷⁸. The TLR3 TIR domain has not been assessed in structural or modelling studies.

It is clear that there's a great deal of variation in the way two TIR domains can interact. TLR2 is believed to differentially engage with MyD88 depending on ligand¹⁷⁷ suggesting that ligand binding does lead to conformational change in TIR domain structure, or conformation is dependent on whether it partners TLR1 or TLR6. The TIR domain is certainly a versatile interaction domain.

1.4. The pivotal role of TLR/IL-1R signalling in innate immunity

The effector molecules produced as a result of TLR signalling have wide-ranging and far-reaching effects on the immune response mounted to an invading microbe and activation of TLRs results in different effector responses depending on the cell type involved. The production of cytokines and chemokines downstream of TLR signalling modulates the inflammatory status of the host which in turn directly affects a wide variety of processes such as immune cell recruitment. TLR signalling is also known to participate in phagocytosis, the production of matrix metalloproteinases, iron sequestration and anti-microbial peptide production¹⁹¹⁻¹⁹⁴ and to be necessary for actin polymerisation, angiogenesis and apoptosis¹⁹⁵⁻¹⁹⁸. TLRs are involved in tissue repair following injury in addition to their broad involvement in host innate defence. Differential TLR ligation is also known to drive the development of an appropriate adaptive immune response¹⁹⁹. These downstream effects are highly co-ordinated by TLRs, as is demonstrated by their involvement in every stage of a process such as the cell activation, migration and apoptosis of neutrophils and macrophages. A variety of roles for TLRs in both the innate and adaptive immune responses are discussed below.

1.4.1. Activation of transcription factors

Effector molecules are produced as a consequence of the activation of transcription factors downstream of the TLR pathways, most notably, NFκB, the IRFs and AP-1. NFκB has been referred to as a “global regulator of gene expression” and the number of target genes for NFκB is now in its hundreds. A full list of these can be found at www.nf-kb.org. Every TLR tested so far signals to NFκB. The NFκB family of transcription factors is evolutionarily conserved and in mammals is made up of five family members so far

identified: RelB, c-Rel, p65 (RelA), p100/p53 and p105/p50²⁰⁰. Mice lacking individual NFκB subunits are very susceptible to microbial infections²⁰¹⁻²⁰³. Some specificity in the TLR response is generated by regulation of these different NFκB subunits, including their phosphorylation at a variety of sites²⁰⁴⁻²⁰⁷. The target genes for NFκB include a large number of immunomodulatory factors such as cytokines and chemokines. The AP-1 family of transcription factors consists of homo- and hetero-dimers of the Jun and Fos family²⁰⁸. The activity of AP-1 is upregulated through phosphorylation by the MAP kinases JNK and ERK²⁰⁹. AP-1 upregulates transcription of genes containing the TPA DNA response element (TRE; 5'-TGAG/CTCA-3') which principally includes genes that express proteins involved in cell cycle regulation and cell survival or apoptosis. AP-1 also controls the expression of proteins involved in the proliferation and differentiation of cells such as lymphoid cells²¹⁰.

The IRF family of transcription factors is made up of IRFs 1-9 and all are critical regulators of innate immune responses²¹¹. IRF1 binds to MyD88 after TLR activation, causing it to translocate to the nucleus where it induces a specific gene subset including IFNβ, iNOS and IL-12p35 although its response may be cell-type specific²¹². IRF3 is activated during the TRIF-dependent pathway downstream of TLR3 and TLR4. IRF5 has an important role in the induction of pro-inflammatory cytokines and interacts with, and is activated by, MyD88 and TRAF6, causing its nuclear translocation where it binds to the interferon-responsive stimulated element (IRSE) motifs in the promoters of genes for pro-inflammatory cytokines such as IL-6, IL-12 and TNFα²¹³. IRF5 is phosphorylated by TBK-1 and IKK-ε but this phosphorylation does not lead to IRF-5 nuclear translocation²¹⁴. IRF7 is a key transcription factor for the induction of type I IFNs and it is activated by both MyD88- and TRIF-dependent pathways^{93,215,216}. Upon stimulation of TLRs (particularly 3, 7, 8 and 9) IRF7 is recruited to a complex containing MyD88, TRAF6, IRAK4 and IRAK1 and the ubiquitin ligase activity of TRAF6 and phosphorylation by IRAK1 are required for its activation^{93,142,217}. Finally IRF8 has also been implicated in the potentiation of NFκB activity downstream of TLR9 signalling in DCs²¹⁸.

1.4.2. Production of immune effector molecules

The release of cytokines and chemokines is the hallmark of the cellular response to the activation of the innate immune system. The term cytokine encompasses a vast array of

protein regulators and, in fact, chemokines are simply cytokines with the ability to induce directed chemotaxis of responsive cells. Activation of IL-1/TLR pathways also induces the production of proteins within the pathway, or pathway inhibitors, to allow feedback and regulation of the pathway. For example, IL-1/TLR signalling induces the degradation of I κ B α to release NF κ B from the cytoplasm, but also induces the transcription of I κ B α feeding back to NF κ B sequestration in the cytoplasm²¹⁹.

1.4.2.1. Chemokines and cell migration

There are two types of cell migration associated with cells of the innate and adaptive immune systems. Homeostatic migration occurs continuously and allows naïve lymphocytes to circulate throughout the body to increase their chance of encountering antigen. No TLR activation is required for this migration to occur. Inducible migration is generally triggered after PRR activation of resident innate tissue cells which encourage further immune cells to the site of infection to augment the killing of invading pathogens thus reducing their spread and likelihood of niche colonisation. This induced migration occurs by a controlled sequence of events and TLR signalling is involved throughout. TLR signalling produces chemotactic factors which attract immune cells to the site of infection or damage. TLR signalling also leads to the upregulation of selectins on endothelial cells and carbohydrate ligands on leukocytes which allow leukocytes to roll along the endothelial surface. Next, chemokines secreted downstream of TLR signalling such as IL-8, growth-related oncogene- α (GRO- α), monocyte chemoattractant proteins (MCP1-4), macrophage inflammatory protein 1 α and β (MIP-1 α/β) and RANTES bind to the luminal surface of the vascular endothelium and activate the rolling leukocytes. This allows firm adhesion of the leukocytes to the vascular endothelium and the consequent migration of leukocytes between the endothelial cells and into tissue interstitium²²⁰

1.4.2.2. Cytokines

TLR signalling induces the production of a vast array of cytokines. Different TLR agonists tend to produce a distinct set of cytokines, despite their stimulation of common pathways, with additional levels of specificity dependent on cell type and cross-talk with other signalling pathways. Due to the presence of different ligands gram-positive and gram-negative bacteria induce different cytokines^{221,222}. TLR7 and TLR9 agonists produce high

levels of type I IFN (prototypically IFN α and IFN β). Of the IFN families it is type I IFNs that are mainly produced via the TLR pathways with TLRs 3, 4, 7, 8 and 9 all able to induce type I IFNs via the IRF transcription factors. TLRs are also able to induce IFN γ production, with TLR8 agonists inducing the highest levels compared to the other TLRs²²³. The IFNs were discovered due to their ability to protect cells from viral infection, but it is now known that they induce production of a wide variety of proteins with various, often cell type-specific, roles including pro- and anti-apoptotic proteins as well as those involved in the proliferation of memory T cells, B cell isotype switching and differentiation, NK cell activation and DC maturation^{224,225}. IL-6 and TNF α are widely produced downstream of TLR signalling, particularly by the TLRs that recognise bacterial products²²⁶. IL-6 is a pleiotropic cytokine with diverse biological functions. With regards to a response to an invading micro-organism it stimulates B-cell differentiation and antibody production but has other functions unrelated to pathogens including the regulation of bone metabolism, for example²²⁷. IL-6 is often considered as an inflammatory cytokine, however many of its activities are associated with the negative control of inflammation mainly due to its induction of protective acute phase proteins from the liver which have anti-protease and scavenger activities. TNF α is a pro-inflammatory cytokine which is cytotoxic to a variety of tumour cells and is an essential factor in mediating the response to bacterial infection. Its pro-inflammatory nature also means it plays a role in the induction of septic shock, autoimmune diseases, rheumatoid arthritis, inflammation and diabetes²²⁸.

1.4.3. TLRs and DCs

Signals for the activation of adaptive immunity via T cell activation and differentiation into their subsets, T helper types 1 or 2 (T_H1 or T_H2) or cytotoxic T lymphocytes (CTLs) are mainly provided by DCs which are activated by microbial components to undergo maturation²²⁹. DCs therefore express a broad selection of TLRs through which maturation is induced²³⁰⁻²³⁴. Immature DCs are phagocytes that circulate in the lymphoid system and engulf antigens, a process which is induced by PRR recognition of microbial structures and induces DCs to produce inflammatory cytokines such as IL-12²³⁵. This process also induces their maturation whereby they lose their capacity for endocytosis and migrate to the draining lymph nodes. Here they present two signals for naïve T cells which are required for T cell activation: an antigen-specific signal, received when the T cell receptor (TCR) binds to an antigenic peptide displayed by the DCs on the appropriate MHC (major

histocompatibility complex) molecule, and a co-stimulatory signal provided by molecules such as CD80 and CD86. The expression of co-stimulatory molecules on DCs is also induced by TLR-mediated recognition of microbial components. The T cells then mature to elicit an antigen-specific adaptive immune response^{229,236}.

The migration of DCs to the site of naïve T cells is also mediated by TLR signals that lead to the down-regulation of inflammatory chemokine receptors on DCs and the upregulation of receptors for lymphoid chemokines²³⁷⁻²³⁹. A particular DC population responds to pathogens recognised via its TLRs and different DC populations may generate distinct immunological outcomes, such as differential cytokine production, even when induced by the same ligand^{56,240}.

1.4.4. TLRs in B cell activation and antibody production

B lymphocytes are somewhat unusual since they express both clonally rearranged antigen receptors and nonclonal PRRs, most notably TLRs. LPS is the most characterised ligand that is able to directly activate B cells. The stimulation of TLRs expressed on B cells can lead to polyclonal activation and production of low-affinity IgM antibodies. For follicular B cells, TLR4 signalling is essential for LPS-induced activation that leads to cell division and isotype switching²⁴¹ via the activation of NFκB p50 homodimers or p50/c-Rel heterodimers, which is in contrast to the predominant p50/p65 dimers activated in most other cells²⁴². ERK is also transiently activated in these cells²⁴³. This activation of TLR4 signalling causes B cells to exit quiescence and enter the G1 phase, and subsequently S phase, of the cell cycle. Without TLR4 signals B cells fail to successfully traverse into S phase²⁴⁴. In addition to controlling cell cycle progression, TLR4 signals to the NFκB subunits c-Rel and NFκB1 to control cell survival^{245,246} potentially via the production of the apoptosis regulators A1, Bcl-xL and Bim^{242,247,248}.

1.4.5. TLRs and T cells

Through their role in DC antigen capture, differentiation and migration (Section 1.4.3), TLRs inform the T helper response, although their bias is a matter of contradiction in the literature. TLR4 and TLR9 have been reported to be most associated with T_H1 responses (through the production of IL-12 by DCs)²⁴⁹⁻²⁵¹, while TLR2 and TLR5 may be associated with the instigation of T_H2 responses^{249,252,253}. However, pathogens that usually activate

TLR2, such as gram-positive bacteria, do not usually induce T_H2 responses *in vivo*²⁵⁴ and other studies of TLR2 signalling point towards a T_H1 bias^{230,233,255}. On the other hand, LPS from *Escherichia coli* and *Porphyromonas gingivalis* have been shown to induce T_H1-type and T_H2-type responses respectively *in vivo*²⁵⁶. It has also been proposed that TLRs initiate responses involving T_H1 cells, whereas an entirely different class of receptors, so far elusive, initiates T_H2 responses²⁵⁷. The role of MyD88 in T cell stimulation is also unclear since it has been reported that the adaptive response to LPS or *Mycobacterium tuberculosis* is intact in MyD88^{-/-} mice whereas others report a central role for MyD88 in directing T_H cell responses²⁵⁸⁻²⁶³.

As well as directing T helper cells, TLR signals also direct DC-mediated antigen cross-presentation to CTLs and this is largely dependent on TLR3^{264,265}. TLR signals also modulate peripheral T cell tolerance and regulation controlled by regulatory T (T_{reg}) cells^{72,266-269}. These cells should be activated without interference in the induction of pathogen-specific immune responses and one mechanism that allows for this is a TLR-mediated block of T_{reg} suppression. This is mediated by IL-6 produced by DCs in response to TLR activation²⁶⁹. This TLR-dependent signal cannot be substituted by other modes of DC activation *in vivo* such as inflammatory cytokines²⁶⁷. IL-6 affects antigen-specific T cells and makes them refractory to suppression by T_{reg} cells²⁶⁹.

1.4.6. TLR signalling and direct anti-microbial activity

TLRs can mediate direct anti-microbial activity in a number of ways including via the production of nitric oxide intermediates and anti-microbial peptides. In *Drosophila* the anti-fungal response mediated by activation of the Toll pathway is due to the direct synthesis of anti-fungal peptides downstream of Toll signalling²⁷⁰. Anti-microbial peptides are also produced downstream of mammalian TLR signalling at epithelial surfaces which form the first line of defence between pathogen and host²⁷¹. One important class of mammalian anti-microbial peptides is the family of defensins. These have a broad spectrum of anti-microbial activity including activity against bacteria, fungi and some enveloped viruses²⁷². Defensins have both microbicidal and anti-inflammatory properties²⁷³ and reports indicate they may have other roles including as chemoattractants for cells of the adaptive immune response^{274,275}. Another important family of anti-microbial peptides is the cathelicidins, which include the well studied human peptide LL-37²⁷⁶. These peptides are found in the

lysosomes of polymorphonuclear leukocytes (PMNs) and have potent anti-microbial activity, and are regulated by vitamin D²⁷⁷.

TLR signalling also contributes to direct anti-microbial activity by inducing the production of reactive oxygen and nitrogen species (ROS and RNS, respectively) which are toxic to invading microbes (the most pathogenic of which have mechanisms of resistance). As well as being directly toxic, the production of ROS and RNS also control other process such as phagocytosis, apoptosis and the production of cytokines²⁷⁸. The overall antimicrobial activity of ROS and RNS has been demonstrated for a wide variety of bacteria, as well as parasites, fungi and viruses²⁷⁸. For example, TLR2 activation leads to NO-dependent killing of intracellular *M. tuberculosis* in murine macrophages²⁷⁹. Conflictingly, the successful control of *M. tuberculosis* in primary human macrophages has been shown to be NO-independent²⁷⁹. ROS generation was found to be upregulated in both neutrophils and monocytes in septic patients²⁸⁰. Many years of research have provided detailed information on the induction and generation of ROS and RNS but their mechanism and specificity of action, particularly *in vivo*, are less well understood. Principally their mechanism of action seems to stem from their ability to inactivate bacterial enzymes through oxidation or reduction reactions, to damage microbial DNA and inhibit membrane transport processes²⁸¹⁻²⁸³. Unfortunately toxic affects on the host also occur at the site of ROS and RNS generation but is often an acceptable and localised price to pay for microbial elimination^{284,285}.

1.4.7. Cell death

A variety of cell death mechanisms have now been described for multicellular organisms which impact the immune system in different ways. These are categorised as controlled and uncontrolled mechanisms of death. Necrosis is the process of uncontrolled cell death which is induced by overwhelming cell stress and is accompanied by a strong inflammatory response due to the release of the contents of dying cells which act as endogenous ligands for PRRs. Controlled cell death has evolved as an essential component of a multicellular lifestyle. It is necessary for cells to die at various stages of a multicellular organism's life as part of embryonic development and normal tissue turnover and controlled cell death ensures that this process is not accompanied by an over-whelming inflammatory response that could be associated with the contents of a dying cell (as occurs in necrosis). Apoptosis

is the most well-studied form of controlled cell death but two other mechanisms have been identified which possess certain characteristics of both apoptosis and necrosis, namely pyroptosis and autophagy. Pyroptosis is a form of programmed cell death that is dependent on caspase-1 and therefore inflammasome activation. Due to the requirement for NLR activation in the inflammasome, pyroptosis may be considered to be an infection-induced cell death. Autophagy is generally a protective process for a cell whereby it is able to engulf large portions of their own cytoplasm under starvation conditions, or remove damaged organelles²⁸⁶. Evidence also suggests it is important in controlling infections, however, by directing intracellular, or ingested, pathogens to lysosomes which results in their destruction. Evidence suggests that TLR signalling has a role to play in each of these cell death mechanisms^{130,287-289}, and that all may participate in the containment and elimination of invading pathogens. However, like so much of a host's immune defence, cell death can be both a defence mechanism and a process to be exploited by an invading pathogen. For example, the inhibition of signalling to NFκB mediated by YopJ from *Yersinia pestis* also induces macrophage cell death which is thought to facilitate the systemic spread of *Y. pestis*²⁹⁰ (Sections 1.6.2 and 1.6.2.1).

The role of TLR signalling in pyroptosis and autophagy is still being elucidated. Certainly for pyroptosis their involvement appears to be indirect, via the priming of macrophages²⁹¹. The role of TLR signalling in autophagy is more established. Both MyD88- and TRIF-dependent pathways appear to be involved. TLR activation induces the association of MyD88 and TRIF with Beclin-1, a key inducer of autophagosome formation. Beclin-1 then dissociates from the anti-apoptotic proteins Bcl-2 and Bcl-XL leading to autophagy²⁹². TLRs also have a role in a newly discovered autophagic mechanism²⁹³.

Apoptosis is also an important part in the elimination of invading microbes, particularly those that persist intracellularly. This is also true in plants where programmed cell death is used to contain a pathogen at the site of infection²⁹⁴. TLR signalling controls the survival of a cell by governing the induction of pro- and anti-apoptotic signalling molecules. The TRIF pathway (Section 1.2.3.3) is the only TLR pathway that can directly mediate apoptosis and control from the other TLR pathways arises from the expression of target genes with a role in apoptotic control. Activation of NFκB promotes cell survival by the induction of anti-apoptotic genes^{295,296}. The induction of apoptosis through TLR signalling (apart from via

TRIF) is potentiated by the inhibition of NF κ B activation, although TLR-mediated cytotoxicity is normally balanced by the induction of the pathway^{288,297-300}. Macrophage cells are often induced to undergo apoptosis when infected by pathogenic intracellular micro-organisms. This may limit the spread of pathogens and pathogen cell death has also been observed during the apoptosis of the host cell³⁰¹. Both TLR2 and TLR4 signalling has been implicated in this direct induction of macrophage apoptosis^{196,288,302,303}. TLR4 signalling is mediated by TRIF, but an involvement of TLR2 in the direct induction of apoptosis is supported by the fact that TRIF-deficient cells are not completely protected against LPS- or poly(I:C)-induced cell death³⁰⁴. This implies another adaptor could confer moderate and delayed apoptosis in the absence of TRIF.

1.4.8. Phagocytosis

The role of TLR signalling in phagocytosis has been controversial, but has been fiercely championed by, in particular, the likes of Dr. J. Blander and it now seems generally accepted that TLR signalling participates in the phagocytosis of invading microbes³⁰⁵. Phagocytosis is an essential, and ancient, defence mechanism for higher metazoans and is performed by specialised cells, such as macrophages. It is literally defined as the “eating process” and is a specific form of endocytosis involving the vesicular internalisation of solid particles. Both invading microbes and apoptotic cells are cleared via a phagocytic pathway.

TLR signalling has been implicated in the regulation of a number of steps in the phagocytic pathway in response to bacterial invasion but not apoptotic cell death¹⁹². TLR signalling has been demonstrated to enhance the rate of phagosome maturation³⁰⁶ and phagosomes carrying TLR ligands are also more able to contribute peptides to major histocompatibility complex (MHC) class II molecules³⁰⁶. The phagocytosis of a number of pathogenic bacteria has been shown to be facilitated by TLR-dependent activation of a variety of effector molecules^{307,308}, such as phosphatidylinositol 3-kinase and Rac1, which regulate the rearrangement of the actin cytoskeleton and extension of the plasma membrane³⁰⁸.

1.5. Pathogenic modulation of TLR/IL-1R signalling

Since TLR signalling plays such a pivotal role in the detection, control and elimination of invading micro-organisms it is entirely expected that pathogenic microbes possess a plethora of strategies to attempt to overcome this host response. Indeed, by very definition a pathogen that successfully colonises, replicates, and causes disease within its host must have subverted TLR signalling and other innate signalling mechanisms in some way. Viral pathogens employ a vast range of evasion strategies, some of which are unique (for example the production of cytokine mimics) and some of which are similar to those employed by bacteria, including the production of signalling pathway inhibitor proteins. Some of the modulation strategies employed by bacteria towards TLR signalling are introduced in the following sections.

1.5.1. Modification and concealment of TLR ligands

A common method of evading detection by TLRs is for pathogens to camouflage or directly modify the molecules that trigger signalling. The central principle of pattern recognition by the innate immune system is that it recognises microbial structures that a pathogen is unable to do without or would be at a disadvantage to alter. However, some pathogens are able to circumvent this, even if it is detrimental for a time. A method used by most extracellular bacterial pathogens to hide TLR surface ligands without compromising function is the expression of a capsule. A capsule is usually composed of polysaccharides or, occasionally, other structures such as the polypeptide capsule of *B. anthracis*. A capsule is able to hide ligands such as lipid A and peptidoglycan whilst allowing the bacteria to attach and enter host cells via protruding molecules such as adhesins.

Another method of hiding TLR ligands is employed by obligate intracellular pathogens, which often replicate in specialised organelles that avoid fusion with lysosomes or escape from the phagosome and replicate in the cytoplasm. *Brucella* uses a type IV secretion system to interact with the ER shortly after invasion and this is required for avoiding fusion with lysosomes and for intracellular replication in macrophages³⁰⁹. More rarely, pathogens may employ mechanisms to abrogate detection by TLRs enabling survival within the phagolysosome. *Coxiella burnetii* provides an example of this³¹⁰. These strategies of concealment avoid intracellular killing and prevent the induction of a full adaptive response.

A wide variety of pathogens also modify their TLR ligands and a well-characterised example of this is the modification of LPS. Such modification of LPS structure not only impairs recognition by PRRs, but may also protect against anti-bacterial peptides. LPS is composed of polysaccharide chains (O-antigens) that are anchored to the outer leaflet of the bacterial envelope by the lipid A portion of the molecule³¹¹ and it is the lipid A which is sensed by the TLR4-MD2 complex^{312,313}. TLR4 responds to hexa-acetylated lipid A molecules with fatty acid side chains of 12-16 carbons in length³¹⁴ and there are a number of gram-negative bacteria that fail to stimulate TLR4 because of lipid A structural differences, frequently in these acyl side chains which may have carbon lengths of up to 20 repeats³¹⁴⁻³¹⁷. For example, *Helicobacter pylori* has a tetra-acetylated lipid A with fatty acid side chains of 16-18 carbons in length³¹⁸. Another example of a lipid A modification leading to weak TLR stimulation includes elimination of an acyl group from the lipid A. *Pseudomonas aeruginosa* actually alters its lipid A structure during disease: initially it expresses a penta-acetylated lipid A which does not stimulate macrophages to release much TNF α or IL-8 (100 fold less than normal lipid A) meaning that minimal other cells are recruited to the site of infection and activated. This likely facilitates initial colonisation of the lung. However, once successfully colonised *P. aeruginosa* expresses a hexa-acetylated LPS that triggers a stronger pro-inflammatory response leading to lung pathology³¹⁹. *Salmonella* sp. employ a similar strategy of lipid A modifications during disease, modifying their lipid A by various mechanisms including deacylation, palmitylation, and addition of aminoarabinose^{320,321}.

The modification of the TLR5 ligand flagellin is also evident in some pathogens and indeed flagellin may represent an exception to the dogma that PAMPs are essential contributors to pathogenicity. TLR5 recognises a conserved N-terminal region of flagellin^{322,323} and so amino acid polymorphisms in this N-terminal domain lead to poor TLR5 signalling³²⁴, as can be seen in some α - and ϵ -proteobacteria, including *H. pylori*. TLR5 is present largely in the gut where damage or invasion of epithelial tissue can result from infection. Thus, mucosal pathogens are frequently found to decrease their flagellin expression once they have entered their host or, if motility is essential, may modify its structure to make it less stimulatory.

1.5.2. Using TLR pathway activation

The blockage of inflammatory responses is the most commonly used survival strategy by pathogens. However, some pathogens actually activate inflammatory pathways for their benefit. For example, *Salmonella* sp. use TLR pathway activation to its advantage, promoting increased phagocytic uptake in order that it may gain access to its replicative niche³²⁵. This strategy is also employed by *Shigella dysenteriae* which produces two forms of lipid A under the control of two versions of the *msbB* gene. One lipid A form is completely acylated and so activates cells and induces leukocyte infiltration which leads to the disruption of the mucosal surface and facilitates bacterial invasion. Long term colonisation by *S. dysenteriae* requires that responses are dampened and it thus produces a less stimulatory lipid A.

Other pathogens also activate immune pathways to induce various cytokines that aid in their colonisation and proliferation. For example, *Yersinia* sp. secrete a virulence antigen (LcrV) that signals through TLR2 to trigger IL-10 secretion which mediates immunosuppression³²⁶. Mycobacteria can also induce the production of anti-inflammatory cytokines such as IL-6, which inhibits T cell activation, and IL-10, which has a variety of immunosuppressive effects including the inhibition of macrophage activation and the production of reactive oxygen and nitrogen intermediates³²⁷. Mycobacteria also reduces the expression of inflammatory cytokines and molecules that trigger adaptive immunity. In fact, IL-10 provides a common target for induction by bacterial pathogens, with *B. pertussis* also exploiting this cytokine to down-regulate the host immune response³²⁸.

The intracellular pathogen *Listeria monocytogenes* activates NFκB as a potential means of increasing its pathogenicity^{329,330}. In endothelial cells this activation causes the increased expression of adhesion molecules, including ICAM-1 and E-selectin, and the macrophage-attracting chemokines IL-8 and MCP-1³²⁹. Together, this attracts phagocytes and promotes tissue infiltration providing *Listeria* with a “Trojan horse” to enter the subendothelial space inside infected cells to enhance bacterial dissemination.

1.5.3. Immunomodulatory proteins

Since PRRs recognise evolutionarily conserved microbial molecules that are essential to the microbe there are a restricted number of changes that can be made to these molecules

before the changes become detrimental to bacterial survival. A common strategy for pathogens, therefore, is to interfere with downstream TLR-mediated signalling or to express TLR antagonists. Bacterial pathogens employ secretion systems to export virulence factors across bacterial membranes either into the extracellular space or directly into host cells. The secretion of toxins and immune modulators is a major use of these secretion systems, along with conjugal DNA transfer. Signalling pathways downstream of most PRRs have common signalling events and intermediates. For example, the NF κ B and MAPK signalling networks are activated by different PRRs, including TLRs and NLRs, and so present attractive targets for microbial subversion strategies. Many viral pathogens directly block signalling by interaction with, or modification of, signalling intermediates in these pathways³³¹⁻³³³ and certain bacterial pathogens also apply this strategy. For example, the *Y. pestis* type III effector YopJ interacts with MKKs and IKKs and blocks MAPK and NF κ B activation³³⁴⁻³³⁶. YopJ is part of a suite of Yops that *Yersinia* sp. produce in order to down-regulate immune signalling and prevent phagocytosis. AvrA, produced by *Salmonella typhimurium*, is homologous to YopJ and demonstrates acetyltransferase activity towards specific MAPKs thus inhibiting JNK and NF κ B signalling pathways and dampening the pro-apoptotic response to *Salmonella*³³⁷. Similarly, the *Bacillus anthracis* lethal factor cleaves MKKs that activate p38 MAPKs thus blocking expression of target genes³³⁸. This leads to the apoptosis of macrophages and DCs which cuts a link between the innate and adaptive immune systems. *Shigella flexneri* expresses a protein kinase OspG that targets ubiquitin-conjugated enzymes affecting phospho-I κ B α degradation and NF κ B activation³³⁹. Other OspG family members have been discovered in both plant and animal pathogens.

1.5.3.1. Pathogenic evasion via TIR domain proteins

In 2000, Bowie *et al.* identified a protein in vaccinia virus (A46) which they reported had homology to the TIR domain of TLRs and their adaptors³⁴⁰. They showed that A46 down-regulates IL-1 signalling to NF κ B and that this down-regulation of NF κ B activity is due to a reduction in p65 transactivation of NF κ B³⁴¹. A46 also prevents JNK and ERK activation downstream of IL-1 and is able to interact directly with TLR4 (but not TLR3), MyD88, Mal, TRIF and TRAM but not SARM³⁴¹. A46 also inhibits signalling downstream of TLR2/6, TLR1/2, TLR4, TLR5, TLR7 and TLR9 and plays a role in the virulence of

vaccinia virus. In 2006, Newman *et al.* identified over 200 bacterial proteins that contained putative TIR domains using a bioinformatic approach³⁴². Furthermore, they showed that one of these proteins (a *Salmonella enteritidis* protein termed TlpA) suppressed NFκB activation in response to IL-1, MyD88 over-expression and constitutive activation of TLR4. In the presence of TlpA, the binding of NFκB to its target sequences was reduced during signalling and that there was a reduction in caspase 8 cleavage of pro-IL-1β. Newman *et al.* also demonstrated that TlpA plays a role in the virulence of *S. enteritidis* and too hypothesised that TIR domain proteins present in pathogens represent an immune evasion strategy. Subsequently a TIR containing protein from an uropathogenic strain of *E. coli* and one from *Brucella* sp. have been investigated and also demonstrated to have roles in evasion of TLR signalling³⁴³⁻³⁴⁶. While much of the work in these studies is very persuasive there are some crucial gaps in the evidence for a physiological role of these TIR domain proteins in immune evasion. Newman *et al.* could not detect an interaction between TlpA and a variety of mammalian TIR domain proteins and no mechanism for the translocation of TlpA into mammalian cells has been identified. Investigations into the *E. coli* and *B. melitensis* TIR domain proteins are much more complete, with information on the translocation of these proteins, crucial residues for signal disruption and interaction with mammalian proteins³⁴³⁻³⁴⁶. A TIR domain protein has also been described from *Paracoccus denitrificans*, a bacterial species that would be generally thought of as non-pathogenic. Newman *et al.* also hint at the presence of many non-pathogenic species in their list of bacteria possessing putative TIR domain proteins. This raises questions as to their function of TIR domain proteins in these species. Perhaps they are involved in the subversion of plant signalling systems, or are proteins required for symbiotic or parasitic relationships.

Successful pathogens will employ a whole range of strategies to overcome the immune signalling pathways of their host. The production of TIR domain proteins may be one of these strategies. The relative impact on virulence of one immunomodulatory strategy is often fairly low. However, some strategies appear more important than others, and this is often reflected in their conservation between and within pathogenic species. These factors have yet to be fully explored in relation to TIR domain proteins. This work focuses on microbial TIR domain proteins, specifically in bacterial pathogens categorised as bioterrorism agents (for project aims see Section 1.7).

1.6. Bacteria as potential bio-terrorism agents

The Centre for Disease Control (CDC) have compiled a list of highly pathogenic bacterial and viral agents that are deemed to be a potential threat to public health and consequently are considered to be agents desirable to an aggressor as bioterrorism agents. The CDC splits these pathogens into three categories (A, B, C). Category A agents are defined as those that can be easily disseminated or transmitted from person to person, those that result in high mortality rates and might cause public panic and therefore have the potential for major public health impact and would require special action for public health preparedness. Category B agents include those that are moderately easy to disseminate and result in moderate morbidity and low mortality rates but that would require special diagnostic capabilities and high disease surveillance. Category C agents are emerging threats, for example organisms that could be engineered for mass dissemination because of their availability and ease of production and dissemination that would then cause high morbidity and mortality. Examples of Category C agents include the emerging infectious agents Nipah virus and Hantavirus (<http://www.bt.cdc.gov/agent/agentlist-category.asp>). The CDC defines the following bacterial species under Category A or Category B: *Bacillus anthracis*, *Yersinia pestis*, *Burkholderia mallei* and *Burkholderia pseudomallei*, *Francisella tularensis*, *Brucella melitensis*, *Salmonella* sp., *E. coli* O157:H7, *Shigella* sp., *Chlamydia psittaci*, *Coxiella burnetti* and *Rickettsia prowaceki*.

1.6.1. *Bacillus anthracis*

Bacillus anthracis is a gram-positive, spore-forming, rod-shaped bacterium that was first isolated from the blood of sheep suffering from anthrax by Casimir Davaine. It was subsequently the first bacterium conclusively demonstrated to cause disease by Robert Koch in 1876 and the first bacterium to be used as an attenuated vaccine in 1881³⁴⁷. Its species name, *anthracis*, derives from the Greek “anthrakis,” meaning coal. This refers to the most common form of the disease, cutaneous anthrax, which is characterised by large black skin lesions. *B. anthracis* is the only bacteria identified so far with a protein capsule (D-glutamate) and the only pathogenic bacteria to carry its own adenyl cyclase virulence factor (edema factor). The spores of *B. anthracis* are highly resilient and can survive extremes of temperature, harsh chemical treatments and low-nutrient environments for decades. *B. anthracis* is able to infect most mammals and in humans most often causes disease through infection of skin lesions (cutaneous anthrax), or through the gastrointestinal

or inhalational routes, disease caused by the latter two routes being the most severe. *B. anthracis* is an extracellular pathogen; its virulence mechanisms allow it to traffic to the lymph nodes after entry and then through the bloodstream, where it can multiply rapidly into internal organs³⁴⁸. Macrophages play a pivotal role in this cycle³⁴⁸⁻³⁵⁰. On entry to the body spores are engulfed by macrophages where they then germinate, move to the lymphoid system and gain access to the blood. Clinical disease includes edema, sepsis and meningitis³⁵¹⁻³⁵³. The virulence of *B. anthracis* is primarily attributed to its toxin production and its possession of a capsule (encoded for by two large plasmids pXO1 and pXO2, respectively). Its capsule prevents *B. anthracis* from being phagocytosed while replicating extracellularly and its toxins modulate the host immune system and cause cellular death. Its toxin has three parts, the protective antigen (PA), the lethal factor (LF) and edema factor (EF)³⁵⁴ and toxic activity only occurs when PA is combined with LF or EF (forming lethal toxin (LT) or edema toxin (ET), respectively). LF is a zinc metalloprotease which has been shown to inactivate MAPK signalling in neutrophils, macrophages, and DCs by cleaving the N-terminus of MAPKKs 1 and 2 which inhibits MAPKK1³⁵⁵⁻³⁵⁸. EF is an adenylate cyclase which causes an elevation in intracellular cAMP leading to fluid outpour from cells and consequently edema. The PA mediates the endocytic entry of EF or LF into target cells. LT causes lysis of macrophages *in vitro* and is the major contributor to virulence in infected animals³⁵⁹⁻³⁶². ET co-operates with LT to impair cytokine secretion from immune cells³⁶³.

1.6.1.1. *Bacillus anthracis* and TLR signalling

The interaction of *B. anthracis* with the innate immune system is somewhat unclear. For example, the role of pro-inflammatory cytokines in toxin-mediated cell death is debated. *In vivo* immune responses to anthrax in the mouse are dependent on the strain of *B. anthracis* and mouse^{364,365}. In addition, while the ability of the IL-1R antagonist to protect mice against lethal toxin challenge suggests the role of an over-active inflammatory response in the pathogenesis of disease³⁴⁹, other studies point to a non-inflammatory mechanism with a key role for apoptosis induced by the anthrax toxins^{366,367}. *B. anthracis* contains putative ligands for TLR2 (lipoprotein, cell wall constituents), TLR4 (anthrolysin) and TLR9 (CpG DNA)³⁶⁸. The capsule of *B. anthracis* hides potential PAMPs and inhibits phagocytosis of vegetative cells by immune cells such as macrophages and neutrophils. Various cytokines are produced from immune cells in response to *B. anthracis* spores, although the receptors

responsible for signalling are unknown; one study ruled out TLR2 involvement³⁶⁹. However, TLR2 is important in the response to vegetative bacteria³⁶⁹. Compared to vegetative bacilli, spores appear to be relatively inactive as TLR ligands, and pre-treatment of macrophages with TLR ligands significantly decreased anthrax-induced cytotoxicity in macrophages in one study³⁷⁰. TNF α has been shown to sensitise macrophages to LT and so it is likely that *B. anthracis* exploits the innate immune response of cytokine activation of cells to ensure their sensitivity to LT. Additionally, an *in vivo* role for TLR2 and TLR4 in *B. anthracis* detection has been suggested by knockout mouse models^{369,371}. As discussed in Section 1.6.1 the *B. anthracis* LF disrupts TLR signalling by inhibiting the MAPKKs and causing the lysis of macrophages but other proteins affecting TLR signalling have not been identified.

1.6.2. *Yersinia pestis*

Y. pestis is one of the three species in the genus *Yersinia* that causes human disease (*Y. pseudotuberculosis* and *Y. enterocolitica* are the other species and both cause gastrointestinal disease). The genus *Yersinia* is named after A. E. J. Yersin, a Swiss bacteriologist who discovered *Y. pestis*³⁷². *Y. pestis* causes a systemic disease referred to as plague. It is primarily a rodent pathogen but readily infects humans and is usually transmitted subcutaneously by the bite of an infected flea or via inhalation, particularly during a pandemic of the disease. There have been three pandemics of plague throughout history which have given rise to three recognised *Y. pestis* biovars: Antiqua, Orientalis and Mediaevalis³⁷³. *Y. pestis* is closely related to *Y. pseudotuberculosis* but with some significant adaptations. For example, *Y. pseudotuberculosis* is a mammalian enteropathogen widely found in the environment whereas *Y. pestis* is a blood-borne mammalian pathogen that is also able to parasitise insects and does not survive well in the environment. Horizontally acquired DNA is likely to have been significant in having enabled *Y. pestis* to adapt to new hosts and indeed *Y. pestis* contains three regions of unusual GC bias, usually caused by the very recent acquisition of DNA (e.g.: from a prophage) or by the inversion or translocation of blocks of DNA. The genes involved in its ability to colonise its insect host appear to be distinct from those related to its ability to colonise a mammalian host³⁷⁴.

After infection with *Y. pestis* bacterial replication occurs first at the site of infection, but subsequently the bacteria enter the lymphatic system via macrophage cells as transport,

spread to the lymph nodes, then into the bloodstream and to organs such as the spleen and liver. Extensive replication within these organs then occurs whereby bacteria return to the bloodstream and the host finally dies of septicemic shock. Due to the fact that *Y. pestis* replicates within cells early in infection but is also able to replicate extracellularly, it is considered to be a facultative intracellular pathogen.

All three of the human pathogenic *Yersinia* sp. carry a 70kb plasmid denoted the plasmid of *Yersinia* virulence (pYV in *Y. pseudotuberculosis*, pCD1 in *Y. pestis*) that is required for replication in lymphoid tissues, for which *Yersinia* have a tropism³⁷⁵. pCD1 encodes for a type III secretion system (TTSS) that allows extracellular *Yersinia* to deliver a set of virulence proteins into host eukaryotic cells³⁷⁶⁻³⁷⁹. This system is composed of three components: a secretion system that delivers proteins to the bacterial surface, a translocation apparatus (minimally represented by LcrV, YopB and YopD) and six effector proteins (YopO, YopH, YopM, YopJ, YopT, and YopE), also referred to as “anti-inflammatory or anti-phagocytic toxins”³⁷⁶⁻³⁷⁹. These Yops allow *Yersinia* to multiply extracellularly by preventing phagocytosis and delaying the onset of the inflammatory response^{290,377-384}. Suppression of phagocytosis enables *Yersinia* to evade macrophage killing and proliferate as extracellular micro-colonies later in infection. *Y. pestis* carries two plasmids (pMT1 and pPCP1), not found in *Y. pseudotuberculosis*, thought to endow *Y. pestis* with increased virulence and vector-borne transmissibility. *Y. pestis* also encodes for another TTSS on its chromosome which is closely related to the TTSS on the *Salmonella* pathogenicity island SPI-2 which promotes replication of the *Salmonella* within macrophages. It is therefore likely that this TTSS contributes to the early phase of the lifecycle of *Y. pestis* within its mammalian host.

1.6.2.1. *Yersinia pestis* and TLR signalling

A reduced inflammatory response is characteristic of *Y. pestis* infection and is partly mediated by down-regulation of TLR signalling. Its type III effector YopJ is a well-researched modulator of TLR signalling and has a number of postulated activities towards TLR pathways. It interacts with MKKs and IKKs resulting in their acetylation (possibly by YopJ itself) in a critical effector loop in both kinases^{385,386}. This acetylation blocks activation of these modified MKK and IKK proteins because the effector loop cannot be

phosphorylated by upstream kinases resulting in reduced MAPK and NF κ B activation³³⁴⁻³³⁶. It has also been reported that YopJ has the ability to remove ubiquitin and SUMO moieties from the IKK and MKK proteins^{334,387} and that expression of YopJ leads to reduced ubiquitination of several TRAF proteins. This allows YopJ to block TLR signalling that diverges before activation of the IKKs or MKKs such as TLR3-dependent IRF3 activation. However, this deubiquitination activity of YopJ is inefficient *in vitro* and its physiological relevance *in vivo* is yet to be determined. The YopJ-mediated downregulation of NF κ B activation by *Yersinia* disrupts the balance between pro- and anti-apoptotic signals (Section 1.4.7) leading to apoptosis of macrophages³⁸⁸. Macrophages are therefore primed to undergo TLR-dependent apoptosis on *Yersinia* infection²⁹⁷. The downregulation of multiple MAPKs also leads to a reduction in pro-inflammatory signals^{336,382,389,390}, particularly TNF α .^{382,389-392}

The other major immunomodulatory protein produced by *Y. pestis* is its major virulence antigen (V-antigen or LcrV), also encoded on the virulence plasmid of *Y. pestis*, *Y. pseudotuberculosis* and *Y. enterocolitica*. LcrV is involved in several functions including regulating the production of Yops and their translocation into host cells. It has also been shown that LcrV can act as an extrabacterial chaperone for the translocation pore formed by YopB and YopD³⁹³ and that once the pore has formed LcrV is released into the environment. LcrV is also protective as a vaccine in *Yersinia* sp. infection³⁹⁴⁻³⁹⁶. LcrV induces IL-10 production via TLR2 activation. This consequently “silences” macrophages against stimulation with other TLR2 agonists via a mechanism that resembles tolerance that also affects signalling via the other TLRs. Whereas the anti-inflammatory Yops likely act at short distance, the secreted LcrV can act as a longer range virulence factor capable of causing systemic immunosuppression.

1.6.3. *Burkholderia pseudomallei*

Burkholderia is a genus of β -proteobacteria that defines a group of virtually ubiquitous, gram-negative, motile, obligatory aerobic rod-shaped bacteria. The genus, named after Burkholder, a plant pathologist at Cornell University, includes both animal and plant pathogens, and environmentally important bacteria. *Burkholderia* sp. have large genomes, their chromosomes are among the largest in the microbial world, allowing them to adopt a myriad of lifestyles.

Of the many *Burkholderia* species, two are categorised as possible biological weapons for potential use against livestock and humans: *B. pseudomallei*, the causative agent of melioidosis and *B. mallei*, the causative agent of glanders, a disease that occurs mostly in horses and related animals. For this reason *B. mallei* is believed to have been used as a bio-weapon in the First World War to infect Russian horses on the Eastern front³⁹⁷. Both *B. pseudomallei* and *B. mallei* are endemic in tropical countries where they are an important public health concern for both humans and livestock³⁹⁸.

The pathogenesis of *B. pseudomallei* is still relatively unknown. Melioidosis is not necessarily associated with a defined set of symptoms and the importance of host genetic background and infection route on the progression of disease have been shown³⁹⁹. *B. pseudomallei* is a facultative intracellular pathogen and is known to infect almost all cell types where it persists in an intracellular compartment. This broad cellular tropism defines its versatility as a pathogen and accounts for the frequently observed wide range of clinical manifestations. Another feature of the disease is the possible long incubation period in re-drudescant melioidosis; up to 62 years has been reported⁴⁰⁰. *B. pseudomallei* virulence factors include exotoxins, siderophores and enzymes like lipases, catalases and proteases. *B. pseudomallei* is also remarkably resistance to a wide variety of antibiotics which limits the options for treatment of melioidosis³⁹⁷. The antibiotic resistance is thought to arise, at least in part, from expression of a polysaccharide capsule which contributes to biofilm formation⁴⁰¹.

1.6.3.1. *Burkholderia pseudomallei* and TLR signalling

Compared to *Y. pestis* little is known about *Burkholderia* sp. interaction with TLRs, although it is clearly able to evade the host innate immune system, potentially for a very long time. Published mechanisms of evasion include its unstimulatory LPS^{402,403}, presence of a capsule that reduces complement deposition⁴⁰⁴ and resists the action of anti-microbial peptides⁴⁰⁵, its poor induction of nitric oxide and cytokine release⁴⁰⁶, its ability to escape from the endosome to the cytosol⁴⁰⁷, its induction of macrophage cell death⁴⁰⁸ and its ability to spread intracellularly through actin polymerisation^{407,409,410}. Most of the work on the interaction of *B. pseudomallei* and TLRs focuses on the unstimulatory nature of many

of its PAMPs and its ability to hide these structures. In addition, however, it is likely that this stealthy bacterium is able to actively interfere with TLR signalling by, as yet, unknown mechanisms. For example, macrophages exposed to *B. pseudomallei* are defective in their ability to induce respiratory burst and TNF α when compared to that induced in response to *E. coli* or *Salmonella typhi*^{403,406}.

As a gram-negative bacterium it has putative ligands for both TLR2 and TLR4. Increased TLR2 and TLR4 expression and mRNA levels have been found in the monocytes and granulocytes of humans with melioidosis and TLR2 and TLR4 have been shown to be activated by *B. pseudomallei in vitro*⁴¹¹ although studies using HEK293 cells transfected with TLRs have been somewhat contradictory. West *et al.* showed that heat-killed *B. pseudomallei* activates TLR2 (in combination with TLR1 or TLR6) and TLR4⁴¹². *B. pseudomallei* LPS and lipid A activated TLR4/MD-2 in these studies. However, Wiersinga *et al.* found that *B. pseudomallei* LPS activated TLR2 but not TLR4. The macrophage cytokine response to *B. pseudomallei* seems entirely dependent on TLR4 but was also increased in the absence of TLR2 suggesting some sort of synergistic role. As for *Y. pestis*, part of the virulence of *B. pseudomallei* appears to be dependent on TLR2 since TLR2 knock-out mice show reduced mortality in response to *B. pseudomallei* infection⁴¹¹, although this mechanism did not appear to be IL-10 dependent.

1.6.4. *Brucella melitensis*

Brucella is a zoonotic pathogen that was first isolated by Sir David Bruce in 1887 from a British soldier who died in Malta from what was known as “Maltese fever”⁴¹³. *Brucellosis* normally presents as a debilitating febrile illness that can progress into a chronic disease often with serious complications such as infection of heart or bones. Several species of *Brucella* are able to infect humans, most commonly *Brucella melitensis* (natural host: cattle and bison), *Brucella abortus* (natural host: sheep) and *Brucella suis* (natural host: pigs). The disease is transmitted to humans by contact with the bodily fluids of infected animals, including via non-pasteurised dairy products.

Brucella sp. are facultative intracellular bacteria that persist and multiply in macrophages. *Brucella* has been called a “stealthy” pathogen as it largely avoids activating the innate immune system and has no classical virulence factors^{414,415}. Their capacity to successfully

survive and replicate within a variety of host cells characterises their pathogenicity. Macrophages, placental trophoblasts and DCs are key targets of infection⁴¹⁶. *Brucella* are phagocytosed by macrophages and DCs via lipid raft mediated macropinocytosis but subsequently establish a replicative niche within a *Brucella* containing vacuole (BCV) or “brucellosome”^{309,417,418}. This brucellosome then moves by altered intracellular trafficking, transiently interacting with early and late endosomes and the lysosome (although avoiding destruction by the lysosome) finally associating with the endoplasmic reticulum (ER) membranes to form a replicative vacuole⁴¹⁹. Here *Brucella* multiply extensively, preventing death of the cell by inhibiting apoptosis⁴²⁰. Killed *Brucella* are also taken up by macrophages but fail to associate with the ER and are rapidly degraded, suggesting that *de novo* protein synthesis and/or secretion is required for bacterial trafficking and survival during infection⁴²¹. Once *Brucella* has established its intracellular niche it is then able to persist chronically, with the infection persisting or relapsing for years⁴²². The way in which *Brucella* controls its gene expression in response to environmental signals has therefore been widely investigated. Several regulators of global gene expression have been identified in *Brucella* that are implicated in its adaptive response to different environments⁴²³⁻⁴²⁵. Many of these genes encode transcriptional regulators, others encode systems crucial during macrophage infection for internalisation and subsequent fusion with the ER, such as the virB type IV secretion system^{309,417} and flagella which may have evolved for a purpose other than motility in *Brucella*^{426,427}. No secreted effector molecules of the VirB type IV secretion system have yet been identified. *Brucella* also responds to the lack of nutrients within the phagosome with what is called a stringent response that involves a halt in the synthesis of periplasmic transporters and an alteration to the TCA cycle⁴²⁸. *Brucella* also use a two-component regulatory system to allow individual bacteria to adjust gene expression in response to environmental stimuli^{429,430}. A blue light signalling system has recently been discovered which appears to contribute to virulence⁴³¹. *Brucella* establishes an intracellular niche and persists chronically in the host which means control of virulence factor expression is particularly important in *Brucella* pathogenesis.

1.6.4.1. *Brucella melitensis* and TLR signalling

In contrast to classical enterobacterial LPS, those of *Brucella* sp. (from both the rough and smooth strains) are several hundred times less active and less toxic than *E. coli* LPS⁴³². The

unconventional LPS of *Brucella* is necessary for entry into cells and early development of the brucellosome. It also has immunomodulatory activities, forming non-functional complexes with the MHC II, and has been shown to impair anti-microbial host responses by inhibiting complement activity, preventing the action of anti-microbial peptides and the synthesis of immune mediators⁴³²⁻⁴³⁴ although the rough strains are more sensitive to normal serum and complement attack. The *Brucella* β -1, 2-glucan is also implicated in early biogenesis of the brucellosome.

The highly subversive nature of *Brucella* sp. and their ability to persist intracellularly suggest they must evade the TLR system in some way. However, apart from the non-stimulatory LPS, few effectors with direct effects on the TLR system have been identified and it is still somewhat unclear as to how *Brucella* is able to remain hidden from the immune system and cause chronic disease. *Brucella* sp. encode for an operon termed *virB* that forms a type IV secretion system (T4SS). A number of studies have confirmed that this operon is clearly involved in virulence^{309,435}, but to date none of its effectors have been identified. Various inflammation and immunity-specific genes are induced during infection with *B. abortus* and *B. melitensis* but not in their *virB* mutants so it does seem that the T4SS is actively involved in host immune regulation. One can speculate that at least some of the T4SS effectors, when fully described, will affect TLR signalling.

One *Brucella* TLR-specific effector protein has been described however. *Brucella* sp. encode for a TIR domain protein which has been postulated to be “Mal-like” as it is able to associate with phosphoinositides through its N-terminal domain and disrupts Mal-dependent TLR signalling. A *Brucella* mutant in this TIR domain protein presented an attenuated phenotype in an immunocompromised mouse model and this likely forms one way in which *Brucella* sp. are able to modulate TLR signalling for their own gain³⁴⁴⁻³⁴⁶.

1.7. Aims of this research

Bacterial species deemed to be bioterrorism threats are by their very nature highly pathogenic. In order to cause disease within a host a pathogen must subvert the host immune system in some way, and since TLR signalling plays such a pivotal role in both the innate and adaptive immune response it is reasonable to assume that highly pathogenic bacteria may target these pathways (and indeed it is evident that they do). One recently postulated evasion strategy involves bacteria using proteins that contain TIR domains to disrupt the host homotypic TIR interactions in TLR signalling (Section 1.5.3.1). This has the advantage of modulating early in the pathway (the association of TIR domains is the first intracellular step in TLR signalling) and that TIR domain interaction is used by all TLRs and the IL-1R giving the potential for widespread disruption of the immune response at this point. The only survey of TIR domain proteins in bacterial species mentioned in the literature is that carried out by Newman *et al.* but their list of putative TIR domain proteins is not available so the presence of TIR domain proteins in potential bioterrorism agents remains unknown.

This study aims to:

- Investigate whether CDC bioterrorism category A and B bacterial pathogens encode for proteins that contain TIR domains
- If found, to assess whether these TIR domain proteins have an effect on mammalian immune signalling *in vitro*.
- To assess the effect of bacterial TIR domain proteins on infection *in vivo* by generating a TIR domain protein deletion mutant.

Chapter 2: General Methods

2.1. Bioinformatic methods

2.1.1. Saturated BLAST

Amino acid sequences (Table 2-1) of known TIR domains (as defined in the literature) were used to initiate a cascade of PSI-BLAST searches, as implemented in the Saturated BLAST program⁴³⁶, to identify proteins with potential TIR domains in a selection of CDC Bioterrorism Category A and B bacterial pathogens. Five iterations of Saturated BLAST were run with all other parameters as default. The results were probed for bacteria of interest by searching for species name and manually recorded. Proteins found in this way were subjected to a round of Saturated BLAST searches to confirm they yielded known Tdps.

Protein seed	Protein ID
Residues 625 – 786 from TLR1, <i>Homo sapiens</i>	CAG38593
Residues 643 – 784 from TLR2, <i>Homo sapiens</i>	AAH33756
Residues 751 – 904 from TLR3, <i>Homo sapiens</i>	AAH59372
Residues 671 – 819 from TLR4, <i>Homo sapiens</i>	CAH72619
Residues 691 – 840 from TLR5, <i>Homo sapiens</i>	AAI09119
Residues 641 – 790 from TLR6, <i>Homo sapiens</i>	BAA78631
Residues 890 – 1035 from TLR7, <i>Homo sapiens</i>	AAQ88659
Residues 892 – 1048 from TLR8, <i>Homo sapiens</i>	AAQ88663
Residues 863 – 1020 from TLR9, <i>Homo sapiens</i>	AAQ89443
Residues 629 – 775 from TLR10, <i>Homo sapiens</i>	AAQ88667
Residues 81 – 170 from Mal, <i>Homo sapiens</i>	NP_001034750
Residues 395 – 527 from TRIF, <i>Homo sapiens</i>	BAC44839
Residues 78 – 180 from TRAM, <i>Homo sapiens</i>	AAO74498
Residues 160 – 294 from MyD88, <i>Homo sapiens</i>	NP_002459
Residues 543 – 696 from Sarm1, <i>Homo sapiens</i>	NP_055892
Residues 167 – 304 from SIGIRR, <i>Homo sapiens</i>	CAG33619
Residues 41 – 173 from A46, <i>Vaccinia virus</i>	XP_636358
Residues 578 – 718 from Tir-1, <i>Caenorhabditis elegans</i>	NP_001021253
Residues 401 – 550 from IL-1RAPL, <i>Homo sapiens</i>	Q9NZN1

Table 2-1: TIR domain proteins used as seeds for Saturated BLAST searches

Amino acid residues of TIR domain proteins used as seed sequences to initiate Saturated BLAST searches. Accession numbers refer to the NCBI nr database.

2.1.2. PSI-BLAST

Eighteen eukaryotic TIR domain sequences (Table 2-2) were used as seeds in PSI-BLAST searches via the NCBI BLAST interface at <http://blast.ncbi.nlm.nih.gov> against the non-redundant (nr) protein database to investigate TIR domain distribution in bacteria, fungi, archaea and viruses. Default search parameters were used until no new results were returned with an e-value cut-off of <0.05. Results were filtered for proteins from whole bacterial, archaeal, fungal or viral genomes and de-duplicated using the “my xBASE” component of xBASE⁴³⁷. Results from subgenomic fragments in nr (e.g. deposits of single proteins) were removed and the final list of proteins transferred to a Microsoft Excel spreadsheet (Appendix B).

Protein seed	Protein ID
Residues 639 - 775 from TLR1, <i>Homo sapiens</i>	CAG38593
Residues 643 - 784 from TLR2, <i>Homo sapiens</i>	AAH33756
Residues 758 - 862 from TLR3, <i>Homo sapiens</i>	AAH59372
Residues 636 - 774 from TLR4, <i>Homo sapiens</i>	CAH72619
Residues 695 - 832 from TLR5, <i>Homo sapiens</i>	AAI09119
Residues 644 - 780 from TLR6, <i>Homo sapiens</i>	BAA78631
Residues 893 - 1034 from TLR7, <i>Homo sapiens</i>	AAQ88659
Residues 882 - 1020 from TLR8, <i>Homo sapiens</i>	AAQ88663
Residues 872 - 1009 from TLR9, <i>Homo sapiens</i>	AAQ89443
Residues 636 - 774 from TLR10, <i>Homo sapiens</i>	AAQ88667
Residues 86 - 168 from Mal, <i>Homo sapiens</i>	NP_001034750
Residues 395 - 527 from TRIF, <i>Homo sapiens</i>	BAC44839
Residues 81 - 174 from TRAM, <i>Homo sapiens</i>	AAO74498
Residues 176 - 305 from MyD88, <i>Homo sapiens</i>	NP_002459
Residues 561 - 700 from Sarm1, <i>Homo sapiens</i>	NP_055892
Residues 167 - 304 from SIGIRR, <i>Homo sapiens</i>	CAG33619
Residues 821 - 915 from TirA, <i>Dictyostelium discoideum</i> AX4	XP_636358
Residues 578 - 718 from Tir-1, <i>Caenorhabditis elegans</i>	NP_001021253

Table 2-2: TIR domain proteins used as seeds for PSI-BLAST searches

Amino acid residues from TIR domain proteins used as seed sequences to initiate PSI-BLAST searches. Accession numbers refer to nr database on NCBI server.

2.1.3. FUGUE

Proteins encoded by bacteria of interest were subjected to structural homology analysis using the FUGUE web server⁴³⁸ (<http://tardis.nibio.go.jp/fugue/prfsearch.html>). Given a query sequence, FUGUE uses parts of the HOMSTRAD structure database to search known domain structures, and calculates the sequence-structure compatibility, producing a list of potential homologues and alignments. This produces a statistical measure (the “Z score”) of how structurally similar two proteins are. The probability that two proteins will have the same secondary structure is classified as follows:

$Z \geq 6.0$	“Certain”	99% confidence
$Z \geq 4.0$	“Likely”	95% confidence
$Z \geq 3.5$	“Marginal”	90% confidence
$Z \geq 2.0$	“Guess”	50% confidence
$Z < 2.0$	“Uncertain”	< 50% confidence

2.1.4. 3D Jury

3D jury is a meta prediction server, that is, it predicts the consensus structure of a given sequence, bringing together a variety of individual structure prediction tools, including FUGUE. It was implemented through the Structure Prediction Meta Server (<http://BioInfo.PL/Meta/>) online and used to give a consensus for the position of α -helices, loop regions and β -sheets for bacterial TIR domain proteins in order to annotate the multiple sequence alignments.

2.1.5. The GOLD database

The Genomes OnLine Database (GOLD) is a curated database of completed and on-going genome sequencing projects⁴³⁹. Numbers of sequenced genomes for particular species can be searched for via their website (<http://www.genomesonline.org>) or the data can be downloaded.

2.1.6. Pfam

Proteins of interest were entered into the Pfam database to investigate domain architectures (<http://pfam.sanger.ac.uk>). The Pfam database is a large collection of protein families (both manually curated (PfamA) and automatically generated (PfamB)) each represented by multiple sequence alignments and hidden Markov models. Pfam will identify previously-

assigned domains to a protein of interest and produce a multiple sequence alignment and schematic representation of domains.

2.1.7. Multiple sequence alignments

Initial multiple sequence alignments after the Saturated BLAST searches were performed using the ClustalW algorithm in MegAlign (DNASTAR, Lasergene[®], Version 7.0, default parameters). After the PSI-BLAST searches multiple sequence alignments on Tdps from selected agents were performed using the ClustalW2 algorithm on the EMBL-EBI server (default parameters) which is compatible with the Jalview editing software which allowed the production of publication-quality coloured alignments. Alignments in Jalview were coloured using the ClustalX colour scheme for conservation of residues (Figure 2-1).

Sequences to align with bacterial TIR domain proteins were chosen from the results of PSI-BLAST searches using the bacterial proteins as seed sequences.

2.2. Buffers and Media

Luria Bertani (LB) broth was prepared with 10 g tryptone, 5 g yeast extract and 5 g NaCl in 1 l of distilled water, adjusted to pH 7.5 and autoclaved. **L-agar** was made with the same constituents plus 1.5% agar.

Blood agar base (BAB) broth was prepared with 15 g proteose peptone, 2.5 g liver digest, 5 g yeast extract (all Oxoid) and 5 g NaCl (Sigma-Aldrich Ltd., UK) in 1 l distilled water.

BAB agar was made with 40 g blood agar base No 2 (Oxoid) in 1 l distilled water, autoclaved at 121°C for 15 min and then cooled to 47°C before the addition of 8 ml filter-sterilised hemin solution made up as follows: 0.25 g hemin (Sigma-Aldrich Ltd., UK) dissolved in 20 ml 1 M NaOH, made up to 100 ml with distilled water and filter sterilised.

SOC broth was purchased from Invitrogen Ltd. UK

Complete Dulbecco's Modified Eagle Medium (cDMEM) was prepared by supplementing DMEM (Gibco, UK) with 2 mM glutamine and 10% heat-inactivated fetal bovine serum (FBS) (Invitrogen, UK).

(A)

Jalview	
blue	(W,L,V,I,M,F): {50%, p}{60%, wlvimafcyhp} (A): {50%, p}{60%, wlvimafcyhp}{85%, t,s,g} (C): {50%, p}{60%, wlvimafcyhp}{85%, s}
red	(K,R): {60%, kr}{85%, q}
green	(T): {50%, ts}{60%, wlvimafcyhp} (S): {50%, ts}{80%, wlvimafcyhp} (N): {50%, n}{85%, d} (Q): {50%, qe}{60%, kr}
pink	(C): {85%, c}
magenta	(D): {50%, de,n} (E): {50%, de,qe}
orange	(G): {always}
cyan	(H,Y): {50%, p}{60%, wlvimafcyhp}
yellow	(P): {always}

(B)

```

AGIHTFRDDDELPRGEEISQHLLE-AIQESKICIVVFSKGYAS
ARLRTFMDEG-VLKGGDVADTI IQ-ALEASRVSIVILSETFAS
LGVSVWFDEAELRIGDSLRRK-IDQGLARSAGVVFSEAFFA
YKIHTFRDDDELRRGEEIGPNLLR-AIDQSKIYVPIISSGYAD
QGIQAYKDDETLPRGERIGPALLK-AIQESRIAVVVFSONYAD
LGAKIFYDAYTLKVGDSLRRK-IDQGLANSKFGIVVLSSEHFFS

```

Figure 2-1: Clustal colourscheme for Jalview alignments

(A) Rules for residue colours in Clustal colourscheme used by Jalview alignment editing software. Amino acid residues are given in round brackets and the rules in curly brackets which include the minimum % and the residues which must meet or exceed this % within the column of residues in the alignment. If a group of residues is concentrated together e.g. “rstv,” then any combination of these residues in total must meet or exceed the given % for the colour to be applied. For residues or residue groups separated by commas, at least one of these must by itself exceed the %. (B) Section of an alignment coloured using this scheme for reference.

HEK-Blue™-DMEM was prepared by supplementing complete DMEM with HEK-Blue™ selection antibiotic mix (InvivoGen, France).

Serum-free medium used in these studies was **Opti-MEM®** (Invitrogen, UK)

PBST wash buffer was composed of phosphate-buffered saline (PBS) supplemented with 0.1% (v/v) Tween®-20 (Sigma-Aldrich, UK).

BLOTTO was prepared by dissolving 5% (w/v) non-fat dried milk powder in PBST.

Transfer buffer had the following constituents:

80 ml 25x Novex® Tris-Glycine Transfer buffer (Invitrogen Ltd., UK)

100 ml methanol

820 ml deionised water

RIPA cell lysis buffer plus protease inhibitors (RIPA_PI) was prepared by adding 20 µl/ml protease inhibitor cocktail (Sigma-Aldrich, UK), 10 µl/ml phenylmethanesulfonyl fluoride (PMSF) at 100mM and 10 µl/ml sodium orthovanadate (NaOV) at 200mM to RIPA buffer purchased from Sigma-Aldrich, UK.

Lysis buffer 1 had the following constituents:

50 mM Tris pH7.5

250 mM NaCl

10 % glycerol

1 mM EDTA

0.05 % CHAPS (w/v)

0.5 % Triton® X-100

Before use 10 µl/ml PMSF at 100 mM, 10 µl/ml NaOV at 200 mM and 30 µl/ml aprotinin at 1 µg/ml were added.

Lysis buffer 2 had the following constituents:

50 mM HEPES

200 mM NaCl

1 mM EDTA pH 7.5

10 % glycerol

1 % NP-40

Before use 10 μ l/ml PMSF at 100 mM, 10 μ l/ml NaOV at 200 mM and 30 μ l/ml aprotinin at 1 μ g/ml were added.

Fixative for confocal microscopy consisted of 3 % (w/v) paraformaldehyde (PFA) in PBS.

Perm/quench solution consisted of 50mM NH₄Cl and 0.2 % (w/v) saponin in PBS kept in the dark.

PGAS consisted of 1 % fish skin gelatine (Sigma-Aldrich Ltd., UK), 0.02 % (w/v) saponin, 0.02 % (w/v) NaN₃ in PBS kept in the dark.

2.3. Animals

All animal studies were carried out in accordance with the UK Scientific Procedures Act 1986. Animal handling and infection studies were carried out by trained staff at Dstl. Pathogen-free 6- to 8-week old female BALB/c mice were obtained from Charles River Laboratories (Margate, UK) and housed in high-efficiency particulate air-filtered barrier units. For challenge with ACDP category III bacteria mice were moved to a similar facility but housed within biological safety cabinets for the duration of the experiments. Mice were always allowed to acclimatise to new surroundings for at least 7 days before experimental work began. Mice were given food and water *ad libitum* and were kept at 25°C with alternating 12 h periods of light and dark. Animals that had reached the humane endpoint described in the UK Home Office project licence used for this work were culled by cervical dislocation. Study plans for the *in vivo* experiments detailed in this work are shown in Table 2-3 and Table 2-4.

2.3.1. Methods of inoculation

For intravenous (i.v.) inoculation of mice with *Y. pestis* strains 100 μ l of inoculum was injected into the tail vein. For subcutaneous (s.c.) inoculation with *Y. pestis* strains 100 μ l of inoculum was injected sub-dermally into the scruff of the neck.

Day no.	Procedure (e.g. vaccination/challenge)
-7	6 mice arrive from supplier and transferred to isolator Caged in 1 group of 6 mice. Acclimatisation period
0	All mice injected i.v. with 10^4 cfu/mouse of <i>Y.pestis</i> GB and <i>Y. pestis</i> $\Delta YpTdp$ in a 1:1 ratio.
2	Cull surviving mice, remove spleens for culture STUDY END

Table 2-3: Study timetable for the assessment of the competitive index of *Y. pestis* $\Delta YpTdp$ in competition with wild-type *Y. pestis* GB

Day no.	Procedure (e.g. vaccination/challenge)
-7	48 BALB/c arrive from supplier. Animals grouped 8 x 6 mice per cage. Acclimatisation period
0	5 groups of 6 mice given 100 µl of the following dilutions of a 1×10^8 cfu/ml <i>Y. pestis</i> $\Delta YpTdp$ starting culture via the s.c. route: 10^{-4} , 10^{-5} , 10^{-6} , 10^{-7} , 10^{-8} 3 groups of 6 mice 100 µl of the following dilutions of a 1×10^8 cfu/ml <i>Y. pestis</i> GB starting culture via the s.c. route: 10^{-5} , 10^{-6} , 10^{-7}
1 – 13	Twice-daily monitoring of clinical signs, animals reach humane endpoint to be killed by cervical dislocation.
14	End of experiment, cull survivors.

Table 2-4: Study timetable for assessment of median lethal dose of *Y. pestis* $\Delta YpTdp$.

2.3.2. Analysis of bacterial colonisation

Mice were culled by cervical dislocation and the spleens were removed and placed in cold PBS. The spleens were then macerated through a cell strainer (Becton Dickinson Labware, US) in 3 ml PBS. Suitable serial dilutions of emulsified tissue were spread onto BAB agar, supplemented with antibiotic if necessary.

2.4. Bacteria

Transformed *Escherichia coli* One Shot[®] TOP10 cells (Invitrogen Ltd., UK) were routinely grown in LB at 37°C with orbital shaking at 180-200 rpm, or streaked for single colonies on L-agar plates. For storage, a single colony of was used to inoculate 5 ml LB and incubated for 16-18 h. 3 ml culture was then centrifuged at 13,000 rpm for 5 min and the pellet was resuspended in 30% (v/v) glycerol and was stored at -70°C. L-agar and LB were both supplemented with 100 µg/ml ampicillin (Sigma-Aldrich Ltd., UK) where appropriate.

Yersinia pestis GB was originally isolated from a human case of *Y. pestis* infection at the Health Protection Agency (HPA), Porton Down, UK. This strain was obtained from Prof. Petra Oyston, Dstl, UK. *Y. pestis* GB was routinely grown in BAB broth at 28°C with orbital shaking at 180 rpm, or streaked onto BAB agar plates. Plates were incubated at 28°C for 48 h for growth of *Y. pestis*. For incubation of *Y. pestis* at 37°C BAB broth was supplemented with 2 mM CaCl₂. Overnight cultures were set up by inoculating 10 ml BAB broth with a 10 µl loopful of colonies from a freshly streaked BAB agar plate. For storage, an overnight culture was set up and incubated 16-18 h at 28°C with orbital shaking. This overnight culture was then diluted 1:1 with 60% (v/v) sterile glycerol and stored at -70°C. Both BAB agar and broth were supplemented with 50µg/ml kanamycin where appropriate.

2.4.1. Production of electrocompetent cells

Electrocompetent *Y. pestis* was produced by Dr. D. Ford to the following method: A loopful of *Y. pestis* from a freshly streaked plate was used to inoculate 10 ml BAB broth supplemented with 50 µg/ml trimethoprim and 0.8 % (v/v) arabinose. This was cultured at 28°C overnight shaking at 180 rpm. These overnights were then used to seed BAB broth as above to an OD₅₉₀ of 0.3 in 10 ml and this was cultured for 3 h at 28°C with shaking at 180 rpm.

2.4.2. Growth curves

Y. pestis was cultured for 16-18 hr at 28°C with orbital shaking. This culture was then diluted 1:10 in 50 ml BAB broth and incubated at the appropriate temperature with orbital shaking for the desired amount of time. At defined intervals the cultures were removed from incubation and 1 ml of culture removed for optical density reading at 590 nm. This 1 ml of culture was then discarded and the cultures returned for incubation.

2.4.3. Surface hydrophobicity assay

Y. pestis was cultured for 16-18 hr at 28°C with orbital shaking. The cultures were then diluted 1:10 to a final volume of 50 ml BAB broth and shaken at 28°C. At specific timepoints culture was removed and washed two times with PBS and the final OD₅₉₀ was adjusted to ~ 1.0. Then, 2 ml of bacterial suspension and 600 µl of *n*-hexadecane (Sigma-Aldrich Ltd., UK) were mixed, vortexed for 60 s, and allowed to stand for 15 min for phase separation at RT before OD₅₉₀ values were recorded for the aqueous phase. Percentage hydrophobicity was calculated as follows:

$$\% \text{ hydrophobicity} = \frac{(\text{OD}_{590} \text{ of washed culture} - \text{OD}_{590} \text{ of aqueous phase})}{\text{OD}_{590} \text{ of washed culture}} \times 100 \%$$

2.4.4. Autoaggregation assay

Y. pestis was cultured for 16-18 hr at 28°C with orbital shaking. The cultures were then diluted 1:10 in BAB broth and shaken at 28°C for 4 h. At this point 3 ml culture was transferred into a cuvette and left to stand at room temperature. The OD₅₉₀ was recorded at different timepoints. A reducing OD₅₉₀ reflects the settling of bacterial aggregates.

2.4.5. Minimum inhibitory concentration (MIC) assay

Polymixin B was appropriately diluted in sterile BAB broth to give a stock concentration of 250 µg/ml. This was then doubly diluted across the rows of a 96-well micro-titre plate in triplicate to give a final volume of 100 µl in each well. A row of wells with no polymixin B were included as a positive control for bacterial growth. A row of wells with broth only served as a negative control. 100 µl of a solution of between 10⁵ and 10⁶ cfu/ml *Y. pestis* was overlaid into the appropriate wells. Bacterial counts in this input culture were determined by enumeration on BAB agar plates. The plates were incubated at 28°C and the

optical density of each well at 600 nm recorded at 24 and 48 h. The % survival of bacteria in concentrations of polymixin B were calculated as follows:

$$\frac{(\text{Mean OD}_{600} \text{ of polymixin B wells} - \text{Mean OD}_{600} \text{ of negative control wells})}{(\text{Mean OD}_{600} \text{ of positive control wells} - \text{Mean OD}_{600} \text{ of negative control wells})} \times 100\%$$

The MIC₅₀ (lowest concentration of polymixin B that inhibits the growth of the bacteria by 50%) was calculated from a one-phase exponential decay best fit curve drawn from the average of two independent experiments.

2.4.6. Salt shock assay

Y. pestis was cultured for 16-18 hr at 28°C with orbital shaking. The cultures were then diluted 1:10 in BAB broth and shaken at 28°C for 4 h. At this point 100 µl of the cultures were added to 10 ml NaCl at 0.05 M and 0.5 M and incubated with orbital shaking at 28°C for 3 h. Serial dilutions of the NaCl cultures were plated onto BAB agar for enumeration of bacteria. Bacteria in the input culture were also enumerated % survival in [NaCl] was then calculated as follows:

$$\left[\frac{\text{cfu NaCl culture}}{\text{cfu input culture}} \right] \times 100 \%$$

2.4.7. Preparation of inoculum for animal dosing

Y. pestis was cultured for 16-18 hr at 28°C with orbital shaking. The culture was then diluted 1:10 in BAB broth and incubated at 28°C with orbital shaking until the OD₅₉₀ of the culture reached 0.6 (approx. 5 h). At this point serial dilutions of the culture were made in PBS and the appropriate dilutions taken for the challenge of mice. For the *in vivo* competitive index study the 10⁻⁴ dilution of the appropriate cultures were mixed together to form the inoculum. The actual cfu was measured by enumeration of bacteria plated onto BAB agar.

2.4.8. Infection of macrophage cell line with bacteria

Y. pestis was cultured for 16-18 hr at 28°C with orbital shaking. Subsequently the OD₅₉₀ of the culture was adjusted to 0.6 in BAB broth and then mixed at a 1:1 ratio with complete DMEM. 200 µl of this solution was used to infect 1 x 10⁶ J774 cells (Section 2.6) giving a multiplicity of infection (MOI) of 10. The actual MOIs were calculated by enumeration of bacteria in the input culture by plating on BAB agar, and by cell counting of the J774s. When calculated empirically the average MOI was +/- 30% of the target inoculum. The bacteria were allowed to infect the macrophages for 60 min at 37°C in a sealed container with one CO₂ gas pack (BioMerieux, France) present. Then, 1 ml gentamicin (Sigma-Aldrich Ltd., UK) per well at a final concentration of 10 µg/ml was used to kill extracellular bacteria by incubation with the cells for 45 min. The macrophages were then washed twice in PBS and lysed in 1 ml distilled H₂O. Serial dilutions of this lysate were plated on BAB agar plates with or without appropriate antibiotics for enumeration of intracellular bacteria.

2.5. DNA

2.5.1. Vectors

The mammalian expression vector pcDNA3.2/V5/GW/D-TOPO[®] (Invitrogen, UK, Figure 2-2A) was used to clone genes for expression in mammalian cell lines. The TOPO[®] cloning vector pCR2.1 (Invitrogen, Figure 2-2B) was used for the routine cloning of PCR products for sequencing. The pRL-TK control luciferase reporter vector was used as an internal luciferase control (Promega, UK Figure 2-2 C). The NFκB-luciferase reporter vector and TIR adaptor-expressing vectors (pMyD88, pMal and pTRIF) were kind gifts from Prof. Andrew Bowie (Trinity College, Dublin, ROI). pK2 was a kind gift from Prof. P. Oyston (Dstl, Porton Down, UK, Table 2-4)

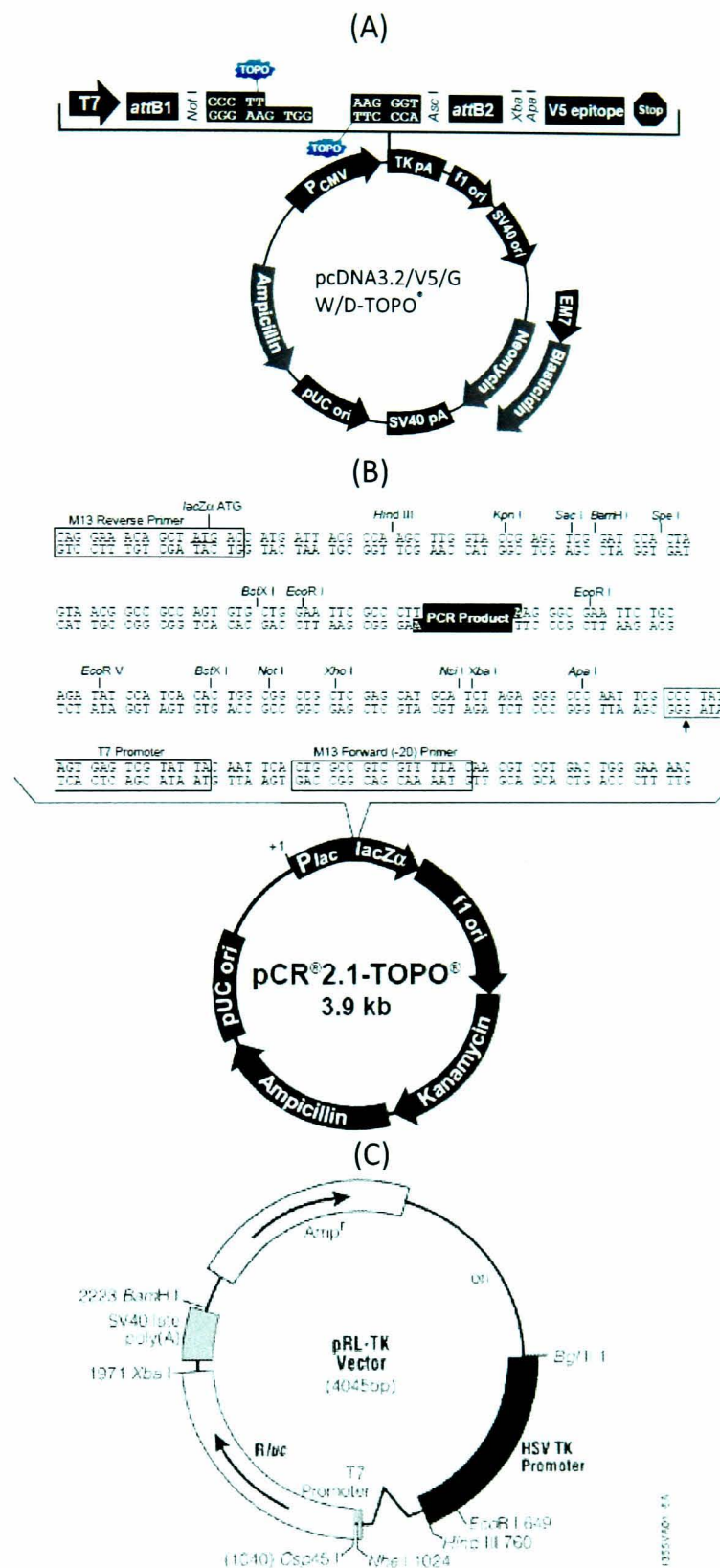


Figure 2-2: Schematic representation of commercially available vectors used in this work

(A) pcDNA3.2V5/GW/D-TOPO[®] vector (Invitrogen) (B) pCR2.1-TOPO (Invitrogen) (C) phRL-TK (Promega)

Vector name	Vector backbone	Antibiotic resistance	Created by	Gifted by	Description
pMyD88	pcDNA3	Eukaryotic: Neomycin Prokaryotic: Ampicillin	Marta Muzio, 1997	Andrew Bowie, TCD	Expresses full-length human MyD88 with AU1 tag
pMal	Information not available	Prokaryotic: Ampicillin	Unknown	Andrew Bowie, TCD	Expresses full-length human Mal with HA tag
pTRIF	Information not available	Prokaryotic: Ampicillin	Unknown	Andrew Bowie, TCD	Expresses full-length human TRIF with Flag tag
pNFκB-luc	pGL3basic (Promega)	Eukaryotic: None Prokaryotic: Ampicillin	Robert Hofmeister	Andrew Bowie, TCD	Reporter construct containing 5 NFκB binding sites upstream of firefly luciferase gene
pK2	pGEM-T-Easy containing kanamycin cassette	Eukaryotic: None Prokaryotic: Kanamycin	Petra Oyston, DstI	Petra Oyston, DstI	Used for amplifying Kan ^R cassette

Table 2-5: Details of vectors used in this study given as gifts

2.5.2. Genomic DNA

Burkholderia pseudomallei K96243 genomic DNA (gDNA) was kindly provided by M. Sarkar-Tyson, *Yersinia pestis* CO92 gDNA was kindly provided by P. Oyston, and *Brucella melitensis* 16M gDNA was kindly provided by S. Perkins (all Dstl, Porton Down, UK).

2.5.3. Polymerase chain reaction (PCR)

The genes encoding bacterial Tdps were amplified from genomic DNA template using PCR and the primers listed in Table 2-6 in 50 μ l reactions. The DNA encoding for residues 130 – 285 of the *YpTdp* gene was amplified from the plasmid pET26b(+)*_YpTIR*, a gift from R. Rana, Imperial College, London, using PCR and the primers listed in Table 2-6 in a 50 μ l reaction. In order to generate a PCR product for the creation of the mutant in *Y. pestis* the kanamycin cassette from vector pK2 was amplified using PCR and the primers listed in Table 2-6. These primers had 20 bases homologous to the kanamycin cassette and 50 nucleotides homologous to the right and left flanking DNA of the gene to be replaced by homologous recombination. These PCRs were carried out using the HotStarTaq[®] Plus DNA polymerase kit (Qiagen, UK). 50 μ l reactions contained 1 μ l gDNA, 0.5 μ l each primer (100 pmol/ μ l), 5 μ l of 10X PCR buffer, 1 μ l dNTP mixture, 0.5 μ l HotStarTaq[®] DNA polymerase and nuclease-free water (Promega, UK) to 50 μ l. Typically, cycling conditions were as follows: 15 min at 95°C for activation of HotStarTaq[®], followed by 30 cycles of 94°C, 30 s for denaturation, 50-55°C, 30 s for annealing, 72°C, 1-3 min extension, followed by 72°C, 10 min for final extension, then hold at 4°C. Specific annealing temperatures and extension times for each PCR can be found in Table 2-6.

Transformed colonies were screened by colony PCR using a T7 promoter primer (5'-TAATACGACTCACTATAGGG-3') and the reverse primers detailed in Table 2-6 using the following process: bacterial colonies for screening taken from agar plates were resuspended in 20 μ l dH₂O, boiled for 5 min and centrifuged at 13,000 rpm for 30 s. Subsequently, 5 μ l of this lysate was screened using PCR in 50 μ l reactions using Taq DNA polymerase (Roche Applied Science, UK). 50 μ l reactions contained 5 μ l colony lysate, 1 μ l each primer (100 pmol/ μ l), 5 μ l of 10x PCR cardload buffer (Qiagen, UK), 1 μ l dNTP mixture, 0.5 μ l Taq

Gene	Primers 5' – 3'	Annealing Temp (°C)	Extension time (sec)
YpTdp	Fwd: <u>CACCATGGCAAGCTGCATCCC</u> Rev: GGGCACAATCTTGTTTACAGTCTCGATAAAT	50	90
BmTdp	Fwd: <u>CACCATGTCTAAAGAGAAACAAGC</u> Rev: GATAAGGGAATGCAGTTCTTTCGC	55	60
BmTdp2	Fwd: <u>CACCATGAATCGTACGCACTGGGC</u> Rev: AAAGGTGATGAGGGCGACGCGCTCGG	55	60
BaTdp	Fwd: <u>CACCATGTATTATCATATTAGAATTA</u> Rev: ATACGTAACCTTTAATCCAGC	50	60
BpTdp	Fwd: <u>CACCATGACAGTTACAATTAAGATGTGGC</u> Rev: GCTTTTTGTTGCATAATGATCGC	55	90
YpTIR	Fwd: <u>CACCATGGCAAGCTGCATCCC</u> Rev: GGGCACAATCTTGTTTACAGTCTCGATAAAT	50	90
Kan + YpTdp flanks	Upstream flank: CAATAACCAATCAAAGCTCACTCAAAGAAGCCACTAAGAGGGACATTATG GATCTGCCACGTTGTGTCTC Downstream flank: AATTTGCCTGTCTCCGTTGTTGGAGTGAAGATATCAAAAACAGGCAATTA GCTCTGCCAGTGTTACAACC	65	60
Exo	Fwd: GCATGACACCGGACATTATC Rev: AGGATGCGTCATCGCCATTG	58	60
Gam	Fwd: TGGGAATTCGAGCTCTAAGG Rev: TGCGAGTGCAGTACTCATTG	58	60
yscC	Fwd: ACAACTGGCTCTGCTAGAAC Rev: TCACAATACGCCACGCTTAG	58	60

Table 2-6: Oligonucleotide PCR primers used in this study

Underlined bases added to 5' end of the Fwd primer allow Directional-TOPO (D-TOPO) cloning into pcDNA3.2. Bases in red represent regions of primer homologous to flanking DNA of a gene, rather than a gene itself. Tdp = TIR domain protein from: Yp (*Yersinia pestis*), Bm (*Brucella melitensis*), Bp (*Burkholderia pseudomallei*), Ba (*Bacillus anthracis*), Bth (*Burkholderia thailandensis*). Kan = kanamycin resistance gene. Fwd = Forward primer, Rev = Reverse primer. PCR for BthTdp was unsuccessful.

DNA polymerase and nuclease-free water (Promega, UK) to 50 µl. Cycling conditions were as follows: 4 min at 94°C, followed by 30 cycles of 94°C, 30 s for denaturation, 65°C, 90 s for annealing, 72°C, 90 s extension, followed by 72°C, 10 min for final extension, then hold at 4°C.

In order to produce the PCR product required for recombination into the *Y. pestis* chromosome the Kanamycin resistance cassette from plasmid pK2 was amplified with the left and right flanking regions of the gene of interest in the *Y. pestis* chromosome incorporated into the primers (Table 2-6). Cycling conditions were as follows: 2 min at 94°C, followed by 30 cycles of 94°C, 60 s for denaturation, 65°C, 60s for annealing, 72°C, 60 s for extension, followed by 72°C, 10 min for final extension then hold at 4°C.

For all PCRs primers were obtained from Euro fins and PCRs were carried out on a 2720 Thermal Cycler (Applied Bio systems, US). DNA was analysed by gel electrophoresis as described in Section 2.5.4.

2.5.4. Agarose gel electrophoresis

Generally analysis of DNA samples was performed by agarose gel electrophoresis using 1.2% pre-cast gels (Invitrogen). PCR samples contained gel loading buffer within the PCR buffer (Cardload buffer, Qiagen, UK) and so samples were diluted 1:4 in dH₂O to a final volume of 20 µl for loading onto the gel. DNA samples not containing loading buffer were diluted 1:10 with DNA loading buffer (Invitrogen Ltd., UK). DirectLoad™ Wide Range DNA ladder (Sigma-Aldrich Ltd., UK) was added to gels alongside the samples for size determination. The gels were run at 70V, 60 mA for 30 min and the DNA was visualised and photographed under UV light using a Gel Doc™ 1000 Molecular Analyst system (Bio-Rad laboratories Ltd., UK).

2.5.5. PCR product purification

PCR fragments were purified from the reaction mixture using QIAquick PCR purification kit (Qiagen, UK) according to the manufacturers' instructions, and eluted in 30 µl nuclease-free distilled water (Promega, UK).

2.5.6. DNA ligation

For PCR product ligation into TOPO vectors the following reaction mixture was used: 1 μ l purified PCR product (purified as Section 2.3.5), 1 μ l vector, 1 μ l salt solution (supplied in TOPO vector kit) plus 3 μ l nuclease-free distilled water (Promega). This was incubated at room temperature (RT) for 5 min. Subsequently, 2 μ l of this ligation mixture was used to transform *E. coli* TOP10 cells (Section 2.5.7).

2.5.7. Transformation of DNA into chemically competent bacteria

Plasmid DNA was transformed into *E. coli* TOP10TM cells (Invitrogen Ltd. UK) by heat shock at 42°C for 30 sec, followed by incubation in SOC broth (Invitrogen Ltd. UK) for 1 h at 37°C, 180 rpm and then the transformants were plated onto selective agar and incubated at 37°C for 16-20 h. Transformants were screened by colony PCR (Section 2.5.3).

2.5.8. Transformation of DNA into electrocompetent bacteria

DNA was electroporated into 1 ml *Y. pestis* at 2.5 V, 200 Ω which was then incubated statically at 28°C overnight with the addition of 500 μ l BAB broth supplemented with 0.8% (v/v) arabinose.

2.5.9. DNA extraction

Plasmid DNA for sequencing was extracted from *E. coli* TOP10TM cells using the QiaSpin Mini prep kit (Qiagen, UK) according to the manufacturer's instructions and eluted in 50 μ l distilled water (Gibco, UK). Plasmid DNA for the transfection of mammalian cell lines was extracted from *E. coli* TOP10TM cells using the QiaSpin Endotoxin-free Maxi-prep kit (Qiagen, UK) according to the manufacturer's instructions and eluted in 500 μ l distilled water (Gibco, UK).

2.5.10. Quantification of DNA

Plasmid DNA was quantified using the absorbance reading at 260 nm as measured using the nanodrop 1000 (Thermo Scientific, US). A ratio of A₂₆₀/A₂₈₀ was used as a measure of DNA purity.

2.5.11. DNA sequencing

DNA sequencing of plasmid DNA was carried out by Cogenics-Lark (Essex, UK) using the T7 promoter forward primer (see Section 2.6.1) and a TKpolyA reverse primer (5' – CTTCCGTGTTTCAGTTAGC – 3'). Sequences were visualised using SeqMan (DNASTAR Lasergene[®] version 7.0).

2.6. Cell culture

2.6.1. Routine maintenance of cell lines

HEK293H cells (Invitrogen, UK) and HEK-Blue[™] hTLR4 cells (InvivoGen, France) were maintained in Complete DMEM or HEK-Blue[™]-DMEM, respectively. Cells were incubated at 37°C in 5% CO₂/95% air (v/v) and maintained as monolayers in sub-confluent growth. The cells were passaged by removal from the monolayer by gentle scraping with a rubber policeman, splitting the cells 1:10 in the appropriate media and seeding into fresh flasks. Cells were stored by freezing in Recovery[™] growth medium (Invitrogen, UK) at a concentration of approximately 10⁶ cells/ml in cryotubes and stored at -80°C.

2.6.2. Seeding of cells for confocal microscopy

Cells for confocal microscopy were seeded onto glass coverslips that had been individually sterilised by autoclaving in 6-well tissue culture plates.

2.6.3. Transient transfection

For the transfection of HEK293 cells with vector DNA for the expression of proteins for Western blot analysis: HEK293H cells (1.5 x 10⁶) were seeded in 100mm dishes in complete DMEM and transfected 24 h later with 24 µg endotoxin-free plasmid DNA as prepared in Section 2.5.9, using Lipofectamine[™] 2000 (Invitrogen Ltd. UK) as manufacturer's instructions. Briefly 60 µl Lipofectamine[™] 2000 was diluted in 1.5 ml Opti-MEM[®] serum free media (Invitrogen Ltd. UK) and incubated for 5 min at room temperature. Meanwhile 24 µg DNA was also diluted in 1.5 ml of Opti-MEM[®]. The diluted Lipofectamine[™] 2000 and DNA were then combined and incubated for 20 min at room temperature. These complexes were then added to the cells and allowed to incubate with the cells for 24 h.

For NFκB luciferase reporter assays HEK293H cells (2×10^4 per well) were seeded into 96-well plates and transfected 24 h later with 60 ng pNFκB-luc, 20 ng pRL-TK, and 150 ng experimental/control vector with Genejuice[®] (Merck Biosciences, UK) as manufacturer's instructions. The cells were then incubated 37°C, 5 % CO₂ for 16 h prior to stimulation.

For NFκB SEAP reporter assays HEK-Blue[™] hTLR4 Blue cells (InvivoGen, France) were seeded (5×10^5 per well) in 6-well plates and transfected 24 h later with 4 μg experimental/control/stimulation vector DNA using Lipofectamine[™] 2000 (Invitrogen Ltd. UK). Cells were left to recover for 24 h before stimulation with exogenous ligand.

2.6.4. Stimulation of cells

For NFκB luciferase reporter assays downstream of IL-1β and TNFα, cells were stimulated *in situ* in the 96-well plates in which they were transfected. The cells were stimulated with 100 ng/ml IL-1β (BD biosciences, UK) or 100 ng/ml TNFα (Sigma Aldrich Ltd. UK) in complete DMEM for 6 h at which point the cells were lysed for analysis. Where appropriate, supernatants were removed for analysis.

For NFκB SEAP reporter assays (exogenous stimulation) HEK-Blue[™] hTLR4 cells were detached from the monolayer by gentle scraping with a rubber policeman, enumerated and adjusted to 2.8×10^5 cells/ml. Subsequently, 180 μl of this suspension was re-seeded with 20 μl *E. coli* K12 LPS (InvivoGen, France) to a final concentration of 1 μg/ml in HEK-Blue[™]-DMEM in a 96-well plate. Cells were then incubated at 37°C with 5% (v/v) CO₂ for 24 h. For NFκB SEAP reporter assays down-stream of TIR adaptor expression (stimulation occurs via protein expressed from introduced DNA vector) constructs expressing stimulant were transfected at the same time as experimental/control vectors and therefore stimulation occurs simultaneously. Where appropriate, supernatants were removed for analysis.

2.6.5. Preparation of cell lysates

At 24 h post transfection media was removed and the cells washed twice with 1ml ice-cold PBS and scraped using a rubber policeman into 1ml ice-cold Cytobuster[™] (Merck Biosciences, UK), RIPA+PI (Section 2.2) or homemade lysis buffers (Section 2.2). The cells were lysed on ice for 5-30 min and then spun at 13,000 rpm for 5 min at 4°C to

remove cell debris. The supernatant was either then used immediately to make SDS-PAGE samples for Western blotting (Section 2.7.2.1) or frozen at -20°C for future use.

The lysis of cells for measurement of luciferase activity was carried out by removing media from the cells, washing the monolayer gently with $50\ \mu\text{l}$ PBS and subsequent incubation with $20\ \mu\text{l}$ Passive Lysis Buffer (PLB, Promega, UK) for 20 min at RT with gentle agitation.

2.6.6. Measurement of luciferase activity

Firefly and Renilla luciferase activity were measured by addition of the substrates for these luciferases supplied within the Dual-Luciferase[®] reporter assay system (Promega, UK) and subsequent analysis of light released by a ThermoFisher MultiSkan luminometer and Ascent software. $100\ \mu\text{l}$ of the firefly luciferase substrate (LARII) was added to the cell lysates by automatic injection using the system in the luminometer and readings were taken using a pre-programmed 10 s integration assay on the Ascent software (Thermo Scientific, UK). $100\ \mu\text{l}$ of Renilla luciferase substrate plus a quenching reagent for the firefly reaction (Stop and Glo[®], Promega, UK) was then added to the lysates by automatic injection and further readings were taken. Results were displayed as relative luciferase units (RLU) and the firefly results were normalised by division by the Renilla readings.

The RLU values in the presence of the bacterial Tdps were then normalised as a % NF κ B activity compared to control (EV) by dividing the mean RLU in the presence of a Tdp by the mean RLU in the presence of EV and multiplying by 100 to give a %. This was done for unstimulated (basal NF κ B activity) and IL-1 β - and TNF α -induced activity for each independent experiment. Table 2-7 demonstrates this for one experiment.

2.6.7. Measurement of alkaline phosphatase activity

Measurement of NF κ B activity in the HEK-Blue[™] hTLR4 cells downstream of TLR4 did not require the lysis of cells as the SEAP enzyme was exported from the cells into the supernatant. Therefore, $40\ \mu\text{l}$ supernatant was removed from cells and added to $160\ \mu\text{l}$ of SEAP substrate present in Quanti-Blue[™] reagent made to the manufacturer's instructions (InvivoGen, France). This was then incubated for 15 - 60 min and optical absorbance at 620

	EV Unstimulated	BthTdp Unstimulated	EV IL-1 β	BthTdp IL-1 β	EV TNF α	BthTdp TNF α
	36.105820	13.958240	449.128600	70.728070	1239.951	368.8932
	47.018120	16.405930	405.904400	61.281320	2481.257	349.9248
	23.833220	10.079630	433.837200	32.558910	2077.023	NR
Mean	35.65239	13.48127	429.6234	54.8561	1932.744	359.409
	Basal NF κ B activity		IL-1 β -induced NF κ B activity		TNF α -induced NF κ B activity	

Table 2-7: Example normalisation of NF κ B activity in the presence and absence of stimulation.

To calculate the % basal NF κ B activity in the presence of BthTdp compared with EV the mean RLU value for unstimulated cells in the presence of BthTdp (green box) was divided by the mean RLU value for unstimulated cells in the presence of EV (red box) multiplied by 100 to give a %. This was repeated for all independent experiments.

nm measured at defined intervals. Results were used when the majority of values (unstimulated and stimulated) were between 0.1 and 1. Normalisation to % NF κ B activity was done in a similar manner to the luciferase reporter assays (Table 2-7).

2.6.8. Cell viability assays

Cells were scraped in the media in which they had been growing and a sample diluted 1:1 with trypan blue. The percentage of dead cells (having taken up the trypan blue dye) was calculated using the Cellometer™ Auto T4 cell counter (PEQLAB Ltd., Germany).

2.6.9. Staining of cells for confocal microscopy

Media was removed from the cells and replaced with fixative (3 % w/v) paraformaldehyde (PFA) in PBS and incubated at RT for 15 min. Fixative was then removed and replaced with perm/quench solution (Section 2-2) which was immediately replaced with fresh perm/quench solution and incubated at RT for 15 min. The perm/quench solution was then removed and replaced with PGAS (Section 2-2) and incubated at 30 min RT or 4°C overnight. Primary antibodies were then diluted 1:500 in PGAS and incubated with the fixed cells for 1 h at RT. The cells were then washed three times with PGAS for 5 min and the twice for 3 min. The secondary antibodies were then diluted in PGAS and incubated with the cells for 1 hr in the dark. The cells were then washed as above with PGAS and once with PBS before being viewed under the confocal microscope.

2.7. Protein methods

2.7.1. Antibodies

Bacterial Tdps were detected using a rabbit-anti-V5 IgG polyclonal antibody (Santa Cruz Biotechnology, Germany) and a goat-anti-rabbit HRP-linked IgG secondary antibody (Bio-Rad laboratories, UK). MyD88 was detected using a rabbit-anti-AU1 primary antibody (Santa Cruz Biotechnology, Germany) and secondary antibody as above. These antibodies were also used for co-immunoprecipitation. For immunofluorescence studies V5-tagged proteins were detected using the primary antibody as above followed by a goat-anti-rabbit IgG-AlexaFluor® 488 secondary antibody. MyD88 was detected using a mouse-anti-MyD88 IgG2a primary antibody followed by a donkey-anti-mouse IgG-TexasRed secondary antibody (all Santa Cruz Biotechnology, Germany).

2.7.2. Western blot

2.7.2.1. The production of SDS Polyacrylamide Gel Electrophoresis (SDS-PAGE) samples

Cell lysates produced according to Section 2.6.5 were diluted 1:1 in 2 x Laemmli sample buffer (Sigma Aldrich Ltd., UK). The samples were then boiled for 3 min and used immediately or stored at RT for use the next day or -20°C for longer-term storage.

2.7.2.2. SDS-PAGE

Lysates were resolved by SDS-PAGE using pre-cast 4–12 % Tris-glycine gels using the Xcell *SureLock* Mini-Cell system and 1 x Tris-glycine running buffer (all Invitrogen Ltd. UK) at 125 V for 2 hr. A mixture of MagicMark™ and SeeBlue Plus™ protein standards (both Invitrogen Ltd., UK) at a 1:15 ratio were used for protein size determination and blotting efficiency.

2.7.2.3. Transfer of Proteins to Membrane

The resolved proteins were transferred to Immobilon-P polyvinylidene difluoride (PVDF) membrane (Sigma-Aldrich, UK) using a semi-dry transfer system (Invitrogen Ltd. UK). The membrane was activated in 100 % methanol, washed in water and then soaked in transfer buffer (Section 2.2). All other components of the stack for transfer (gel, filter paper) were also soaked in transfer buffer. A constant voltage of 20 V was then applied for 40 min.

2.7.2.4. Antibody Blotting

PVDF membranes were blocked for non-specific binding by incubation in BLOTTO (Section 2.2) at RT for 2 h. The membrane was washed for 5 minutes in PBST (Section 2.2) and then incubated for 2 h at RT or at 4°C overnight with primary antibody diluted 1:1000 in BLOTTO. Next, the membrane was washed a further three times in PBST and incubated with a horseradish peroxidase-linked secondary antibody diluted 1:1000 or 1:2000 in BLOTTO for 1 h at RT.

2.7.2.5. Detection of immunoblot by Enhanced Chemiluminescence (ECL)

Following incubation of Western blots with secondary antibody (Section 2.7.2.4), the PVDF membranes were washed for 3 x 5 min and then for 1 x 15 min with PBST and then incubated with ECLPlus™ reagent according to manufacturer's instructions (GE healthcare, UK). The membranes were wrapped in SaranWrap™ and placed in an X-ray film cassette for exposure to autoradiography film, enabling visualisation of the Western blot.

2.7.3. Co-immunoprecipitation

Cells in 100 mm dishes were transiently transfected with vectors expressing the two proteins of interest (Section 2.6.3) then lysed in 850 µl of the appropriate lysis buffer (Sections 2.2, 2.6.5). Then, 50 µl of this lysate was used to make SDS-PAGE samples and the remaining lysate split for co-immunoprecipitation using an antibody to one of the proteins attached to protein G sepharose beads (Sigma-Aldrich Ltd., UK). Antibody was either pre-coupled to the beads overnight at 4°C, or separate antibody and beads added to the lysate for coupling. The lysate was incubated with beads plus antibody overnight at 4°C. The beads were then sedimented at 1000 rpm for 3 min, the supernatant removed and the beads washed in combinations of lysis buffer and then PBS between 5 and 7 times. Finally the beads were resuspended in 50 µl Laemmli buffer (Sigma-Aldrich Ltd., UK) and boiled for 3 min.

2.7.4. Enzyme-linked immunosorbant assay (ELISA)

For the determination of IL-8 concentrations in cell supernatants a BD OptEIA™ Set Human IL-8 (Becton Dickinson (BD) Biosciences) was used to manufacturers' instructions. Briefly, 96-well plates were coated with 100 µl per well of mouse anti-human IL-8 antibody diluted 1:250 in coating buffer (BD biosciences, UK). Plates were covered and incubated at 4°C overnight or a maximum of 72 h. Plates were washed twice in wash buffer (Reagent Set B, BD biosciences, UK) and then blocked with 250 µl per well of assay diluent (BD biosciences, UK) and incubated at RT for 1-2 h before further washing. Either IL-8 standards (in the range of 0.03 - 0.2 ng/ml) or samples were added at 100 µl per well and incubated for 2 h at RT, then plates were washed 3 times. 100 µl of biotinylated anti-human IL-8 antibody (BD biosciences, UK) diluted 1:250 in assay diluent plus Streptavidin conjugated to horseradish peroxidase (SAv-HRP) reagent (BD biosciences, UK) diluted

1:250 in the Detection antibody mixture were added to each well. Plates were incubated at RT for 2 h and then washed 7 times. Then 100 μ l of substrate solution was added to each well and incubated in the dark for 30 mins followed by the addition of 50 μ l of Stop solution added to each well and the absorbance from each well measured at 450 nm using a ThermoFisher microplate reader. Standard curves were constructed relating IL-8 concentrations to absorbance at 450 nm and were used to determine IL-8 concentrations.

2.8. Statistics

All transformations of data and statistical tests were performed using GraphPad Prism[®] 5 software (GraphPad, US). A *p* value of <0.05 was considered significant for all studies.

Chapter 3: Identification of TIR domain proteins in bacteria

3.1. Introduction

Since the recent discovery that proteins containing TIR domains are present in bacteria, it has been postulated that the function of these proteins in bacteria is to interact with, and modulate, eukaryotic TIR-dependent immune signalling pathways in order to evade these responses. Pathogenic organisms engage in a wide variety of immunomodulatory activities and disruption of early detection methods, such as TLR signalling, is of paramount importance. This fact, combined with the experimental data on bacterial TIR domain proteins, means it is logical to postulate this role for bacterial TIR domain proteins in immune subversion, and the disruption of their immunomodulatory activities at this point could form a common point of intervention for therapy. It would therefore be interesting to know whether highly pathogenic organisms deemed to be a public health risk encode proteins containing TIR domains capable of disrupting the mammalian immune response.

Although Newman *et al.* reported that they had produced a list of bacterial Tdps before their subsequent evaluation of the Tdp from *S. enteritidis*³⁴², this list was not published. Therefore, in order to assess whether Tdps are present in highly pathogenic bacteria deemed to be a potential public health threat, a new survey of Tdps in bacteria will need to be carried out. Searches of this nature are done by taking a protein sequence known to contain an area of interest (i.e. the TIR domain) and comparing this sequence to other sequences in a database and assessing their similarity. This has been made infinitely easier by the advent of automated computer tools.

The enormous pace with which genetics and computational biology have progressed now means that all researchers have a wide variety of sophisticated and intuitive computational tools with which to probe protein structure, function and evolutionary relationships available at their fingertips before even reaching the bench. One of the most useful advances in this field is the creation of large curated databases of sequence information, allowing one to search for genes or proteins by organism, protein name, function, structure or homology. A leader in this area is the National Centre for Biotechnology Information (NCBI). Not only do they provide up-to-date databases of nucleotide and protein sequences but also a vast array of tools for their investigation. One of the most useful and widely used

tools created by NCBI is their Basic Local Alignment Search Tool (BLAST). This program uses an algorithm that allows the researcher to compare a query sequence (seed) with a database of sequences (both nucleotide and amino acid) to identify sequences that resemble the seed. The search for homologous sequences is an indispensable tool in the study of evolution and the function of proteins. The presence or absence of particular proteins or domains within whole groups of organisms informs the timeline of evolution. BLAST would therefore be a useful tool for investigating whether bacterial species possess proteins that contain TIR domains using seed sequences of already-defined TIR domains.

BLAST finds homologous sequences by locating short matching sequences (“words”) between the query sequence and those in the database, rather than comparing the whole length of the protein. For the protein search version of BLAST (BLAST-p) the default word size is 3 amino acids. This process of finding initial words is called “seeding.” BLAST then begins to make local alignments and matches are reported that are statistically similar to the seed sequence (measured by the “expect” (e) value for which a threshold is set; $e < 0.05$ is the default value). In this way BLAST-p finds the protein sequences most homologous to a protein of interest. TIR domains show relatively little sequence conservation either within, or between, species, however, and are therefore likely to have significantly diverged throughout evolution. BLAST-p would be insufficient to find these hits. An iterative version of the program, however, was designed just for this purpose. In this search strategy a single protein sequence is entered again as a “seed” and a round of BLAST-p is initiated. Results are listed in the standard way, but these proteins are now combined into a general “profile” sequence which summarises significant features present in these sequences. A BLAST-p search is now run using this profile. A larger group of proteins is now found and this group is used to construct another profile and the process is then repeated for a set number of iterations or until no new results are found. Before each iteration the list of proteins found by the previous iteration can be checked and the next iteration must then be manually initiated.

A derivative of PSI-BLAST was developed at the Burnham Institute in California called Saturated BLAST. Saturated BLAST automatically carries out a user-defined number of PSI-BLAST iterations without the researcher having to manually initiate each iteration. The program, along with an appropriate database of sequences to search, needs to be

downloaded rather than using a web server. This program was used by Newman *et al.* for their survey of Tdps in bacteria and so may prove useful here.

Once a list of Tdps in bacteria of interest has been accumulated, using the search strategies discussed, other bioinformatic tools can be used to confirm the presence of a TIR domain in these proteins. The fact that TIR domains show relatively little sequence conservation suggests that only a proportion of the residues within the domain are crucial for function and that their secondary and tertiary structure are also important factors. Distant homologues identified using PSI-BLAST can therefore be confirmed using bioinformatic programs that investigate the similarity in secondary structure between proteins in addition to tools investigating their primary sequence. In addition, reverse PSI-BLAST searches should be initiated using the bacterial Tdp result as a seed to ensure the original seed can be found in this way.

Initially Saturated BLAST using the NCBI nr sequence database was chosen as the search strategy for identifying Tdps in bacterial species. A selection of known TIR domain sequences were chosen as seeds (Table 2-1). These were primarily mammalian TIR domain sequences since the bacteria of interest in this study are mammalian pathogens and in order to interact with, and modulate, a mammalian immune response it seemed logical that these sequences would be most similar to mammalian sequences. Tdp seeds from other phylogenetic groups were then included to evaluate whether these produced new bacterial Tdp results. During the use of Saturated BLAST it became apparent that this bioinformatics approach was limited in the manner it was being employed and thus an alternative approach was then taken using the PSI-BLAST search tool on the NCBI web server. This approach is more time-consuming as the results are manually monitored and collated but was both intrinsically more reliable, and more intelligently used.

3.2. Aims and objectives

The aim of this Chapter is to investigate whether proteins containing TIR domains are encoded within the genomes of bacterial species classified as bioterrorism agents, and to investigate their sequence and structural features bioinformatically before functional studies are carried out. Tdps have already been identified in bacterial species and been shown to modulate immune signalling (as discussed in Section 1.5.3.1). Since this function depends

on the interaction of TIR domains, their sequence and structural features may provide information as to their likely mode of action.

The specific aims of this Chapter are to:

- Compile a list of TIR domain proteins within Category A and B bacterial pathogens using a PSI-BLAST search strategy (either Saturated BLAST or PSI-BLAST on the NCBI server).
- Confirm the presence of a TIR domain within these proteins using reverse PSI-BLAST searches, a secondary structure homology tool (FUGUE) and domain alignments (Clustal W, Pfam).
- Down-select a list of proteins for functional characterisation of their effect on mammalian immune signalling *in vitro*
- Probe the sequence features of the down-selected proteins using multiple sequence alignments (Clustal W).

3.2.1. Nomenclature

Proteins containing TIR domains have been given a variety of acronyms in the literature including “TIR-containing proteins” (Tcps), in the case of the bacterial TIR proteins from *E. coli* and *B. melitensis*⁴⁴⁰, and “TIR-like proteins” (Tlps) in the case of the TIR domain proteins from *S. enteritidis* and *P. denitrificans*^{342,441}. The “TIR-like” nomenclature is misleading as it does not infer a directly evolutionary relationship. Thus, throughout this study proteins containing TIR domains have been referred to as “TIR domain proteins” and therefore will use the acronym “Tdp” for the bacterial TIR domain protein nomenclature.

3.3. Results

3.3.1. Bacterial TIR domain protein results from Saturated BLAST

Initially the bioinformatics program Saturated BLAST was used to find bacterial proteins with homology to known TIR protein sequences. The program was downloaded onto the Dstl server by Bry Lingard (Dstl, Porton Down) and run on the Windows operating system using the NCBI nr database also downloaded to the Dstl server in September 2006. Nineteen protein sequences were used as seeds for these bioinformatic searches (Table 2-1, Section 2.1). Each seed was entered into the program and the number of iterations to be run was set at five (all other parameters as default). When these iterations had finished, proteins in bacteria of interest were identified by searching for the species name. All results from bacteria of interest were recorded manually. These proteins were then subjected to reverse Saturated BLAST searches using the same parameters (Section 2.1.1), secondary fold prediction using the homology search tool FUGUE (Section 2.1.3) and multiple alignments using the ClustalW algorithm (Section 2.1.7). The Saturated BLAST searches produced many proteins in Category A and B agents but it became apparent during the confirmatory bioinformatic tests that most of these did not meet the criteria for possessing a TIR domain. This raised concerns that these searches had produced many false positives. Nevertheless, using the confirmatory tests it was decided that four proteins from Category A and B agents were likely to contain a TIR domain (Table 3-1). One protein identified is the *S. enteritidis* TIR protein TlpA which therefore does confirm the ability of this search strategy to find previously characterised bacterial Tdps. The three newly discovered proteins (y2426 in *Y. pestis* KIM, BMEI1674 in *B. melitensis* 16M and BPSL0748 in *B. pseudomallei* K96243), plus one from a model organism for the Category B agent *B. pseudomallei* (BTH_I3242 from *B. thailandensis*) were down-selected for experimental investigation and are discussed briefly below.

Category A	TIR domain protein?	Protein
Bacillus anthracis	No	-
<i>Yersinia pestis</i>	Yes (1)	Equivalent to y2426 in <i>Y. Pestis</i> KIM, conserved across strains
Variola virus	No	-
<i>Francisella tularensis</i>	No	-
Filoviruses	No	-
Arenaviruses	No	-
Category B		
<i>Brucella</i> sp.	Yes (1)	Equivalent to BMEI1674 in <i>B. melitensis</i> 16M, conserved across strains.
<i>Salmonella</i> sp.	Yes (1), certain strains	TlpA from <i>Salmonella enteritidis</i>
<i>E. coli</i> O157:H7	No	-
<i>Shigella</i> sp.	No	-
<i>Burkholderia mallei</i>	No	-
<i>Burkholderia pseudomallei</i>	Yes (1), certain strains	BPSL0748 in <i>Burkholderia pseudomallei</i> K96243.
<i>Chlamydia psittaci</i>	No	-
<i>Coxiella burnetti</i>	No	-
<i>Rickettsia prowaceki</i>	No	-
Alphaviruses	No	-

Table 3-1: TIR domain proteins in CDC Category A and B agents (Saturated BLAST search strategy)

This table details the distribution of TIR domain proteins in CDC Category A and B agents as found using the Saturated BLAST search strategy followed by further down-selection using reverse Saturated BLAST searches, assessment of secondary structure homology (FUGUE) and multiple sequence alignments.

3.3.1.1. *Yersinia pestis*

The Saturated BLAST searches and confirmatory analysis revealed one Tdp conserved across genome sequenced *Y. pestis* strains corresponding to y2426 in *Y. pestis* KIM (referred to as YpTdp throughout this manuscript to avoid strain specificity). This protein produced human Tdps on reverse Saturated BLAST, its TIR domain aligned well with other TIR domains and it was classified as “Likely” (Section 2.1.3) to contain a TIR domain from FUGUE analysis ($p < 0.05$).

3.3.1.2. *Brucella melitensis*

The Saturated BLAST searches and confirmatory analysis revealed one Tdp in *Brucella* sp., corresponding to BMEI1674 in *B. melitensis* 16M. This protein is conserved across *Brucella* sp. and so is referred to as BmTdp throughout this manuscript to avoid strain specificity. BmTdp produced human Tdps on reverse Saturated BLAST, its TIR domain aligned well with other TIR domains and it was classified as “Certain” (Section 2.1.3) to be a TIR domain from FUGUE analysis ($p < 0.001$)

3.3.1.3. *Burkholderia pseudomallei* and *Burkholderia mallei*

The Saturated BLAST searches and confirmatory analysis found no Tdps in *B. mallei*. The searches did find two Tdps in species of *Burkholderia* that are not considered to be pathogenic (*B. thailandensis* and *B. xenovorans*), although *B. thailandensis* is studied for its pathogenicity in immunocompromised patients, particularly those suffering with cystic fibrosis and *B. thailandensis* is also used as an ACDP (Advisory Committee on Dangerous Pathogens) level 2 model organism for *B. pseudomallei* (which is an ACDP level 3 pathogen).

The Saturated BLAST searches did find a potential Tdp in *B. pseudomallei*. However, this protein (BPSL0748 in strain K96243, called BpTdp throughout this thesis) gave mixed results from the confirmatory bioinformatic analysis. In reverse Saturated BLAST analysis it only produced two human Tdps in the final iterations, but in multiple sequence alignment analysis it appeared to possess some sequence motifs characteristic of a TIR domain and had strong sequence conservation in Box 2. FUGUE analysis, however, did not confirm its identity as a TIR domain. When the Tdp from vaccinia virus (A46) was subjected to similar

bioinformatic tests it too produced conflicting findings (some sequence conservation but not deemed to be structurally homologous to TIR domains using FUGUE) and yet functionally the data for its ability to disrupt TIR-dependent signalling events was strong. It was therefore decided that BpTdp should be down-selected for experimental investigation.

3.3.2. TIR domain protein results from PSI-BLAST

For a variety of reasons it was realised that the Saturated BLAST searches had not produced the most reliable, or easily collatable, results. Therefore the search for Tdps in bacterial species was performed again using the PSI-BLAST search tool on the NCBI web server in 2008. Eighteen characterised eukaryotic TIR domain sequences were used as seeds and the results were collated into one list by Dr. Nick Loman at the University of Birmingham. The way in which the searches were run is as follows. Figure 3-1 shows the front screen of a PSI-BLAST search. The seed sequence is entered into the box marked in red. The database of sequences to compare the seed sequence to is selected from a drop-down menu (blue arrow). The type of protein Blast is selected (green arrow). The parameters of the search, such as word size, or the statistical cut off for the inclusion of alignments, can also be changed. Features that are altered from default are then highlighted in yellow. In these searches all parameters were left as default except the number of results returned in one iteration (1000).

After the first iteration is initiated a results screen will appear. The results are shown graphically (top 100 results, Figure 3-2A), as a list (Figure 3-2B), and as detailed pairwise alignments Figure 3-2C). The list of sequences producing significant alignments is used to form the profile for the next iteration of the search which is started by pressing “Go” (Figure 3-2B, red arrow). The results table of sequences from the second iteration is shown in Figure 3-3. “New” sequences, not found in the previous search are now involved in creating the sequence profile for the next search (Figure 3-3). Eventually no new sequences will be produced and these PSI-BLAST searches were run until this point.

blastn blastp blastx tblastn tblastx

BLASTP programs search protein databases using a protein query. [more...](#) [Reset page](#) [Bookmark](#)

Enter Query Sequence

Enter accession number, nt, or FASTA sequence Clear From To

Or, upload file

Job Title Enter a descriptive title for your BLAST search

Align two or more sequences

Choose Search Set

Database

Organism Enter organism common name, binomial, or tax id. Only 20 top taxa will be shown

Exclude Models (XM/XP) Uncultured/environmental sample sequences

Entrez Query Enter an Entrez query to limit search

Program Selection

Algorithm blastp (protein-protein BLAST) PSI-BLAST (Position-Specific Iterated BLAST) PHI-BLAST (Pattern Hit Initiated BLAST) Choose a BLAST algorithm

BLAST Search database Non-redundant protein sequences (nr) using PSI-BLAST(Position-Specific Iterated BLAST) Show results in a new window

Algorithm parameters Note: Parameter values that differ from the default are highlighted in yellow and marked with * sign

General Parameters

Max target sequences Select the maximum number of aligned sequences to display

Short queries Automatically adjust parameters for short input sequences

Expect threshold

Word size

Max matches in a query range

Scoring Parameters

Matrix

Gap Costs

Compositional adjustments

Filters and Masking

Filter Low complexity regions

Mask Mask for lookup table only Mask lower case letters

PSI/PHI BLAST

Upload PSM

PSI-BLAST Threshold

Pseudocount

BLAST Search database Non-redundant protein sequences (nr) using PSI-BLAST(Position-Specific Iterated BLAST) Show results in a new window

Figure 3-1: Screen shot of the first page of the web-based PSI-BLAST search

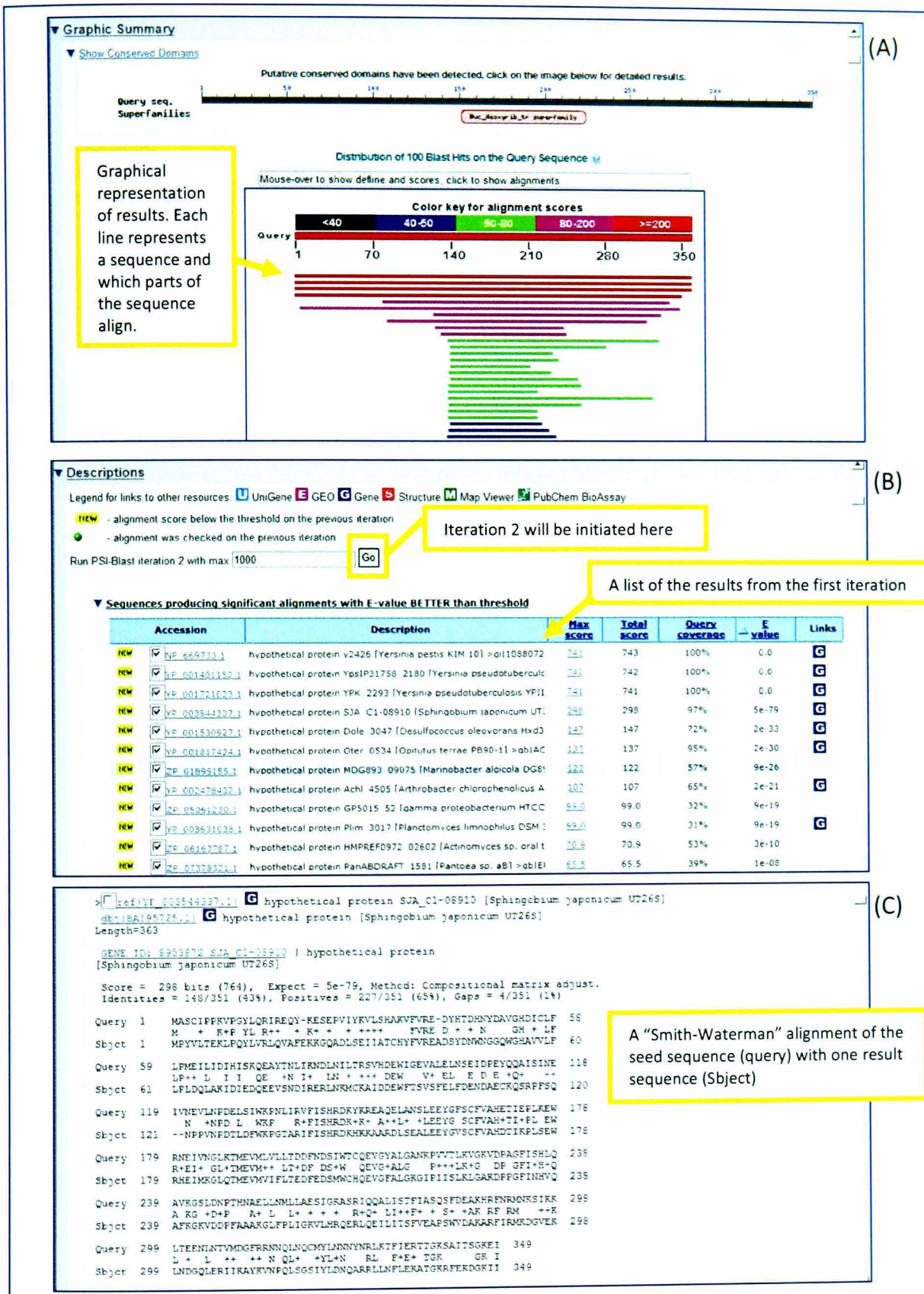



Figure 3-2: Screen shots of PSI-BLAST results

(A) Graphical representation of aligned hits, (B) List of sequences whose alignment score is better than threshold and will be used to make the sequence profile for the next iteration of searches (C) Full Smith-Waterman alignments are shown for each significant hit.

Descriptions

Legend for links to other resources: [U](#) UniGene [E](#) GEO [G](#) Gene [S](#) Structure [M](#) Map Viewer [P](#) PubChem BioAssay

NEW - alignment score below the threshold on the previous iteration
 - alignment was checked on the previous iteration

Run PSI-Blast iteration 3 with max

Sequences producing significant alignments with E-value BETTER than threshold






































Accession	Description	Max score	Total score	Query coverage	E value	Links
 YF_669733.1	hypothetical protein v2426 [Yersinia pestis KIM 10] >qi 1088072	523	523	100%	2e-146	G
 YF_001401152.1	hypothetical protein YpsIP31758_2180 [Yersinia pseudotubercu	522	522	100%	3e-146	G
 YF_001721023.1	hypothetical protein YPK_2293 [Yersinia pseudotuberculosis YPII	521	521	100%	7e-146	G
 YF_003544337.1	hypothetical protein SJA_C1-08910 [Sphingobium japonicum UT:	446	446	97%	3e-123	G
 YF_001817424.1	hypothetical protein Oter_0534 [Opitutus terrae PB90-1] >qb AC	370	370	96%	2e-100	G
 YF_001530927.1	hypothetical protein Dole_3047 [Desulfococcus oleovorans Hxd3	294	294	81%	1e-77	G
 YF_002478432.1	hypothetical protein AchI_4505 [Arthrobacter chlorophenolicus A	260	260	69%	2e-67	G
 ZF_01895155.1	hypothetical protein MDG893_09075 [Mannibacter alqicola DG8:	235	235	66%	7e-60	
 ZF_05061230.1	hypothetical protein GPS015_52 [gamma proteobacterium HTCC	198	198	58%	8e-49	
 ZF_06163787.1	hypothetical protein HMPREF0972_02602 [Actinomyces sp. oral t	198	198	53%	1e-48	
 ZF_06608649.1	conserved hypothetical protein [Actinomyces odontolyticus F030:	188	188	52%	9e-46	
 YF_003631038.1	hypothetical protein Plm_3017 [Planctomyces limnophilus DSM :	162	162	51%	8e-38	G
 ZF_07378321.1	hypothetical protein PanABDRAFT_1581 [Pantoea sp. aB] >qb E	141	141	51%	1e-31	
 YF_003422761.1	hypothetical protein mru_0017 [Methanobrevibacter ruminantium	129	129	38%	4e-28	G
 ZF_03127954.1	hypothetical protein CFE428DRAFT_1119 [Chthoniobacter flavus	128	128	30%	9e-28	
 YF_003478749.1	hypothetical protein Nmaq_0601 [Natrialba maqadii ATCC 43099	128	128	33%	1e-27	G
 YF_003403464.1	hypothetical protein Htur_1906 [Haloterrigena turkmenica DSM 5	125	125	33%	8e-27	G
 ZF_06882326.1	TIR protein [Clostridium lentocellum DSM 5427] >ab EFH00401:	124	124	29%	2e-26	
 YF_932769.1	putative transmembrane sensor protein [Azoarcus sp. BH72] >e	118	118	30%	1e-24	G
 ZF_02207914.1	hypothetical protein COPEUT_02740 [Coprococcus eutactus ATC	117	117	52%	2e-24	
NEW  YF_003357256.1	hypothetical protein MCP_2201 [Methanocella paludicola SANA	106	106	39%	5e-21	G
NEW  YF_003356930.1	hypothetical protein MCP_1875 [Methanocella paludicola SANA	105	105	29%	9e-21	G
 ZF_02635815.1	hypothetical protein AC1_0162 [Clostridium perfringens B str. A	105	105	27%	1e-20	
NEW  YF_556469.1	hypothetical protein Bxe_C1258 [Burkholderia xenovorans LB40	102	102	39%	5e-20	G
 ZF_05920392.1	conserved hypothetical protein [Pasteurella daamatis ATCC 433:	102	102	25%	1e-19	
 YF_002379525.1	hypothetical protein PCC7424_4289 [Cyanotheca sp. PCC 7424]	102	102	26%	1e-19	G
NEW  YF_001792827.1	PASTA domain-containing protein [Leptothrix cholodnii SP-6] >q	97.9	97.9	29%	2e-18	G
NEW  ZF_04291326.1	PASTA domain containing protein [Bacillus cereus R309803] >ab	97.5	97.5	60%	2e-18	
NEW  ZF_04547760.1	conserved hypothetical protein [Bacteroides sp. D1] >ref ZP_05	96.3	96.3	37%	6e-18	
NEW  YF_003167540.1	protein of unknown function DUF323 [Candidatus Accumulibacter	95.2	95.2	48%	1e-17	G
NEW  ZF_01115188.1	TIR domain protein [Reinekea sp. MED297] >ab EAR08896.1 TI	92.5	92.5	39%	9e-17	
 YF_001657146.1	hypothetical protein MAE_21320 [Microcystis aeruginosa NIES-8:	91.7	91.7	25%	1e-16	G
 CAO87660.1	unnamed protein product [Microcystis aeruginosa PCC 7806]	91.3	91.3	25%	2e-16	
NEW  YF_001762975.1	TIR protein [Shewanella woodyi ATCC 51908] >ab ACA88880.1	89.8	89.8	40%	5e-16	G
NEW  YF_003847289.1	TIR protein [Gallionella capsiferiformans ES-2] >ab ADL55525:	89.8	89.8	35%	5e-16	G
NEW  YF_003847279.1	TIR protein [Gallionella capsiferiformans ES-2] >ab ADL55515:	88.6	88.6	34%	1e-15	G
NEW  YF_003407886.1	TIR protein [Geodermatophilus obscurus DSM 43160] >ab ADB7	86.7	86.7	53%	4e-15	G

Figure 3-3: Screen shot of the second iteration of a PSI-BLAST search

Green circles next to the results represent sequences that were statistically significant in the first iteration. A yellow “new” symbol denotes a new sequence to this iteration.

For the PSI-BLAST searches the survey of Tdps was extended beyond bacterial species to include fungi, archaea and viruses to assess the distribution of Tdps in the unicellular (or noncellular, in the cases of viruses) world. The searches were run with all sixteen seeds and then the results were formatted for bacteria, fungi, archaea and viruses. The results were then collated into a list giving a final number of 922 bacterial proteins containing a TIR domain (for summary of results see Table 3-3, a full list of results can be found in Appendix B). Each time a search was run with a new seed sequence some new bacterial Tdps were found (although this number reduced with ongoing searches). This implies that the final list of 922 proteins is not exhaustive. When weighted against the number of completed and ongoing genome sequencing projects using the GOLD database⁴³⁹, the numbers of Tdps in bacterial phyla generally correlate with the proportion of genomes sequenced, with the most notable exception of the Cyanobacteria (accounting for 13.8% of Tdps but only 3.19% of sequencing projects). Tdps were also found in Bacteroidetes, Chlorobi, Proteobacteria, Firmicutes, Fusobacteria, Nitrospirae, Acidobacteria, Verrucomicrobia, Aquificae, Chloroflexi, Actinobacteria, Planctomycetes, Spirochaetes and Tenericutes (Table 3-3).

With regards to fungal species: a single Tdp was found in fungi (hypothetical protein An11g08390 from *Aspergillus niger*). Six archaeal proteins were found to contain TIR domains (two from *Methanococcoides burtonii*, one from *Methanocsarcina barkeri* one from *Thermofilum pendens* and two from an uncultured archaean). One archaeal protein contains a SEF/IL-17 (SEFIR) domain and three contain Domain of Unknown Function (DUF)-1863 domains (Table 3-3). Many of the bacterial proteins identified were also annotated as containing SEFIR or DUF1863 domains. PFAM classifies these domains with TIR domains within the STIR domain superfamily⁴⁴². However, given the presence of all three domains together in the PSI-BLAST output their classification as three separate domains is probably unnecessary, rather they are just variants of the TIR domain. Reverse PSI-BLAST searches and the structural homology prediction tool FUGUE both bring out TIR domains when a SEFIR domain is used as the seed and this is also the case for DUF1863 domains. This is the first report of the presence of STIR domains in both fungi and archaea. No Tdps were identified in viruses.

Table 3-2: Summary table of TIR domain proteins in bacterial and archaeal species.

BACTERIA						
Phylum	Family	Genus	Number of genomes with Tdps	Tdps	Genome sequencing projects	% Genomes with TIR
Acidobacteria	Acidobacteriaceae	n/a	1	3		
	Solibacteraceae	Solibacter	1	7		
Total Acidobacteria			2	10	5	40
Actinobacteria	Coriobacteriaceae	Collinsella	2	2		
	Corynebacteriaceae	Corynebacterium	1	1		
	Frankiaceae	Frankia	3	60		
	Micrococcaceae	Arthrobacter	4	4		
	Micromonosporaceae	Salinispora	1	2		
	Mycobacteriaceae	Mycobacterium	2	2		
	Nocardiaceae	Rhodococcus	1	4		
	Nocardioidaceae	Nocardioides	1	2		
	Nocardiopsaceae	Thermobifida	1	1		
	Pseudonocardiaceae	Saccharopolyspora	1	1		
	Streptomycetaceae	Streptomyces	24	49		
	n/a	n/a	1	1		
Total Actinobacteria			42	129	269	15.6133
Aquificae	Aquificaceae	Hydrogenivirga	1	1		
Total Aquificae			1	1	11	9.09090
Bacteroidetes	Bacteroidaceae	Bacteroides	9	11		
	Cyclobacteriaceae	Algoriphagus	3	3		
	Flavobacteriaceae	Kordia	1	1		
		Polaribacter	1	1		
		Psychroflexus	4	5		
		Robiginitalea	1	1		
		Cytophaga	1	1		
	Flexibacteraceae	Microscilla	2	3		
		Parabacteroides	1	1		
		Porphyromonas	2	4		
	Porphyromonadaceae	Alistipes	1	1		
		Pedobacter	1	1		
	Rikenellaceae		2	2		
Sphingobacteriaceae						
	n/a	n/a	2	2		
Total Bacteroidetes			29	35	118	24.5762
Chlorobi	Chlorobiaceae	Chlorobaculum	1	7		
		Chlorobium	3	22		
		Chloroherpeton	1	4		
		Pelodictyon	1	27		
		Prosthecochloris	1	18		
Total Chlorobi			7	78	12	58.3333
Chloroflexi	Chloroflexaceae	Chloroflexus	2	3		
Total Chloroflexi			2	3	21	9.52381
Cyanobacteria	Nostocaceae	Anabaena	1	4		
		Nodularia	5	5		
		Nostoc	11	27		
	Prochlorococcaceae	Prochlorococcus	1	1		
		n/a	Acaryochloris	3	10	
		Crocospaera	1	1		
		Cyanothece	38	83		
		Gloeobacter	1	1		
		Lyngbya	1	1		
		Microcystis	1	6		

		Synechococcus	4	6		
		Synechocystis	1	1		
		Thermosynechococcus	1	1		
		Trichodesmium	1	1		
Total Cyanobacteria			70	148	77	90.9090
Deinococcus-Thermus	Thermaceae	Thermus	2	2		
Total Deinococcus-Thermus			2	2	14	14.2857
Firmicutes	Bacillaceae	Bacillus	15	15		
		Geobacillus	2	2		
	Clostridiaceae	Alkaliphilus	1	1		
		Clostridium	31	48		
	Enterococcaceae	Enterococcus	2	3		
	Erysipelotrichaceae	n/a	2	3		
	Eubacteriaceae	Anaerofustis	1	2		
		Eubacterium	3	4		
	Halanaerobiaceae	Halothermothrix	1	1		
	Lachnospiraceae	Coprococcus	1	3		
		Dorea	4	5		
		Roseburia	1	1		
	Lactobacillaceae	Lactobacillus	1	1		
	Leuconostocaceae	Leuconostoc	1	2		
	Listeriaceae	Listeria	1	1		
	Peptococcaceae	Desulfotobacterium	3	4		
	Ruminococcaceae	Anaerotruncus	3	3		
		Faecalibacterium	1	1		
		Ruminococcus	2	2		
	Staphylococcaceae	Staphylococcus	2	2		
	Streptococcaceae	Streptococcus	3	3		
	Syntrophomonadaceae	Syntrophomonas	1	1		
	Veillonellaceae	Mitsuokella	1	1		
Total Firmicutes			83	109	643	12.9082
Fusobacteria	Fusobacteriaceae	Fusobacterium	3	3		
Total Fusobacteria			3	3	28	10.7142
Planctomycetes	Planctomycetaceae	Gemmata	1	1		
		Planctomyces	3	3		
		Rhodopirellula	1	5		
Total Planctomycetes			5	9	10	50
Proteobacteria	Acetobacteraceae	Gluconacetobacter	2	2		
	Acidithiobacillaceae	Acidithiobacillus	1	1		
	Aeromonadaceae	Aeromonas	1	1		
	Alcaligenaceae	Bordetella	1	2		
	Alteromonadaceae	Marinobacter	2	2		
		Saccharophagus	1	2		
	Aurantimonadaceae	Aurantimonas	1	1		
	Bartonellaceae	Bartonella	2	2		
	Beijerinckiaceae	Beijerinckia	2	4		
	Bradyrhizobiaceae	Bradyrhizobium	3	8		
		Nitrobacter	3	4		
		Oligotropha	2	2		
		Rhodopseudomonas	6	10		
	Brucellaceae	Brucella	6	9		
	Burkholderiaceae	Burkholderia	11	12		
		Ralstonia	2	2		
	Campylobacteraceae	Campylobacter	1	1		
	Caulobacteraceae	Caulobacter	2	3		
	Chromatiaceae	Nitrosococcus	1	1		
	Colwelliaceae	Colwellia	1	3		
	Comamonadaceae	Acidovorax	2	5		
		Diaphorobacter	1	2		
		Polaromonas	2	4		
		Rhodoferax	1	3		
	Cystobacteraceae	Stigmatella	3	3		
	Desulfobacteraceae	Desulfatibacillum	3	4		
		Desulfococcus	1	2		
	Desulfobulbaceae	Desulfotalea	1	1		

Desulfovibrionaceae	Desulfovibrio	2	2
Desulfuromonadaceae	Desulfuromonas	1	1
Ectothiorhodospiraceae	Nitrococcus	1	1
Enterobacteriaceae	Escherichia	4	4
	Klebsiella	1	1
	Pectobacterium	1	1
	Providencia	1	1
	Salmonella	8	8
	Yersinia	5	7
Erythrobacteraceae	Erythrobacter	6	8
Geobacteraceae	Geobacter	8	19
Helicobacteraceae	Helicobacter	6	6
Hydrogenophilaceae	Thiobacillus	1	2
Hyphomonadaceae	Hyphomonas	1	2
	Maricaulis	1	1
Idiomarinaceae	Idiomarina	1	1
Mariprofundaceae	Mariprofundus	2	2
Methylobacteriaceae	Methylobacterium	11	23
Methylococcaceae	Methylococcus	1	1
Moraxellaceae	Acinetobacter	2	2
Moritellaceae	Moritella	2	3
Myxococcaceae	Anaeromyxobacter	2	6
	Myxococcus	1	1
Nannocystaceae	Plesiocystis	3	4
Neisseriaceae	Chromobacterium	1	1
Nitrosomonadaceae	Nitrosomonas	1	1
	Nitrospira	1	1
Oxalobacteraceae	Herminiimonas	1	3
	Janthinobacterium	1	3
Pasteurellaceae	Actinobacillus	2	4
	Haemophilus	3	3
	Histophilus	1	1
	Pelobacter	1	3
Pelobacteraceae	Pelobacter	1	3
Phyllobacteriaceae	Parvibaculum	1	1
Piscirickettsiaceae	Thiomicrospira	1	3
Polyangiaceae	Sorangium	1	10
Pseudoalteromonadaceae	Pseudoalteromonas	4	6
Pseudomonadaceae	Pseudomonas	6	8
Psychromonadaceae	Psychromonas	1	2
Rhizobiaceae	Agrobacterium	1	1
	Rhizobium	4	7
	Sinorhizobium	2	2
	Paracoccus	1	1
Rhodobacteraceae	Rhodobacter	2	3
	Roseovarius	2	3
	Azoarcus	1	4
Rhodocyclaceae	Dechloromonas	1	5
	Thauera	4	6
	Magnetospirillum	1	2
Rhodospirillaceae	Rhodospirillum	1	1
	Shewanella	12	23
Shewanellaceae	Shewanella	12	23
	Sphingomonas	2	3
Sphingomonadaceae	Zymomonas	1	1
	Syntrophus	1	4
Syntrophaceae	Syntrophus	1	4
Syntrophobacteraceae	Syntrophobacter	1	1
Thiotrichaceae	Beggiatoa	2	2
Vibrionaceae	Aliivibrio	3	3
	Photobacterium	2	2
	Vibrio	12	14
	Xanthobacter	2	3
Xanthobacteraceae	Xanthobacter	2	3
	Xanthomonas	4	4
Xanthomonadaceae	Xylella	4	4
	Congregibacter	2	2
n/a	Endoriftia	1	1
	Leptothrix	1	3
	Magnetococcus	1	1
	Reinekea	2	2

		Sulfurovum	1	8		
		n/a	5	5		
Total Proteobacteria			242	374	1062	22.7871
Spirochaetes	Spirochaetaceae	Treponema	1	2		
Total Spirochaetes			1	2	52	1.92307
Tenericutes	Entomoplasmataceae	Mesoplasma	1	1		
	Mycoplasmataceae	Mycoplasma	2	2		
Total Tenericutes			3	3	9	33.3333
Verrucomicrobia	Opitutaceae	Opitutus	1	3		
	Verrucomicrobia subdivision 3	n/a	3	3		
	Verrucomicrobiaceae	Verrucomicrobium	1	7		
	n/a	Chthoniobacter	3	3		
Total Verrucomicrobia			8	16	9	88.8888
Total Bacteria			500	922	2416	20.6953

ARCHAEA

Phylum	Family	Genus	Number of genomes with Tdps	Tdps	Genome sequencing projects	% genomes with TIR
Crenarchaeota	Thermofilaceae	Thermofilum	1	1		
Total Crenarchaeota			1	1	46	2.17391
Euryarchaeota	Methanosarcinaceae	Methanococcoides	1	1		
Euryarchaeota		Methanococcoides	1	1		
Euryarchaeota		Methanosarcina	1	1		
Total Euryarchaeota			3	3	94	3.19148
Uncultured	n/a	n/a	2	2		
Total Archaea			6	7	142	4.22535

Table 3-3: Summary table of TIR domain proteins in bacterial and archaeal species.

The PSI-BLAST searches revealed six Tdps in CDC category A and B agents (Table 3-4); three of these are common with those identified in the Saturated BLAST searches (Tdps from *Y. pestis*, *B. melitensis*, and *S. enteritidis*). The Tdp in *B. thailandensis* was also confirmed. The Tdp from *B. pseudomallei* identified in the Saturated BLAST searches was not identified by PSI-BLAST, but this search identified two further Tdp in *B. pseudomallei* and one in *B. anthracis*. Results that differ from the Saturated BLAST searches are highlighted in blue in the table. These six Tdps were confirmed using reverse PSI-BLAST searches, structural homology using FUGUE and multiple alignments using Pfam and ClustalW2. These findings are summarised below and in Table 3-5 at the end of the chapter.

3.3.2.1. *Yersinia pestis*

The PSI-BLAST results reveal the same as the Saturated BLAST results in that *Y. pestis* strains encode for one protein that contains a TIR domain which corresponds to y2426 in *Y. pestis* KIM (YpTdp). YpTdp is 358 amino acids in length (Appendix A) and exists in all *Y. pestis* strains present in the NCBI nr database. It is annotated as a hypothetical protein in all strains but *Y. pestis* CO92 and *Y. pestis* Angola where it is annotated as a pseudogene due to the fact that in these sequences the neighbouring insertion sequence (IS285) is annotated as overlapping the end of the *Tdp* gene by 23 nucleotides. This is, in fact, no different than for the genes annotated as hypotheticals and so this appears to be an anomaly of annotation. In some *Y. pestis* strains the gene encoding this Tdp contains three extra nucleotides, in frame, which encode an additional serine residue.

The *YpTdp* gene, along with a number of other genes, is in between two transposases. The genomic environment also includes an insertion sequence and an integrase implying horizontal acquisition, potentially of phage origin. In many pathogens, phages have been instrumental in the acquisition of virulence traits^{443,444}. This TIR gene also exists in sequenced strains of *Yersinia pseudotuberculosis* and *Yersinia intermedia* but not in *Yersinia enterocolitica*. The region of the genome in which this gene occurs is also of below average GC content (46%). *Y. pestis* contains three regions of low GC content usually caused by the very recent acquisition of DNA (e.g. from a prophage) or by the inversion or

Category A	TIR domain protein?	Protein
<i>Bacillus anthracis</i>	Yes (1)	Equivalent to BA4098 in <i>B. anthracis</i> Ames, conserved across strains
<i>Yersinia pestis</i>	Yes (1)	Equivalent to y2426 in <i>Y. Pestis</i> KIM, conserved across strains
Variola virus	No	-
<i>Francisella tularensis</i>	No	-
Filoviruses	No	-
Arenaviruses	No	-
Category B		
<i>Brucella</i> sp.	Yes (2)	Equivalent to BMEI1674 and BMEI1216 in <i>B. melitensis</i> 16M, conserved across strains
<i>Salmonella</i> sp.	Yes (1), certain strains	TlpA from <i>Salmonella enteritidis</i>
<i>E. coli</i> O157:H7	No	-
<i>Shigella</i> sp.	No	-
<i>Burkholderia mallei</i>	No	-
<i>Burkholderia pseudomallei</i>	Yes (2), certain strains	BpseD_010100000475 from <i>B. pseudomallei</i> DM98 and Bpse7_010100021343 from <i>B. pseudomallei</i> 7894
<i>Chlamydia psittaci</i>	No	-
<i>Coxiella burnetti</i>	No	-
<i>Rickettsia prowaceki</i>	No	-
Alphaviruses	No	-

Table 3-4: TIR domain proteins in CDC Category A and B agents (PSI-BLAST search strategy)

This table details the distribution of TIR domain proteins in CDC Category A and B agents as found using the PSI-BLAST search strategy followed by further down-selection using reverse PSI-BLAST searches, assessment of secondary structure homology (FUGUE) and multiple sequence alignments.

translocation of blocks of DNA. The gene for YpTdp is next to the so-called *Yersinia* “high pathogenicity island” involved in iron sequestration and survival of *Y. pestis* in the flea.

After this sequence was down-selected from the PSI-BLAST results it was subjected to reverse PSI-BLAST analysis to confirm its identity as a Tdp. Mammalian Tdps appeared after just two iterations and included human SARM, Mal, TLR1 and TLR6. By the third iteration all other human TLRs except TLR7, TLR8 and TLR9 had appeared along with human IL-18R, MyD88, *Drosophila* Toll, *C. elegans* tir-1 and TirA from *Dictyostelium* indicating that YpTdp is able to find TIR domain proteins when it is used as a seed sequence. The eukaryotic protein that YpTdp is most closely related to is a protein from the Rotifer *Adineta vaga*, a microscopic animal that lives in freshwater feeding on dead bacteria and algae. YpTdp was also subjected to secondary fold analysis using FUGUE which confirmed it is “likely” to contain a TIR domain ($p < 0.05$). Figure 3-4 shows an alignment of y2426 from *Y. pestis* KIM with a variety of Tdps. From this it is clear that the TIR domain from YpTdp shares homology in regions important for the definition and function of eukaryotic TIR domains, including in “Box 1” and in the β C helix. However, differences are also clear: YpTdp lacks the conserved “Box 2” motif RDxxPG¹⁶², although it does contain the conserved proline residue demonstrated to be important for eukaryotic TLR signalling function¹⁹. YpTdp also lacks a “Box 3” motif, although the importance of this region for function is less clear^{160,162,445}

3.3.2.2. *Burkholderia mallei* and *Burkholderia pseudomallei*

In line with the Saturated BLAST results the PSI-BLAST analysis found no Tdps in *B. mallei*. Unlike Saturated BLAST, the PSI-BLAST analysis produced two Tdps residing within *B. pseudomallei* strains, one in *B. pseudomallei* DM98 (BpseD_01010000475) and one in *B. pseudomallei* 7894 (Bpse7_010100021343). These are not the only *B. pseudomallei* strains to be sequenced, however, so these two proteins are not conserved. TIR domains in these proteins were confirmed by reverse PSI-BLAST searches, PFAM and FUGUE analysis but Bpse7_010100021343 and BpseD_01010000475 were not down-selected for experimental investigation because of the difficulty in obtaining genomic DNA from these *B. pseudomallei* species. An interesting point from the bioinformatic analysis of these proteins is that the eukaryotic protein most similar to BpseD_01010000475 is a hypothetical protein from the lancelet *Branchiotoma floridae*, an early invertebrate

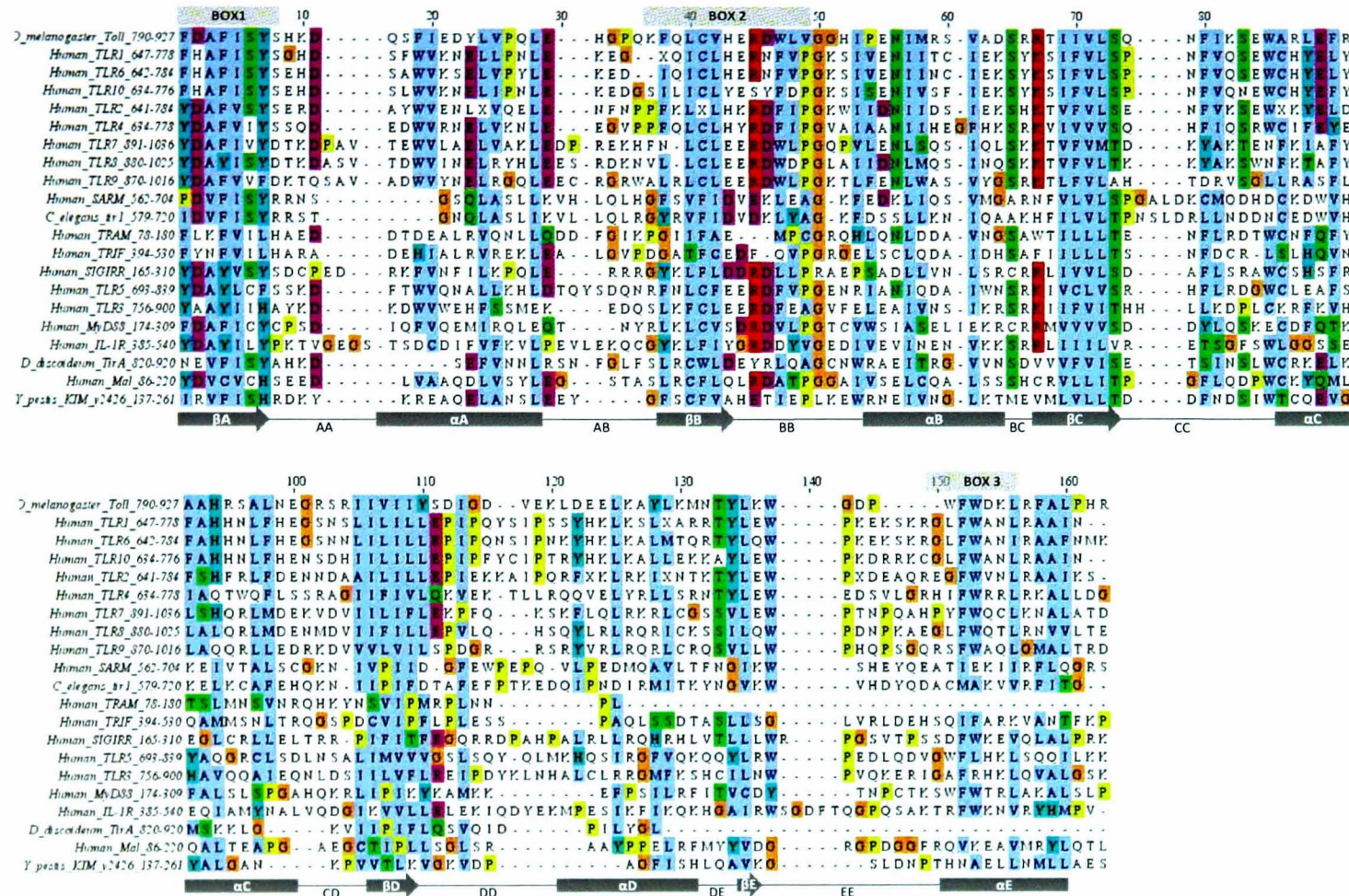


Figure 3-4: Multiple sequence alignment of y2426 from *Y. pestis* KIM with eukaryotic TIR domain proteins
 Multiple sequence alignment carried out using the ClustalW2 algorithm on the EBI web server (<http://www.ebi.ac.uk/tools/clustalw2>)¹⁶⁵ and coloured according to the Clustal X colourscheme using Jalview (Section 2.1.7). TIR domain sequences taken from *Homo sapiens*, *Caenorhabditis elegans*, *Dictyostelium discoideum* and *Drosophila melanogaster*. The grey boxes correspond to areas of α -helix and the grey arrows correspond to areas of β -sheet. The lines connecting these structures correspond to the loop regions of sequence. Secondary structure predicted using 3D Jury web server¹⁶⁶ and published crystal structures^{162,163,167,168}

normally found buried in sand in shallow parts of temperate or tropical seas, an environment in which *B. pseudomallei* might very well reside.

The *B. pseudomallei* protein identified as a possible Tdp from the Saturated BLAST searches (BPSL0748, Section 3.3.1.3) did not fall within the threshold ($e < 0.05$) for these PSI-BLAST searches and was therefore subsequently considered likely to be a false positive from the Saturated BLAST search.

Tdps were found in other *Burkholderia* sp. not characterised as potential bioterrorism agents including *B. thailandensis* BTH_I3242 (BthTdp) which was also a result from the Saturated BLAST searches and went forward for *in vitro* investigation. The genomic environment around the *BTH_I3242* gene suggests it is likely to be of phage origin. Reverse PSI-BLAST and FUGUE analysis confirm the presence of a TIR domain with greatest similarity to plant TIR domains. Tdps were also found in *Burkholderia ambifaria*, *multivorans*, *phymatum*, *vietnamiensis*, *xenovorans*, sp. 383 and sp. H160 (Table 3-3).

3.3.2.3. *Bacillus anthracis*

Unlike the Saturated BLAST searches, the PSI-BLAST searches found *Bacillus anthracis* strains to have one Tdp, in *B. anthracis* Ames (Appendix A). This is BA4098 (referred to throughout this thesis as BaTdp). This protein is conserved across *B. anthracis* strains but not across other *Bacillus* sp. although does show some homology (54% identity) to a protein in *Bacillus thuringiensis*. The genomic environment surrounding the *BA4098* suggests it is in a region of phage DNA. A reverse PSI-BLAST pulls out one protein from *Dictyostelium discoideum* AX4 at iteration one and a plant TIR domain protein. Otherwise this reverse search does not produce other eukaryotic proteins. FUGUE does not find any highly scoring matches for BaTdp, and no matches for TIR domain structures. The highest match is for histidine biosynthetic enzyme ($Z = 4.44$). Pfam does, however, recognise BaTdp as containing a TIR domain. This suggests that in primary sequence part of BaTdp is homologous to TIR domain proteins, but that structurally it may differ from previously solved TIR domain structures. The multiple sequence alignment of BaTdp with homologous TIR domain proteins as found during the reverse PSI-BLAST search (Figure 3-5) shows that BaTdp shows a high degree of homology at Box 1, but very little at Box 2.

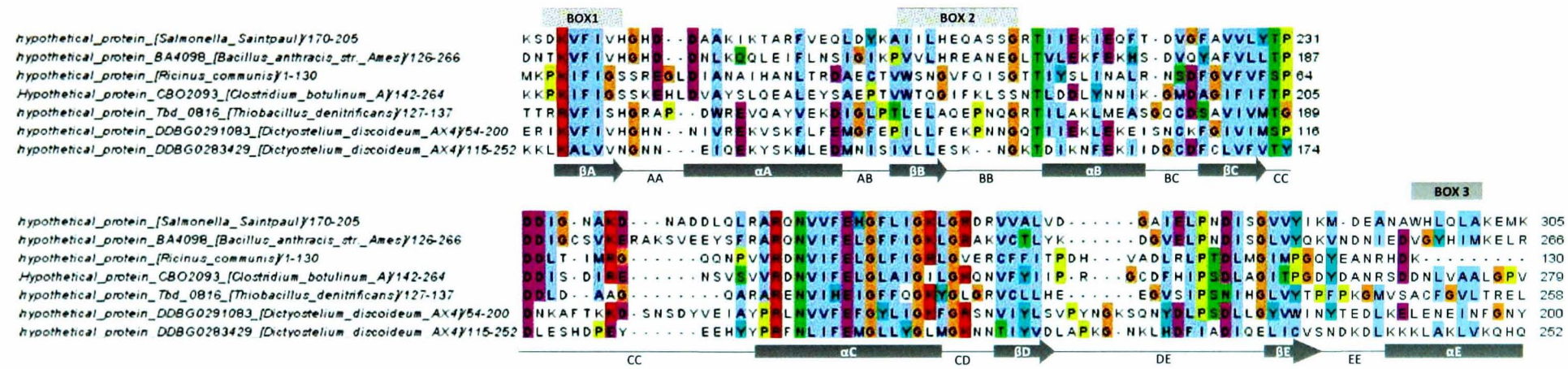


Figure 3-5: Multiple sequence alignment of BaTdp with homologous TIR domain proteins

Multiple sequence alignment carried out using the ClustalW2 algorithm on the EBI web server (<http://www.ebi.ac.uk/tools/clustalw2>)¹⁶⁵ and coloured according to the Clustal X colourscheme using Jalview (Section 2.1.7). TIR domain sequences for alignment with BA4098 were taken from reverse PSI-BLAST results when BA4098 was used as a seed and include the following proteins (NCBI accession numbers): ZP_02346495.1, YP_314574.1, XP_635389.1, XP_002537270.1, YP_001254590.1, XP_639069.1. The grey boxes correspond to areas of α -helix and the grey arrows correspond to areas of β -sheet. The lines connecting these structures correspond to the loop regions of sequence. Secondary structure predicted using 3D Jury web server¹⁶⁶ and published crystal structures^{162,163,167,168}

and its sequence here is almost unrecognisable from the archetypal Box 2 sequence from mammalian TIR domains as first described by Xu *et al.*¹⁶². BaTdp also shows limited homology at Box 3. Interestingly, BaTdp is also missing the α D helix and DD loop of traditionally described TIR domains.

3.3.2.4. *Brucella melitensis*

In addition to the Tdp identified by Saturated BLAST (BMEI1674, termed BmTdp), the PSI-BLAST searches found one additional Tdp conserved across *Brucella* species (BMEI1216 in *B. melitensis* 16M, referred to throughout this manuscript as BmTdp2).

3.3.2.4.1. BmTdp

BmTdp is 250 amino acids long (Appendix A) with the TIR domain predicted to be at its C-terminus (approx. residues 120-250). It is annotated as a hypothetical protein and the gene encoding this protein is located in a 20 kb genomic island on chromosome 1. The genomic environment here suggests this island has been acquired recently via a phage-mediated integration event. During a reverse PSI-BLAST search mammalian Tdps did not feature in the results. Instead this protein produced plant Tdps from the first iteration suggesting the TIR domain in BmTdp is more closely related to the TIR domains within plant resistance proteins. The results of the FUGUE analysis suggest BmTdp may have some structural homology to the annexins. These are a large family of intracellular phospholipid-binding proteins which also have extracellular roles in innate immune signalling and apoptosis, although no annexin family proteins have ever been identified in prokaryotes. This is further discussed in Section 3.4. The multiple sequence alignment of BmTdp with homologous TIR domain proteins as found during the reverse PSI-BLAST search (Figure 3-6) shows that BmTdp has a high degree of homology with other TIR domain proteins at Box 1, but that the Box 2 region is not only quite different from the proteins it is most homologous to, but is also almost unrecognisable from a mammalian TIR domain protein Box 2 as originally described by Xu *et al.*¹⁶². The TIR domain of BmTdp is also truncated at its C-terminal end. It lacks the DE and EE loops, β E sheet and α E helix, and consequently, Box 3.

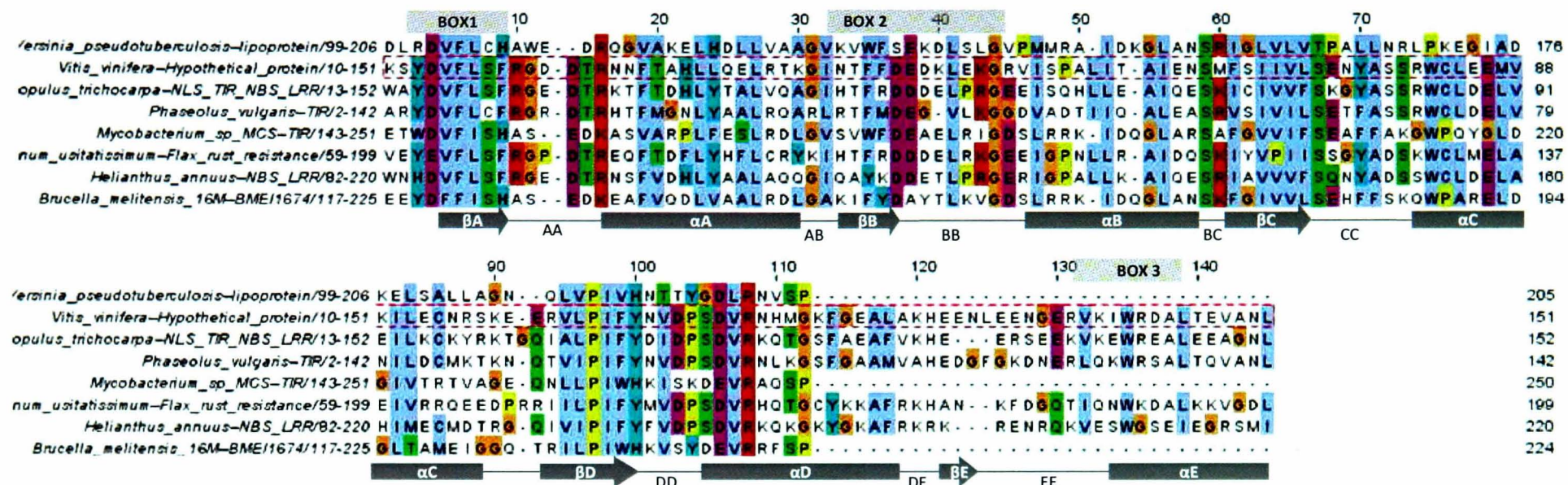


Figure 3-6: Multiple sequence alignment of BMEI1674 with homologous TIR domain proteins

Multiple sequence alignment carried out using the ClustalW2 algorithm on the EBI web server (<http://www.ebi.ac.uk/tools/clustalw2>)¹⁶⁵ and coloured according to the Clustal X colourscheme using Jalview (Section 2.1.7). TIR domain sequences for alignment with BMEI1674 were taken from reverse PSI-BLAST results when BMEI1674 is used as a seed and include the following proteins (NCBI accession numbers): ABI16465.1, CAN83385.1, AAN73010.1, YP_638640.1, AAD25976.1, XP_002310389.1. The grey boxes correspond to areas of α -helix and the grey arrows correspond to areas of β -sheet. The lines connecting these structures correspond to the loop regions of sequence. Secondary structure predicted using 3D Jury web server¹⁶⁶ and published crystal structures^{162,163,167,168}

3.3.2.4.2. BmTdp2

BmTdp2 is 178 amino acids long with the TIR domain ostensibly taking up the entire protein. BmTdp2 is “Certain” to contain a TIR domain by FUGUE analysis ($p < 0.01$). During reverse PSI-BLAST searches plant proteins containing TIR domains are visible at iteration two and mammalian Tdps are visible from iteration three, including human TLR1, TLR2, TLR10, TLR6, TLR4, MyD88 and SIGIRR. The multiple sequence alignment of BmTdp2 with homologous TIR domain proteins as found during the reverse PSI-BLAST search (Figure 3-7) shows that it has a high degree of homology with other TIR domain proteins at Boxes 1, 2 and 3 although Box 2 differs somewhat from the originally described sequence. Interestingly though, BmTdp2 is missing the α D helix and DD loop. In the PdTIR structure, to which BmTdp2 shows high homology by FUGUE analysis, the DD and EE loops were shown to mediate the dimer interface. The lack of a DD loop in BmTdp2 perhaps suggests it acts as a monomer or that, if dimeric, this structure is mediated by the BB loop, as for mammalian TIR domains.

The bioinformatic characteristics of all the Tdps from potential bacterial bioterrorism agents are summarised in Table 3-5.

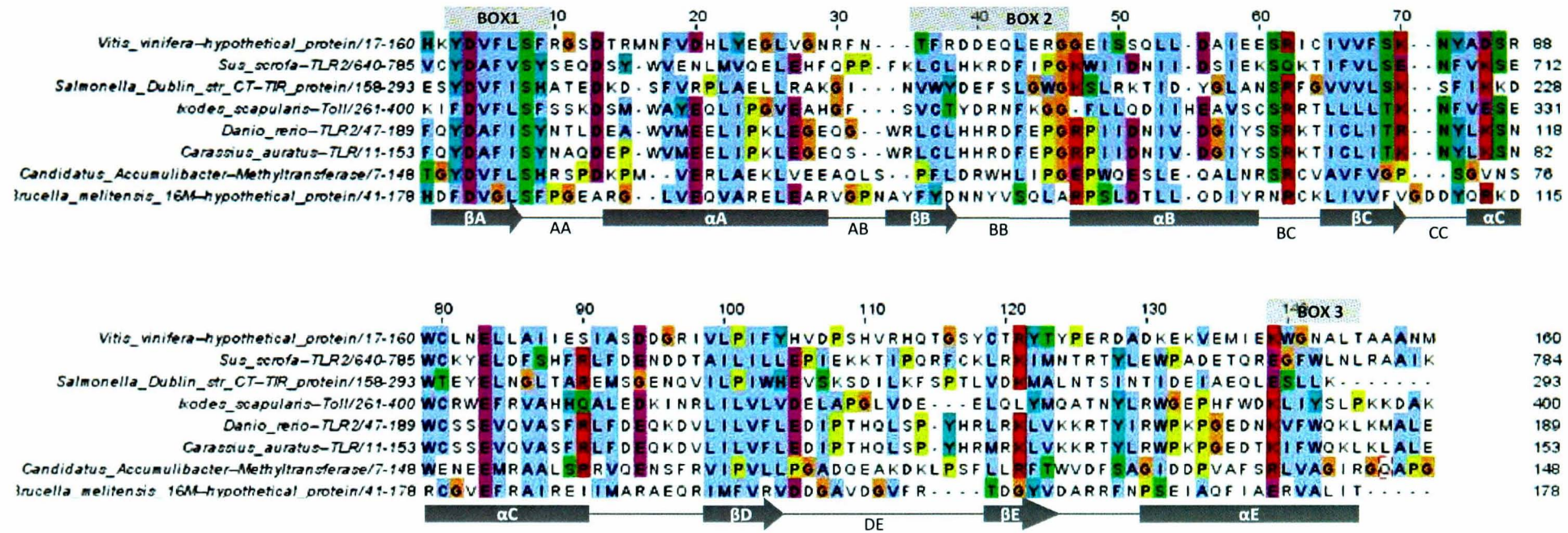


Figure 3-7: Multiple sequence alignment of BMEI1216 with homologous TIR domain proteins

Multiple sequence alignment carried out using the ClustalW2 algorithm on the EBI web server (<http://www.ebi.ac.uk/tools/clustalw2>)¹⁶⁵ and coloured according to the Clustal X colourscheme using Jalview (Section 2.1.7). TIR domain sequences for alignment with BMEI1216 were taken from the reverse PSI-BLAST results when BMEI1216 is used as a seed and include the following proteins (NCBI accession numbers): YP_002216067.1, XP_002406802, YP_003167638.1, AAO53555.1, AAQ91321.1, NP_998926.1, XP_002274306.1. The grey boxes correspond to areas of α -helix and the grey arrows correspond to areas of β -sheet. The lines connecting these structures correspond to the loop regions of sequence. Secondary structure was predicted using 3D Jury web server¹⁶⁶ and published crystal structures^{162,163,167,168}







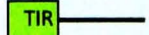
Protein	Conserved?	Amino acids	Annotation	Location of domains	Searches	Reverse PSI-BLAST	Top FUGUE results	Down-selected for in vitro investigation?	Multiple alignment
YpTdp (y2426 in <i>Y. pestis</i> KIM)	Conserved across <i>Y. pestis</i> strains.	358	Hypothetical protein	TIR 137-285 	Saturated BLAST & PSI-BLAST	Mammalian Tdps at Iteration 2	TIR (Z = 20.61 against <i>Paracoccus denitrificans</i> TIR structure)	Yes	Figure 3-4
BpseD_01010000475	Only found in <i>Burkholderia pseudomallei</i> DM98	156	Putative lipoprotein	TIR 22-154 	PSI-BLAST	Plant and other eukaryotic proteins at iteration 2.	TIR (Z = 27.78 against <i>Paracoccus denitrificans</i> TIR structure)	No	NA
Bpse7_010100021343	Only found in <i>Burkholderia pseudomallei</i> 7894	295	nucleotide-binding protein containing TIR -like domain	TIR 140-295 	PSI-BLAST	Protein from <i>Dictyostelium dicosodium</i> AX4 at iteration 1, mammalian Tdps at iteration 5.	No significant matches	No	NA
BaTdp (BA4098 in <i>B. anthracis</i> Ames)	Conserved across <i>B. anthracis</i> strains.	273	Hypothetical protein	TIR: 128-252 	PSI-BLAST	Protein from <i>Dictyostelium dicosodium</i> AX4 at iteration 1	Histidine biosynthesis enzyme (z = 4.44)	Yes	Figure 3-5
BmTdp (BME11674 in <i>B. melitensis</i> 16M)	Conserved across <i>Brucella</i> species	250	Hypothetical protein	TIR: 	Saturated BLAST & PSI-BLAST	Plant Tdps at iteration 1.	TIR (Z = 33.35 against <i>Paracoccus denitrificans</i> TIR structure)	Yes	Figure 3-6
BmTdp2 (BME11216 in <i>B. melitensis</i> 16M)	Conserved across <i>Brucella</i> species	178	Hypothetical protein	TIR: 1-178 	PSI-BLAST	Plant Tdps at iteration 2, mammalian Tdps at iteration 3.	TIR (Z = 15.57 against <i>Paracoccus denitrificans</i> TIR structure)	Yes	Figure 3-7
Bth_I3242	Only found in <i>Burkholderia thailandensis</i> E264	325	Hypothetical protein	TIR 1-120 	Saturated BLAST & PSI-BLAST	Mammalian Tdps at iteration 2	TIR (Z = 12.03 against P681 mutant of human TLR2 structure)	Yes	NA

Table 3-5: Summary table of the bioinformatic characteristics of TIR domain proteins from CDC category A and B bacteria

This table details all the TIR domain proteins found in CDC category A and B bacteria from the PSI-BLAST searches, and their bioinformatic characteristics. One TIR domain protein was also investigated from an environmental organisms (*Burkholderia thailandensis*) (light grey shaded row).

3.4. Conclusions

The survey of Tdps in bacteria carried out by Newman *et al.* in which 200 bacterial proteins with TIR domains were found, and their work on TlpA from *Salmonella enteritidis* paved the way for them, and others, to put forward a “subversion hypothesis” for the function of proteins that contain TIR domains in bacterial species. A bioinformatic search for Tdps in micro-organisms has also been carried out in this work, including analysis of the bioinformatic distribution and characteristics of the proteins probed with particular attention focussed on a group of highly pathogenic bacteria and viruses classed as potential bio-terror agents.

Due to their low sequence homology any search for Tdps will require in-depth bioinformatic scrutiny. The Saturated BLAST search tool, as used by Newman *et al.* for the discovery of TlpA in *S. enteritidis* aims to make these searches easier by automating the iterations. However, in this study this search tool proved problematic for a number of reasons including the fact that it was not able to be run on its preferred operating system (LINUX) which made the collation of data difficult. Additionally, its features were not used to their full advantage (statistical cut offs etc.) due to inexperience, and the inclusion of vaccinia virus A46 as a TIR domain seed likely increased false positive results. Through this work (A46 was absent from the PSI-BLAST results), and that of others, it is now clear that A46 is unlikely to contain a TIR domain³³¹. In fact, there was no evidence for a TIR domain in A46 or any other viral protein using BLAST or PSI-BLAST—homology search methods that allow unbiased searching of sequence libraries and provide an objective statistical evaluation of each alignment. Searches starting with known TIR domains do not find A46 and searches starting with A46 do not find TIR domains. Instead, both BLAST and PFAM searches reveal homology of A46 to other vaccinia proteins of known structure (B14 and A52), which contain a Bcl-2 fold³⁶. The PSI-BLAST search tool does rely on the divergent evolution of proteins, so it is reasonable to suggest that A46 may have evolved to have TIR-*like* properties by convergent evolution. There are conflicting views on how likely the convergent evolution of domain architectures is, however^{446,447}.

Subsequently the survey of Tdps in bacteria was carried out using PSI-BLAST without A46 as a seed. Results were collated for bacteria, archaea, fungi and viruses. As already mentioned Tdps were completely absent from viruses in these results and not widespread in

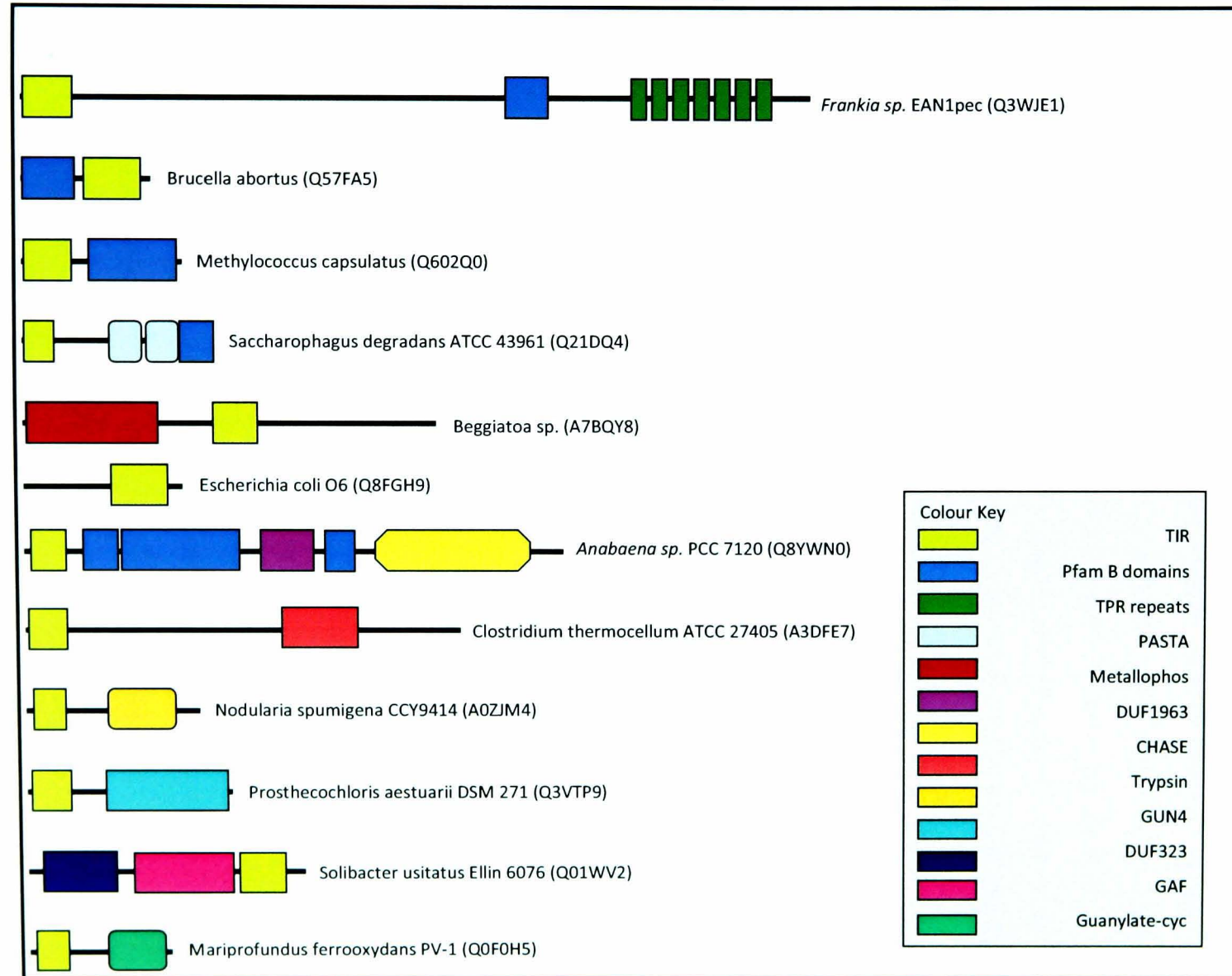
archaea or fungi. This bioinformatic survey did, however, find 922 Tdps across bacterial species. This number of proteins far exceeds that found by Newman *et al.* using the Saturated BLAST search tool, despite the same statistical cut off for similarity being used ($p < 0.05$). Even taking into account the fact that its features were not being used to their optimal effect, this bioinformatic tool did not appear particularly effective at finding and collating Tdps. Although not all 922 proteins found by PSI-BLAST have been tested for their likely validity as Tdps, a proportion of the proteins were tested using reverse PSI-BLAST searches and 3D homology search tools and all the proteins tested were returned as being highly likely to contain a TIR domain. The bioinformatic analysis reported in this chapter show that Tdps in bacteria show a very sporadic distribution (Appendix B); they are present in bacterial species classically thought of as “pathogenic” and “non-pathogenic” and are often not particularly well-conserved. For example, the *tlpA* gene occurs in only 5 of >70 genome-sequenced strains of *Salmonella enterica*, while *tcpB* occurs in only a minority of uropathogenic *E. coli* isolates, so neither gene can be considered an essential conserved component of enteropathogenesis or uropathogenesis, respectively. This sporadic occurrence of genes encoding bacterial Tdps may be seen as problematic for the subversion hypothesis. However, the patchy phylogenetic distribution of *Tdp* genes in bacteria which seldom, if ever, follow vertical lines of descent, need not count against the subversion hypothesis. One sees similar patchiness in the genomic distribution of well-established subversion factors, such as type-III secretion effectors, where it is a hallmark of horizontal gene transfer.

However, two other lines of evidence from the bioinformatic survey suggest that the subversion hypothesis cannot explain the function of all bacterial Tdps. Firstly, when one looks at the broad phylogenetic distribution of bacterial Tdps, one finds the vast majority of these proteins are encoded within the genomes of environmental organisms not usually thought of as pathogens. Perhaps the starkest example of this is their over-representation within the cyanobacteria which seldom, if ever, engage in subversive interactions with metazoans or plants. It is also worth noting that the closest homologue of the *TcpB* TIR domain (52% identity) occurs in a marine flavobacterium that has no credible role in human disease. However, on the eco-evo view of bacterial pathogenomics⁴⁴⁸ a role for bacterial Tdps in “non-pathogens” as agents of subversion against microbial eukaryotic predators or competitors cannot be ruled out.

Secondly, the survey confirms the already-observed association of TIR domains with other apoptosis domains and also reveals that TIR domains in bacteria are promiscuous in their co-occurrence with other domains in individual proteins - dozens of domain architectures were found around TIR domains (Figure 3-8). This counts against any unified theory that attempts to shoe-horn all bacterial Tdps into a single functional category. In fact, together, these two lines of evidence suggest that the TIR domain is no different from many other “eukaryotic signalling domains”, which were first associated with signalling in eukaryotes, but then found to occur widely in bacteria. In almost all such cases, the signalling function occurs in a specific context in eukaryotes that is not shared by bacteria. Instead, the micro-organisms adopt and adapt the domains for their own uses. For example, tetratricopeptide repeats mediate protein-protein interaction in humans and bacteria, but in different contexts (in eukaryotes as scaffolds for the assembly of multiprotein complexes in the nucleus or peroxisome or for binding cargo on microtubules; in bacteria as chaperones in type III secretion)⁴⁴⁹. Similarly, serine-threonine protein kinases, although prominent in signalling in humans, are also intimately integrated into bacterial signalling pathways (particularly within the mycobacteria)⁴⁵⁰.

As well as casting doubt on the subversion hypothesis the bioinformatic results give other insights into the history of the TIR domain within proteins. Their sporadic distribution and frequent occurrence within regions of phage or otherwise-acquired DNA suggest the genes for Tdps have been mobile. Their absence in archaea and fungi but their presence in other early eukaryotes such as *D. dicosedium* suggests that perhaps these genes were transferred from prokaryotes to single-celled eukaryotes via horizontal gene transfer, or potentially during mitochondrial endosymbiosis. The Tdp from *D. dicosedium* is required for immune cell function and for vegetative amoeba to feed on live bacteria. The presence of a Tdp in *D. dicosedium* and its role in feeding suggests an ancient foraging mechanism was adapted for defence purposes well before the diversification of animals. Unlike apoptotic domains there is a suggestion that TIR domains were useful to organisms before the evolution of multi-cellularity, or perhaps during the evolution of multi-cellularity. Multi-cellularity first appeared in cyanobacteria and it is within this species of bacteria that TIR domain proteins appear to be over-represented.

Figure 3-8: Diverse domain architectures of bacterial proteins containing TIR domains



Explanation for domain names: TIR, Toll/interleukin-1 receptor; PFAM B-domains, miscellaneous automatically annotated domains of unknown function; TPR repeats, tetratricopeptide repeats, a common protein-protein interaction domain; PASTA, small globular domain found at C-terminus of penicillin-binding proteins and bacterial serine/threonine kinases involved in binding to peptidoglycan precursors; Metallophos, a calcineurin-like metallo-phosphoesterase domain found in many proteins involved in phosphorylation; DUF1963, one of many domains of unknown function; CHASE, an extracellular ligand-binding domain from receptor-like proteins; Trypsin, a serine protease domain; GUN4, a domain involved in regulation of chlorophyll synthesis and intracellular signaling in chloroplasts; DUF323, another domain of unknown function; GAF, a domain present in phytochromes and cGMP-specific phosphodiesterases; Guanylate_cyc, catalytic domain of adenylate and guanylate cyclases and Mrr-cat, a type IV restriction endonuclease domain. Figure re-drawn from results displayed by PFAM (<http://pfam.sanger.ac.uk/>).

Another interesting feature of the bioinformatic searches is that certain mammalian TIR domains did not produce homologues in bacterial species. For example, TLRs can be divided into five sub-families: TLR2, TLR3, TLR4, TLR5, and TLR9 sub-families. The TLR2 family contains TLR1, TLR2, TLR6 and TLR10. TLR1 and TLR6 seem to have arisen by evolutionary duplication. The TLR9 subfamily contains TLR7, TLR8 and TLR9, which all recognise nucleic acids. TLR3, TLR4 and TLR5 are each alone in their own subfamily⁴⁵¹. The TIR domains from TLR3, TLR5 and TLR7, TLR8 and TLR9 did not produce bacterial results when used as seeds. Neither did the TIR domain from the adaptor TRIF. This adaptor protein and these TLRs (with exceptions) are involved in the recognition of nucleic acids and therefore primarily viruses. All TIR domain sequences from the TLR2 family produced bacterial results. In addition, some of the bacterial Tdps were more closely related to the Tdps from plants rather than animals. The immune pathways within plants and animals that use TIR domains are postulated to have evolved independently⁴⁵²⁻⁴⁵⁴. In addition some of the bacterial Tdps show interesting differences in their secondary structure. For example, BmTdp is truncated at its C-terminal end by approximately the same number of residues that are removed after caspase-1 cleavage of Mal at its C-terminal end⁴⁵⁵. Also, two of the proteins, BaTdp and BmTdp2 lack an α D helix and DD loop perhaps suggesting a common lineage between these proteins. None of the bacterial Tdps show a particularly high level of sequence conservation with the hallmark boxes of sequence in mammalian Tdps. Separate TIR domain sequence hallmarks are probably appropriate for bacterial Tdps and it would be interesting to characterise these across the 922 bacterial proteins identified.

Despite questions surrounding the subversion hypothesis being raised by these bioinformatic results, they do not necessarily indicate that the hypothesis should be completely rejected. It may be that a subversive role is an exception, rather than the rule, or that these domains can “moonlight” as subversion proteins in addition to another role. Bacterial TIR domains occur in a wide variety of domain architectures in a wide variety of bacteria and are therefore likely to play diverse roles in bacterial physiology of which innate immune subversion may be one, particularly in highly pathogenic organisms. Future studies of bacterial TIR domain proteins, particularly in classical “non-pathogen,” may enable the identification of other functions.

Chapter 4: The effect of bacterial TIR domain proteins on mammalian immune signalling

4.1. Introduction

Previous studies have demonstrated that if mammalian cells are stimulated with IL-1R or TLR agonists in the presence of bacterial TIR domain proteins (Tdps) then immune signalling readouts, such as transcription factor activity or cytokine production, are modulated in their presence^{342,343}. Three different bacterial Tdps have so far been investigated for their effect on mammalian immune signalling. The first bacterial Tdp to be identified was TIR-like protein A (TlpA) in *Salmonella enterica* serovar *Enteritidis*³⁴². In this study, Newman *et al.* showed that TlpA down-regulated NFκB activation downstream of TLR4, IL-1R and MyD88, which are all TIR domain-dependent signalling pathways, but not downstream of TNFα stimulation, which is a TIR domain-independent signalling pathway to NFκB³⁴². They demonstrated that TlpA reduces the DNA binding activity of NFκB and can induce caspase-1 activation and thus the secretion of IL-1β. They could not, however, demonstrate an interaction between TlpA and a variety of TIR domain-containing proteins. Subsequently, Tdps were investigated from *Brucella melitensis* and *Escherichia coli*. A Tdp from *B. melitensis*, equivalent to BmTdp identified in this study (Chapter 3), has now been investigated by three research groups. With regards to its effect on signalling these groups have produced conflicting findings; Salcedo *et al.* showed that BmTdp could down-regulate signals downstream of murine TLR2 but not human TLR2, and had no effect on any TLR9 signalling tested³⁴⁶. Two other studies have shown that it is able to down-regulate signalling from TLR2 and TLR4^{344,345}, although its ability to affect signalling downstream of the over-expression of Mal is conflicting in these studies. BmTdp has been postulated to be “Mal-like” in that it is able to bind phospholipids and exerts its effects on TLR2 and TLR4 signalling. Sengupta *et al.* demonstrate that this is via the induced degradation of Mal by BmTdp³⁴⁴. The third Tdp that has been investigated is from an uropathogenic strain of *E. coli*, and is denoted TcpC³⁴³. Cirl *et al.* showed that TcpC could down-regulate signalling to NFκB downstream of TLR2 and TLR4 and that it could bind MyD88³⁴³. From these proteins studied so far it appears that different bacterial Tdps specifically affect signalling from different TLRs, or the IL-1R.

In this study, six Tdps were down-selected following bioinformatic identification for further investigation (Chapter 3). One protein is equivalent to the Tdp from *Brucella* sp. investigated by other groups but studies on the other five Tdps have not previously been reported. The Tdps come from bacteria with very different characteristics: five are from pathogenic bacteria categorised as potential bioterrorism agents: *Burkholderia pseudomallei*, *Yersinia pestis*, *Brucella melitensis* and *Bacillus anthracis*. The first three are gram-negative bacteria with an intracellular aspect of their lifestyle whereas *B. anthracis* is a spore-forming gram-positive bacterium able to replicate within macrophages once germination has occurred. All four pathogens rely somewhat on the modulation of the innate immune response, including TLR signalling, to survive and replicate within the host, most notably *Yersinia pestis* and *Brucella melitensis* as discussed in Section 1.6. The sixth protein is from *Burkholderia thailandensis* which is considered to be “non-pathogenic” but a close relative of *B. pseudomallei* and is often employed as a model for this organism. Tdps from these different bacterial species were down-selected to enable a determination of the effect of the Tdps on TIR domain-dependent signalling.

4.2. Aims and objectives

The aim of this chapter was to screen the candidate Tdps down-selected from the bioinformatic studies in Chapter 3 for their effect on mammalian immune signalling *in vitro* in order to determine whether Tdps from disparate organisms had a similar activity.

Specific objectives of this chapter were to:

- Clone each gene encoding the selected Tdp into a mammalian expression vector and confirm sequence
- Confirm Tdp expression from these constructs in a mammalian cell line
- Set up a reporter assay for NFκB activity downstream of IL-1/TLR signalling in this cell line
- Screen all the candidates for their affect on IL-1/TLR signalling downstream of a variety of stimulants
- Assess the specificity of action via TIR-independent signalling assays and dose-dependent effects

Four Tdps (YpTdp, BthTdp, BmTdp, BpTdp) were down-selected from the Saturated BLAST searches and their genes were cloned into an expression vector for investigation of their effect on signalling to NF κ B. Following the subsequent PSI-BLAST searches, two further candidates were selected for investigation (BaTdp, BmTdp2) and one protein from the Saturated BLAST searches was discounted (BpTdp). Results for all of these proteins can be seen in the following Sections. Figure 4-1 and Table 4-1 summarise the candidates selected from the bioinformatic studies in Chapter 3 and demonstrate how the selection informed the experimental work described in this Chapter.

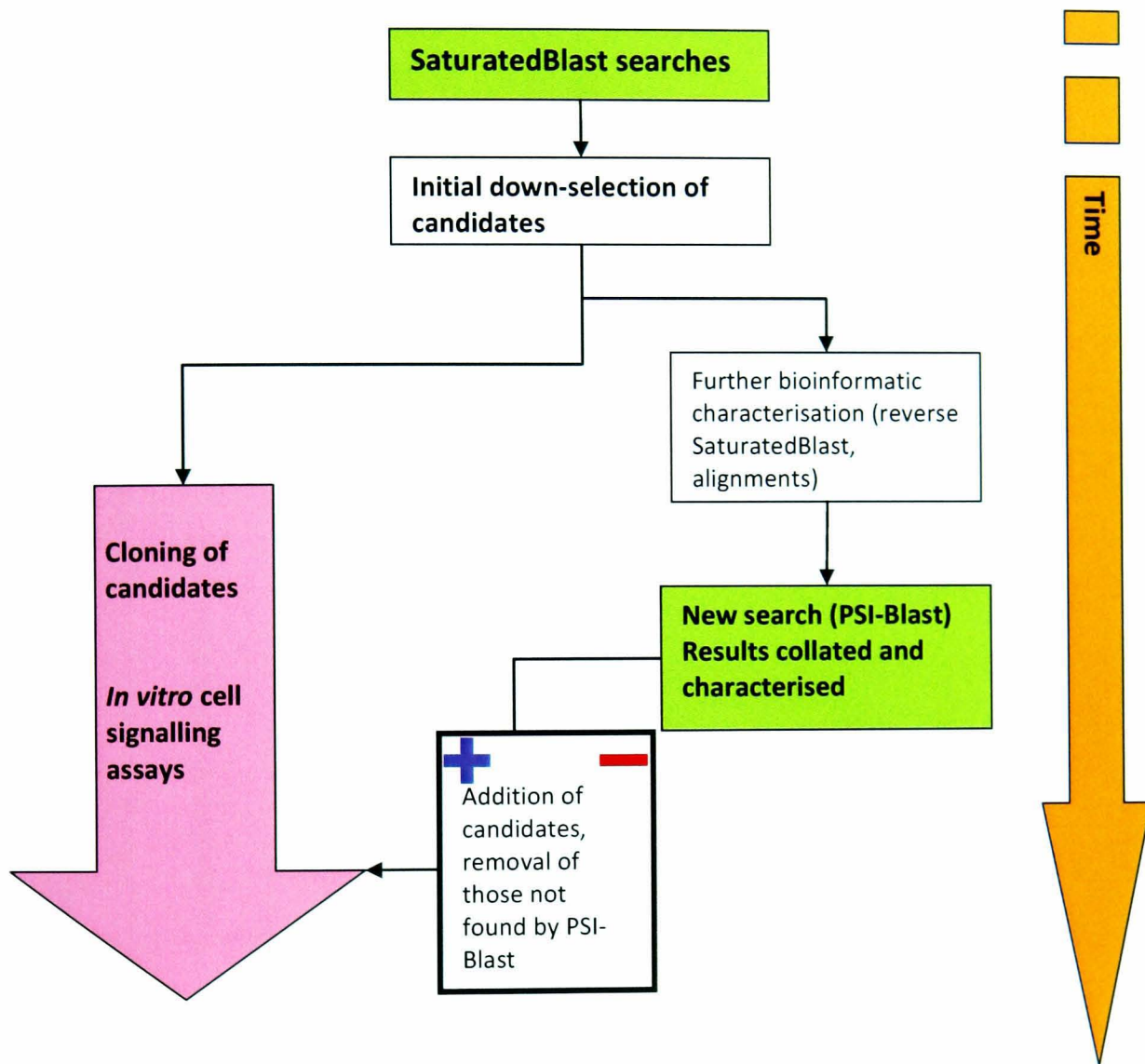


Figure 4-1: Flow diagram explaining the link between the bioinformatic searches and subsequent experimental work

Protein name in this document	Bacterial species	Result of which searches	Reason for down-selection	Colour code on figures
YpTdp	<i>Yersinia pestis</i>	Saturated BLAST & PSI-BLAST	CDC category A agent, strong candidate bioinformatically	Pink
BaTdp	<i>Bacillus anthracis</i>	PSI-BLAST	CDC category A agent, strong candidate bioinformatically	Green
BthTdp	<i>Burkholderia thailandensis</i>	Saturated BLAST & PSI-BLAST	Model organism for Category B agent <i>B. pseudomallei</i> but “non-pathogenic.” Interesting to assess affect on mammalian immune signalling	Red
BmTdp	<i>Brucella melitensis</i>	Saturated BLAST & PSI-BLAST	CDC category B agent, strong candidate bioinformatically	Blue
BmTdp2	<i>Brucella melitensis</i>	PSI-BLAST	CDC category B agent, strong candidate bioinformatically	Orange
BpTdp	<i>Burkholderia pseudomallei</i>	Saturated BLAST, later discounted	Weak candidate bioinformatically but only <i>B. pseudomallei</i> candidate from Saturated BLAST. Down-selected before completion of PSI-BLAST searches.	Purple

Table 4-1: Bacterial TIR domain proteins down-selected for initial *in vitro* signalling assays
Amino acid sequences for these proteins can be found in Appendix A

4.3. Results

4.3.1. Cloning of the genes encoding selected bacterial TIR domain proteins

The genes for expression of the six candidate proteins were amplified from genomic DNA by PCR. These PCR products were then purified and ligated into the mammalian expression vector pcDNA3.2 using a directional TOPO method. This vector allows the protein of interest to be expressed with a V5 tag. This is a small tag comprised of fifteen amino acids of the sequence GKIPNPLLGLDST. PCR reactions were successful for five out of the six candidates (data not shown) but were unsuccessful for BthTdp. The genome of *Burkholderia* sp. is naturally very GC rich meaning that hairpins are a frequent occurrence and PCR from this genomic DNA can be difficult. The *BthTdp* gene was therefore synthesised, attached to a V5 tag, and cloned into the expression vector pcDNA3.1. This vector is similar to pcDNA3.2 but it is not a TOPO vector and transcription termination is provided by the bovine growth hormone (BGH) polyadenylation (polyA) site instead of the thymidine kinase (TK) polyA site. The genes cloned into both vectors are under the control of the same promoter in the same vector backbone and therefore should express to similar levels. Cloning of authentic genes into the expression vectors was confirmed by sequencing (Appendix C).

4.3.2. Expression of bacterial TIR domain proteins in HEK293 cells

HEK293 cells were chosen as the cell line in which to carry out immune signalling assays. HEK293 cells naturally express appreciable levels of the IL-1R but show little, or no, expression of the TLRs⁴⁵⁶. Thus the cells are amenable to the study of the IL-1R pathway alone, and for the study of individual TLR pathways via the stable transfection of TLR-expressing constructs. A variant of HEK293 cells (HEK293H cells) were chosen for the IL-1-induced NF κ B activity assays since these cells show greater adherence to the wells of tissue culture plates making the addition of media/washing of cells easier. Confirmation that the genes encoding the bacterial Tdps cloned into pcDNA3.2 or pcDNA3.1 were expressed as V5-tagged proteins in HEK293H cells was carried out before immune signalling assays were undertaken. HEK293H cells were transfected with each Tdp-expressing construct or control vector (pcDNA3.2_Cat, see Section 4.3.3) and incubated for 24 h to allow expression. At this time the cells were lysed, cleared of debris and used to produce SDS-PAGE samples (Section 2.7.2.1). The samples were separated by PAGE and analysed by Western blot using a primary antibody for the V5 tag (Figure 4-2).

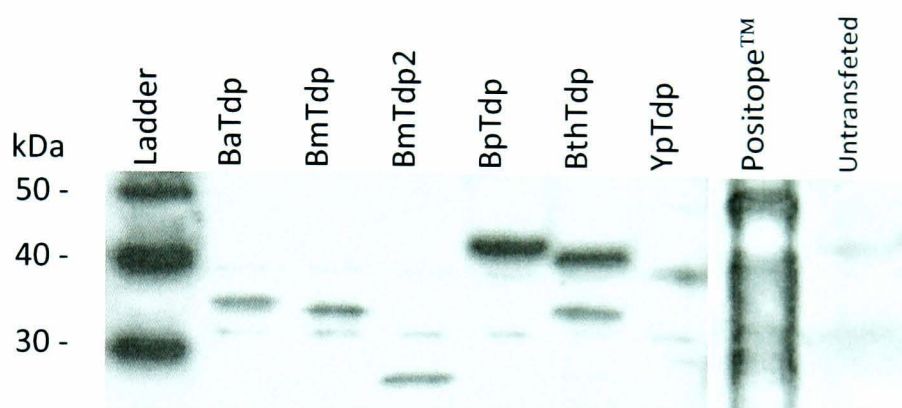


Figure 4-2: Expression of bacterial TIR domain proteins in HEK293H cells.

In order to show expression from cloned *Tdp* genes HEK293H cells were transfected with Tdp-expressing vectors and after 24 h expression the cells were lysed, cleared of cell debris and used to make reduced SDS-PAGE samples. Lysates were separated by PAGE and blotted onto PVDF membrane. After blocking, this membrane was incubated with rabbit anti-V5 antibody and then anti-rabbit-HRP secondary antibody before detection using ECL substrates. Tdp = TIR domain protein from Ba (*Bacillus anthracis*), Bm (*Brucella melitensis*), Bp (*Burkholderia pseudomallei*), Bth (*Burkholderia thailandensis*), and Yp (*Yersinia pestis*). Positope™ (Invitrogen) is a positive control protein containing a V5 tag. Total protein sizes predicted/observed (kDa): BaTdp-V5 = 35.51/c.36, BmTdp-V5 = 32.17/c.34, BmTdp2-V5 = 24.71/c.26, BpTdp-V5 = 44.03/c.42, BthTdp-V5 = 40.22/c.41, YpTdp-V5 = 42.27/c.40, Positope™ = 53.00.

4.3.3. Setting up the NF κ B luciferase reporter assay

In order to assess IL-1 signalling to NF κ B in the presence of bacterial Tdps, a luciferase reporter assay was set up using a reporter vector encoding the gene for firefly luciferase located downstream of five NF κ B binding sites. The IL-1 pathway is activated by exogenous addition of IL-1 β which signals to activate NF κ B thus inducing transcription of the luciferase gene and production of this enzyme. When its substrate luciferin is introduced, the enzyme converts luciferin to oxyluciferin with the concurrent production of light. The amount of light produced is proportional to the amount of luciferase enzyme present, and thus the activity of NF κ B and the immune signalling pathway (Figure 4-3). To ensure that any change in luciferase activity observed is due to the modulation of signalling, rather than the viability of the cells, a control luciferase vector was used expressing the *Renilla reniformis* luciferase gene under the control of the constitutive HSV-thymidine kinase promoter (pRL-TK). This promoter is relatively weak but is useful for providing neutral constitutive expression of the *Renilla* luciferase.

Light emitted as a result of both the *Renilla* and firefly luciferase activity can be measured using a luminometer and the ratio of firefly activity over *Renilla* activity gives a relative luciferase unit (RLU) reading. Changes in the activity of a pathway leading to NF κ B (in the presence of Tdps, for example) can be correlated with changes in the RLU. This system can also be used to investigate TNF α signalling to NF κ B through the TNF receptor (TNFR) since HEK293 cells also naturally express this receptor. TNF α signalling is a useful control pathway when studying the effects of Tdps since this pathway is independent of TIR domain interactions.

Additionally, HEK293 cells stably transfected with human TLR4 (HEK-Blue™ hTLR4 cells) were used to assess the effect of the bacterial Tdps on signalling initiated by LPS. These HEK-Blue™ hTLR4 cells were stably transfected with an NF κ B reporter system whereby activation of NF κ B caused the expression of secreted embryonic alkaline phosphatase (SEAP). SEAP catalyses the hydrolysis of para-nitrophenyl phosphate (pNpp) producing the yellow end product para-nitrophenol. This can be measured using light absorbance with the level of colour change correlating with pathway activation and therefore the effect of Tdps on signalling can be inferred.

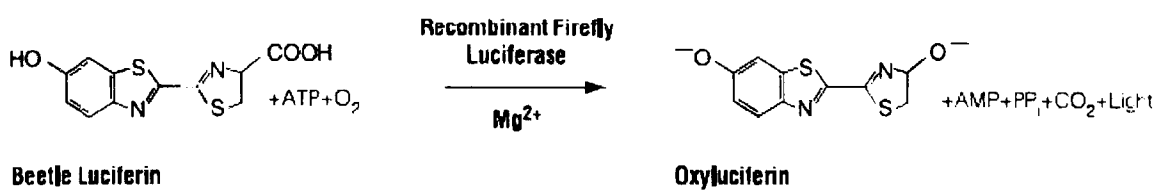


Figure 4-3: The catalysis of luciferin into oxyluciferin with the concurrent emission of light as catalysed by firefly luciferase.

The first screening assay for the action of the selected Tdps was to investigate their effect on the IL-1 pathway. This assay was to be conducted in the presence and absence of the six down-selected bacterial proteins. Empty vector DNA is often employed as a control, and for keeping the amount of DNA transfected constant. However, since pcDNA3.2 is a TOPO vector, it is linear in its empty form. A control vector supplied with the TOPO vector contains the gene for chloramphenicol acetyltransferase (Cat) which confers chloramphenicol resistance. To assess its utility as a control vector, the effect of Cat on IL-1 β signalling to NF κ B was assessed. HEK293H cells were seeded into a 96-well plate and transfected with pcDNA3.2_Cat in addition to the NF κ B luciferase reporter vector and control *Renilla* luciferase vector. Control cells were transfected only with the luciferase vectors. The cells were then stimulated with IL-1 β or PBS and lysed after 6 hours of stimulation for the measurement of luciferase activity. Figure 4-4 shows that the presence of Cat had no effect on IL-1 β signalling to NF κ B ($p = 0.9810$, unpaired t-test) and pcDNA3.2_Cat was suitable for use as a control vector.

4.3.4. The effect of Tdps on IL-1 β signalling to NF κ B.

In order to test the effect of the bacterial Tdps on IL-1 signalling HEK293H cells were transfected with the six candidate Tdp-expressing vectors or control vector in at least triplicate. Subsequently, 24 h after transfection NF κ B activation was induced by stimulation with 100 ng/ml IL-1 β for 6 h at which time the cells were lysed and luciferase activity was analysed. PBS was used as a control stimulant. A stimulation event was deemed to be successful if the luciferase activity from the IL-1 β -stimulated cells was significantly increased over unstimulated (PBS) cells ($p < 0.05$, one-way ANOVA with Bonferroni's post test).

Luciferase activity is expressed as relative luciferase units (RLU) which are calculated by dividing the amount of light emitted from the firefly luciferase reaction (in arbitrary units) by the amount of light emitted from the renilla luciferase reaction (in arbitrary units).

Although RLU values were relatively consistent between wells in the same experiment, values changed hugely between experiments on different days. However the difference between RLU values for unstimulated and stimulated cells remained relatively constant. This variation in RLU values on different days likely reflects the age and health of the cells which will affect the amount of IL-1R naturally expressed, and enzymatic reactions within

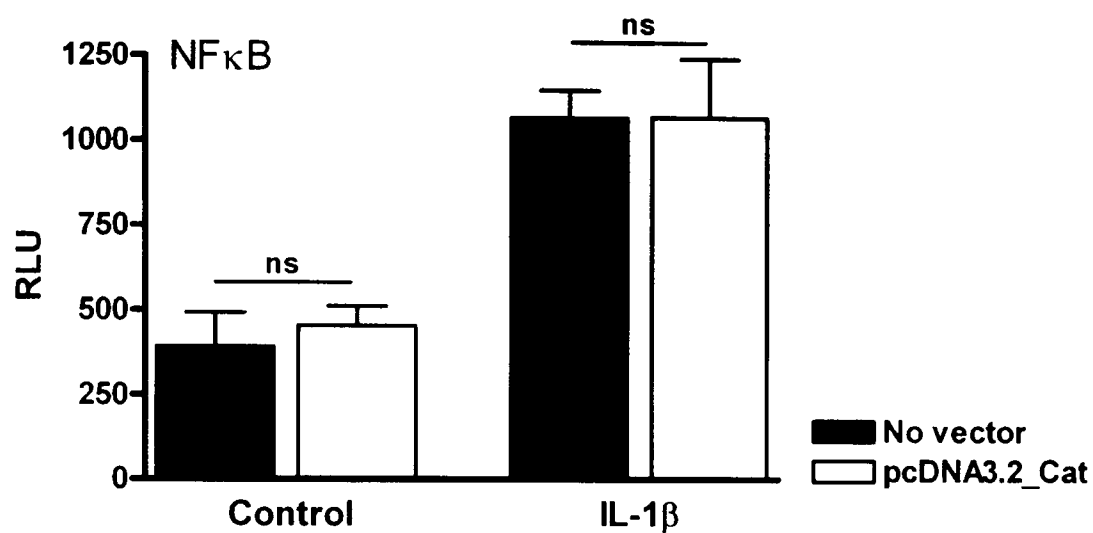


Figure 4-4: The effect of chloramphenicol acetyltransferase on NFκB activity downstream of IL-1β stimulation.

HEK293H cells were transfected with the pNFκB-luc and pTK-renilla reporter vectors alone (black bars), or along with pcDNA3.2_Cat (white bars). After 24 h the cells were stimulated with PBS (control) or 100 ng/ml IL-1β for 6 hr and luciferase activity was measured as described. $p = 0.5927$ unstimulated control, $p = 0.9810$ IL-1β stimulation (unpaired t-test).

the cells. Figure 4-5 shows a graph of the data from each well from one representative experiment for each bacterial Tdp. Initially each experiment contained triplicate wells for each condition, but due to the variation in the assay and the fact that occasionally a value was not returned for a well (if the *Renilla* luciferase activity was recorded as zero for example), subsequently up to six wells per condition were used. Significant induction of NFκB activity on stimulation with IL-1β, and the significance of the effect of each bacterial Tdp in each experiment were analysed by one-way ANOVA with Bonferroni's post test. Experiments for each Tdp were conducted five times (significant stimulation events).

In order to normalise the differences in RLU values between experiments, and to compare each bacterial Tdp for its affect on IL-1β signalling, average RLU values in the presence of control vector (stimulated or unstimulated) were normalised to 100% for each experiment. Signalling in the presence of each Tdp was then expressed as % of this control signalling (calculation detailed in Table 2-7, Section 2.6.6). The results for IL-1β signalling are summarised in Figure 4-6. A one-sample column t-test was used to assess whether the NFκB activity in the presence of each Tdp differed significantly from 100%.

Modified NFκB activity after IL-1β stimulation was demonstrated by the addition of 3 out of 6 Tdps tested. NFκB activity was reduced to 52.9% of control signalling in the presence of YpTdp ($p = 0.0036$) indicating that the over-expression of YpTdp is able to down-regulate IL-1β signalling to NFκB in this system. Similarly, in the presence of BthTdp NFκB activity was 31.7% of control signalling ($p = 0.0009$) suggesting that IL-1β signalling is modulated in the presence of BthTdp. Somewhat surprisingly, when BmTdp2 was expressed in this system NFκB activity after IL-1β stimulation increased by 92% ($p = 0.0119$). This could mean that the TIR domain from BmTdp2 is actually facilitating the binding of downstream adaptor proteins in this case. Whether this is physiologically relevant remains to be investigated. Using $p < 0.05$ as a cut-off for this hypothesis test meant that there was no difference in signalling in the presence of BaTdp, BmTdp or BpTdp ($p = 0.8692, 0.4063$ and 0.5769 respectively). This is unsurprising for BpTdp since the PSI-BLAST searches discounted this protein as a Tdp. Somewhat surprisingly, like BmTdp2, BmTdp may cause an up-regulation of signalling to NFκB in the presence of IL-1β (based on individual assay data), although this is not statistically significant when independent experiments are averaged.

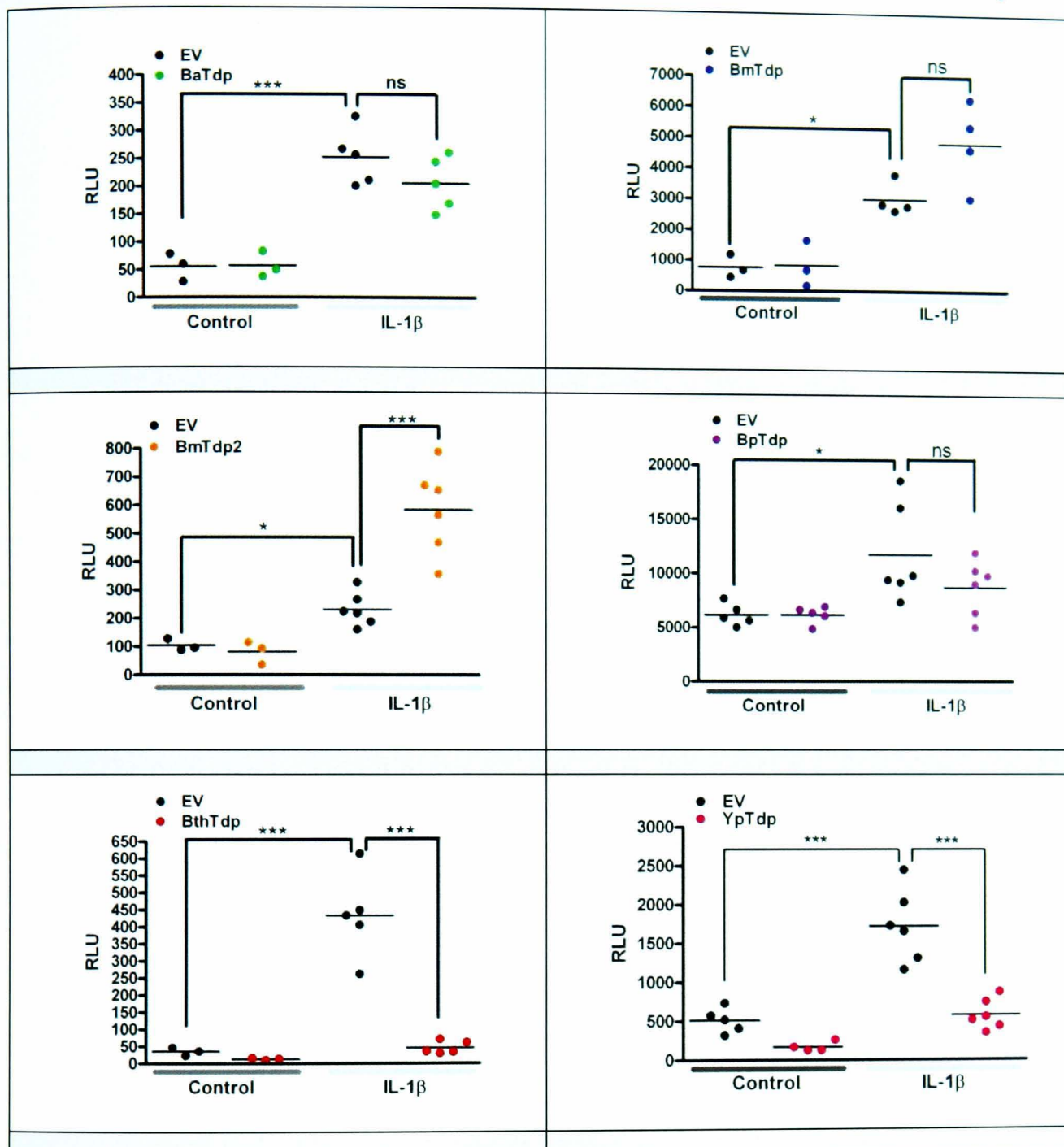


Figure 4-5: Results from representative IL-1 β signalling experiments

RLU values for each well in a representative IL-1 β -induced NF κ B activity experiment for each bacterial Tdp. * denotes $p < 0.05$, ** denotes $p < 0.01$, *** denotes $p < 0.001$ using a one-way ANOVA with Bonferroni's post-test. RLU – relative luciferase units.

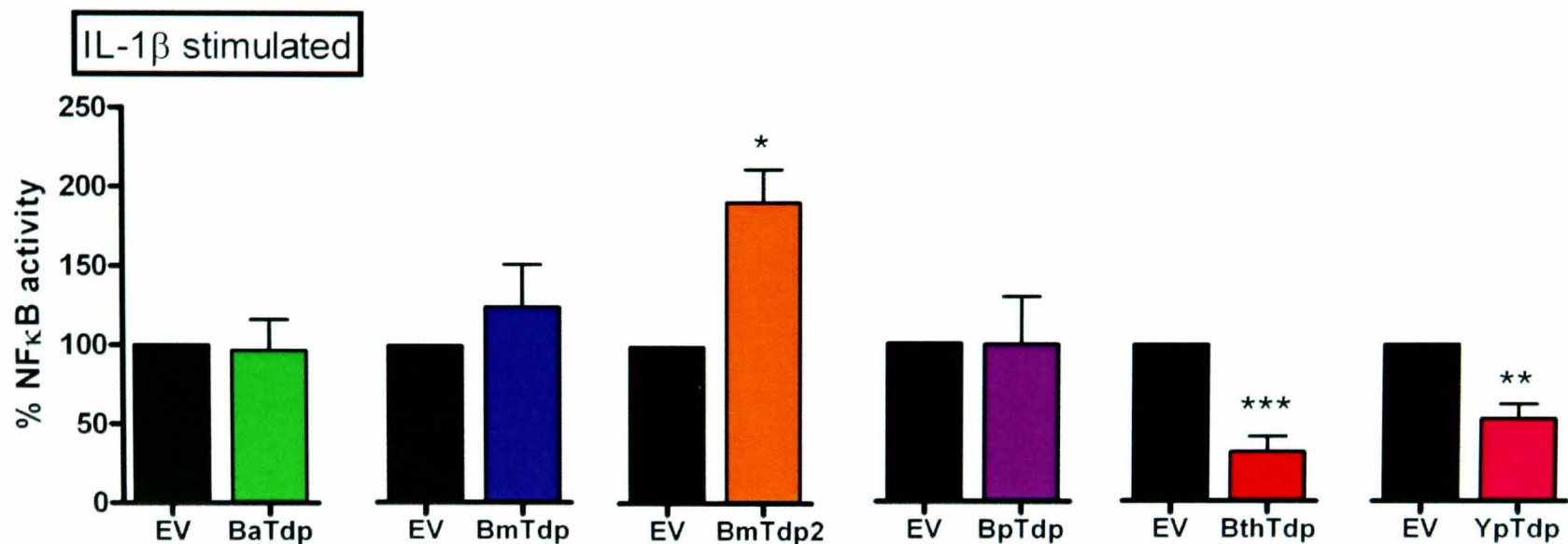


Figure 4-6: The effect of selected bacterial Tdps on IL-1 β -induced NF κ B activity.

HEK293H cells were transfected with Tdp-expressing vectors or control vector. Subsequently, 24 h post-transfection they were stimulated with IL-1 β at 100 ng/ml and then luciferase activity measured as described. PBS was the control stimulant for all experiments (Figure 4-7). RLU values for cells stimulated with IL-1 β in the presence of control vector were normalised to 100% for each experiment and signalling in the presence of the Tdps is expressed as a % of this signalling. Data is expressed as the mean \pm SEM of five biological replicates each being the mean of at least three technical replicates. * denotes $p < 0.05$, ** denotes $p < 0.01$, *** denotes $p < 0.001$ by column t-test compared to 100%

4.3.5. The effect of Tdps on basal NFκB activity

Control conditions in the luciferase assays also included the absence of pathway stimulation to assess the affect of each bacterial Tdp on the basal activity of NFκB in the absence of exogenous stimulant (Figure 4-7). Here basal NFκB activity in the presence of control vector is normalised to 100% for the purposes of comparing each Tdp. These studies indicate that BthTdp down-regulates basal NFκB activity to 24.8 % of control ($p = 0.0002$). This undermines a TIR-dependent affect for BthTdp on NFκB activity. None of the other Tdps had any significant affect on NFκB activation in the absence of stimulation.

4.3.6. The effect of Tdps on TNFα signalling to NFκB.

In order to assess whether the observed effects of the bacterial Tdps on IL-1β signalling to NFκB was likely to be due to disruption at the level of TIR domain interactions, the NFκB reporter assay was also carried out downstream of TNFα signalling. TNFα signals through the TNFR receptor in a manner that does not rely on any interaction between TIR domains. Figure 4-8 shows the effect of each bacterial Tdp on TNFα signalling to NFκB. NFκB activity induced by TNFα in the presence of control vector was normalised to 100% for each experiment. None of the bacterial Tdps had a significant effect on TNFα signalling to NFκB, although there is an indication of an effect in the presence of BthTdp but more studies would be needed to confirm this. This contributes to the supposition that the effect of BthTdp on NFκB activity may not be entirely TIR-mediated. The lack of affect on TNFα signalling from YpTdp and BmTdp2 suggests that their action on the IL-1β signalling pathway is likely to be TIR-mediated.

4.3.7. Specificity of the effect of YpTdp and BthTdp on IL-1β signalling to NFκB.

YpTdp and BthTdp were tested for their specificity of action on the IL-1β pathway to NFκB by investigating their effect at varying doses. Varying amounts of the YpTdp- or BthTdp-expressing vectors were transfected into HEK293H cells with NFκB- and control luciferase reporter vectors. The amount of DNA transfected was kept constant by the addition of control vector DNA. NFκB activity induced by IL-1β in the presence of control vector was normalised to 100% for each experiment and activity in the presence of YpTdp or BthTdp is expressed as a % in comparison. PBS was the control stimulant for

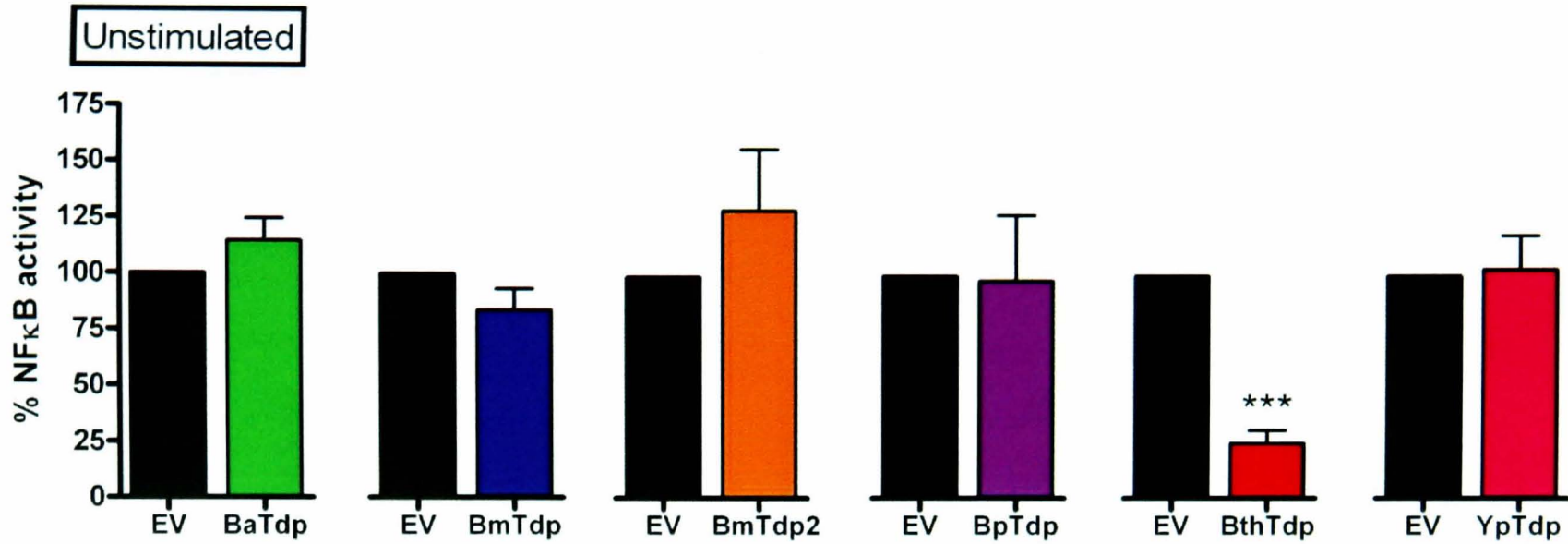


Figure 4-7: The effect of selected bacterial Tdps on the basal activity of NFκB (in the absence of any exogenous immune stimulation).

During the experiments to determine the effect of bacterial Tdps on IL-1β signalling to NFκB control wells were included: HEK293H cells were transfected with the Tdp-expressing vectors or control vector. Subsequently, 24 h post-transfection they were incubated with PBS for 6 h and then luciferase activity measured. RLU values for cells incubated with PBS in the presence of control vector were normalised to 100% for each experiment (basal NFκB activity) and NFκB activity in the presence of the Tdps is expressed as a % of this activity. Data is expressed as the mean ± SEM of five biological replicates each being the mean of at least three technical replicates. *** denotes $p < 0.001$ by column t-test compared to 100%

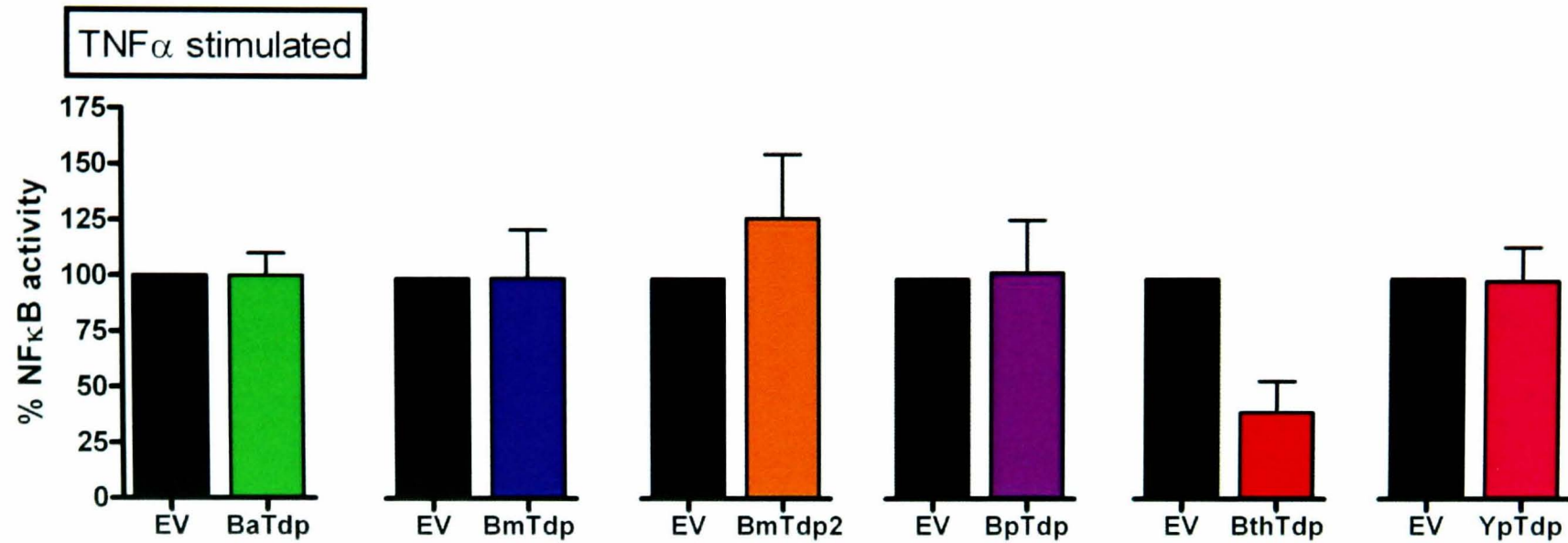


Figure 4-8: The effect of selected bacterial Tdps on NF κ B activity downstream of TNF α stimulation

HEK293H cells were transfected with the Tdp-expressing vectors or control vector. Subsequently, 24 h post-transfection they were stimulated with TNF α at 100 ng/ml and then luciferase activity was measured. PBS was used as the control stimulant for these experiments (data not shown). RLU values for cells stimulated with TNF α in the presence of control vector were normalised to 100% for each experiment and signalling in the presence of the Tdps is expressed as a % of this signalling. Data is expressed as the mean \pm SEM of three biological replicates each being the mean of at least three technical replicates.

these assays (data not shown). YpTdp reduced IL-1 β -induced NF κ B activity when the highest concentration of vector was transfected (150 ng, Figure 4-9, $p = 0.0455$, column t-test). Linear regression analysis gives a correlation value (r^2) of 0.6259 for the correlation between dose of pcDNA3.2_*YpTdp* (and hence likely amount of YpTdp present in the cells) and NF κ B activity. This suggests that the altered dose of YpTdp vector correlates well with NF κ B activity but that there are likely to be other factors involved (an r^2 value of > 0.7 is considered to be high and therefore a good correlation between x and y). This may be expected since transfection efficiency and pipetting accuracy are likely to impact on the correlation. In addition there will be saturation in the system (the amount of DNA able to be transfected and concentrations of IL-1R in the cells). Considering all the variables it seems there is a good correlation between amount of YpTdp and level of IL-1 β induced NF κ B activity. A similar analysis was carried out for BthTdp (Figure 4-9). BthTdp causes a significant reduction in NF κ B activity at every dose of vector transfected suggesting that perhaps more functionally available protein is expressed per ng of vector than YpTdp, or that BthTdp has a higher affinity for the human TIR domain proteins in the pathway. BthTdp certainly appears to express better in the HEK293H cells than YpTdp when compared by Western blot (Figure 4-4). Linear regression analysis gave an r^2 value of 0.7720 for the correlation between amount of pcDNA3.2_*BthTdp* transfected and NF κ B activity which indicates a good correlation between the amount of BthTdp in the cells and the extent to which NF κ B activity is reduced.

4.3.8. The effect of Tdps on LPS signalling to NF κ B.

HEK-Blue™ hTLR4 cells, with a SEAP reporter system for NF κ B activity (Section 4.1), were used to assess the effect of the bacterial Tdps on signalling initiated by LPS. BpTdp and BthTdp were excluded from these experiments since BpTdp was discounted as a Tdp and studies suggested that BthTdp may have a non-specific effect on NF κ B activation. HEK-Blue™ hTLR4 cells were seeded into 6-well plates and transfected 24 h later with the Tdp constructs or control vector. At 24 h post-transfection the cells were stimulated with *E. coli* K12 LPS (or PBS) for 24 h and subsequently the media was removed from the cells was assessed for its alkaline phosphatase activity. A stimulation event was deemed to be successful if the absorbance of light at 620 nm (A_{620}) in the media from stimulated cells

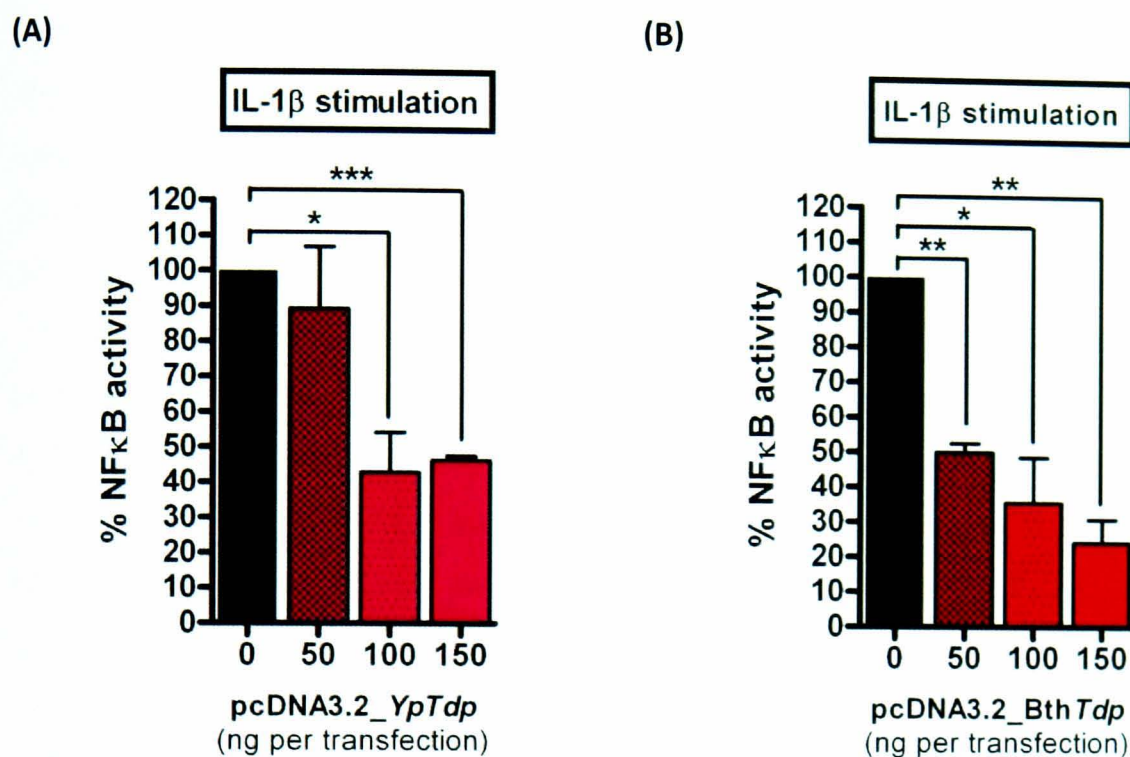


Figure 4-9: The dose-dependent affect of YpTdp and BthTdp on IL-1 β signalling to NF κ B.

HEK293H cells were transfected with different amounts of YpTdp- or BthTdp- expressing vectors. Total DNA was kept constant at 230 ng with the addition of control vector. Subsequently, 24 h post-transfection the cells were stimulated with 100 ng/ml IL-1 β for 6 h and then luciferase activity measured as described. PBS was the control stimulant for these assays (data not shown). RLU values for cells stimulated with IL-1 β in the presence of control vector only were normalised to 100 % for each experiment and signalling in the presence of varying amounts of YpTdp/BthTdp is expressed as a % of this control signalling. Data is expressed as the mean \pm SEM of three biological replicates each being the mean of at least three technical replicates.

was significantly increased over unstimulated cells ($p < 0.05$, one-way ANOVA with Bonferroni's post test). Due to the presence of transfected TLR4 within these cells the variability in reporter activity (SEAP) within and between experiments was vastly reduced when compared to the luciferase assays which relied on endogenous expression of the IL-1 and TNF α receptors. Therefore an experiment containing triplicate wells was repeated on three separate occasions for each Tdp. Figure 4-10 shows a graph of one representative experiment for each Tdp. Activity in the presence of control vector was normalised to 100% for each experiment and signalling in the presence of the Tdps was expressed as a % of this for comparison of Tdps across experiments (Figure 4-11). In these assays, NF κ B activity was reduced to 83% of control signalling in the presence of YpTdp ($p = 0.0323$) indicating that YpTdp is likely to down-regulate LPS signalling to NF κ B. In the presence of BmTdp, NF κ B activity was 77% of control signalling ($p = 0.0129$) suggesting that LPS signalling is also modulated in the presence of BmTdp. BaTdp may also modulate LPS-dependent signalling to NF κ B although the data generated here does not demonstrate significant activity (77% of control signalling, $p = 0.0984$). LPS signalling in the presence of BmTdp2 was not significantly different from control ($p = 0.8193$). NF κ B activity in these TLR4 cells in the absence of LPS stimulation (basal activity) was again assessed and none of the bacterial Tdps tested had an effect on basal NF κ B activity in this TLR4 background (Figure 4-12).

Unlike the NF κ B luciferase reporter assay the HEK-Blue™ hTLR4 SEAP reporter system does not include a reporter control for cell viability (neutral constitutive expression of SEAP). Conceivably, the reduction in LPS signalling observed in the presence of BmTdp and YpTdp could be caused by a reduction in viability of these cells. In the protocol for stimulation of the HEK-Blue™ hTLR4 cells post-transfection, the cells are scraped, counted and re-seeded in the presence of LPS. In order to assess whether the expression of the bacterial Tdps had an effect on cell viability the cells were scraped in the media in which they were seeded and counted in the presence of trypan blue. The results indicate that a reduction in NF κ B activity in the presence of YpTdp and BmTdp does not correlate with a reduction in cell viability (Figure 4-13). Transfection with empty vector alone

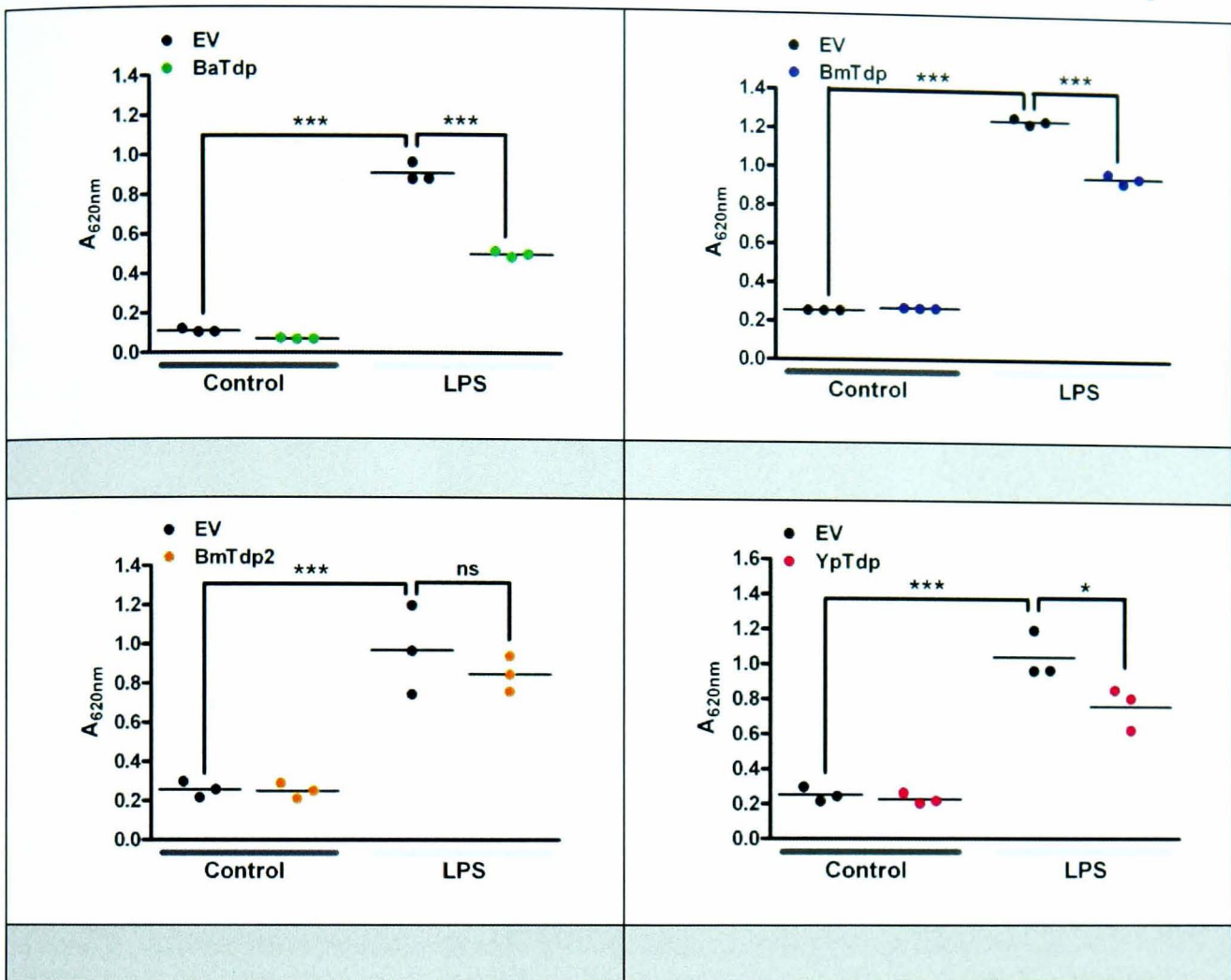


Figure 4-10: Results from representative LPS signalling experiments

The graphs depict the absorbance of light at 620 nm for each well in a representative LPS-induced NF κ B activity experiment for each bacterial Tdp. * denotes $p < 0.05$, *** denotes $p < 0.001$.

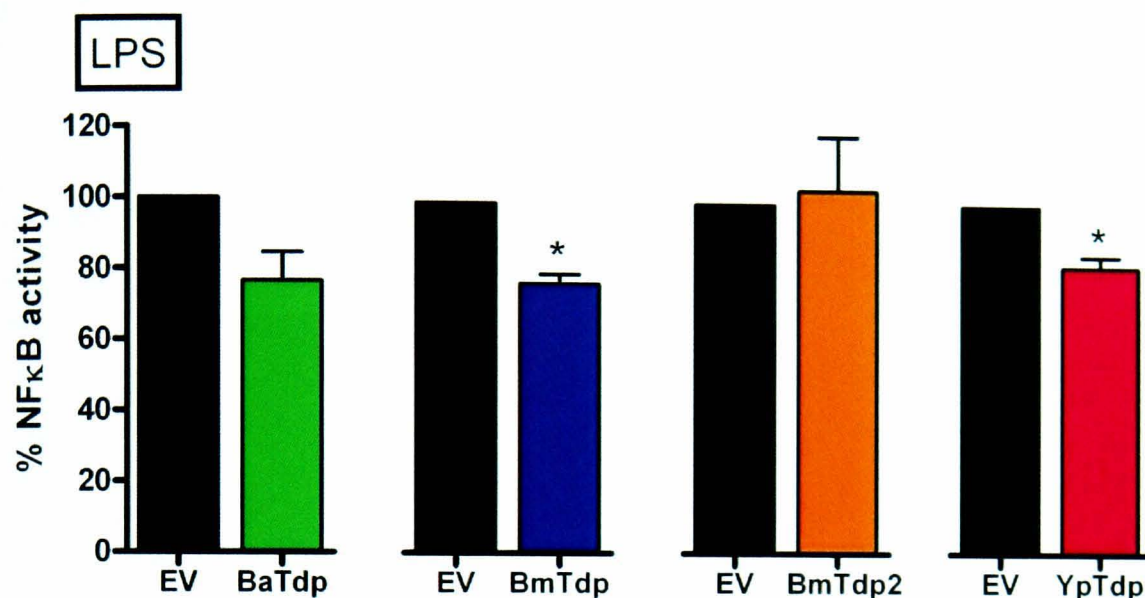


Figure 4-11: The effect of selected Tdps on NFκB activity downstream of LPS stimulation

HEK293H cells were transfected with Tdp-expressing vectors or control vector. Subsequently, 24 h post-transfection the cells were scraped and counted, and reseeded in the presence of *E. coli* K12 LPS to a final concentration of 1 μg/ml. PBS was the control stimulant for all experiments (Figure 4-12). After 24 h stimulation the media from the cells was removed and assessed for alkaline phosphatase (SEAP) activity. SEAP activity in the presence of control vector was normalised to 100% and activity in the presence of the bacterial Tdps expressed as a % of this. Data is expressed as the mean ± SEM of three biological replicates each being the mean of at least three technical replicates.

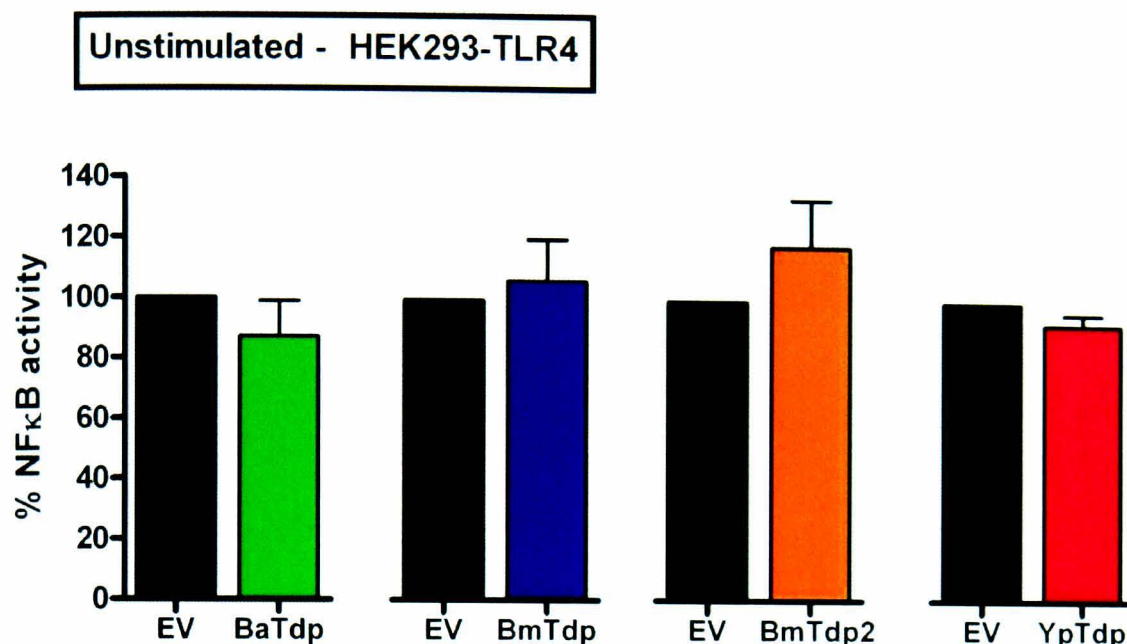


Figure 4-12: The effect of selected bacterial Tdps on basal NF κ B activity (absence of any exogenous immune stimulation) in HEK-Blue™ hTLR4 cells

During the experiments to determine the effect of bacterial Tdps on LPS signalling to NF κ B control wells were included: HEK293H cells were transfected with the Tdp-expressing vectors or control vector. Subsequently, 24 h post-transfection the cells were scraped and counted, and reseeded in the presence of PBS for 24 h. Then the media from the cells was removed and assessed for alkaline phosphatase (SEAP) activity. SEAP activity in the presence of control vector was normalised to 100% and activity in the presence of the bacterial Tdps expressed as a % of this. Data is expressed as the mean \pm SEM of three biological replicates each being the mean of at least three technical replicates.

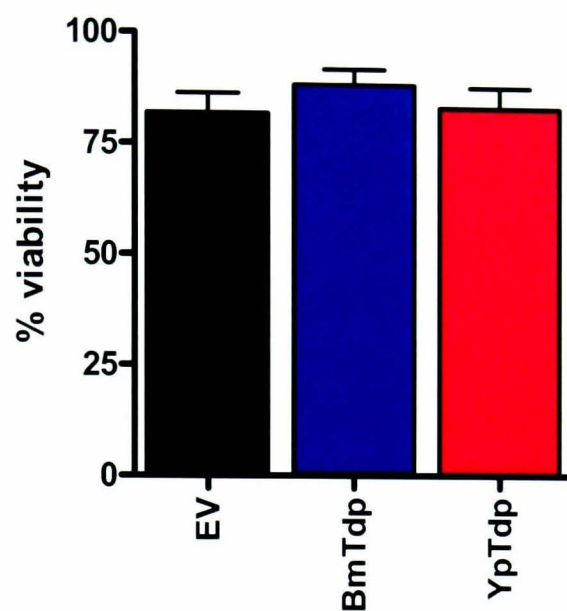


Figure 4-13: Percentage viability of HEK-Blue™ hTLR4 cells 24 h after transfection with Tdp constructs

HEK293-TLR4 cells were transfected with Tdp-expressing vectors. After 24 h the cells were removed from the well by gentle scraping in their original media and counted in the presence of trypan blue at a 1:1 (v/v) ratio in order to assess their viability. % viability is shown for BmTdp and YpTdp since these proteins demonstrated a modulating the LPS response.

caused the death of 18% of cells and this was not significantly different in the presence of YpTdp (17%) or BmTdp (12%).

4.4. Conclusions

Of the five candidate bacterial proteins found to contain a TIR domain in the PSI-BLAST searches, YpTdp demonstrated a specific and significant effect on both IL-1 β and LPS (TIR-dependent) signalling to NF κ B. BmTdp was seen to down-regulate LPS signalling, whereas the second Tdp in *Brucella* sp (BmTdp2) appeared to exert an unusual effect on IL-1 β signalling to NF κ B by actually increasing the activation of NF κ B down-stream of this signal. There was also an indication that BaTdp may have an effect on LPS signalling to NF κ B (Figure 4-10 and Figure 4-11). One important point to note is that, in general, these reporter assays produced a fairly large amount of variability in the data (although the SEAP reporter assays were much improved on the initial luciferase assay system). This is likely attributed to the age and health of the cells, and the multiple steps within the assay where variability could occur including, particularly for the luciferase assays, the transient transfection of three or more vectors at one time. Therefore, far from being the initial screening method for Tdp activity anticipated, additional experiments would be necessary for conclusive results.

Looking at the results from these assays, however, and taking each bacterial Tdp in turn: BaTdp had no significant effect on immune signalling downstream of IL-1 or TNF α but there is an indication that it may affect LPS signalling to NF κ B. Initially this may seem unusual since *B. anthracis* is a gram-positive bacterium and does not possess LPS as a stimulant for TLR4. However, TLR4 is the receptor for a wide variety of molecules aside from LPS, including anthrolysin³⁶⁸ (a molecule possessed by *B. anthracis*) and endogenous danger signals. Therefore it is not inconceivable that during infection *B. anthracis* would aim to disrupt TLR4 signalling.

BmTdp had no significant effect on immune signalling downstream of IL-1 or TNF α , although there is an indication of up-regulation of IL-1-dependent signalling. Previous reports on BmTdp are somewhat conflicting (Section 4.1). However, a down-modulatory

effect of this protein on TLR4 signalling is generally accepted. In this work, a down-regulation of LPS signalling to NF κ B in the presence of BmTdp has also been observed. In Chapter 3 the structural homology of BmTdp to the annexin family of proteins was introduced. Annexins have been shown to be ligands for TLR4⁴⁵⁷ and although proteins from the annexin family are not thought to exist in bacterial species, an alternative hypothesis to disruption at the level of the TIR domain is that BmTdp may be sufficiently similar to the annexin family to block the TLR4 ligand binding site and therefore LPS stimulation of this receptor.

A second Tdp in *Brucella* sp., which has not been previously reported, does not appear to have any significant affect on basal NF κ B activity, or that induced by TNF α or LPS. However, it appears to facilitate NF κ B activity after IL-1 β stimulation. This is unlikely to be attributed to endotoxin contamination of the vector stimulating any low-level expression of TLR4 in HEK293 cells since there was no up-regulation observed in HEK-Blue™ hTLR4 cells. Further studies would be needed to probe this further. *B. melitensis* causes significant immune modulation in its host⁴¹⁴, and this may include the up-regulation of certain pathways for its own needs, whether this is in order to encourage immune cells to the site of infection to provide its niche environment, or for the up-regulation of anti-inflammatory molecules.

BthTdp showed a consistent and significant down-regulation of NF κ B activity, but this also included an effect on the basal activity of NF κ B and some indication that it affected NF κ B activity downstream of TNF α signalling. These results suggest that BthTdp may be acting on a TIR-independent signal to NF κ B, on NF κ B itself, or globally on transcription. BthTdp acted in some senses as a control protein in these human immune signalling assays since it is from a bacterial species largely avirulent to humans. However, it was still able to down-regulate a human immune signalling pathway. This may suggest that these assays do not act as a reliable method to assign physiological function to these proteins, or that *B. thailandensis* does encode proteins that engage in modulation of immune signalling pathways. Some studies, and information from patients, suggest that *B. thailandensis* may

be more virulent than is often thought⁴⁵⁸, or perhaps it is engaged in the modulation of plant or insect immune pathways.

Table 4-2 summarises the results of these *in vitro* signalling assays. Looking at previous studies of bacterial Tdps, and the assertion that their role is one of immune modulation, it may have been expected that more of these Tdps would have a measurable effect on each of the pathways investigated. Out of the five Tdps tested only YpTdp showed any effect on both IL-1 β and LPS signalling and, in general, the results showed variability and fairly marginal effects. Bearing in mind that this system also relies on the over-expression of these proteins within cells, these results perhaps add weight to the argument introduced here that the modulation of IL-1/TLR signalling pathways is not the primary, or physiological, role of bacterial Tdps. These assays, however, are limited and there may be other explanations for the lack of observed modulation of signalling by these Tdps. It has been postulated that BmTdp may have species-specific effects on TLR signalling pathways³⁴⁶, and this may be the case for the other Tdps. Only human IL-1/TLR signalling has been assessed in these studies. Similarly, only NF κ B activation induced by IL-1 β , LPS or TNF α has been investigated here. These bacterial Tdps may exert their effects on other TIR-dependent signalling pathways, for example downstream of other TLRs involved in the recognition of bacteria such as TLR2 or TLR5. Finally, as discussed at the beginning of this Section, these reporter assays, in general, showed a considerable degree of variability, meaning that larger sample sizes and complementary tests will be necessary to fully explore the effect of these bacterial Tdps on TIR-dependent signalling in this way.

In these limited studies it does, however, appear that the Tdp from *Y. pestis* exerts an effect on human TIR-dependent signalling. In Chapter 5 this protein will be more fully investigated for its effects of TIR-dependent signalling, and confirmation for the results seen here will be sought.

	Basal (HEK293)	IL-1β	TNFα	Basal (HEK-Blue™ hTLR4)	LPS
BaTdp	↔	↔	↔	↔	↔
BmTdp	↔	↔	↔	↔	↓
BmTdp2	↔	↑	↔	↔	↔
BpTdp	↔	↔	↔	ND	ND
BthTdp	↓	↓	↔	ND	ND
YpTdp	↔	↓	↔	↔	↓

Table 4-2: A summary of the effect of selected bacterial TIR domain proteins on TIR -dependent (IL-1/LPS) and -independent (basal, TNF α) signalling to NF κ B

↔ no significant change, ↓ NF κ B activity significantly reduced, ↑ NF κ B activity significantly increased, ND not determined

Chapter 5: Further *in vitro* investigation of YpTdp and its effects on mammalian immune signalling

5.1. Introduction

In Chapter 4 the effect of YpTdp on IL-1 β -, TNF α - and LPS-dependent signalling to NF κ B was investigated. YpTdp significantly down-regulated NF κ B activity induced by IL-1 β and LPS stimulation, but not TNF α stimulation. YpTdp was down-selected for more in-depth, and confirmatory, studies of its effect on TIR-dependent immune signalling pathways downstream of signals other than IL-1 β and LPS, and using methods in addition to the NF κ B reporter assays to confirm these results. NF κ B reporter assays are a powerful technique for assessing the activation of a wide variety of signalling pathways. However, the luciferase assays, as carried out here, were plagued by variability which, as discussed in Chapter 4, likely arose from the requirement to transfect up to five plasmids into the cells at once and the reliance on endogenous expression of receptors. An assessment of other readouts of pathway activation should help to solidify the data on the effect of YpTdp on TLR signalling. The activation of NF κ B is a distal step in the TLR pathway. Other measureable outputs proximal to this include the modification of pathway intermediates (phosphorylation/ubiquitination) or their degradation (e.g.: I κ B α) all of which can be monitored by Western blotting. The binding and dissociation of proteins within the pathway could be monitored by a technique such as Forster resonance energy transfer (FRET), although whether this would be powerful enough to see changes in signalling in the presence of an interfering protein is not clear. At the level of transcription factor activity, apart from reporter assays, their binding to promoters could be measured by an assay such as an electrophoretic molecular shift assay (EMSA) and the appearance of selected mRNA transcripts could be monitored by real time reverse transcriptase PCR (qRT-PCR) or globally by microarray. Finally the production of protein downstream of pathway activation could be monitored by ELISA and Western blotting. In order to investigate the effect of YpTdp on pathway activation a technique was chosen to investigate one process proximal to NF κ B activation (the degradation of I κ B α) and one distally (the production of Il-8).

In addition, YpTdp will also be tested for its interaction with mammalian Tdps to assess at which point in the assembly of a signalling platform at the TIR domain it acts. This Chapter also aims to investigate whether the signalling effects observed in the presence of YpTdp are attributable to its TIR domain or whether other parts of the protein contribute to any effect. In order to do this the region of DNA that encodes solely for the TIR domain of YpTdp (YpTIR) will be cloned and expressed in HEK293 cells for the same assays carried out with YpTdp in Chapter 4. The evaluation of just the TIR domain of a bacterial TIR domain protein has not been previously reported. Using bioinformatics, the TIR domain has been identified as covering approximately residues 137 to 285 in YpTdp. YpTIR will therefore be expressed as residues 130 to 285. These residues were chosen to give 7 residues around the proposed TIR domain.

5.2. Aims and objectives

The aim of this chapter is to confirm an effect of YpTdp on TIR-dependent mammalian immune signalling and to investigate specifically which pathways and molecules are affected by YpTdp expression.

Specific objectives of this chapter are to:

- Clone and express the TIR domain of YpTdp (residues 130-285, YpTIR) to investigate whether the effects on mammalian immune signalling observed in Chapter 4 could be attributed solely to this domain, or whether regions of the protein outside of the TIR domain contribute.
- Investigate the effect of YpTIR expression in immune signalling experiments as described in Chapter 4 (IL-1 β and TNF α -induced signalling to NF κ B via luciferase reporter assays and LPS-induced signalling to NF κ B via an alkaline phosphatase reporter assay) and compare directly to YpTdp activity.
- Determine effects of YpTdp and YpTIR on immune signalling by methods other than NF κ B activity reporter assays to consolidate results.

- Determine the effects of YpTdp and YpTIR on immune signalling induced by the over-expression of the TIR adaptor proteins. When compared to their effects on signalling induced by exogenous stimulation this may give an indication as to where in the pathways YpTdp may be exerting its effect.
- Assess whether YpTdp is able to interact with mammalian TIR domain containing molecules.

5.3. Results

5.3.1. Cloning and expression of the YpTdp TIR domain (YpTIR)

From bioinformatic analysis, the TIR domain from YpTdp is predicted to occur at amino acids residues 130 – 285 (Section 3.3.2.1). DNA to encode this region from the *YPO1883* gene in *Y. pestis* CO92 was amplified by PCR from the vector pET 26b(+)_YPTIRo kindly provided by Dr. Rohini Rana at Imperial College, London. This PCR product was ligated into pcDNA3.2, transformed into *E. coli*, and its sequence was checked (Appendix C). This vector (pcDNA3.2_YpTIR) was then purified free of endotoxin and transfected into HEK293 cells for confirmation of expression by Western blotting (Figure 5-1).

5.3.2. The effect of YpTIR on IL-1 β , TNF α and LPS signalling to NF κ B

Like YpTdp (Chapter 4), YpTIR was expressed in HEK293 and HEK-Blue™ hTLR4 cells and its affect on basal NF κ B activity, and NF κ B activity downstream of IL-1 β , TNF α or LPS was assessed using the reporter assays as detailed in Section 4.3.4. Figure 5-2 shows the normalised results for these assays in comparison with the results for full-length YpTdp from Chapter 4. These results show that YpTIR had no significant affect on IL-1 β -, TNF α - or LPS-induced signalling to NF κ B ($p = 0.8884, 0.6291$ and 0.1906 respectively) which indicates that the down-regulation of NF κ B activity seen in the presence of YpTdp is not attributable solely to the TIR domain, or that when expressed alone the YpTdp TIR domain is not folded as it is in the full length protein. As before, control experiments without any stimulation were carried out for each stimulation event and YpTIR had no effect on basal NF κ B activity (data not shown).

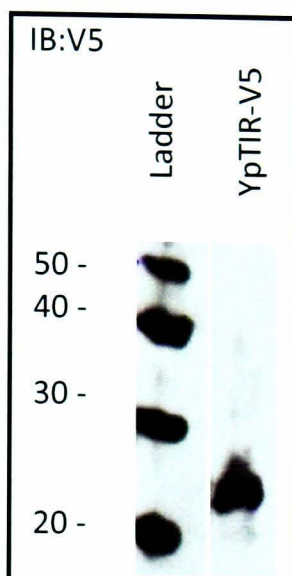


Figure 5-1: Confirmation of the expression of YpTIR-V5 in HEK293 cells by Western blotting

HEK293H cells were transfected with pcDNA3.2_YpTIR and 24 h later the cells were lysed, cleared of cell debris and used to make reduced SDS-PAGE samples. These samples were run on a Tris-Glycine gel alongside MagicMark™ ladder (Invitrogen) and blotted onto PVDF membrane. After blocking, the membranes were incubated with rabbit anti-V5 antibody and then goat-anti-rabbit IgG-HRP antibody before detection of protein using ECL substrates. YpTIR-V5 = 19 kDa

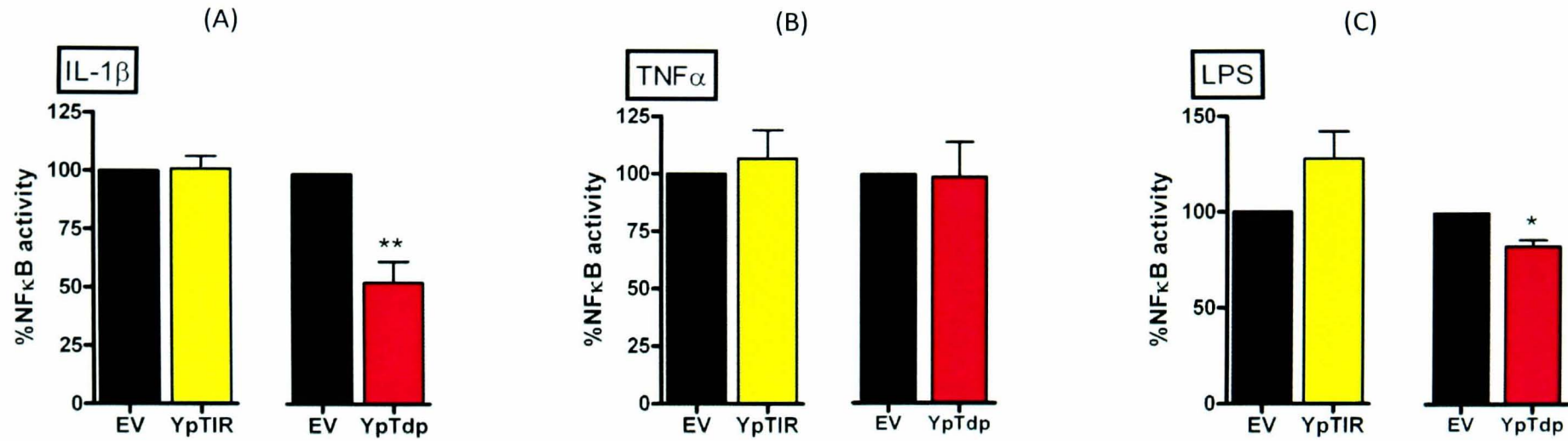


Figure 5-2: The effect of YpTIR on NFκB activity after IL-1β, TNFα or LPS stimulation.

(A) and (B) HEK293H cells were transfected with pcDNA3.2_YpTIR, or _Cat and, at 24 h post-transfection, stimulated with IL-1β or TNFα for 6 h at which point luciferase activity was measured. Data is expressed as the mean of five separate experiments containing at least three biological replicates ± SEM (C) HEK-Blue™ hTLR4 cells were transfected as above and stimulated with *E. coli* K12 LPS for 24 h. The media was then assayed for alkaline phosphatase activity. Data is expressed as the mean of three separate experiments containing three biological replicates ± SEM. For all experiments the data for cells stimulated in the presence of control vector (black bars) were normalised to 100% and signalling in the presence of YpTIR is expressed as a % of this signalling (yellow bars). The results from YpTdp (Chapter 4) are also displayed for comparison (pink bars). Addition of PBS formed the control stimulation for these experiments (data not shown). * denotes $p < 0.05$, ** denotes $p < 0.01$ column t-test.

5.3.3. IL-8 production

The chemokine IL-8 is produced on stimulation of both the IL-1R and TLR4 pathways. Cell culture media from cells used in IL-1 β -stimulated luciferase assays, or LPS-stimulated SEAP reporter assays was removed and stored at -20°C. Media from replicate wells was pooled. Subsequently, these samples were analysed for IL-8 content by ELISA to assess whether the production of IL-8 in the presence of YpTdp or YpTIR was altered, when compared with control. In line with the reporter assays (luciferase in particular) the amount of IL-8 secreted varied between experiments (generally corresponding with level of NF κ B activation). Figure 5-3 shows the concentration of IL-8 in the media for a representative NF κ B reporter experiment. Media from replicate wells was pooled and assayed in duplicate wells on the ELISA plate.

In the presence of YpTdp, IL-8 secretion from HEK293H cells stimulated with IL-1 β is reduced when compared with control ($p < 0.05$ one-way ANOVA with Bonferroni's post test, Figure 5-3). However, there is no effect on the amount of IL-8 secreted in the presence of YpTIR. These results reflect the IL-1 β -dependent signalling assays to NF κ B whereby YpTdp causes a reduction in NF κ B-induced luciferase activity, whereas YpTIR does not. A similar reflection of the IL-1 β -dependent NF κ B activity assays is seen with IL-8 secretion down-stream of TNF α stimulation where neither YpTdp nor YpTIR have any effect on IL-8 secretion (one-way ANOVA with Bonferroni's post test, Figure 5-3). However, the IL-8 results from LPS stimulation of HEK-Blue™ hTLR4 cells do not follow the trend of the reporter assay. In these experiments, neither YpTdp nor YpTIR have any measurable effect on IL-8 production downstream of LPS stimulation (one-way ANOVA with Bonferroni's post test, Figure 5-3), whereas YpTdp was shown to significantly down-regulate NF κ B activity after LPS stimulation (Figure 4-8). This may indicate that IL-8 is being produced from a pathway involving a transcription factor other than NF κ B in this assay.

5.3.4. I κ B α degradation

An indirect method to assess the activation status of NF κ B is to monitor the presence of its inhibitor protein I κ B α . In a resting cell I κ B α holds NF κ B in the cytoplasm, unable to translocate to the nucleus and initiate transcription. The regulation of NF κ B in this way

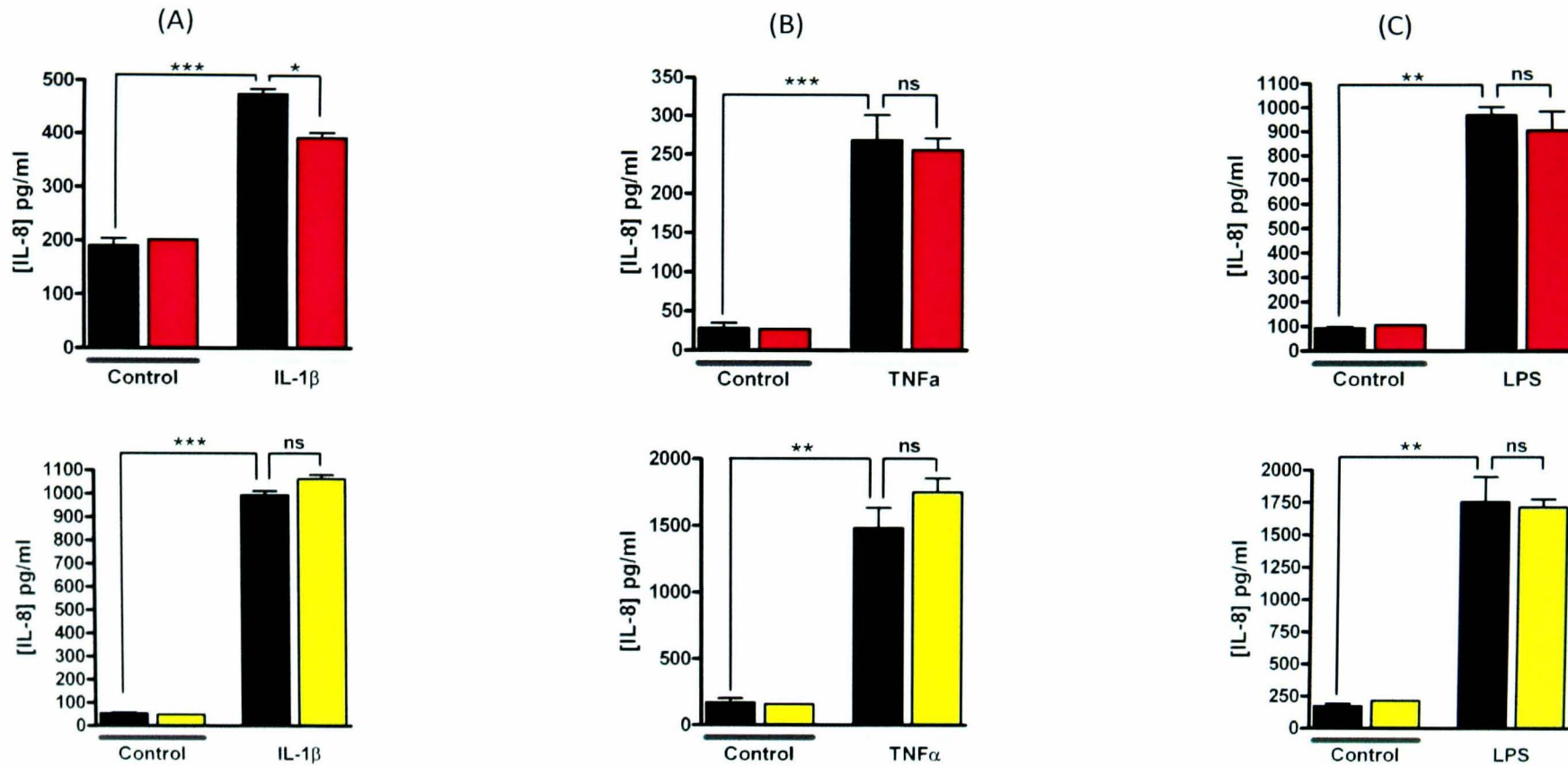


Figure 5-3: Effect of YpTdp/YpTIR on IL-8 production downstream of IL-1 β , TNF α or LPS stimulation.

Graphs show a representative ELISA for YpTdp and YpTIR and their effect on IL-1 β -, TNF α - or LPS-induced production of IL-8. Media was removed from IL-1 β - (A) and TNF α - (B) induced NF κ B luciferase assays or LPS- (C) induced NF κ B SEAP assays. The concentration of IL-8 in the media was assayed by ELISA and calculated from a standard curve performed on each plate. Media from technical replicates within signalling assays was pooled and represented in duplicate on the plate. Addition of PBS formed the control stimulation for these experiments. Data is expressed as the mean IL-8 concentration between duplicate wells \pm SEM. * denotes $p < 0.05$, ** denotes $p < 0.01$, *** denotes $p < 0.001$ one-way ANOVA with Bonferroni's post test.

means that it can be quickly activated in the absence of transcription or translation. On stimulation of a pathway leading to NF κ B activation, I κ B α is phosphorylated and degraded by the 26S proteasome (Section 1.2.3). As an alternative approach to assess signalling to NF κ B in the presence of YpTdp, I κ B α degradation after stimulation of cells was monitored by Western blotting. Initially I κ B α levels were monitored at timepoints after IL-1 β -stimulation of HEK293 cells in the presence and absence of YpTdp and YpTIR. Figure 5-4 shows that I κ B α is degraded just 15 min after pathway stimulation and is at its lowest level in this time course at 30-45 min. In the presence of YpTdp and YpTIR, however, I κ B α degradation appears delayed and is at its lowest level in this time course at 60 min (Figure 5-4). The presence of YpTdp and YpTIR also appears to ameliorate the feedback loop in which activation of NF κ B induces the expression of I κ B α causing its levels to rise after signalling. A histogram representation of the fold change in I κ B levels demonstrates more clearly how the resynthesis of I κ B α after signalling appears to have been blunted (Figure 5-4 C). In the absence of YpTdp/YpTIR, I κ B α was re-synthesised to unstimulated levels by 120 min, consistent with previous data of this type³⁰⁰. However, in the presence of YpTdp/YpTIR re-synthesis is delayed to 240 - 480 min, and to a lower level than in control cells.

5.3.5. Interaction studies

The reporter assays and cytokine analysis suggest that YpTdp is able to disrupt signalling, possibly by binding the TIR domain of either the receptor or adaptor proteins. For IL-1 β signalling the receptor is the IL-1R and the adaptor proteins are IL-1RAPL and MyD88. For LPS signalling the receptor is TLR4 and the adaptors used could either be a combination of MyD88 and Mal or TRIF and TRAM (Section 1.2.3). Studies to investigate whether YpTdp is able to bind to MyD88, which participates in both IL-1R and TLR4 signalling were therefore carried out to investigate the hypothesised binding. In order to do this co-immunoprecipitation (co-IP) and co-immunofluorescence (co-IF) studies were performed.

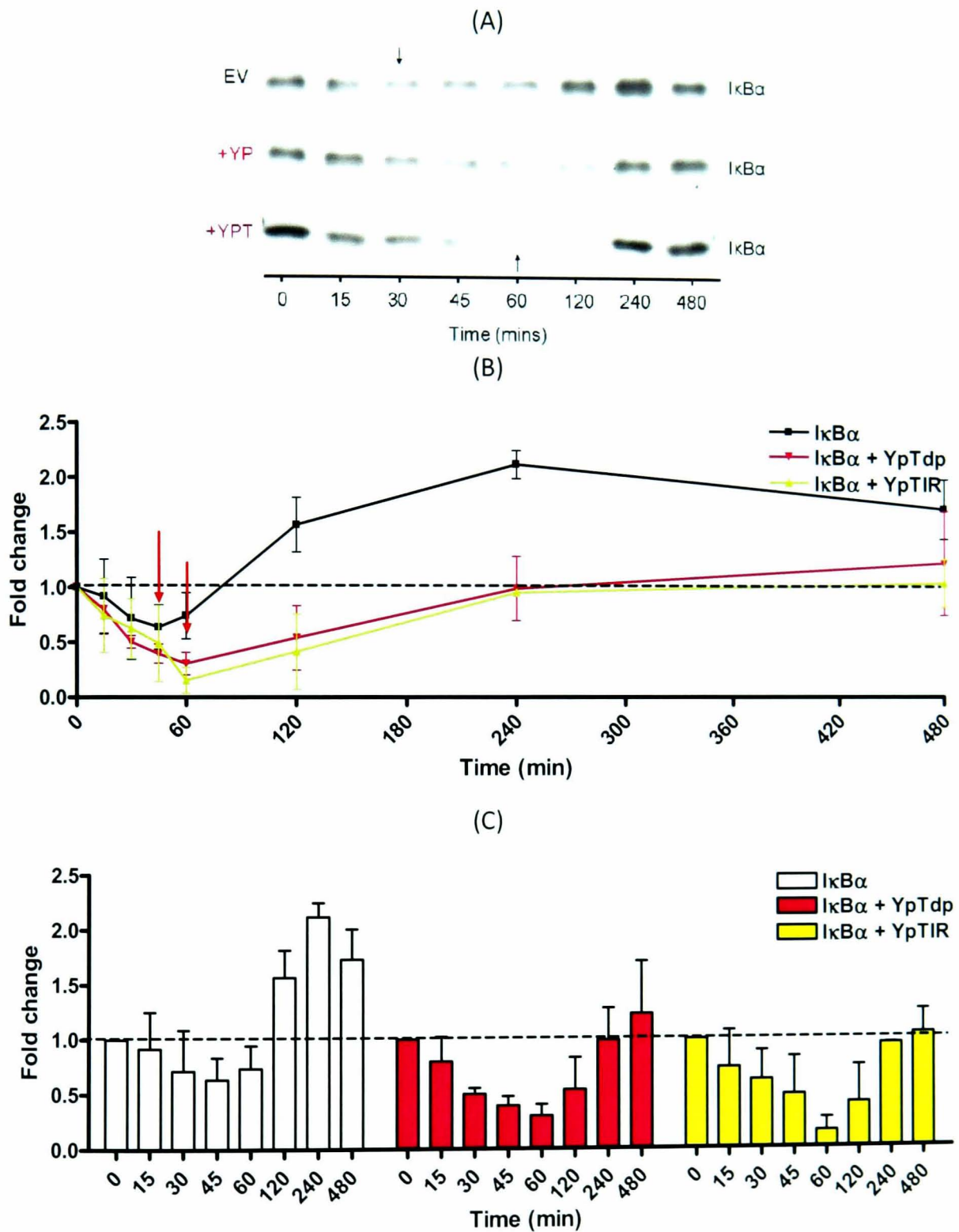


Figure 5-4: The effect of YpTdp and YpTIR on $I\kappa B\alpha$ levels after $IL-1\beta$ stimulation.

Cells were stimulated with $IL-1\beta$, lysed at defined timepoints, and samples were used for Western blotting with an antibody to $I\kappa B\alpha$ (A). Densitometry was performed on the Western blot and $I\kappa B\alpha$ levels normalised to a β -actin control. Fold change of $I\kappa B\alpha$ levels compared to $T = 0$ in the presence and absence of YpTdp/YpTIR is shown by line graph (B) and by column graph (C).

To probe any interaction between YpTdp and MyD88 by co-IF, HEK293H cells were immobilised onto sterilised glass coverslips and transfected with equal amounts of YpTdp- and MyD88-expressing vectors. At 24 h post-transfection the cells were fixed in paraformaldehyde, permeabilised and incubated with YpTdp- and/or MyD88-specific primary antibodies followed by fluorescent secondary antibodies. The co-IF studies showed that MyD88 had a distinct pattern of location when over-expressed in HEK293 cells (Figure 5-5). It appears to be located at the plasma membrane of the cells, and in a distinct pattern intracellularly, perhaps at endosomes (although these were not stained for). Figure 5-6 shows that YpTdp did not share this distinct location of expression when co-expressed in HEK293H cells with MyD88 inferring that the proteins do not interact when over-expressed together.

For the co-IP studies HEK293H cells were seeded into 100 mm dishes and transfected 24 h later with equal amounts of YpTdp- and MyD88-expressing vectors. The cells were lysed 24 h after transfection and the lysate was split for IP with AU1- (the MyD88 tag) or V5- antibodies. The co-IP studies did not clearly demonstrate an interaction between YpTdp and MyD88. A variety of different permeations of the co-IP were attempted. Lysis buffers of different strengths were employed to lyse the cells initially including two homemade buffers (Lysis buffer #1 and #2, Section 2.2). The strongest lysis buffer tried was RIPA buffer, often employed for the solubilisation of membrane proteins, which gave the best visible expression of YpTdp. In addition, the co-IP experiments were attempted with and without pre-coupling of the antibodies to the protein G beads and with incubation of the beads with the cell lysate for 1 h at room temperature and overnight at 4°C. The washing of the lysate away from the beads was attempted with lysis buffer only, or with a regimen of buffers that gradually reduced in stringency (down to PBS). The use of a co-IP kit was also tried whereby the beads are trapped within a column (the protein G IP kit, Sigma-Aldrich Ltd., UK). These various methods either produced very little visible expression of YpTdp in the cell lysate (weak lysis buffer) and therefore no pulldown of YpTdp with the V5- or MyD88-specific antibody, or good visible YpTdp expression (RIPA lysis buffer) but

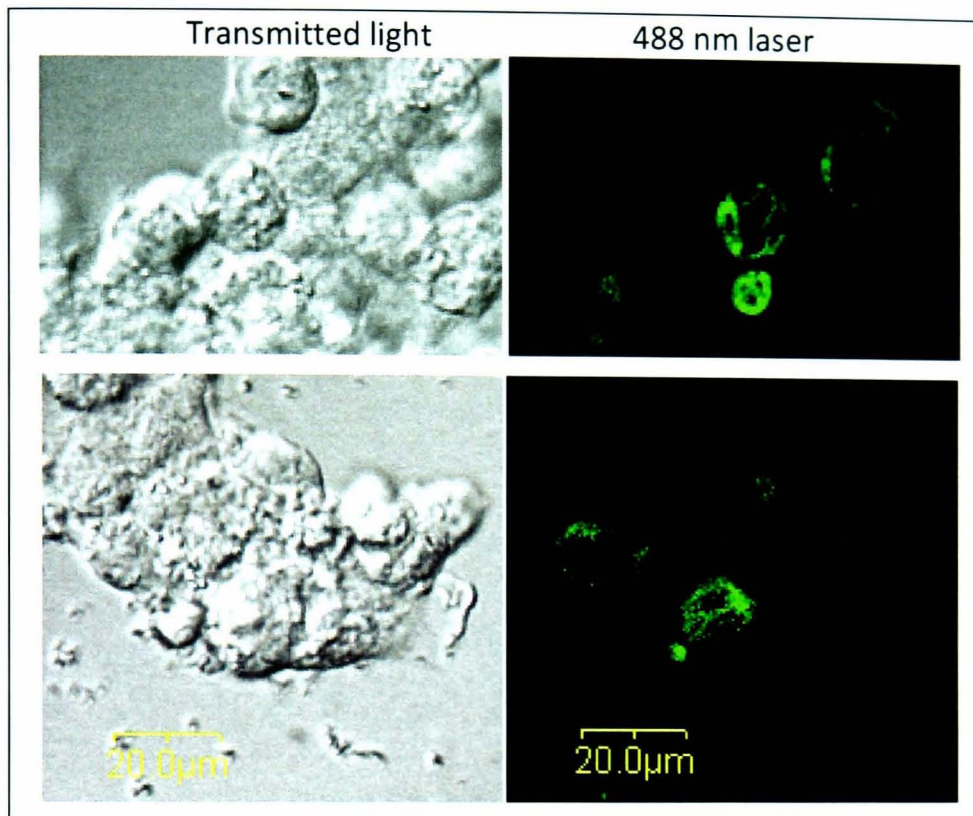


Figure 5-5: Intracellular pattern of expression of MyD88 over-expressed in HEK293H cells.

HEK293H cells were seeded onto glass coverslips and transfected 24 h later with a vector expressing MyD88. After 24 h expression the cells were fixed and permeabilised and probed with an anti-MyD88 primary antibody followed by a secondary antibody tagged with the AlexaFluor®488 fluorophore. The cells were viewed under a confocal microscope at a 60 x magnification and excited with a 488 nm laser.

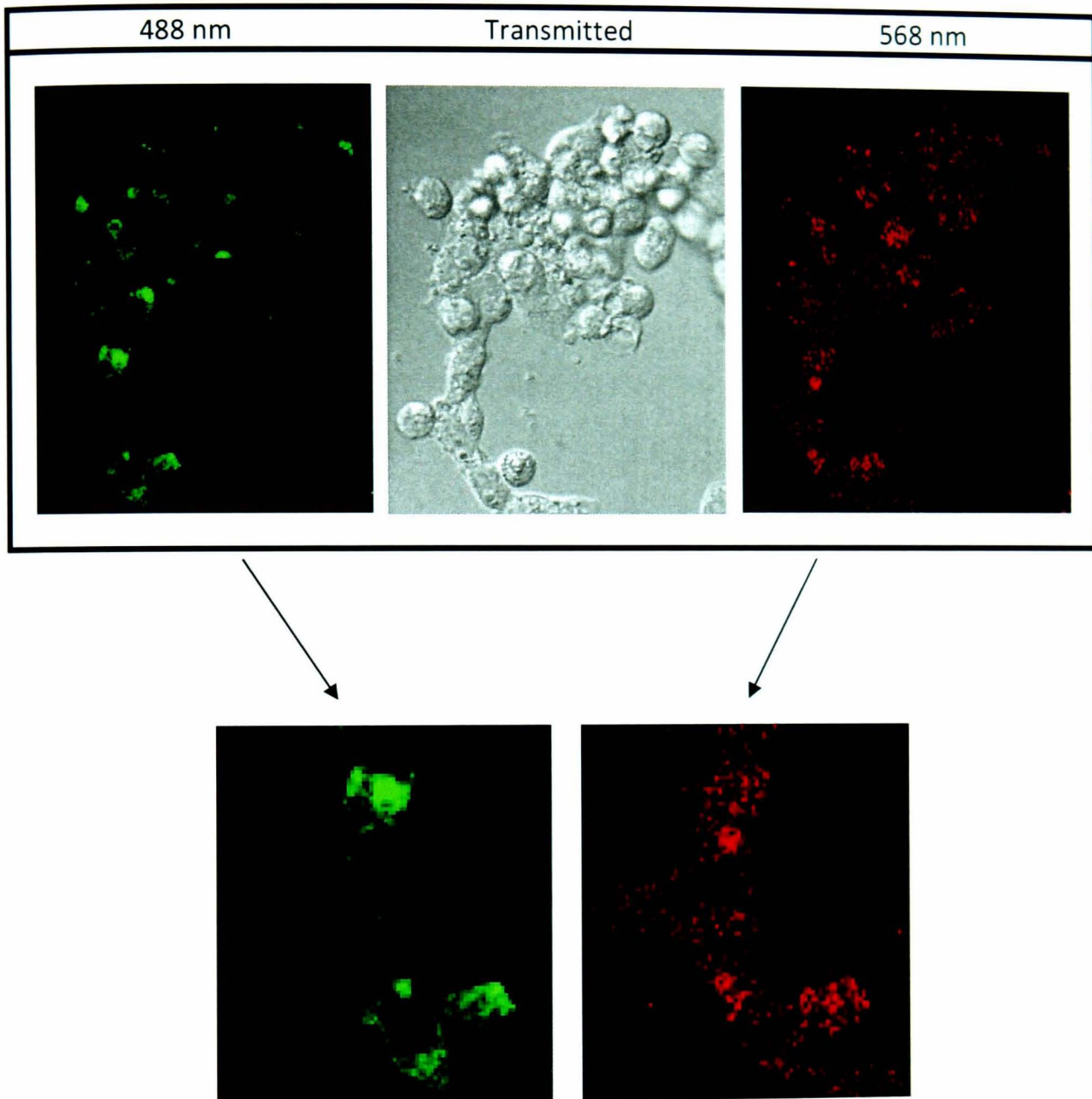


Figure 5-6: The intracellular expression pattern of YpTdp and MyD88 when over-expressed together in HEK293H cells.

HEK293H cells were seeded onto glass coverslips and transfected 24 h later with equal amounts of vectors expressing MyD88 and YpTdp-V5. After 24 h expression the cells were fixed and permeabilised and probed with anti-MyD88 and anti-V5 primary antibodies followed by secondary antibodies tagged with the AlexaFluor[®]488 fluorophore (MyD88) or the TexasRed fluorophore (YpTdp). The cells were viewed under a confocal microscope at a 60 x magnification and excited with a 488 nm or 568 nm laser. Inserts are enlarged and cropped.

then no interaction with MyD88 (high stringency washes), or non-specific interactions (low stringency washes). An example of an experiment such as this is shown in Figure 5-7. Here the cells were lysed with lysis buffer #2 (high stringency), incubated with pre-coupled beads overnight and then washed with a medium stringency set of washes (lysis buffer followed by PBS). Here IP with the V5-antibody in the presence of YpTdp did precipitate MyD88. Unfortunately MyD88 is also precipitated using a V5-tag antibody in the presence of Cat, although a smaller band is seen than for YpTdp (Figure 5-7). Despite the optimisation of this assay the balance between no binding and non-specific binding could not be achieved suggesting that there is either no interaction between YpTdp and MyD88, or that the assay was not appropriate to measure this interaction.

5.3.6. TIR adaptor-induced signalling to NFκB

In HEK293 cells NFκB transcriptional activity can also be induced by exogenous over-expression of the four TIR adaptor proteins that activate signalling (MyD88, Mal, TRIF and TRAM). Several experimental approaches have been used to show that overexpression of MyD88 results in the formation of functional homodimers, thereby bypassing the need for ligand-mediated TLR4 oligomerisation and recruitment of MyD88 to the TLR/IL-1R complex^{77,184}, and this also appears to be the case for the other adaptors. In order to attempt to determine whether YpTdp is able to bind with a receptor or adaptor during signalling, the effect on signalling induced by over-expression of MyD88, Mal or TRIF was assessed downstream of TLR4 in the presence of YpTdp and YpTIR. HEK-Blue™ hTLR4 cells were seeded into 6-well plates and transfected 24 h later with vectors expressing YpTdp, YpTIR or control vector along with vectors expressing MyD88, Mal or TRIF. NFκB activity was evident 24 h after transfection of MyD88, Mal or TRIF DNA and therefore media from the cells was sampled at this point and assessed for alkaline phosphatase activity. Signalling in the presence of control vector was normalised to 100% and signalling in the presence of YpTdp or YpTIR is expressed as a % of this control signalling (Figure 5-8). The results indicate that neither YpTdp nor YpTIR have any significant affect on signalling downstream of MyD88 or TRAM. Interestingly YpTdp does reduce Mal-induced NFκB activity slightly (NFκB activity is 85 % of control signalling in the presence of

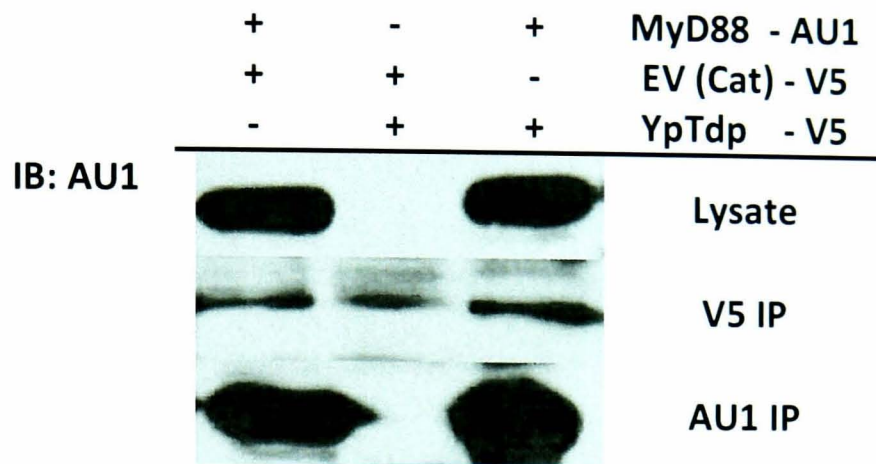


Figure 5-7: Co-immunoprecipitation of YpTdp and MyD88

HEK293 cells were transfected with vectors expressing MyD88-AU1 and YpTdp-V5 in equal amounts. At 24 h post-transfection the cells were lysed in the presence of protease inhibitors and the lysate split in order to be immunoprecipitated using a V5 antibody or AU1 antibody attached to protein G sepharose beads. Immunoprecipitation was allowed to occur overnight at which point the samples were washed and analysed by SDS-PAGE and Western blotting. This shows the IPs immunoblotted with AU1 primary antibody.

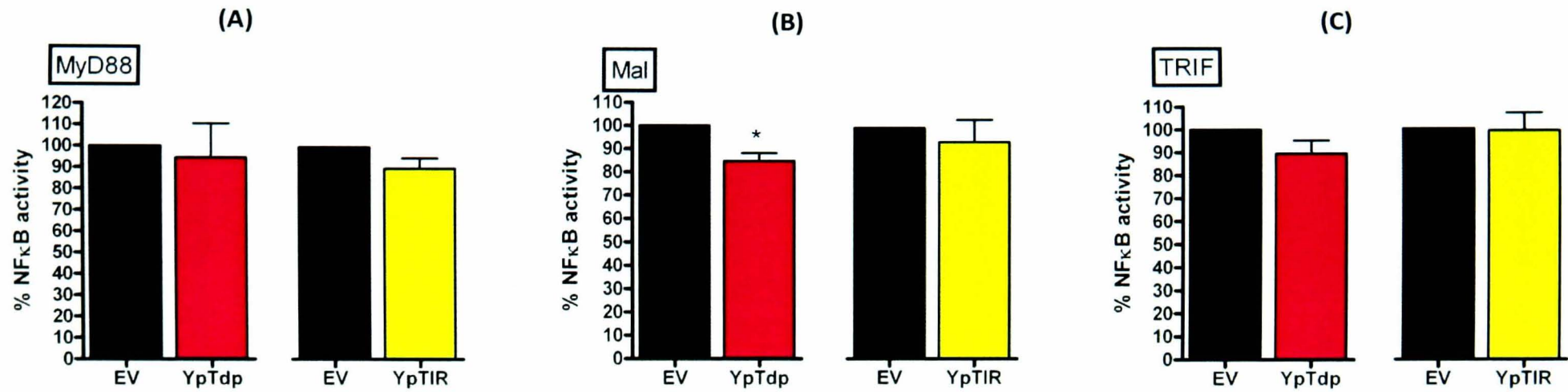


Figure 5-8: The effect of YpTdp and YpTIR on MyD88-, Mal-, or TRIF-induced signalling to NFκB.

HEK-Blue™ hTLR4 cells were transfected with pcDNA_YpTdp, _YpTIR or _cat and vector expressing human MyD88 (A), Mal (B) or TRIF (C). Subsequently, 24 hr after transfection media from the cells was analysed for SEAP activity.

MyD88-induced NFκB activity in presence of YpTdp = 94.32% (p = 0.7575), YpTIR = 89.89% (p = 0.1757)

Mal-induced NFκB activity in presence of YpTdp = 84.74% (p = 0.0108), YpTIR = 93.78% (p = 0.5863)

TRIF-induced NFκB activity in presence of YpTdp = 89.40% (p = 0.1700), YpTIR = 99.01% (p = 0.9059).

Data is expressed as the mean of at least three separate experiments containing three biological replicates ± SEM.

YpTdp, $p = 0.011$, column t-test), but this effect is abrogated when the TIR domain is expressed alone (YpTIR). One of the *B. melitensis* proteins investigated in Chapter 4 that has also been investigated in the literature (BmTdp) has also been shown to selectively affect Mal signalling, although an effect on signalling induced by the overexpression of Mal could only be demonstrated in one of the two studies that have investigated this^{344,345}. Neither YpTdp nor YpTIR had any effect on basal NF κ B activation in these assays (data not shown).

5.4. Conclusions

The aim of this chapter was to confirm and investigate further the effect of YpTdp on mammalian immune signalling. In order to do this the effect of YpTdp on IL-1/TLR signalling was investigated by methods other than transcription factor reporter assays, such as the degradation of I κ B α and the analysis of chemokine production. In addition, the TIR domain only from YpTdp was cloned and expressed in HEK293 cells in order to assess whether the effect on immune signalling seen in the presence of YpTdp could be attributed to the TIR domain in this protein.

The affect of YpTdp on IL-1 β -dependent NF κ B activation was supported by a reduction in IL-1 β -induced IL-8 production in the presence of YpTdp, and a delay in the degradation of I κ B α and a reduction in its subsequent feedback expression. In comparison, when these assays were carried out in the presence of YpTIR, all assays suggested it had no effect on the pathways, apart from when IL-1 pathway activation was assessed via I κ B α degradation. Given that YpTIR had no effect on IL-1 β -dependent NF κ B activation or production of IL-8, it is surprising to see that it reduced IL-1 β -dependent degradation of I κ B α . A delay in I κ B α degradation and an absence of its subsequent feedback expression is expected in the presence of YpTdp because the immune signalling and cytokine assays showed a drop in NF κ B activity in the presence of this protein. However, the lack of affect of YpTIR on IL-1-dependent NF κ B activation or IL-8 production suggests that the immunomodulatory properties of YpTdp have been lost in the truncation of this protein. The reason for the conflict between the results from the NF κ B reporter assays/IL-8 production and the results from the I κ B α degradation analysis is unclear. The majority of the assays, however, do suggest that the effects on IL-1/TLR signalling seen in the presence of YpTdp are lost in

truncation of the protein to give the TIR domain alone (including the disruption of Mal-induced signalling by YpTdp). There are a number of reasons why this may be the case and these are discussed below and shown pictorially in Figure 5-9.

One hypothesis is that the effects observed with YpTdp are mediated by regions of the protein outside of the TIR domain. No conserved domain architectures have been identified for the other parts of the protein and it does not appear to be homologous to other proteins. However, perhaps it is this part of the protein that contacts the receptor/adaptor proteins in the Il-1/TLR pathways (Figure 5-9B). Alternatively, and perhaps most likely, it may be that YpTdp binds to the mammalian Tdps at the level of the TIR domain but that other proteins are prevented from binding to the platform by the absence of another interaction domain (e.g.: a death domain for IRAK binding) and steric hindrance (Figure 5-9A). Alternatively it may be that the TIR domain of YpTdp is not folded properly when expressed alone (Figure 5-9C). This is considered unlikely, however, since collaborators at Imperial College have demonstrated a similar fold in YpTIR as for MyD88 by 1D NMR (personal communication).

A number of studies carried out here confirm that YpTdp can play a role in the modulation of mammalian immune signalling. IL-8 production downstream of IL-1 β stimulation is reduced in the presence of YpTdp, and the degradation of I κ B α after IL-1 β stimulation appears delayed and blunted. In addition YpTdp causes the down-regulation of TLR4 signalling to NF κ B induced by over-expression of the adaptor Mal. However, there are inconsistencies: IL-8 production after LPS stimulation of TLR4 is unchanged in the presence of YpTdp, whereas LPS-dependent NF κ B activity is reduced in the presence of YpTdp. It may be that the NF κ B activity activated in response to LPS in this system does not affect the *IL-8* gene. NF κ B regulates a large number of genes and the specificity of the immune response downstream of different signals occurs at a number of levels including the differential use of NF κ B subunits. Thus, it may be that the way in which YpTdp modulates signalling to NF κ B (as seen in the reporter assays) does not have an effect on

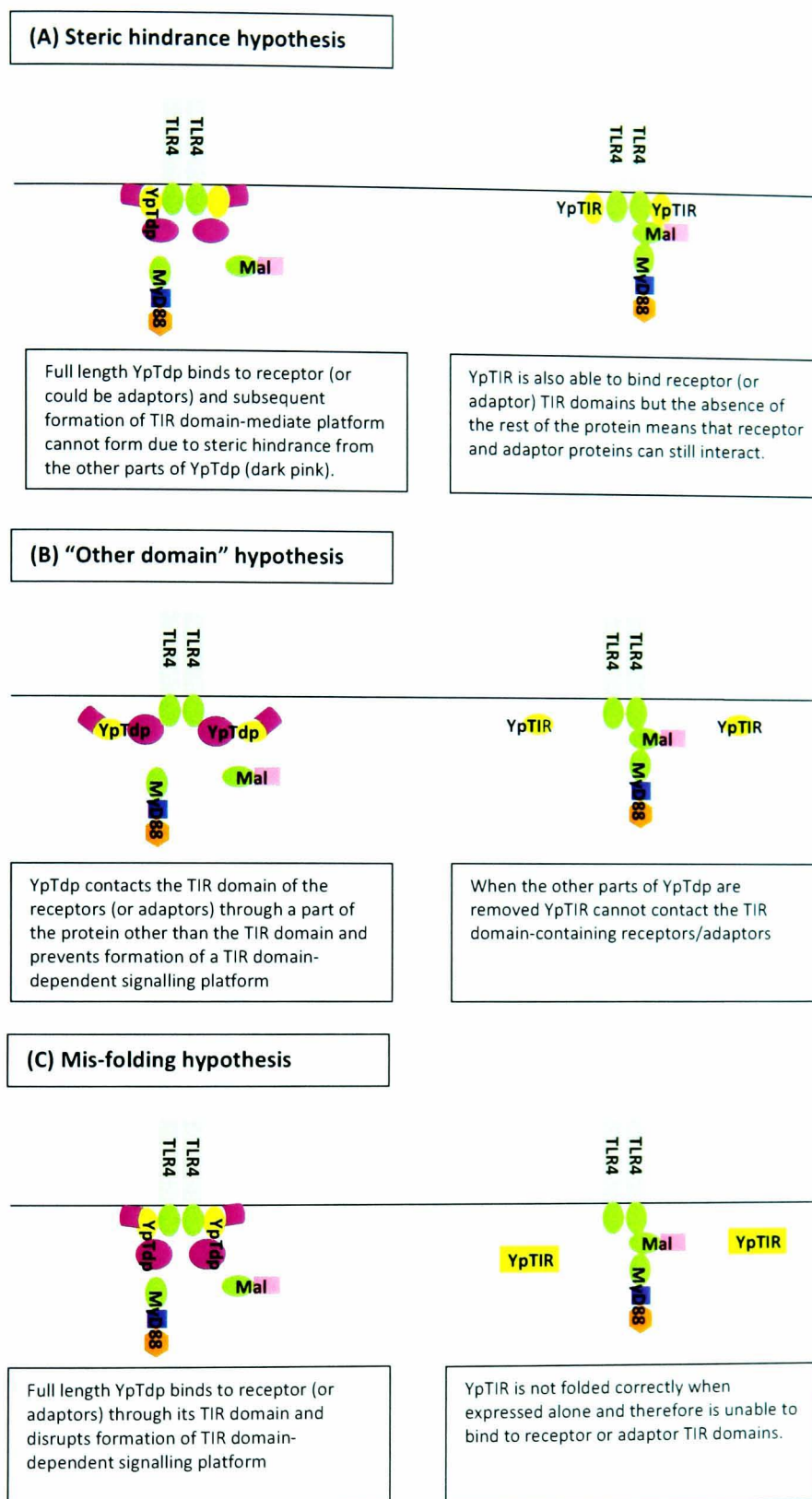


Figure 5-9: Hypotheses for the different experimental observations between YpTdp and YpTIR

transcription of the *IL-8* gene. Further analysis of other intermediates of this pathway, and other cytokines, would be useful to confirm the effect of YpTdp on LPS signalling. The effect of YpTdp on Mal-induced signalling to NF κ B suggests that any observed modulation of LPS-induced signalling is likely to be via interaction with, or modulation of the activities of, Mal.

It is also of paramount importance to investigate the interaction of YpTdp with other Tdps. The interaction of a bacterial Tdp with a mammalian counterpart is something which is absent from most of the limited number of publications focussing on the disruption of signalling by bacterial Tdps³⁴², and yet it seems crucial to the full elucidation of their function. Unfortunately, the interaction studies attempted here proved inconclusive. However, collaborators at Imperial College, London carried out GST pulldown experiments using purified YpTIR and MyD88. Here they saw a specific interaction between YpTIR and MyD88 which became apparent on a Western blot when the eluate from the column was concentrated three times (Dr. R. Rana, personal communication). This suggests that YpTIR is able to bind MyD88 but whether this binding occurs at physiological levels is yet to be determined and a GST-pulldown with full length YpTdp has not been possible due to the fact that obtaining a high yield of pure YpTdp has proved very difficult. The co-IF studies attempted in this chapter showed that YpTdp and MyD88 did not co-localise suggesting that these proteins do not interact. It would be interesting to investigate whether an interaction occurred after stimulation of the cells.

Co-IP studies with MyD88 and YpTdp suffered from a number of problems: The appearance of YpTdp in HEK293 cell lysates by Western blot was not to a high level and this is potentially due to aggregation and insolubility of the protein. Collaborators at Imperial College, London found the full-length YpTdp very difficult to express in large, pure amounts since it had a strong propensity to form large insoluble aggregates (Dr. R. Rana, personal communication) which may be cleared from a lysate, or difficult to detect using Western blot. It is also possible that YpTdp may be associated with membranous or nuclear material in HEK293 cells which is cleared when the lysates are centrifuged. This suggestion is given some weight by the fact that RIPA lysis buffer, often employed for the solubilisation of membrane proteins, improved the appearance of YpTdp by Western

blotting. Regardless of the reason behind the difficulty in expressing and visualising YpTdp, the co-IP technique may not be best suited for demonstrating its interactions. An assay whereby purified proteins are employed, rather than cell lysates, may be beneficial and indeed GST-pulldown between YpTIR and MyD88 does yield a visible interaction. It has not been possible to use purified YpTdp in these assays for the reasons given above, and a GST-pulldown experiment introduces a level of artificiality over a co-IP.

Neither YpTdp nor YpTIR affected NF κ B activation as induced by the over-expression of the TIR adaptor proteins MyD88 or TRAM but, as discussed, YpTdp did down-regulate signalling induced by the over-expression of Mal. The *B. melitensis* protein BMEI1674 (BmTdp) also acts of Mal-specific signalling pathways and has been postulated to be “Mal-like” for its ability to interfere in TLR2 and TLR4 signalling and its ability to bind phospholipids. An experiment to investigate whether YpTdp was also able to bind phospholipids was conducted once but no interaction was identified (data not shown). This would be an important avenue of investigation for future studies and would suggest that efforts in studying the interactions of YpTdp should be focussed on Mal instead of MyD88.

The lack of effect of YpTdp on MyD88-induced NF κ B activity suggests that the down-regulation of NF κ B activation observed in the presence of YpTdp when cells are stimulated with IL-1 β is due to YpTdp disrupting signalling by binding to the IL-1R or IL-1APL, rather than MyD88. However, this may not correlate with the observed interaction between YpTIR and MyD88 in the GST pulldown experiments performed by collaborators. It is also possible that the over-expression of MyD88 (and TRAM) in order to induce signalling creates a vast excess of the adaptor proteins that may be enough to overcome any interaction with YpTdp/YpTIR that would disrupt signalling to NF κ B (although this does not seem to be the case for Mal). A dose-dependent assessment of the amount of the vectors expressing the adaptor proteins to transfect that would give NF κ B activation was carried out and the lowest dose of adaptor vector that gave significant NF κ B activation was employed. However, this still may be enough to overcome YpTdp inhibition in the case of MyD88 and TRAM.

In conclusion it seems likely that when over-expressed in a mammalian cell line YpTdp is able to disrupt IL-1/TLR signalling. However, the mechanism of its disruption, including at which point it binds, has yet to be fully elucidated.

Chapter 6: Assessment of the contribution to the virulence of *Yersinia pestis* from YpTdp

6.1. Introduction

Previous studies with bacterial Tdps have not provided a clear indication regarding their roles in bacterial virulence. This is partly due to the fact that they have so far been investigated in bacteria that, while pathogenic, do not cause lethal disease in an animal model, or the disease caused in the model does not necessarily correlate well with the disease in its natural host. *Salmonella enterica* serovar Enteritidis, investigated by Newman *et al.*³⁴² most frequently causes a gastrointestinal disease of livestock and humans but is lethal in the oral infection murine model used in their study. The *TlpA* mutant was not significantly attenuated in its lethality in this model but was defective in its ability to colonise the spleen. *In vitro*, the *TlpA* mutant was significantly attenuated in its replication within a J774 macrophage cell line, but not in its uptake into these macrophages. Other Tdp mutants present different characteristics. The *BmTdp* mutant of *B. melitensis* was not found to be defective in intracellular replication within macrophages or HeLa cells but did show an attenuated phenotype in the mouse model used³⁴⁵. However, brucellosis is not generally a lethal disease in wild-type mice; in fact mice are remarkably resistant to *Brucella*, unlike the debilitating phenotype of *Brucella* infection in other mammals/humans. Therefore IRF knockout mice were used for the infections giving a somewhat artificial aspect to the study. Similarly the uropathogenic strain of *E. coli* investigated by Cirl *et al.* in their study of *TcpC*³⁴³ is not lethal in a mouse model, or indeed in immunocompetent patients. The *TcpC* mutant was attenuated in a urinary tract infection (UTI) model in mice, as determined by the reduced appearance of the *TcpC* mutant bacteria in the urine and kidneys compared to wild-type, and the pathology of the kidneys in this model was worse during the wild-type infection where they showed a higher number of abscesses compared to mutant bacterial infection. From these studies there is some indication that bacterial Tdps play a role in the virulence of their cognate organism but it also seems important to investigate the effect of removal of a bacterial Tdp on a highly virulent organism such as *Y. pestis*. In order to investigate whether YpTdp is involved in the virulent colonisation and replication of *Y. pestis* within a host, the gene encoding YpTdp will be genetically removed from *Y. pestis* GB and the ability of this mutant bacteria to be taken up by, and replicate within, a murine

macrophage cell line will be assessed. In addition, its ability to compete for niche and colonise the spleen in a mouse model of infection will be investigated in two ways: using a competitive index (CI) study, and by the assessment of its median lethal dose (MLD) in mice in comparison with wild-type.

The pathogenesis of *Y. pestis* in mice has been investigated by a number of groups. One study, specifically looking at *Y. pestis* GB (the strain used here) and its pathogenesis in BALB/c mice found the course of disease to have three stages. The first phase (up to day 3) showed a small number of intracellular bacteria within macrophages and neutrophils, with a high amount of neutrophil apoptosis. This, and other evidence, suggests that neutrophils are able to control bacterial numbers whereas the macrophage has been suggested to be a “safe haven” for the bacteria. After day 3 *Y. pestis* GB was exclusively found in macrophage cells and numbers reached between 10^3 and 10^4 cfu per spleen. At days 4 and 5 post-infection there was a decrease in bacterial numbers and escape of bacteria into the extracellular environment⁴⁵⁹.

It is clear from the lifestyle of *Y. pestis* that resident macrophages are a primary target for immunomodulation⁴⁶⁰. If the YpTdp mutant of *Y. pestis* is defective in its ability to reduce TLR signalling, it may be that macrophage cells are better able to resist entry or survival of *Y. pestis*. Modulation of macrophage function and survival has been demonstrated for other *Y. pestis* mutants defective in immunomodulatory strategies^{461,462}. In addition, if the *Y. pestis* Tdp mutant is defective in its entry to, and survival within, macrophage cells the disease severity and colonisation *in vivo* may be expected to be less than that of wild-type bacteria in the second and third phases of infection. However, in a highly virulent pathogen such as *Y. pestis* the removal of one immunomodulatory protein may not produce such dramatic effects. Of the known immunomodulatory strategies in *Y. pestis*, in general these must act in concert to overwhelm the host immune response. For example, deletion of YopJ, the archetypal *Yersinia* immunomodulatory effector, in *Y. pestis* has no effect on the virulence, systemic spread or colonisation of *Y. pestis*⁴⁶³. At the other end of the scale, deletion of the TLR2-dependent immunomodulator LcrV in *Y. pestis* increases the MLD in mice from 10 cfu to $>10^7$ cfu⁴⁶⁴. The point at which YpTdp falls on this scale is yet to be determined.

Previous studies on bacterial Tdp mutants have focussed on characterising the virulence and immunomodulatory phenotype. However, since there is evidence to suggest that these proteins may have other roles it would also be interesting to investigate other characteristics of the mutant, including growth and sensitivity to stresses, information which has not been assimilated on other bacterial Tdp mutants. To this end its growth *in vitro* will be assessed and literature searching and experimental findings will lead the search for other phenotypes.

6.2. Aims and objectives

The aim of this chapter is to investigate the role of YpTdp in the virulence of *Y. pestis*.

This will be achieved by addressing the following objectives:

- Genetically remove the gene for YpTdp (*YpTdp*) from *Y. pestis* GB by homologous recombination between this gene and a kanamycin construct using the “lambda red swap” method⁴⁶⁵. Confirm the mutant via PCR screening and sequencing.
- Assess the growth of the *Yersinia pestis YpTdp* mutant ($\Delta YpTdp$) *in vitro*.
- Investigate the ability of *Y. pestis* $\Delta YpTdp$ to replicate within a macrophage cell line.
- Evaluate the median lethal dose of *Y. pestis* $\Delta YpTdp$ in a murine model of infection.
- Determine the competitive index value for *Y. pestis* $\Delta YpTdp$ in competition with wild-type *Y. pestis* GB
- If virulence phenotype not identified, investigate clues to other phenotypes.

6.3. Results

6.3.1. Production and confirmation of *Yersinia pestis* Δ YpTdp

A genetic knockout of the gene encoding for YpTdp was achieved using the “lambda (λ) red swap” method of Datsenko and Wanner⁴⁶⁵. In this method a PCR product encoding for a knockout mutation of the gene of interest, flanked by its surrounding chromosomal DNA, is introduced into the bacterial strain of interest by electroporation. This strain is already transformed with a “helper plasmid” pAJD434 which encodes for the λ -red recombinase to facilitate the recombination of the PCR product with chromosomal DNA. Figure 6-1 shows the mutant making process and confirmatory PCRs for making a *YpTdp* knockout of *Y. pestis* GB (steps highlighted in yellow). A kanamycin resistance cassette (to replace *YpTdp*) was amplified from the vector pK2⁴⁶⁶ surrounded by 50 bp of DNA homologous to the DNA immediately flanking either side of the *YpTdp* gene including the START and STOP codons (to minimise polar effects) and the PCR product was electroporated into *Y. pestis* GB (Figure 6-1, Steps 1 & 2). Integration of this PCR product into the bacterial chromosome then occurs due to regions of the PCR product DNA being homologous to the chromosomal regions surrounding the gene to be removed. Recombination is aided by the recombinase enzyme expressed on the pAJD434 plasmid also present within the cell. Bacterial colonies were screened for their ability to grow on media containing kanamycin, and by PCR using primers outside the gene of interest in order to see a size difference in the PCR product of the mutant (“flanking PCR”, Figure 6-1, Step 3). This reflects the fact that the gene for kanamycin resistance (*KanR*) is smaller than the gene of interest; the sizes of PCR products for this confirmatory PCR are 1231 bp for *KanR* and 1338 bp for *YpTdp*. A confirmatory PCR was also carried out with a kan-specific PCR primer which would give a positive result only on mutant colonies (“Kan-specific PCR”, Figure 6-1, Step 3). Once a potential *YpTdp* mutant was identified the helper recombinase plasmid was cured by growth of the strain at 37°C (Figure 6-1, Step 4). Loss of the recombinase plasmid was confirmed by the loss of PCR products corresponding to the *exo* and *gam* genes from the helper plasmid (Figure 6-1). The presence of the *Y. pestis* virulence plasmid (pCD1) was confirmed by PCR amplification of the *yscC* gene from this plasmid. The replacement of the *YpTdp* gene with a kanamycin cassette was confirmed by amplifying the new insert using PCR, cloning this product into pCR2.1 and subsequent sequencing of this construct.

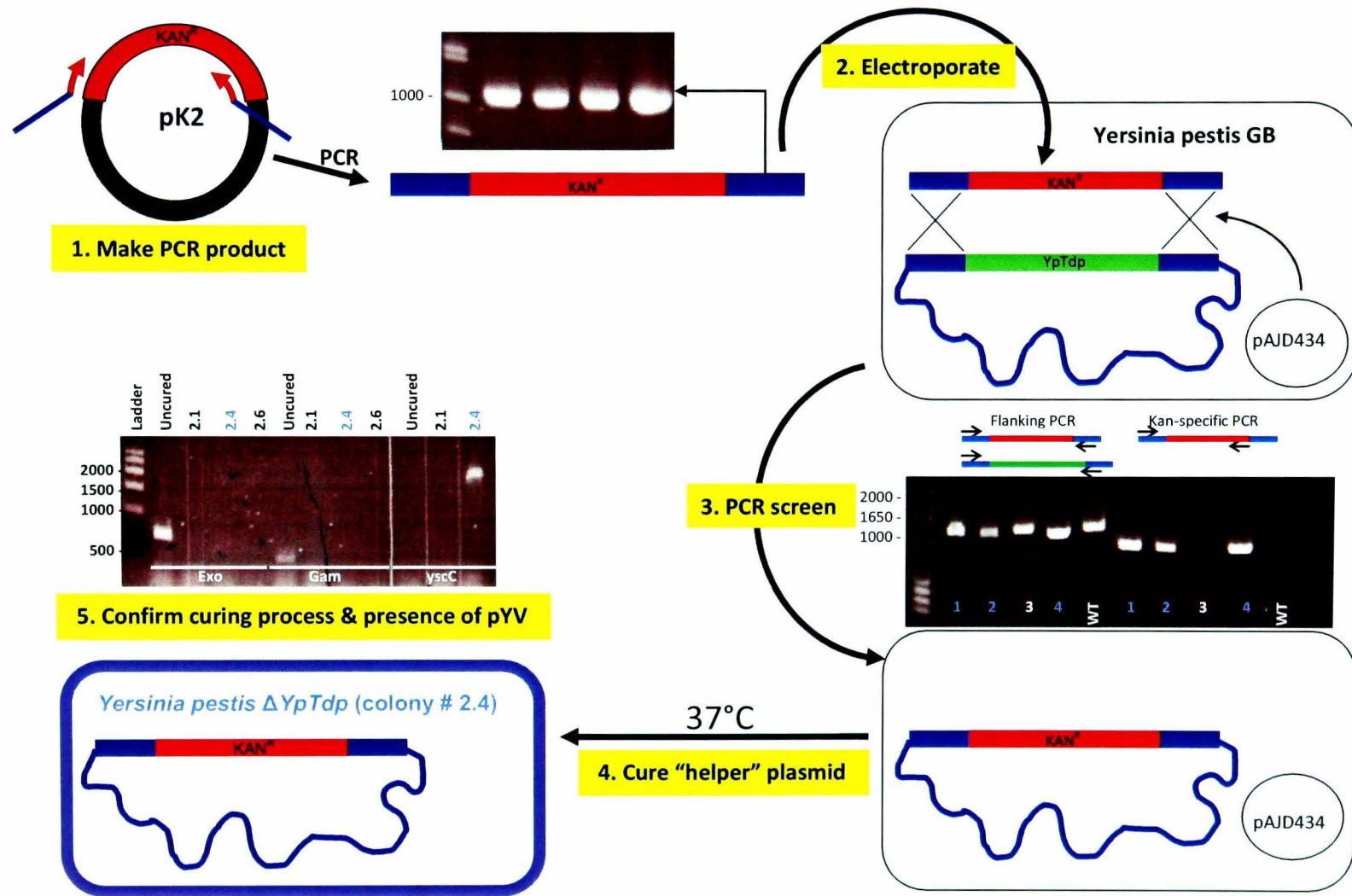


Figure 6-1: Schematic representation of the steps carried out in the creation of a *Y. pestis* *YpTdp* gene knockout.

6.3.2. Growth of *Yersinia pestis* $\Delta YpTdp$ in vitro

The growth of the *Y. pestis* $\Delta YpTdp$ mutant in comparison with wild-type *Y. pestis* GB was assessed by optical density reading and enumeration of serially diluted bacteria on agar plates. The growth of wild-type and mutant *Y. pestis* were compared at 28°C. Growth at 28°C imitates the lifestyle of *Y. pestis* within the flea since this is approximately its body temperature. Stationary phase cultures of *Y. pestis* GB and *Y. pestis* $\Delta YpTdp$, grown overnight in BAB broth were diluted 1:10 (v/v) in BAB broth (time = 0 h) and their growth was monitored by absorbance of light at 590 nm (Figure 6-2 A). These initial growth curves at 28°C appeared to indicate that the *YpTdp* mutant has a growth defect compared to wild-type. However, in performing these experiments it became apparent that after approximately 3 h of growth, *Y. pestis* $\Delta YpTdp$ started to form large aggregates. Wild-type *Y. pestis* strains have an auto-aggregation phenotype which is believed to be due to the addition of complex sugars to surface proteins and aids in the blockage of the flea stomach by *Y. pestis* to enhance its dissemination³⁷⁴. This aggregation phenotype can make it difficult to obtain an optical density (OD) reading for *Y. pestis* cultures. However, the aggregates generally break up easily with gentle shaking and pipetting and an OD reading can be obtained. The *Y. pestis* $\Delta YpTdp$ mutant, however, appeared to be forming larger flocculent clumps that were difficult to disperse and this was likely to be affecting the OD readings. The clumping of the mutant could be visualised in broth culture noticeably (Figure 6-2B). The growth curves were therefore repeated after vortexing and pipetting of the cultures before OD readings were taken which somewhat dispersed the aggregates and gave a more accurate growth curve (Figure 6-2A). In addition, culture was removed at defined timepoints, serially diluted and plated for the enumeration of bacteria (Figure 6-3). The results of the growth curves with vortexing, and dilution plating, demonstrate that the *Y. pestis* $\Delta YpTdp$ mutant has the same growth kinetics as wild-type *Y. pestis*.

The increased auto-aggregation observed with the $\Delta YpTdp$ mutant was quantified using a sedimentation assay. This relies on the fact that a culture with more aggregates will sediment more quickly than a smooth culture, if undisturbed. This sedimentation of bacteria in culture is associated with a reduction in OD and sedimentation was monitored in this

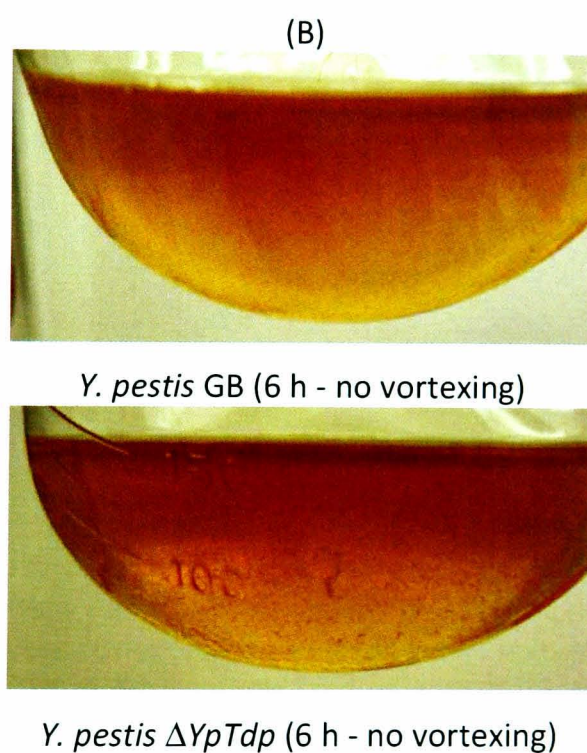
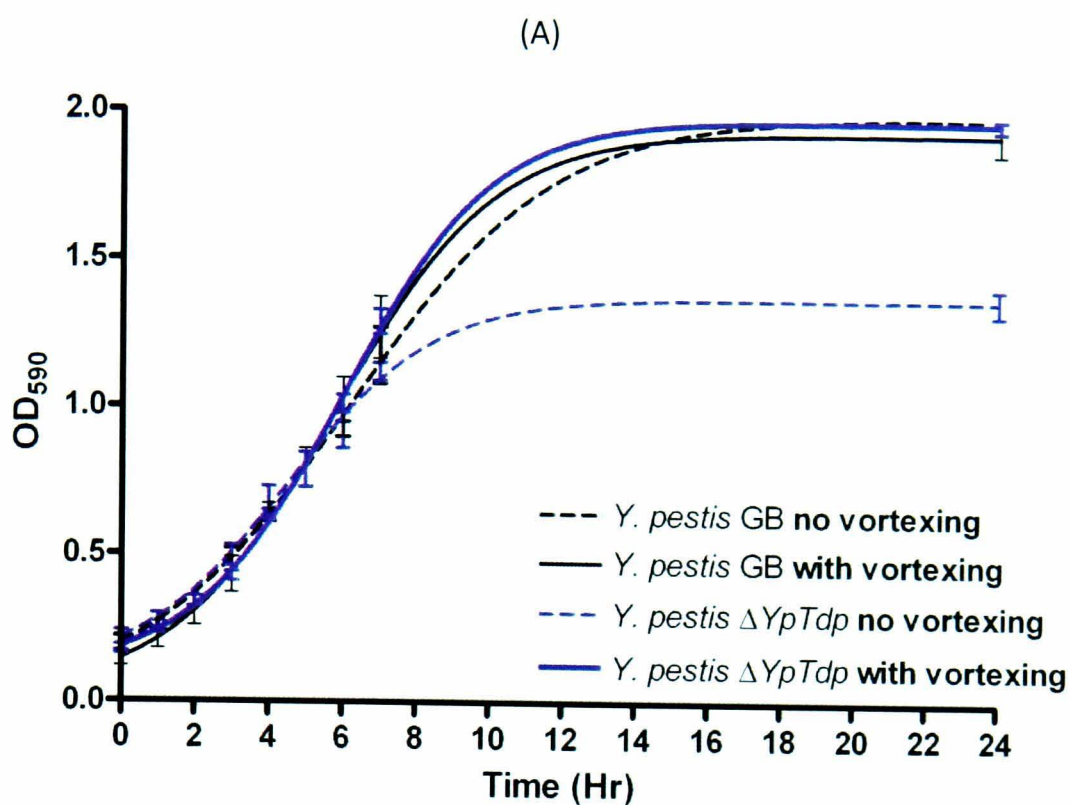


Figure 6-2: Growth of *Y. pestis* GB and *Y. pestis* $\Delta YpTdp$ in BAB broth.

An overnight culture of *Y. pestis* GB or $\Delta YpTdp$ was diluted 1:10 (v/v) to a total of 50 ml in BAB broth and incubated at 28°C with orbital shaking. (A) The OD₅₉₀ of the culture was measured hourly until 7 h and then at 24 h. A best fit curve was drawn using the Boltzman sigmoidal function in the GraphPad™ Prism statistical package. Data is expressed as the mean ± SEM of three independent experiments (B) Cultures were photographed after 6 h of growth.

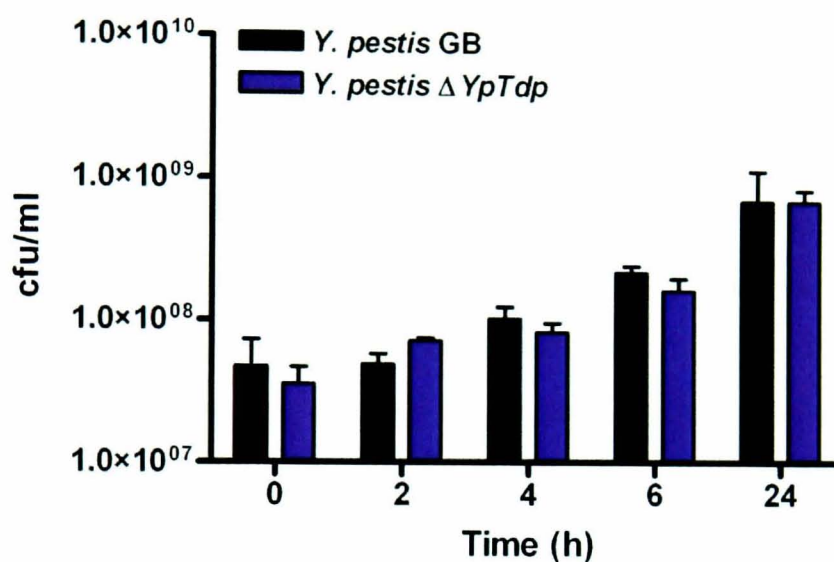


Figure 6-3: Enumeration of *Y. pestis* GB and *Y. pestis* $\Delta YpTdp$ at timepoints during broth culture

An overnight culture of *Y. pestis* GB or $\Delta YpTdp$ was diluted 1:10 (v/v) to a total of 50 ml in BAB broth and incubated at 28°C with orbital shaking. At defined timepoints after initial inoculation 1 ml culture was removed, serially diluted and plated for the enumeration of colonies. Cultures were vortexed prior to the samples being taken. Data is expressed as the mean \pm SEM cfu/ml taken from counts on duplicate dilution plates from two independent experiments.

way for the wild-type and $\Delta YpTdp$ mutant (Figure 6-4). Overnight cultures were diluted 1:10 and incubated at 28°C for 4 h. At this time 3 ml culture was removed and placed in a cuvette. The OD₅₉₀ of this culture was taken at defined timepoints with as little disturbance of the cuvette as possible. From this it is apparent that the $\Delta YpTdp$ culture sediments at a faster rate than the wild-type *Y. pestis* GB.

The increased auto-aggregation of the *Y. pestis* $\Delta YpTdp$ mutant in broth may suggest an alteration in the membrane characteristics of the bacteria particularly that the membrane may have become more hydrophobic in nature and therefore the bacterial cells clump together in response to the hydrophilic broth environment. In order to investigate this *Y. pestis* and *Y. pestis* $\Delta YpTdp$ were tested for their hydrophobicity using the bacterial adhesion to hydrocarbon (BAH) test^{467,468}. Overnight cultures of *Y. pestis* and *Y. pestis* $\Delta YpTdp$ were diluted 1:10 (v/v) in 50 ml cultures and grown for 24 h. Their relative hydrophobicity was measured at 4, 6 and 24 h. Results from this test show that there is no difference in the hydrophobicity of the bacteria at these time-points (Figure 6-5).

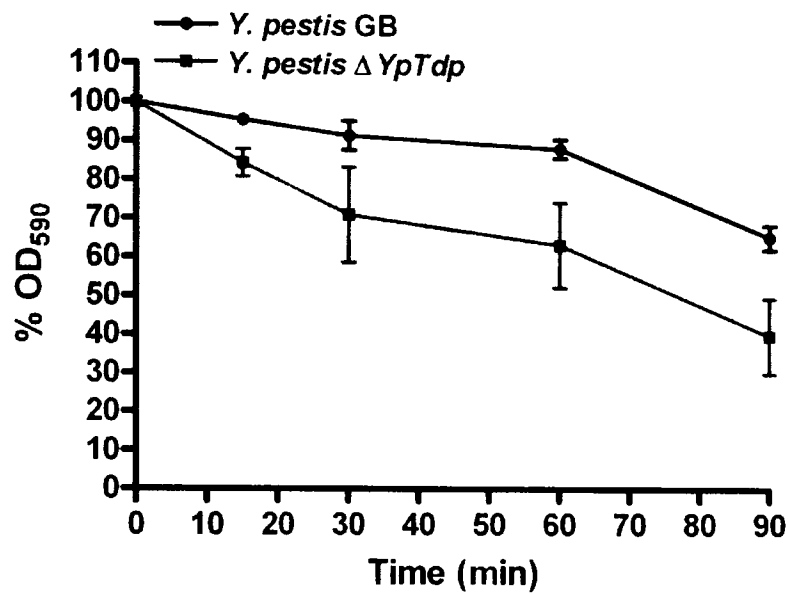


Figure 6-4: Sedimentation of *Y. pestis* GB and *Y. pestis* Δ*YpTdp* in culture

Overnight cultures of *Y. pestis* GB or Δ*YpTdp* were diluted 1:10 (v/v) to a total of 50 ml in BAB broth and incubated at 28°C with orbital shaking. After 4 h growth 3 ml of the culture was removed and placed into a cuvette. At various timepoints after this the OD₅₉₀ was measured with as little disturbance to the cuvette as possible. The OD₅₉₀ at T = 0 was normalised to 100% and the OD₅₉₀ at points after this calculated as a % of this starting OD₅₉₀. Data is expressed as the mean ± SEM from three independent experiments.

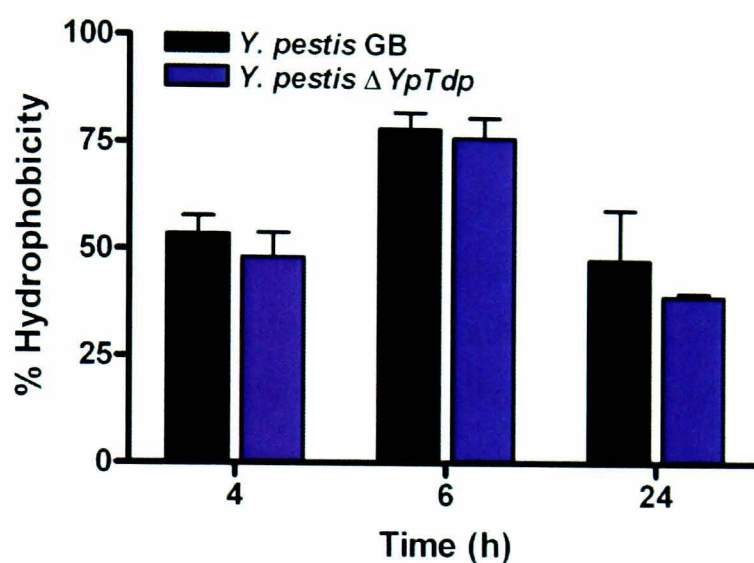


Figure 6-5: Hydrophobicity of *Y. pestis* GB and $\Delta YpTdp$

Overnight cultures of *Y. pestis* GB or $\Delta YpTdp$ were diluted 1:10 (v/v) in a total of 50 ml in BAB broth and incubated at 28°C with orbital shaking. At defined timepoints, culture was removed, washed twice with PBS and resuspended in PBS to an OD₅₉₀ of ~1. Subsequently, 2 ml of this culture was overlaid with 600 μ l hexadecane, vortexed for 1 min and then left to stand for 15 min. At this point the OD₅₉₀ of the aqueous phase was measured and % culture that partitions with hydrocarbon (% hydrophobicity) measured as detailed in the Materials and Methods. Data is expressed as the mean \pm SEM from % hydrophobicity calculated from three independent experiments where enumeration of bacteria was carried out on duplicate dilution plates.

6.3.3. Uptake and replication of *Yersinia pestis* $\Delta YpTdp$ in a macrophage cell line

To assess the interaction of the Tdp mutant of *Y. pestis* with macrophages its uptake into, and replication within, the murine macrophage cell line J774 was assessed. The bacteria were allowed to infect the macrophages at a multiplicity of infection (MOI) of 10 for 60 min, after which extracellular bacteria were killed by incubating the cells with 10 $\mu\text{g/ml}$ gentamicin for 45 min. This timepoint was considered T = 0 h. At 0 h and 24 h, the macrophages were lysed, and intracellular CFU were enumerated by dilution plating of the lysates. Figure 6-6 and two-way ANOVA analysis show that at T = 0 h there is no difference in number of wild-type or mutant bacteria within the macrophage. This suggests that the *Y. pestis* $\Delta YpTdp$ mutant is not attenuated in its ability to gain entry into this macrophage cell line. There is also no difference in the numbers of bacteria within the macrophages at T = 24 suggesting that *Y. pestis* $\Delta YpTdp$ is also not attenuated in its ability to replicate within this macrophage cell line.

6.3.4. Virulence of *Yersinia pestis* $\Delta YpTdp$ in a murine model

In order to assess the effect that removing YpTdp from *Y. pestis* GB has on its ability to colonise a host and cause disease, two *in vivo* studies were conducted: a competitive index (CI) study and an experiment to determine the median lethal dose (MLD) for *Y. pestis* $\Delta YpTdp$, i.e. the dose of *Y. pestis* $\Delta YpTdp$ that kills 50% of a population. In a CI study both wild-type and mutant bacteria are introduced into a host at a 1:1 ratio and allowed to colonise for a defined amount of time. At this point the animals are culled and the colonisation of the spleen by either wild-type or mutant bacteria is assessed. The ratio of colonisation compared with input informs the researcher about the ability of the mutant bacteria to compete with the wild-type bacteria for niche. In a MLD study animals are given a variety of doses of mutant bacteria and their time to death is monitored. A calculation (Reed-Meunch) can then be applied to calculate the dose of mutant bacteria that would kill half a population of mice, and this can be compared to the MLD for the wild-type strain.

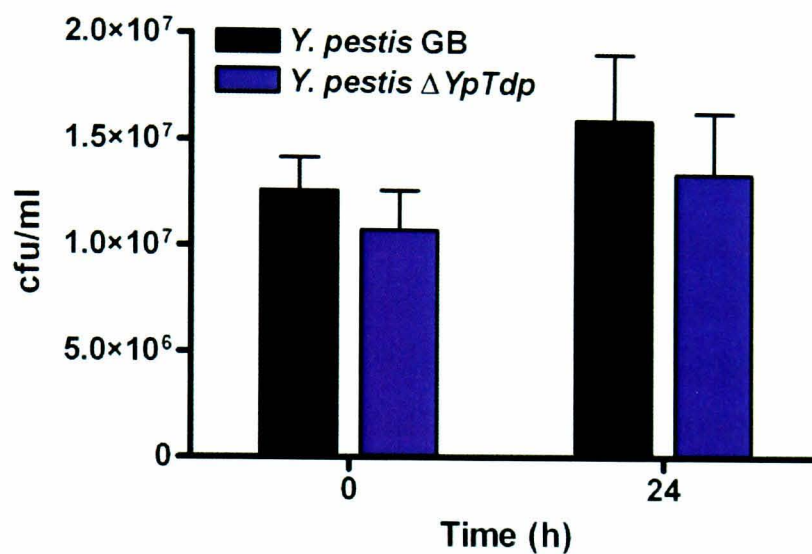


Figure 6-6: The intracellular growth of *Yersinia pestis* GB and *Yersinia pestis* $\Delta YpTdp$ in J774 murine macrophages

J774 macrophages were seeded at 1×10^6 cells per well in a 24-well plate and 16 h later infected with 1×10^7 cfu *Y. pestis* GB or *Y. pestis* $\Delta YpTdp$ (MOI 10) for 60 min. At this time the bacterial suspension was removed from the cells and extracellular bacteria killed using 10 μ g/ml gentamicin for 45 min. At this point (considered T = 0 h), the cells were lysed and the lysates diluted for the enumeration of bacteria within the cells. A 2 μ g/ml solution of gentamicin was added to the cells for the T = 24 h timepoint and then at T = 24 the cells were washed, lysed and diluted as before. Data is expressed as the mean \pm SEM cfu/ml as calculated from duplicate dilution plates from three independent experiments with two technical replicates (wells).

For the CI study stationary phase cultures of wild-type and mutant bacteria were diluted 1:10 (v/v) and allowed to reach log phase (an OD₅₉₀ of 0.6). These cultures were then diluted to 10⁻⁴ (approx 1000 cfu) and mixed at a 1:1 ratio. This mixture was used to inoculate six BALB/c mice via the intravenous (i.v.) route. At a point when it was clear the bacteria had extensively colonised the host (where the mice were showing significant clinical signs) the mice were culled and their spleens were removed. For this study this point was at 72 h post-challenge (phase 2 of *Y. pestis* infection). The spleens were then disrupted by maceration through a fine sieve and plated onto BAB and BAB-kanamycin plates for the enumeration of bacteria. The ratio of colonies on the BAB-kan plates divided by the total bacteria present (as informed by the BAB plates) gives a competitive index value. For this study a value of less than 0.2 was deemed to indicate a reduction in ability to compete for nutrients and colonise a host of the mutant bacteria (i.e. one fifth of mutant bacteria compared to wild-type are able to colonise the spleen) in line with other studies⁴⁶⁹. The results of the *in vivo* CI experiment are summarised in Table 6-1. Results were only used for four of the six mice inoculated since two of the mice were considered unlikely to have received the whole dose due to problems with the i.v. dosing. The *in vivo* CI results indicate that the *Y. pestis* $\Delta YpTdp$ mutant is not attenuated in its ability to compete with wild-type for niche since the average CI value for *Y. pestis* $\Delta YpTdp$ in competition with wild-type is 2.04. Enumeration of bacteria from spleen 1 indicated that there were more mutant bacteria within the spleen than total bacteria; a 1:1 output ratio was therefore assumed for this mouse. Results from the other three animals demonstrate that there are approximately the same numbers of mutant bacteria as wild-type bacteria within the spleens of these mice.

For the determination of the median lethal dose of *Y. pestis* $\Delta YpTdp$, groups of six BALB/c mice were challenged by the sub-cutaneous route with dilutions of a *Y. pestis* $\Delta YpTdp$ culture ranging from 10⁻⁴ to 10⁻⁸. The neat culture contained 2 x 10⁸ cfu/ml *Y. pestis* $\Delta YpTdp$ (Table 2-4, Section 2.3). The sub-cutaneous route best mimics *Y. pestis* infection by its most natural route – via the bite of an infected flea. In addition, entry via the sub-cutaneous route means that the bacteria must encounter a host of immune barriers (more so

Spleen number	Total CFU/spleen (as determined by counts on BAB plates)	<i>Y. pestis</i> $\Delta YpTdp$ CFU/spleen (as determined by counts on BAB-kan plates)	<i>Y. pestis</i> GB CFU/ spleen = Total CFU – <i>Y.</i> <i>pestis</i> $\Delta YpTdp$ CFU	Ratio WT : $\Delta YpTdp$
1	1.20×10^7	1.29×10^7	-9.00×10^5	Assume 1:1*
2	5.67×10^7	3.84×10^7	1.83×10^7	1 : 2.1
3	3.38×10^7	2.22×10^7	1.16×10^7	1 : 1.91
4	7.05×10^7	4.81×10^7	2.24×10^7	1 : 2.1

Table 6-1: Bacterial numbers per spleen from the *in vivo* competitive index study

BALB/c mice were inoculated via the i.v. route with 1000 cfu of a 1:1 mixture of *Y. pestis* GB and *Y. pestis* $\Delta YpTdp$. After 48 h the mice were culled and their spleens removed and macerated for the enumeration of total bacteria per spleen, and of numbers of *Y. pestis* $\Delta YpTdp$ mutant bacteria per spleen. A ratio of wild-type to mutant bacteria having colonised each animal could then be calculated. *Assumed to be 1:1

than direct entry into the bloodstream as for i.v. dosing). The MLD of *Y. pestis* GB is approximately 1 cfu⁴⁷⁰. Groups of mice given *Y. pestis* GB at three different dilutions of a 2×10^8 cfu/ml neat culture (10^{-5} to 10^{-7}) were used as a control for the experiment. The mice were monitored twice a day for two weeks and deaths recorded. Mice were culled at a humane endpoint based on a symptom scoring system by researchers independent from the study.

Figure 6-7 shows survival curves comparing wild-type and mutant bacteria at comparable doses (10^{-5} , 10^{-6} and 10^{-7} dilutions equivalent to approximately 200, 20 and 2 cfu). Table 6-2 summarises the median time to death across all the groups.

These results indicate that there is no significant difference between wild-type and mutant *Y. pestis* with regards to numbers of survivors after challenge or time to death. The Reed-Meunch equation was conducted to ascertain the MLD for *Y. pestis* $\Delta YpTdp$ (Figure 6-8). In order to calculate the MLD using this equation 100% of the group given the lowest dose need to survive and 100% of the group given the highest dose must succumb to infection. Unfortunately one mouse succumbed in the lowest dose group (10^{-8} dilution) and so an assumption had to be made that all mice would survive at a log lower dose (10^{-9} dilution) for the equation to work. The analysis showed that the MLD for *Y. pestis* $\Delta YpTdp$ is 1.27 cfu and so $\Delta YpTdp$ is not an attenuating mutation. Mice given wild-type *Y. pestis* died with the expected characteristics and within the expected timeframe indicating that the growth and administration of the bacteria should not have affected the results.

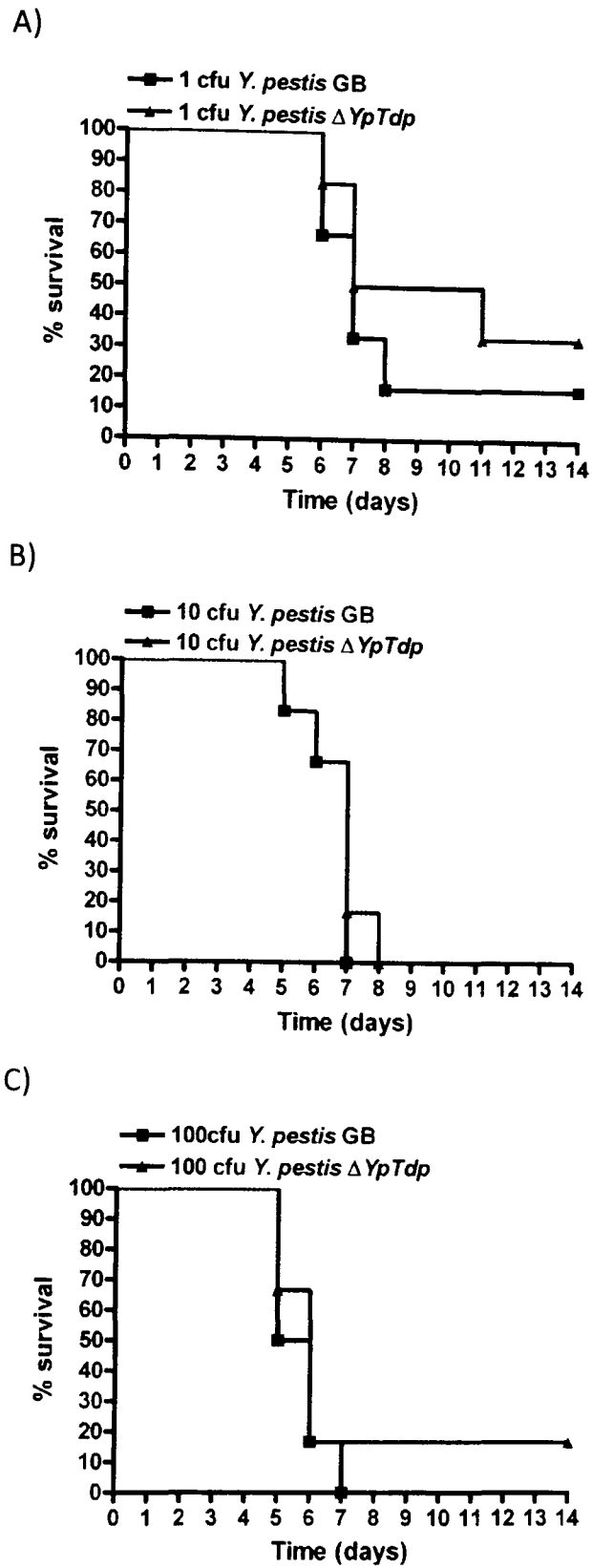


Figure 6-7: Survival curves for the three comparable doses of *Y. pestis* GB and *Y. pestis* $\Delta YpTdp$ given during the MLD study.

Six BALB/c mice were dosed via the s.c. route with *Y. pestis* GB and *Y. pestis* $\Delta YpTdp$ at a dose of (A) 1 cfu, (B) 10 cfu, (C) 100 cfu and their survival monitored over a period of 14 days.

	<i>Y. pestis</i> GB				<i>Y. pestis</i> $\Delta YpTdp$			
Dose (dilution of 2×10^8 cfu/ml)→	10^{-7}	10^{-6}	10^{-5}	10^{-8}	10^{-7}	10^{-6}	10^{-5}	10^{-4}
Number of survivors at end of experiment (out of 6)	1	0	0	5	2	0	1	0
Median time to death (days)	7	7	5.5	≥ 14	9	7	6	5

Table 6-2: A summary of the number of surviving mice in each dose group in the MLD study and their median time to death

Six BALB/c mice were dosed via the s.c. route with dilutions of a starting *Y. pestis* GB of *Y. pestis* $\Delta YpTdp$ culture (as detailed in the table). Their survival was monitored over a period of 14 days.

Dilution	Alive	Dead	Cumulative Alive ↓	Cumulative Dead ↑	% mortality
-4	0	6	0	22	100
-5	1	5	1	16	94.0
-6	0	6	1	11	91.7
-7	2	4	3	5	62.5
-8	5	1	8	1	11.0
-9	6	0	14	0	0

$$\frac{(\% \text{ mortality at dilution immediately above 50\% mortality}) - 50\%}{(\% \text{ mortality at dilution immediately above 50\% mortality}) - (\% \text{ mortality at dilution immediately below 50\%})} = \frac{62.5 - 50}{62.5 - 11}$$

$$= \frac{12.5}{51.5}$$

$$= 0.243 \text{p (index)}$$

What is the dilution that produced the mortality rate immediately above 50%? = -7

Apply the index value to this dilution = -7.243

The dilution of *Y. pestis* Δ*YpTdp* that would have contained 1MLD in 100μl is therefore = 10^{-7.243}

From the dose calculations in this study the “Neat” solution used to make the above dilutions contained : 2.26 x 10⁷ cfu/100μl

A 10^{-7.243} dilution of this is : **1.29 cfu = MLD**

Figure 6-8: Reed-Meunch calculation for MLD of *Y. pestis* Δ*YpTdp*.

6.3.5. Other characteristics of the *Y. pestis* $\Delta YpTdp$

Since the *Y. pestis* $\Delta YpTdp$ mutant did not show any altered virulence characteristics in the models used here, and with an increased auto-aggregation phenotype observed, additional experiments were carried out to investigate other characteristics of the mutant. The auto-aggregation phenotype of *Y. pestis* wild-type strains has recently been attributed to the presence of complex sugars on outer membrane proteins when grown at 28°C⁴⁷¹. The removal of a phosphoglucomutase protein involved in the synthesis of these sugars renders *Y. pestis* CO92 unable to aggregate. At the same time this mutant is also 1000-fold more sensitive to polymixin B⁴⁷¹. To investigate the response of *Y. pestis* $\Delta YpTdp$ to polymixin B an experiment to determine the minimum inhibitory concentration 50 (MIC₅₀) of polymixin B to *Y. pestis* $\Delta YpTdp$ was carried out. Approximately 8×10^4 cfu of *Y. pestis* GB or $\Delta YpTdp$ were incubated with varying concentrations of polymixin B for 24 h. At this point the OD₆₀₀ of each well was measured and used to calculate the percentage survival compared to control wells containing no polymixin B. The resultant kill curves show that there is no difference between the response of *Y. pestis* GB and $\Delta YpTdp$ to polymixin B (Figure 6-9). The MIC₅₀ for *Y. pestis* GB as calculated from a one phase exponential decay best-fit curve is 25.1 µg/ml for wild-type and 22.7 µg/ml for $\Delta YpTdp$ indicating that the *Y. pestis* $\Delta YpTdp$ does not differ in its susceptibility to polymixin B from *Y. pestis* GB.

The gene for YpTdp in *Y. pestis* strain 201 (biovar *Microtus*) has been shown to be up-regulated in response to high-salinity stress in two microarray studies^{472,473}. In one of the studies, where 25 environmental stresses were investigated, high salinity gave rise to the greatest change in expression of *YpTdp*. To investigate the response of the *Y. pestis* $\Delta YpTdp$ mutant to high salinity both wild-type and mutant *Y. pestis* were exposed for 3 h to a concentration of NaCl that is approximately equivalent to that in sea water (0.5 M). As a control, the strains were exposed to the approximate concentration of NaCl in BAB broth (0.05M) (Figure 6-10). Surviving bacteria were enumerated by dilution plating onto BAB agar. This experiment indicated that while the *Y. pestis* $\Delta YpTdp$ mutant is able to survive comparably to wild-type bacteria when exposed to 0.05 M NaCl, it demonstrates significantly reduced survival when exposed to 0.5M NaCl (2.54% mean survival for *Y. pestis* $\Delta YpTdp$ compared to 7.04% for wild-type).

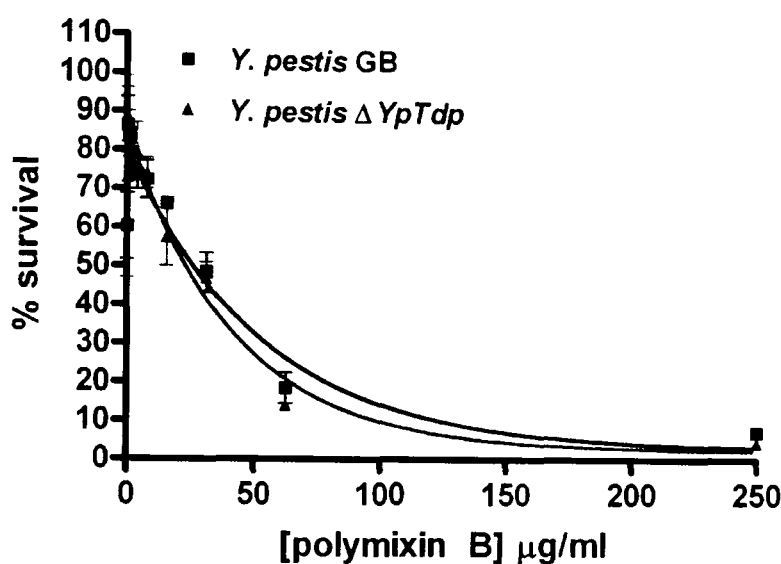


Figure 6-9: Survival of *Y. pestis* GB and $\Delta YpTdp$ in different concentrations of polymixin B

Overnight cultures of *Y. pestis* GB and $\Delta YpTdp$ were diluted to an $OD_{590} \sim 0.1$ and incubated for 1 h at 28°C with orbital shaking. The cultures were then diluted to 10^{-2} (approximately 10^5 to 10^6 cfu/ml) and 100 μ l culture added to a 96-well plate containing varying concentrations of polymixin B, as well as a positive control with no polymixin B and a negative control containing only BAB broth. The plate was incubated for 24 h and then the OD_{590} of the wells measured. Percentage survival was calculated by dividing the OD of the experimental wells by the OD for the positive control growth, both minus the OD from the negative control wells. Data is expressed as the mean of two independent experiments, each with triplicate technical replicates \pm SEM.

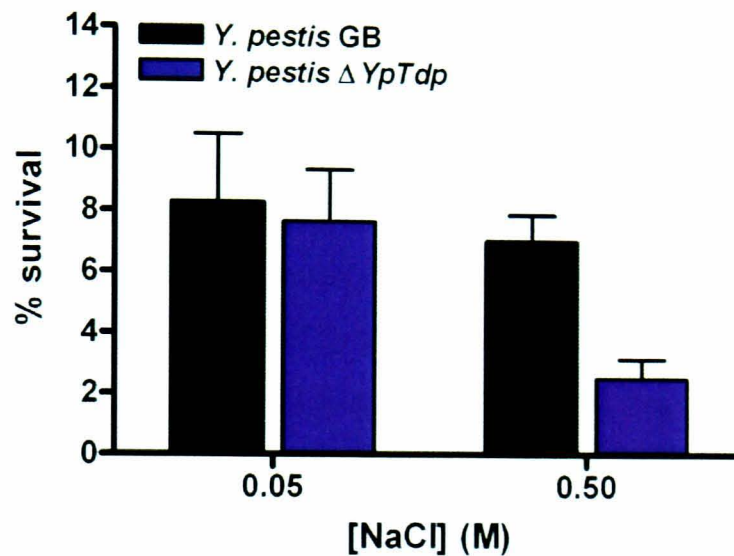


Figure 6-10: The survival of *Y. pestis* GB and $\Delta YpTdp$ in sodium chloride

Overnight cultures were diluted 1:10 (v/v) to a total of 10 ml BAB broth and incubated until an OD_{590} of ~ 0.4 was reached (c. 1×10^7 cfu/ml). Then, 100 μ l culture was used to inoculate 10 ml NaCl at 0.05 M or 0.5 M and incubated at 28°C with orbital shaking for 3 h. At this point the cultures were serially diluted and plated for the enumeration of bacteria. The input culture was also serially diluted and plated onto BAB agar in order to calculate the survival from initial inoculum. The counts were taken from duplicate plating of the dilutions, and the experiment carried out on three separate days. Data is expressed as the mean \pm SEM.

6.4. Conclusions

Previous studies of bacterial Tdps have investigated the effect that removing a Tdp has on the virulence characteristics of its cognate bacteria. However, the bacteria investigated so far have not necessarily been particularly pathogenic, or the models used have not necessarily reflected the natural disease. Other characteristics of the mutant bacteria which may contribute to an altered virulence, such as growth, have not been reported. Here we investigate a highly pathogenic bacterial species, *Y. pestis*, for its growth and virulence characteristics after removal of YpTdp.

On removal of the *YpTdp* gene from *Y. pestis* GB the mutant was assessed for its ability to grow in broth culture. Initially it appeared that the mutant had a growth defect when compared, in a growth curve measured by optical density, to wild-type bacteria. However, on closer inspection the *Y. pestis* $\Delta YpTdp$ mutant had a more aggressive auto-aggregation phenotype than *Y. pestis* GB which meant OD readings were difficult to accurately obtain. Vortexing and pipetting up and down of the cultures was able to break up the clumps to some extent and another growth curve was obtained, this time with no significant difference between the mutant and wild-type. This was confirmed by the enumeration of bacteria on BAB agar plates at defined points in the curve. This observed increase in autoaggregation was confirmed using a sedimentation assay but was found not to depend on a change in the hydrophobic nature of the *Y. pestis* $\Delta YpTdp$ mutant compared to wild-type. Recently, the gene *pgmA* which encodes for a phosphoglucomutase, has been found to be responsible for the autoaggregation phenotype of *Y. pestis*. Removal of this gene was also shown not to affect the hydrophobicity of *Y. pestis* but instead to affect the addition of complex sugars to proteins on the bacterial cell surface⁴⁷¹. Whether the removal of YpTdp similarly affects the bacterial cell surface has yet to be determined.

In three different virulence studies the *YpTdp* mutant did not demonstrate an attenuation. It was not defective in its ability to be taken up by, or replicate within, a macrophage cell line. Other macrophage cell lines, including of human origin, and *ex vivo* cells may also be useful in confirming this phenotype. In two mouse models of *Y. pestis* infection the mutant was not shown to be attenuated. In a competitive index study a mixture of wild-type and

mutant bacteria are given intravenously giving an acute model of colonisation. *Y. pestis* $\Delta YpTdp$ was able to colonise the spleens of BALB/c mice to a similar level as wild-type *Y. pestis*³⁷⁴. In an MLD study a range of doses of wild-type and mutant bacteria were given subcutaneously to groups of mice. This route of entry better reflects a natural flea bite infection and provides the invading bacteria with immune cell interaction at the site of infection that subsequently carry the *Y. pestis* around the body. In this model of infection no increased survival or reduced time to death was observed with the *YpTdp* mutant. These results are comparable those observed with the *Y. pestis* virulence factor YopJ. While YopJ has been extensively investigated for its immunomodulatory abilities^{290,334,336,382,385-387,474}, it does not bestow *Y. pestis* with significant fitness advantage alone^{463,475,476}. This suggests that the *Y. pestis* $\Delta YpTdp$ mutant should be investigated for more subtle effects *in vivo*, such as spleen and lymph node colonisation, or in other models, such as *Y. pestis* colonisation of the flea. YopJ also appears to play a more central role in virulence in *Y. pseudotuberculosis*⁴⁷⁷, and it would therefore be interesting to assess the role of YpTdp in *Y. pseudotuberculosis* virulence. This may be complicated by the fact, however, that *Y. pseudotuberculosis* strains express an additional TIR domain protein (Appendix B).

The addition of complex sugars to surface proteins of *Y. pestis* and its resulting aggregation causes blockage of the flea stomach which subsequently aids in the dissemination of *Y. pestis*. The addition of these sugars also causes *Y. pestis* to be relatively resistant to polymixin B. The removal of *pgmA* causes a reduction in aggregation and an increased susceptibility to polymixin B⁴⁷¹. We sought to discover whether the increased autoaggregation phenotype made *Y. pestis* $\Delta YpTdp$ more resistant to polymixin B. However, MIC experiments did not demonstrate an increased resistance since the MIC₅₀ of *Y. pestis* $\Delta YpTdp$ is 22.7 $\mu\text{g/ml}$ compared to 25.1 $\mu\text{g/ml}$ for *Y. pestis* GB. Given the inherent resistance of *Y. pestis* to polymixin B it may be that the resistance of *Y. pestis* to polymixin B cannot be much improved.

Reported microarray studies provided a further potential phenotype for the *Y. pestis* $\Delta YpTdp$ mutant since *YpTdp* has been shown to be upregulated in response to high salinity^{472,473}. Experiments reported in this chapter demonstrate that the mutant was

compromised in its ability to survive salt shock in comparison with wild-type *Y. pestis*. This indicates that the removal of YpTdp is not only affecting the bacteria (probably at the membrane level) in such a way as to make it form larger aggregates, but also in such a way that it is unable to control the flux of water and ions across the membrane. In one microarray paper that identified the upregulation of *YpTdp* under high salinity, the experiment was also repeated with using a *Y. pestis* $\Delta OmpR$ mutant strain⁴⁷³. OmpR is a transcription factor that differentially regulates the expression of *OmpF* and *OmpC*, two outer membrane porin proteins that sense and control the response of *Y. pestis* to changes in osmolarity of its environment⁴⁷⁸. In the *OmpR* mutant background the up-regulation of *YpTdp* in response to high-salinity is abrogated⁴⁷³. This may indicate that *YpTdp* expression is also regulated by OmpR, or that the dysregulation of osmoregulatory control after removal of OmpR means the trigger for *YpTdp* to be upregulated in high salinity is lost.

In conclusion, these initial phenotype studies indicate that if the effects of YpTdp on immune signalling observed *in vitro* also affect its infection *in vivo* these effects are likely to be subtle and were not demonstrated in the fairly acute *in vivo* models used here. Models of *Y. pestis* organ colonisation may give insights into the more subtle effects on virulence that removal of YpTdp likely confers. The other phenotypic attributes of the *Y. pestis* $\Delta YpTdp$ mutant identified here (increased aggregation and inability to survive salt shock) suggest YpTdp may affect the membrane of *Y. pestis* in a way that means its removal causes increased aggregation and a lack of osmoregulatory control. Further studies are certainly warranted, to investigate this function.

Chapter 7: General discussion

In 2006 Newman *et al.* performed a bioinformatics survey to identify TIR domains in bacterial proteins. They found more than 200 bacterial TIR domain proteins (Tdps) and focussed their research efforts on a Tdp, TlpA, from *Salmonella enterica* serovar *Enteritidis*. They showed that this protein impaired TLR- and MyD88-mediated activation of NFκB¹³ and that a *tlpA* deletion mutant was attenuated in cell culture and mouse models of infection. Despite being unable to demonstrate an interaction between TlpA and host proteins, they postulated that the function of TlpA was to disrupt host immune signalling via TIR-TIR interaction with host proteins and that bacterial Tdps were a new class of virulence factor. This paved the way for a number of subsequent studies with bacterial Tdps, which have each found that bacterial Tdps are able to disrupt host immune signalling and that deletion mutants in these proteins are attenuated³⁴³. This work has led to a “subversion hypothesis”: that the primary function of bacterial Tdps is to subvert the mammalian immune response by interacting with eukaryotic TIR-mediated signalling. As discussed in Chapter 3, the bioinformatic work carried out here casts doubt over the subversion hypothesis. The bioinformatic investigation found at least an equivalent number of Tdps in bacterial species not considered to engage in subversion of a host immune response, and did not find the proteins to be consistently conserved. However, one cannot ignore the growing wealth of data on a number of bacterial Tdps and their role in immune subversion and the likelihood that, at least for some bacterial Tdps, their role is one of signalling disruption.

The bioinformatic work in this study also gives a small glimpse into the interesting evolutionary history that TIR domain proteins appear to have had, including their frequent horizontal transfer, promiscuous association with other domains, and possible link to the advent of multicellularity. The list of proteins produced in this study (Appendix B) could be further probed for information on these observations. The sequence and structural characteristics of the bacterial Tdps investigated here, as found by more in depth bioinformatic scrutiny, suggest that bacterial Tdps may themselves group into families, and the production of a phylogenetic tree based on the Tdp sequence information would provide

insight into this. Finally, the bioinformatics work attempted here also highlights the importance of the considered use of bioinformatic tools. Although not used to its full advantage, the Saturated BLAST program did not appear to give much advantage over the traditional PSI-BLAST search strategy and the output from all bioinformatic assessments, including multiple sequence and structural alignments should be constantly monitored and checked with complementary tests.

Since a large body of experimental data supports some role for bacterial Tdps in immune evasion, particularly in pathogenic bacteria, four bacterial Tdps from highly pathogenic organisms (YpTdp from *Yersinia pestis*, BaTdp from *Bacillus anthracis* and BmTdp and BmTdp2 from *Brucella melitensis*) were downselected and screened for their ability to disrupt two TIR domain-dependent mammalian signalling pathways (IL-1 β - and LPS-induced signalling to NF κ B) and a TIR domain-independent signalling pathway (TNF α -induced signalling to NF κ B). Their effect on basal activity of NF κ B was also assessed. One bacterial Tdp from an environmental organism was also investigated in these studies (BthTdp from *Burkholderia thailandensis*), and initially a sixth candidate was included (found in the Saturated BLAST searches) that was later ruled out as a Tdp. All four proteins from pathogenic bacteria demonstrated the ability to modulate immune signalling *in vitro*. However, the protein from *B. thailandensis* also produced a marked decrease in signalling to NF κ B which was unexpected. *B. thailandensis* is not considered to be pathogenic and, while there have been a few isolated human cases of disease, these have been concurrent with other confounding factors. Current knowledge also indicates that *B. thailandensis* does not naturally or regularly infect any hosts within the environment. The fact that the Tdp from *B. thailandensis* shows an effect on NF κ B activation when over-expressed in these assays again calls into question the subversion hypothesis and the suitability of these assays for the investigation of Tdp function. By their very nature TIR domains are homotypic interaction domains, and therefore when they are over-expressed in cells one may expect that they would have the ability to interact with one or more human TIR domain proteins. Whether this is their physiological role is less easy to assess from these reporter assays.

Since NF κ B reporter assays are only one way of measuring immune signalling, YpTdp was down-selected for further investigation of its ability to disrupt human immune signalling *in vitro* and whether any observed disruption was via the homotypic interaction between TIR domains. The gene encoding YpTdp was also removed from *Y. pestis* and growth and virulence characteristics of this *Tdp* mutant were investigated. The signalling studies with YpTdp confirmed that when over-expressed in HEK293 cells it has the ability to disrupt immune signalling as demonstrated by reduced IL-8 production and delayed I κ B α degradation downstream of IL-1 β stimulation. YpTdp also reduced NF κ B activation induced by the over-expression of Mal. In combination with the LPS signalling data (that YpTdp disrupts LPS signalling to NF κ B) this suggests YpTdp is able to disrupt the association of Mal and TLR4. The involvement of the TIR domain from YpTdp in these effects, as investigated by the expression of the TIR domain alone (YpTIR) in these assays, was not conclusive. In the NF κ B reporter assays and assessment of IL-8 production YpTIR had no effect. In the I κ B α degradation studies, however, it demonstrated an identical effect to YpTdp; that is that the degradation of I κ B α was delayed in its presence. It is difficult to say whether the NF κ B reporter assays and IL-8 production are more sensitive or accurate read-outs of immune signalling compared to endogenous I κ B α degradation. Various hypotheses for why YpTIR might be unable to disrupt immune signalling, as suggested by the cytokine output and reporter assays, were discussed in Section 5.4.

When YpTdp is removed from *Y. pestis* the studies carried out in this work suggest that YpTdp has no significant role in the virulence of *Y. pestis*. The *YpTdp* deletion mutant (*Y. pestis* Δ *YpTdp*) was not defective in its replication within a macrophage cell line, its colonisation of the mouse spleen when given via the intravenous (i.v.) route in competition with wild-type *Y. pestis*, or in its ability to kill mice via the sub-cutaneous (s.c.) route. Obviously there are limitations of these models. Although macrophages are the niche host cell of *Y. pestis*, the murine macrophage cell line J774 is unlikely to very accurately reflect macrophages *in vivo*. It would therefore be interesting to test the *Y. pestis* Δ *YpTdp* mutant for its ability to gain access to, and replicate within, primary macrophages. In addition an experiment to investigate the colonisation of *Y. pestis* Δ *YpTdp* in comparison to wild-type *Y. pestis* at different timepoints may highlight a more subtle affect of YpTdp on the

virulence of *Y. pestis*. In addition to the s.c. route used in the MLD study, which reflects one of the common routes of infection for *Y. pestis* via the bite of an infected flea, an experiment to investigate the role of YpTdp in inhalational infection (common during pneumonic plague) may provide additional insights. The models used here to assess the virulence of *Y. pestis* $\Delta YpTdp$ were acute, and while they do not provide a complete picture of how YpTdp may contribute to every aspect of *Y. pestis* infection, these studies suggest that YpTdp does not play a central role in virulence. As discussed, this has also proved the case for the archetypal *Y. pestis* immunomodulatory protein YopJ. However, YopJ has been shown to augment the function of other immunomodulatory proteins⁴⁶³, and the interaction of YpTdp with other *Yersinia* immune effectors would be interesting to investigate.

Having postulated that bacterial Tdps may have roles other than in immune evasion and with an observed lack of effect on virulence after removing the YpTdp clues to other functions have been sought. Bioinformatic analyses in conjunction with literature searching and experimental observations have opened up a number of possibilities for an alternative function for YpTdp which will need to be further investigated. Possibilities for an alternative function of YpTdp, and the support for and against these ideas are discussed below, along with suggested further investigation for each of these functions.

7.1. Osmoregulation-related function

A number of studies have indicated that the *YpTdp* gene is up-regulated during conditions of high salinity^{472,473}. One study also found that while *YpTdp* is up-regulated after exposure to 0.5M NaCl for 20 min (32.3 fold increase in expression) this upregulation is abrogated in an *OmpR* mutant background⁴⁷³. Initial experimental data from these studies also indicate a potential role in osmoregulation. The *YpTdp* mutant is significantly attenuated in its ability to survive when exposed to high salinity (0.5M NaCl for 3 h) in comparison to wild-type *Y. pestis*, but there is no difference in survival when exposed to 0.05M NaCl, the approximate concentration of NaCl in BAB broth. NaCl at 0.5 M reflects the approximate levels of salt in sea water, and represents a high saline environmental condition. *Y. pestis* has little contact with harsh environmental conditions, however, since it survives poorly outside of a host organism. However, *Y. pestis* may encounter various osmotic stresses during its

colonisation of different hosts. Physiological levels of NaCl within the bloodstream of a mammalian host are approximately 0.1 M. The osmotic environment of a flea has not been investigated but it has been shown that fleas are stimulated to feed when NaCl concentrations are between 0.15 M and 0.2 M NaCl suggesting that the flea stomach may present a somewhat raised salt level environment⁴⁷⁹. Alternatively, this postulated role for YpTdp may be an evolutionary remnant from the life-style of *Yersinia pseudotuberculosis*, an organism more likely to encounter differing osmotic conditions in the environment.

The increased auto-aggregation phenotype of the *YpTdp* mutant may also link into a role in osmoregulation for YpTdp since any affect on osmoregulation by YpTdp may manifest itself at the cell membrane, and auto-aggregation may also be dependent on membrane characteristics of the bacteria. Interestingly, the increased expression of *YpTdp* observed under salt shock is ameliorated in an *ompR* mutant background⁴⁷³ indicating a possible direct, or indirect (through the change in OmpC and OmpF expression), link between *YpTdp* and OmpR as discussed in Section 6.4. The removal of OmpR, and therefore a change in expression of OmpC and OmpF, is likely to affect the membrane characteristics of the bacteria. So far no link between these porins and the auto-aggregation phenotype has been made, however.

7.2. Phage-related function

The gene for *YpTdp* sits just outside of the *Yersinia* high pathogenicity island (HPI) thought to have been acquired via phage transfer of DNA which is responsible for *Yersinia* sp. ability to scavenge iron from its host and its ability to colonise the flea⁴⁸⁰. The region around *YpTdp* also suggests phage origin and so it is possible that *YpTdp* once was, or still is, part of a prophage. The aggregation phenotype observed in wild-type *Y. pestis* species is linked to biofilm formation^{481,482} and it is thought that phage may play an important role here. The production of phage during biofilm formation is thought to increase the diversity in the biofilm and help the formation of new micro-colonies⁴⁸³. The removal of *YpTdp* may have disrupted the ability of phage to be produced leading to reduced death of cells within the aggregates and a reduction of new sub-populations (new aggregates) being formed, giving rise to less, but larger, aggregates within the *Y. pestis* $\Delta YpTdp$ broth culture. In

addition, the area of YpTdp that contains the TIR domain also shows some homology to a nucleoside 2-deoxyribosyltransferase (NDRT) enzyme (Figure 7-1) which may support a phage-related function for YpTdp. These enzymes catalyse the cleavage of the glycosidic bonds of 2' deoxyribonucleosides and phage require a NDRT enzyme to form part of the dNTP synthetase complex formed during phage-infection of the bacterial cell to maintain high rates of DNA accumulation⁴⁸⁴. Alternatively, there may be a link between a phage-related function for YpTdp and the observed link to osmoregularity and the Omps. Omps were originally identified as receptors for bacteriophage, and many are necessary for infection by phages⁴⁸⁵. The λ phage-encoded Lom protein is thought to be an ancestor of the gene family that includes OmpX and it this protein is able to confer adhesion of *E. coli* to human cells.

7.3. Biofilm formation

As discussed, the auto-aggregation phenotype of wild-type *Y. pestis* species is considered to be linked to biofilm formation⁴⁸¹. Therefore since the *YpTdp* mutant forms larger aggregates *in vitro* YpTdp may act as a negative regulator of biofilm formation, or affect the production of other biofilm regulators such as hmsP⁴⁸⁶. Apart from the increased auto-aggregation phenotype, however, there is currently little evidence to support a role for YpTdp in biofilm formation. The capacity of bacterial cells to bind certain dyes like Congo Red is also an indicative phenotype of biofilm formation, and auto-aggregation in liquid medium and formation of pigmented colonies on media containing Congo Red or hemin correlates with the ability to block the flea proventriculus³⁷⁴. When grown on media containing Congo Red or hemin both wild-type and $\Delta YpTdp$ take up the stain to a similar extent, although whether any difference in an increase in biofilm formation would be visible by the uptake of stain (compared to an absence of uptake) is not certain. Further studies would therefore be essential to elucidate whether there is a role for YpTdp in the formation of *Y. pestis* biofilms.

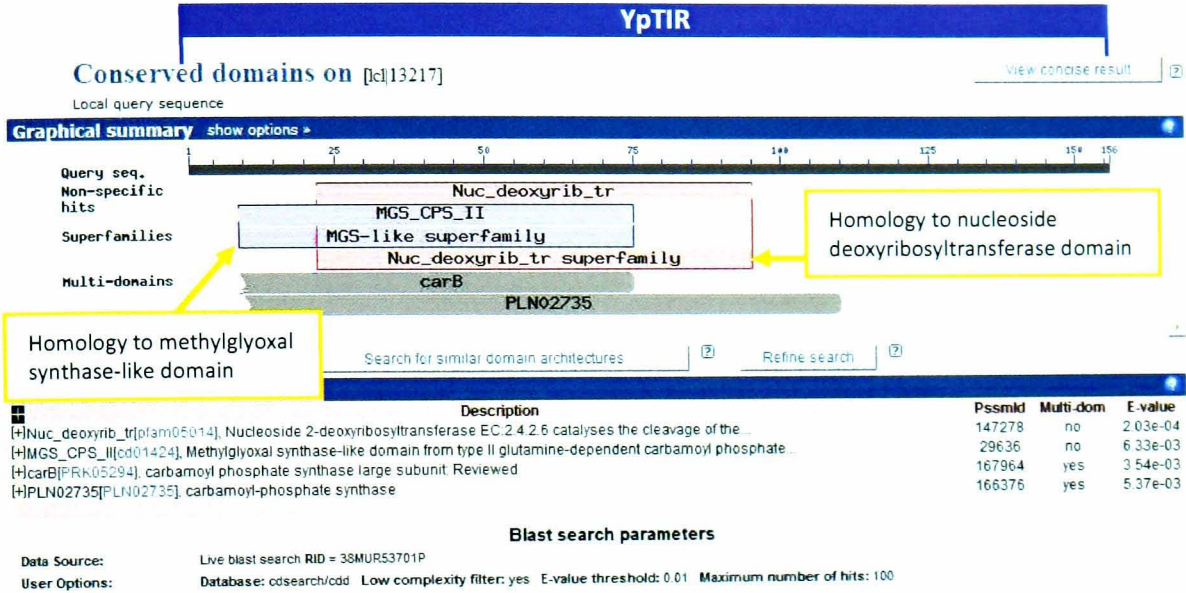


Figure 7-1: Screen shot from a Conserved Domains Database (CDD) search using YpTIR

The YpTIR sequence was entered into a search of the CDD on the NCBI web server and the above results were returned. The region of sequence homologous to the nucleoside deoxyribosyltransferase domain is shown in pink and the region of sequence with homology to the methylglyoxal synthase-like domain is shown in blue. Expect (e) values for the pairwise alignment of these sequences are also reported.

7.4. Methylglyoxyl synthase

Recently it has been discovered that a phosphoglucomutase is required for the *Y. pestis* clumping phenotype⁴⁸⁷. In the enteropathogenic *Yersiniae* species autoaggregation is mediated by YadA, an adhesin, and is due to hydrophobic interactions between the bacteria and a host environment⁴⁸⁸. In *Y. pestis*, however, YadA is non-functional^{489,490} and its basis for autoaggregation was unclear. However, a recent study demonstrated that the enzyme phosphoglucomutase (PgmA) was essential for the phenotype and that a transposon mutant in *PgmA* lost the autoaggregation phenotype and was more sensitive to the anti-microbial polymixin B. Pgm catalyses the interconversion between glucose 6-phosphate (G-6-P) and glucose 1-phosphate (G-1-P). The conversion of G-6-P to G-1-P initiates the pathway that leads to the formation of nucleotide sugars, for example UDP-glucose. These nucleotide sugars can be used to modify cellular components such as LPS and secreted matrix components and Pgms have been shown to have a role in virulence and sensitivity to anti-microbials in other organisms⁴⁹¹⁻⁴⁹³. In *Y. pestis* deletion of *pgmA* had no effect on virulence but did increase its sensitivity to polymixin B over 1000-fold. Deletion of *YpTdp* from *Y. pestis* GB has no effect on virulence, or its susceptibility to polymixin B but appears to increase its autoaggregation in broth culture when grown at 28°C and this is not due to a change in hydrophobicity of the mutant bacteria. A highly speculative prediction might be that YpTdp is involved in this sugar metabolism and that removal of YpTdp has dysregulated the system in some way. This prediction is given some weight by the bioinformatic assessment of the TIR domain from YpTdp. The area of sequence that includes the TIR domain also shows homology to a methylglyoxal synthase-like domain from a type II glutamine-dependent carbamoyl phosphate synthase (CPS)⁴⁹⁴ (Figure 7-1). A methylglyoxal synthase is an enzyme that catalyses the conversion of dihydroxyacetone phosphate (DHAP) to methylglyoxal and phosphate which is essentially a carbon-oxygen lyase reaction on the phosphate group. In the CPS the methylglyoxal synthase domain forms a regulatory domain that binds to the allosteric effector ornithine. A link between the deletion of a potential methylglyoxal synthase-type enzyme and an increase in autoaggregation is not immediately clear. However, methylglyoxal synthase has been shown to have a role in sugar metabolism in bacteria⁴⁹⁵ and it is conceivable that it may also impact on the production of sugars for addition to outer membrane proteins, and

therefore auto-aggregation, as does the phosphoglucomutase enzyme of *Y. pestis*. In fact both a phosphoglucomutase and a methylglyoxal synthase are proposed to have a role in the utilisation of polyglucose by the bacterium *Desulfovibrio gigas* (Figure 7-2) and the availability of glucose has been shown to affect aggregation in *E. coli*⁴⁹⁶. A role in sugar metabolism for YpTdp may also link into the observed reduction in survival of the *Y. pestis* $\Delta YpTdp$ mutant in high salinity. Bacteria are able to respond to osmotic stress in two ways: solutes can be pumped in or out of the cell to maintain an osmotic balance across the membrane, or compatible solutes can be synthesised within the cell. Compatible solutes are molecules that are able to accumulate within the cell without becoming toxic. In this way solute concentrations within the cell can be raised to match high concentrations outside (for example, in conditions of high salinity). Examples of compatible solutes include betaines, amino acids and the sugar trehalose. A role for YpTdp in sugar metabolism may therefore affect the production of compatible solutes in times of osmotic stress.

7.5. Further work

This study has demonstrated that YpTdp has the ability to modulate the mammalian immune system *in vitro* but this function does not appear to affect the virulence of *Y. pestis* GB through the models used here. Further work will be needed to assess the effect of YpTdp on the more subtle manifestations of virulence such as organ colonisation. In addition, the unusual phenotypes of the *Y. pestis* $\Delta YpTdp$ mutant should be further explored.

Initially it should be confirmed that the production of the $\Delta YpTdp$ mutant has not altered the expression of any other genes. This could be achieved by assessing the expression of neighbouring genes by RT-PCR, or by the complementation of the *Y. pestis* $\Delta YpTdp$ mutant through expression of YpTdp from a plasmid. Complementation is often successfully achieved if the gene is expressed from a plasmid under the control of its native promoter. An initial investigation of the possible location of the native promoter for *YpTdp* has proved unsuccessful.

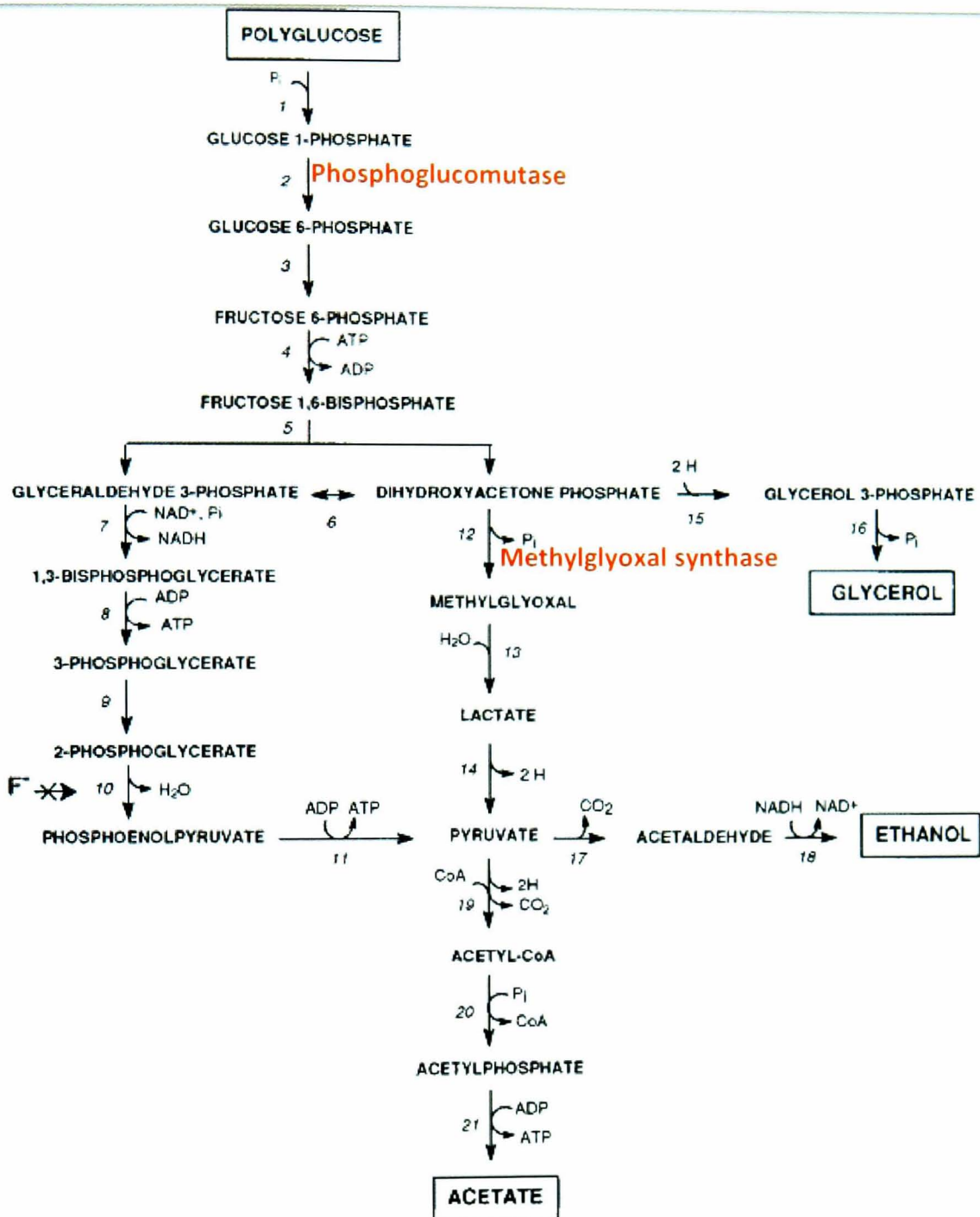


Figure 7-2: Proposed metabolic pathways for polyglucose use by *Desulfovibrio gigas*

This pathway demonstrates how the affects of a phosphoglucomutase enzyme and a methylglyoxal synthase enzyme may be linked. Adapted from Fareleira *et al.* 1997⁴⁹⁷

The role of YpTdp in the virulence of *Y. pestis* should be investigated in other, less acute, models of *Y. pestis* infection, and in other hosts. It would be interesting to investigate the ability of *Y. pestis* $\Delta YpTdp$ to be taken up by, and replicate within, primary macrophages using a variety of timepoints during infection. In addition the cytokines produced by these macrophages on infection with *Y. pestis* $\Delta YpTdp$ in comparison with wild-type *Y. pestis* GB would provide additional insights into the role of YpTdp as a immunomodulator.

The colonisation of the spleen, liver and lymph nodes by *Y. pestis* $\Delta YpTdp$ compared to wild-type *Y. pestis* should be investigated in an s.c. and inhalational *Y. pestis* mouse infection model at various timepoints. It may be that YpTdp confers an early advantage during infection.

In addition to the further investigation of YpTdp as an immunomodulatory protein and virulence factor, other possible roles for YpTdp could be investigated. Most of the other possible roles for YpTdp that have been postulated in this section are borne from analysis of the *YpTdp* gene location within the chromosome and YpTdp protein homology. However, a potential role in osmoregulation, or a function dependent on NaCl concentrations, is backed up with, albeit limited, experimental observation, both in this study and in the literature. This would therefore be a prudent starting point for investigations into other possible functions for the *Y. pestis* Tdp. The survival of *Y. pestis* $\Delta YpTdp$ (and a complemented mutant if it were achieved) after salt shock in a wider range of NaCl concentrations would need to be investigated. The NaCl concentrations within a flea stomach have not been published. However, the fact that elevated NaCl concentrations in food induce fleas to feed suggests that the flea environment may be one of higher salinity. The colonisation and survival of *Y. pestis* $\Delta YpTdp$ in fleas compared with wild-type could therefore be investigated both as an alternative function of YpTdp, and as another virulence model.

As for the other postulated functions, the ability of *Y. pestis* GB and *Y. pestis* $\Delta YpTdp$ to produce any phage-like particles may help to confirm any phage-related function and, in the same vein, the ability of *Y. pestis* $\Delta YpTdp$ to grow on DNA as a carbon source in defined

media could confirm or deny its likely identity as a deoxyribosyltransferase enzyme. Further investigation of the increased auto-aggregation phenotype of *Y. pestis* $\Delta YpTdp$ including microscopic inspection of the aggregates, and an assessment of the addition of sugars to proteins on the outer membrane would give information about the reason for the observed aggregation phenotype and whether it was linked to the pathway involved in wild-type *Y. pestis* aggregation. This would, in turn, inform the possible role for YpTdp as a methylglyoxal synthase enzyme, or whether the aggregation phenotype observed was more related to an osmoregulatory function. The role of YpTdp as a methylglyoxal synthase enzyme could be assessed by growing the *Y. pestis* $\Delta YpTdp$ on a variety of different sugars as the carbon source. Deletion of a methylglyoxal synthase in *E. coli* has been shown to alter the panel of sugars on which it can grow⁴⁹⁵.

7.6. Concluding remarks

An immunomodulatory function for bacterial TIR domain proteins is being vigorously pursued in the literature and a growing body of evidence convincingly suggests that at least some of these proteins do possess this function. However, it seems that a variety of questions surrounding bacterial TIR domain proteins are also being conveniently ignored. The bioinformatic data on the identity of TIR domain proteins across bacterial species is the most detailed analysis of these proteins to have been performed so far and gives a fascinating insight into the distribution and promiscuous nature of these domains. The data presented here, on the immunomodulatory role of TIR domain proteins, and other functions they may possess, is somewhat incomplete and often inconclusive. It has become apparent that the affect of bacterial TIR domain proteins on signalling may be subtle, and relatively pathway/species specific, and so a much larger volume of work is needed to fully elucidate the *in vitro* affects of the range of bacterial TIR domain proteins investigated here. The further investigation of the *Y. pestis* Tdp has helped to confirm its possible immunomodulatory role but the phenotypic observations on the *Y. pestis* $\Delta YpTdp$ mutant raise more questions than they answer. However, there are a number of solid conclusions that can be drawn and a variety of fascinating questions to be answered. Firstly, TIR domain proteins do exist widely in bacterial species and seem to have had an interesting evolutionary history. I would suggest that these are versatile domains that can be, and have

been, co-opted for a variety of different purposes in different organisms. Over time a full analysis of these proteins from very different bacterial species will be very valuable. Some of the bacterial TIR domain proteins tested here are clearly able to modulate human immune signalling *in vitro* and a wider panel of TIR-dependent signalling pathways, from different species, should shed further light on this. The TIR domain protein from *Y. pestis* certainly has the capability to modulate mammalian immune signalling but the overall effect of this, like many single immunomodulatory proteins, is likely to be subtle and potentially involve co-ordination with other strategies. In addition there is a strong possibility that TIR domain proteins, and the protein in *Y. pestis*, may “moon-light” in other roles. A number of roles for YpTdp, some very speculative, have been presented here and should make for interesting further investigation. The role of TIR domains in bacteria is certainly not as straightforward a question as it may have originally seemed but is definitely an exciting one to pursue.

References

- 1 Kennedy,R.B. *et al.* (2009) The immunology of smallpox vaccines. *Curr. Opin. Immunol.* 21, 314-320
- 2 Greenberg,S. and Grinstein,S. (2002) Phagocytosis and innate immunity. *Curr. Opin. Immunol.* 14, 136-145
- 3 Li,Z. *et al.* (2004) The generation of antibody diversity through somatic hypermutation and class switch recombination. *Genes & Development* 18, 1-11
- 4 Thompson,C.B. (1995) New insights into V(D)J recombination and its role in the evolution of the immune system. *Immunity* 3, 531-539
- 5 Janeway,C.A. (1989) Approaching the Asymptote? Evolution and Revolution in Immunology. *Cold Spring Harb. Symp. Quant. Biol.* 54, 1-13
- 6 Meylan,E. *et al.* (2006) Intracellular pattern recognition receptors in the host response. *Nature* 442, 39-44
- 7 Osterloh,A. and Breloer,M. Heat shock proteins: linking danger and pathogen recognition. *Med. Microbiol. Immunol. (Berl).*
- 8 Williams,J.H.H. and Ireland,H.E. (2007) Sensing danger - Hsp72 and HMGB1 as candidate signals. *J. Leukoc. Biol.* 83, 489-492
- 9 Alnemri,E. (2010) Sensing Cytoplasmic Danger Signals by the Inflammasome. *J. Clin. Immunol.* 30, 512-519
- 10 Lemaitre B *et al.* (1996) The dorsoventral regulatory gene cassette spatzle/Toll/cactus controls the potent antifungal response in *Drosophila* adults. *Cell* 86, 973-983
- 11 Anderson Kathryn V. *et al.* (1985) Establishment of dorsal-ventral polarity in the *Drosophila* embryo: Genetic studies on the role of the Toll gene product. *Cell* 42, 779-789
- 12 Hashimoto,C. *et al.* (1988) The Toll gene of drosophila, required for dorsal-ventral embryonic polarity, appears to encode a transmembrane protein. *Cell* 52, 269-279
- 13 Gay,N.J. and Keith,F.J. (1991) *Drosophila* Toll and IL-1 receptor. *Nature* 351, 355-356
- 14 Chen,G.K. *et al.* (2007) Immune-like phagocyte activity in the social amoeba. *Science* 317, 678-681
- 15 Georgel,P. *et al.* (2009) The Heterogeneous Allelic Repertoire of Human Toll-Like Receptor (TLR) Genes. *PLoS ONE* 4, e7803
- 16 Krieg,A.M. (2007) TLR9 and DNA 'feel' RAGE. *Nature Immunology* 8, 475-477

- 17 Grover,A. *et al.* (2008) Mycobacterial infection induces the secretion of high-mobility group box 1 protein. *Cellular Microbiology* 10, 1390-1404
- 18 Philpott,D.J. and Girardin,S.E. (2004) The role of Toll-like receptors and Nod proteins in bacterial infection. *Mol. Immunol.* 41, 1099-1108
- 19 Poltorak A *et al.* (1998) Defective LPS signaling in C3H/HeJ and C57BL/10ScCr mice: mutations in TLR4 gene. *Science* 282, 2085-2088
- 20 Qureshi,S.T. *et al.* (1999) Endotoxin-tolerant Mice Have Mutations in Toll-like Receptor 4 (Tlr4). *The Journal of Experimental Medicine* 189, 615-625
- 21 Heine,H. *et al.* (1999) Cutting Edge: Cells That Carry A Null Allele for Toll-Like Receptor 2 Are Capable of Responding to Endotoxin. *J Immunol* 162, 6971-6975
- 22 Enkhbayar,P. *et al.* (2004) Structural principles of Leucine-Rich repeat (LRR) proteins. *Proteins-Structure Function and Genetics* 54, 394-403
- 23 Kajava,A.V. *et al.* (2009) A network of hydrogen bonds on the surface of TLR2 controls ligand positioning and cell signaling. *J Biol Chem* 285, 6227-6234
- 24 Bell JK *et al.* (2005) The molecular structure of human Toll-like receptor 3 ligand-binding domain. *Proc. Natl. Acad. Sci. U. S. A.* 102, 10976-10980
- 25 Choe Jungwoo *et al.* (2005) Crystal Structure of Human Toll-Like Receptor 3 (TLR3) Ectodomain. *Science* 309, 581-585
- 26 Lin,L. *et al.* (2008) Structural basis of toll-like receptor 3 signaling with double-stranded RNA. *Science*, 379-381
- 27 Alexopoulou,L. *et al.* (2001) Recognition of double-stranded RNA and activation of NF-kappaB by Toll-like receptor 3. *Nature (London)* 413, 732-738
- 28 Leonard,J.N. *et al.* (2008) The TLR3 signaling complex forms by cooperative receptor dimerization. *Proc Natl Acad Sci* 105, 258-263
- 29 Lan,T. *et al.* (2009) Synthetic oligoribonucleotides-containing secondary structures act as agonists of Toll-like receptors 7 and 8. *Biochem Biophys Res Commun* 386, 443-448
- 30 Cekaite,L. *et al.* (2007) Gene expression analysis in blood cells in response to unmodified and 2'-modified siRNAs reveals TLR-dependent and independent effects. *J Mol Biol* 365, 90-108
- 31 Gantier,M.P. *et al.* (2008) TLR7 Is Involved in Sequence-Specific Sensing of Single-Stranded RNAs in Human Macrophages. *J Immunol* 180, 2117-2124
- 32 Sioud,M. (2006) Innate sensing of self and non-self RNAs by Toll-like receptors. *Trends in Molecular Medicine* 12, 167-176

- 33 Heil, F. *et al.* (2004) Species-specific recognition of single-stranded RNA via toll-like receptor 7 and 8. *Science* 303, 1526-1529
- 34 Judge, A.D. *et al.* (2005) Sequence-dependent stimulation of the mammalian innate immune response by synthetic siRNA. *Nat Biotech* 23, 457-462
- 35 Sioud, M. (2006) Single-stranded small interfering RNA are more immunostimulatory than their double-stranded counterparts: a central role for 2'-hydroxyl uridines in immune responses. *Eur J Immunol* 36, 1222-1230
- 36 Hornung, V. *et al.* (2008) RNA Recognition via TLR7 and TLR8. *Handb Exp Pharmacol.* 183, 71-86
- 37 Gay, N.J. and Gangloff, M. (2007) Structure and Function of Toll Receptors and Their Ligands. *Annu. Rev. Biochem.* 76, 141-165
- 38 Jin, M.S. *et al.* (2007) Crystal structure of the TLR1-TLR2 heterodimer induced by binding of a tri-acylated lipopeptide. *Cell* 130, 1071-1082
- 39 Park, B.S. *et al.* (2009) The structural basis of lipopolysaccharide recognition by the TLR4-MD-2 complex. *Nature* 458, 1191-U130
- 40 Kim, H.M. *et al.* (2007) Crystal structure of the TLR4-MD-2 complex with bound endotoxin antagonist eritoran. *Cell* 130, 906-917
- 41 Gangloff, M. *et al.* (2008) Structural insight into the mechanism of activation of the Toll receptor by the dimeric ligand Spatzle. *J. Biol. Chem.* 283, 14629-14635
- 42 Bell, J.K. *et al.* (2005) The molecular structure of the Toll-like receptor 3 ligand-binding domain. *Proc. Natl. Acad. Sci. U. S. A.* 102, 10976-10980
- 43 Bell, J.K. *et al.* (2003) Leucine-rich repeats and pathogen recognition in Toll-like receptors. *Trends in Immunology* 24, 528-533
- 44 Gioannini, T.L. *et al.* (2004) Isolation of an endotoxin-MD-2 complex that produces Toll-like receptor 4-dependent cell activation at picomolar concentrations. *Proc. Natl. Acad. Sci. U. S. A.* 101, 4186-4191
- 45 Jiang, Z.F. *et al.* (2005) CD14 is required for MyD88-independent LPS signaling. *Nature Immunology* 6, 565-570
- 46 Wetzler, L.M. (2003) The role of Toll-like receptor 2 in microbial disease and immunity. *Vaccine* 21, S55-S60
- 47 Hoebe, K. *et al.* (2005) CD36 is a sensor of diacylglycerides. *Nature* 433, 523-527

- 48 Ozinsky,A. *et al.* (2000) The repertoire for pattern recognition of pathogens by the innate immune system is defined by cooperation between Toll-like receptors. *Proceedings of the National Academy of Sciences* 97, 13766-13771
- 49 Weber,A.N.R. *et al.* (2005) Ligand-Receptor and Receptor-Receptor Interactions Act in Concert to Activate Signaling in the Drosophila Toll Pathway. *J. Biol. Chem.* 280, 22793-22799
- 50 Latz,E. *et al.* (2007) Ligand-induced conformational changes allosterically activate Toll-like receptor 9. *Nat Immunol* 8, 772-779
- 51 Gay,N.J. *et al.* (2006) Opinion - Toll-like receptors as molecular switches. *Nature Reviews Immunology* 6, 693-698
- 52 Gay,E.A. *et al.* (2004) Functional selectivity of D-2 receptor ligands in a Chinese hamster ovary hD(2L) cell line: Evidence for induction of ligand-specific receptor states. *Mol. Pharmacol.* 66, 97-105
- 53 Haas,T. *et al.* (2008) The DNA Sugar Backbone 2' Deoxyribose Determines Toll-like Receptor 9 Activation. *Immunity* 28, 315-323
- 54 Hornung,V. *et al.* (2002) Quantitative Expression of Toll-Like Receptor 1-10 mRNA in Cellular Subsets of Human Peripheral Blood Mononuclear Cells and Sensitivity to CpG Oligodeoxynucleotides. *J Immunol* 168, 4531-4537
- 55 Muzio,M. *et al.* (2000) Toll-like receptor family and signalling pathway. *Biochem. Soc. Trans.* 28, 563-566
- 56 Ito,T. *et al.* (2002) Interferon-alpha and interleukin-12 are induced differentially by toll-like receptor 7 ligands in human blood dendritic cell subsets. *J. Exp. Med.* 195, 1507-1512
- 57 Krug,A. *et al.* (2001) Toll-like receptor expression reveals CpG DNA as a unique microbial stimulus for plasmacytoid dendritic cells which synergizes with CD40 ligand to induce high amounts of IL-12. *Eur. J. Immunol.* 31, 3026-3037
- 58 Muzio,M. *et al.* (2000) Differential expression and regulation of toll-like receptors (TLR) in human leukocytes: Selective expression of TLR3 in dendritic cells. *J. Immunol.* 164, 5998-6004
- 59 Visintin,A. *et al.* (2001) Regulation of Toll-like receptors in human monocytes and dendritic cells. *J. Immunol.* 166, 249-255
- 60 Jarrossay,D. *et al.* (2001) Specialization and complementarity in microbial molecule recognition by human myeloid and plasmacytoid dendritic cells. *Eur. J. Immunol.* 31, 3388-3393

- 61 Kadowaki,N. *et al.* (2001) Subsets of human dendritic cell precursors express different toll-like receptors and respond to different microbial antigens. *J exp med* 194, 863-869
- 62 Miettinen,M. *et al.* (2001) IFNs activate toll-like receptor gene expression in viral infections. *Genes Immun* 2, 349-355
- 63 Matsuguchi,T. *et al.* (2000) Gene expressions of Toll-like receptor 2, but not Toll-like receptor 4, is induced by LPS and inflammatory cytokines in mouse macrophages. *J Immunol* 165, 5767-5772
- 64 Matsuguchi,T. *et al.* (2000) Gene expressions of lipopolysaccharide receptors, toll-like receptors 2 and 4, are differently regulated in mouse T lymphocytes. *Blood* 95, 1378-1385
- 65 Zarembek,K.A. and Godowski,P.J. (2002) Tissue Expression of Human Toll-Like Receptors and Differential Regulation of Toll-Like Receptor mRNAs in Leukocytes in Response to Microbes, Their Products, and Cytokines. *J Immunol* 169, 1136
- 66 Underhill,D.M. *et al.* (1999) The Toll-like receptor 2 is recruited to macrophage phagosomes and discriminates between pathogens. *Nature* 401, 811-815
- 67 Latz,E. *et al.* (2002) Lipopolysaccharide rapidly traffics to and from the Golgi apparatus with the toll-like receptor 4-MD-2-CD14 complex in a process that is distinct from the initiation of signal transduction. *J Biol Chem* 277, 47834-47843
- 68 Eaton-Bassiri,A. *et al.* (2004) Toll-like receptor 9 can be expressed at the cell surface of distinct populations of tonsils and human peripheral blood mononuclear cells. *Infect Immun* 72, 7202-7211
- 69 Hornef,M.W. *et al.* (2003) Intracellular recognition of lipopolysaccharide by toll-like receptor 4 in intestinal epithelial cells. *J exp med* 198, 1225-1235
- 70 Akira,S. *et al.* (2006) Pathogen Recognition and Innate Immunity. *Cell* 124, 783-801
- 71 Yoneyama,M. *et al.* (2004) The RNA helicase RIG-I has an essential function in double-stranded RNA-induced innate antiviral responses. *Nat Immunol* 5, 730-737
- 72 Schulz Oliver *et al.* (2005) Toll-like receptor 3 promotes cross-priming to virus-infected cells. *Nature* 433, 887-892
- 73 Matsumoto,M. *et al.* (2003) Subcellular localization of Toll-like receptor 3 in human dendritic cells. *J Immunol* 171, 3154-3162
- 74 Akazawa,T. *et al.* (2007) Antitumor NK activation induced by the Toll-like receptor 3-TICAM-1 (TRIF) pathway in myeloid dendritic cells. *Proc Natl Acad Sci* 104, 252-257
- 75 Kagan,J.C. *et al.* (2008) TRAM couples endocytosis of Toll-like receptor 4 to the induction of interferon- β . *Nat Immunol* 9, 361-368

- 76 Janssens,S. *et al.* (2002) Regulation of interleukin-1-and lipopolysaccharide-induced NF-kappa B activation by alternative splicing of MyD88. *Curr. Biol.* 12, 467-471
- 77 Burns,K. *et al.* (1998) MyD88, an adapter protein involved in interleukin-1 signaling. *J. Biol. Chem.* 273, 12203-12209
- 78 Wesche,H. *et al.* (1997) MyD88: An adapter that recruits IRAK to the IL-1 receptor complex. *Immunity* 7, 837-847
- 79 Medzhitov,R. *et al.* (1998) MyD88 is an adaptor protein in the hToll/IL-1 receptor family signaling pathways. *Mol. Cell* 2, 253-258
- 80 Davis,C.N. *et al.* (2006) MyD88-dependent and -independent signaling by IL-1 in neurons probed by bifunctional toll/IL-1 receptor domain/BB-loop mimetics. *Proc. Natl. Acad. Sci. U. S. A.* 103, 2953-2958
- 81 Ulrichts,P. *et al.* (2007) MAPPIT analysis of TLR adaptor complexes. *FEBS Lett.* 581, 629-636
- 82 Kawai,T. *et al.* (1999) Unresponsiveness of MyD88-Deficient Mice to Endotoxin. *Immunity* 11, 115-122
- 83 Muraille,E. *et al.* (2003) Genetically Resistant Mice Lacking MyD88-Adapter Protein Display a High Susceptibility to Leishmania major Infection Associated with a Polarized Th2 Response. *J Immunol* 170, 4237-4241
- 84 Takeuchi,O. and Akira,S. (2002) Genetic approaches to the study of Toll-like receptor function. *Microbes and Infection* 4, 887-895
- 85 Häcker,H. *et al.* (2000) Immune cell activation by bacterial CpG-DNA through myeloid differentiation marker 88 and tumor necrosis factor receptor-associated factor TRAF6. *J. Exp. Med.* 192, 595-600
- 86 Schnare,M. *et al.* (2000) Recognition of CpG DNA is mediated by signaling pathways dependent on the adaptor protein MyD88. *Curr Biol* 10, 1139-1142
- 87 Burns,K. *et al.* (2003) Inhibition of Interleukin 1 Receptor/Toll-like Receptor Signaling through the Alternatively Spliced, Short Form of MyD88 Is Due to Its Failure to Recruit IRAK-4. *J. Exp. Med.* 197, 263-268
- 88 Suzuki,N. *et al.* (2002) Severe impairment of interleukin-1 and Toll-like receptor signalling in mice lacking IRAK-4. *Nature (London)* 416, 750-756
- 89 Li,S. *et al.* (2002) IRAK-4: A novel member of the IRAK family with the properties of an IRAK-kinase. *Proceedings of the National Academy of Sciences* 99, 5567-5572
- 90 Cao,Z. *et al.* (1996) TRAF6 is a signal transducer for interleukin-1. *Nature (London)* 383, 443-446

- 91 O'Neill, L.A.J. and Bowie, A.G. (2007) The family of five: TIR-domain-containing adaptors in Toll-like receptor signalling. *Nature Reviews Immunology* 7, 353-364
- 92 Huang, Y.S. *et al.* (2005) Novel role and regulation of the interleukin-1 receptor associated kinase (IRAK) family proteins. *Cell Mol Immunol* 2, 36-39
- 93 Uematsu, S. *et al.* (2005) Interleukin-1 receptor-associated kinase-1 plays an essential role for Toll-like receptor (TLR)7- and TLR9-mediated interferon- α induction. *J exp med* 201, 915-923
- 94 Keating, S.E. *et al.* (2007) IRAK-2 participates in multiple toll-like receptor signaling pathways to NF κ B via activation of TRAF6 ubiquitination. *J Biol Chem* 282, 33435-33443
- 95 Wang, C. *et al.* (2001) TAK1 is a ubiquitin-dependent kinase of MKK and IKK. *Nature* 412, 346-351
- 96 Baud, V. *et al.* (1999) Signaling by proinflammatory cytokines: oligomerization of TRAF2 and TRAF6 is sufficient for JNK and IKK activation and target gene induction via an amino-terminal effector domain. *Genes & Dev* 13, 1297-1308
- 97 Muroi, M. *et al.* (2008) TRAF6 distinctively mediates MyD88- and IRAK-1-induced activation of NF- κ B. *J Leukoc Biol* 83, 702-707
- 98 Chen, Z.J. (2005) Ubiquitin signalling in the NF- κ B pathway. *Nat Cell Biol* 7, 758-765
- 99 Fukushima, T. *et al.* (2007) Ubiquitin-conjugating enzyme Ubc13 is a critical component of TNF receptor-associated factor (TRAF)-mediated inflammatory responses. *Proc Natl Acad Sci* 104, 6371-6376
- 100 Yamamoto, M. *et al.* (2006) Key function for the Ubc13 E2 ubiquitin-conjugating enzyme in immune receptor signaling. *Nat Immunol* 7, 962-970
- 101 Deng, L. *et al.* (2000) Activation of the I κ B Kinase Complex by TRAF6 Requires a Dimeric Ubiquitin-Conjugating Enzyme Complex and a Unique Polyubiquitin Chain. *Cell* 103, 351-361
- 102 Qian, Y. *et al.* (2001) IRAK-mediated Translocation of TRAF6 and TAB2 in the Interleukin-1-induced Activation of NF κ B. *J. Biol. Chem.* 276, 41661-41667
- 103 Jiang, Z. *et al.* (2002) Interleukin-1 (IL-1) Receptor-Associated Kinase-Dependent IL-1-Induced Signaling Complexes Phosphorylate TAK1 and TAB2 at the Plasma Membrane and Activate TAK1 in the Cytosol. *Mol. Cell. Biol.* 22, 7158-7167
- 104 Dinarello, C.A. (2004) Infection, fever, and exogenous and endogenous pyrogens: some concepts have changed. *Journal of Endotoxin Research* 10, 201-222

- 105 Dinarello, C.A. (2000) Proinflammatory cytokines. *Chest* 118, 503-508
- 106 Alam, M.N. *et al.* (2004) Interleukin-1 beta modulates state-dependent discharge activity of preoptic area and basal forebrain neurons: role in sleep regulation. *Eur. J. Neurosci.* 20, 207-216
- 107 Manfredi, A. *et al.* (2003) Interleukin-1 beta enhances non-rapid eye movement sleep when microinjected into the dorsal raphe nucleus and inhibits serotonergic neurons in vitro. *Eur. J. Neurosci.* 18, 1041-1049
- 108 DeSarro, G. *et al.* (1997) Comparative, behavioural and electrocortical effects of tumor necrosis factor-alpha and interleukin-1 microinjected into the locus coeruleus of rat. *Life Sci.* 60, 555-564
- 109 Dunne, A. and O'Neill, L.A.J. (2003) The interleukin-1 receptor/Toll-like receptor superfamily: signal transduction during inflammation and host defense. *Sci Stke* 2003, re3
- 110 O'Neill L.A.J. and Dower, S.K. (2000) IL-1 Receptor Family. *Academic Press Cytokine Reference*, 1565-1585
- 111 Li, X.X. and Qin, J.Z. (2005) Modulation of Toll-interleukin 1 receptor mediated signaling. *Journal of Molecular Medicine-Jmm* 83, 258-266
- 112 Burns, K. *et al.* (2000) Tollip, a new component of the IL-1RI pathway, links IRAK to the IL-1 receptor. *Nature Cell Biology* 2, 346-351
- 113 O'Neill, L. (2000) The Toll/interleukin-1 receptor domain: a molecular switch for inflammation and host defence. *Biochem. Soc. Trans.* 28, 557-563
- 114 Bahi, N. *et al.* (2003) IL1 receptor accessory protein like, a protein involved in X-linked mental retardation, interacts with Neuronal Calcium Sensor-1 and regulates exocytosis. *Hum. Mol. Genet.* 12, 1415-1425
- 115 Fitzgerald, K.A. *et al.* (2001) Mal (MyD88-adaptor-like) is required for Toll-like receptor-4 signal transduction. *Nature* 413, 78-83
- 116 Horng, T. *et al.* (2001) TIRAP: an adapter molecule in the Toll signaling pathway. *Nature Immunology* 2, 835-841
- 117 Dunne, A. *et al.* (2003) Structural complementarity of Toll/interleukin-1 receptor domains in toll-like receptors and the adaptors Mal and MyD88. *J. Biol. Chem.* 278, 41443-41451
- 118 Yamamoto, M. *et al.* (2002) Essential role for TIRAP in activation of the signalling cascade shared by TLR2 and TLR4. *Nature (London)* 420, 324-329

- 119 Dunne, A. *et al.* (2003) Structural complementarity of Toll/interleukin-1 receptor domains in toll-like receptors and the adaptors Mal and MyD88. *J. Biol. Chem.* 278, 41443-41451
- 120 Sheedy F.J. and O'Neill, L.A.J. (2007) The Troll in Toll: Mal and Tram as bridges for TLR2 and TLR4 signalling. *J Leukoc Biol.* 82, 196-203
- 121 Kagan, J.C. and Medzhitov, R. (2006) Phosphoinositide-Mediated Adaptor Recruitment Controls Toll-like Receptor Signaling. *Cell* 125, 943-955
- 122 Miggin Sinead M *et al.* (2006) NF- κ B activation by the Toll-IL-1 receptor domain protein MyD88 adapter-like is regulated by caspase-1. *Proceedings of the National Academy of Sciences* 104, 3372-3377
- 123 Piao, W. *et al.* (2008) Tyrosine phosphorylation of MyD88 adapter-like (Mal) is critical for signal transduction and blocked in endotoxin tolerance. *J. Biol. Chem.* 283, 3109-3119
- 124 Gray, P. *et al.* (2006) MyD88 Adapter-like (Mal) Is Phosphorylated by Bruton's Tyrosine Kinase during TLR2 and TLR4 Signal Transduction. *J. Biol. Chem.* 281, 10489-10495
- 125 Yamamoto, M. *et al.* (2003) Role of adaptor TRIF in the MyD88-independent toll-like receptor signaling pathway. *Science* 301, 640-643
- 126 Oshiumi, H. *et al.* (2003) TIR-containing Adapter Molecule (TICAM)-2, a Bridging Adapter Recruiting to Toll-like Receptor 4 TICAM-1 That Induces Interferon- β . *J. Biol. Chem.* 278, 49751-49762
- 127 Fitzgerald, K.A. *et al.* (2003) LPS-TLR4 signaling to IRF-3/7 and NF- κ B involves the toll adaptors TRAM and TRIF. *J. Exp. Med.* 198, 1043-1055
- 128 Oshiumi, H. *et al.* (2003) TICAM-1, an adaptor molecule that participates in Toll-like receptor 3-mediated interferon- β induction. *Nature Immunology* 4, 161-167
- 129 Meylan, E. *et al.* (2004) RIP1 is an essential mediator of Toll-like receptor 3-induced NF- κ B activation. *Nature Immunology* 5, 503-507
- 130 Kaiser, W.J. and Offermann, M.K. (2005) Apoptosis induced by the toll-like receptor adaptor TRIF is dependent on its receptor interacting protein homotypic interaction motif. *J. Immunol.* 174, 4942-4952
- 131 Funami, K. *et al.* (2008) Homo-oligomerization Is Essential for Toll/Interleukin-1 Receptor Domain-containing Adaptor Molecule-1-mediated NF- κ B and Interferon Regulatory Factor-3 Activation. *J. Biol. Chem.* 283, 18283-18291

- 132 Cusson-Hermance N *et al.* (2005) RIP1 mediates the Trif-dependent Toll-like receptor 3- and 4-induced NF-(kappa)B activation but does not contribute to interferon regulator factor 3 activation. *J. Biol. Chem.* 280, 36560-36566
- 133 Funami,K. *et al.* (2007) Spatiotemporal mobilization of Toll/IL-1 receptor domain-containing adaptor molecule-1 in response to dsRNA. *J. Immunol.* 179, 6867-6872
- 134 Hacker,H. *et al.* (2006) Specificity in Toll-like receptor signalling through distinct effector functions of TRAF3 and TRAF6. *Nature* 439, 204-207
- 135 Sasai,M. *et al.* (2005) Cutting edge: NF-kappa B-activating kinase-associated protein 1 participates in TLR3/Toll-IL-1 homology domain-containing adapter molecule-1-mediated IFN regulatory factor 3 activation. *J. Immunol.* 174, 27-30
- 136 Oganessian,G. *et al.* (2006) Critical role of TRAF3 in the Toll-like receptor-dependent and -independent antiviral response. *Nature (London)* 439, 208-211
- 137 Sato,S. *et al.* (2003) Toll/IL-1 receptor domain-containing adaptor inducing IFN-beta (TRIF) associates with TNF receptor-associated factor 6 and TANK-Binding kinase 1, and activates two distinct transcription factors, NF-kappa B and IFN-regulatory factor-3, in the toll-like receptor signaling. *J. Immunol.* 171, 4304-4310
- 138 Fitzgerald Katherine A *et al.* (2003) IKKepsilon and TBK1 are essential components of the IRF3 signaling pathway. *Nature Immunology* 4, 491-496
- 139 McWhirter,S.M. *et al.* (2004) IFN-regulatory factor 3-dependent gene expression is defective in Tbk1-deficient mouse embryonic fibroblasts. *Proc. Natl. Acad. Sci. U. S. A.* 101, 233-238
- 140 Sharma,S. *et al.* (2003) Triggering the interferon antiviral response through an IKK-related pathway. *Science* 300, 1148-1151
- 141 Servant,M.J. *et al.* (2003) Identification of the minimal phosphoacceptor site required for in vivo activation of interferon regulatory factor 3 in response to virus and double-stranded RNA. *J. Biol. Chem.* 278, 9441-9447
- 142 Mori,M. *et al.* (2004) Identification of Ser-386 of interferon regulatory factor 3 as critical target for inducible phosphorylation that determines activation. *J. Biol. Chem.* 279, 9698-9702
- 143 Jiang,Z.F. *et al.* (2004) Toll-like receptor 3-mediated activation of NF-kappa B and IRF3 diverges at Toll-IL-1 receptor domain-containing adapter inducing INF-beta. *Proc. Natl. Acad. Sci. U. S. A.* 101, 3533-3538
- 144 Gohda,J. *et al.* (2004) Cutting edge: TNFR-associated factor (TRAF) 6 is essential for MyD88-dependent pathway but not toll/IL-1 receptor domain-containing adaptor-inducing IFN-beta (TRIF)-dependent pathway in TLR signaling. *J. Immunol.* 173, 2913-2917

- 145 Tojima, Y. *et al.* (2000) NAK is an I kappa B kinase-activating kinase. *Nature* 404, 778-782
- 146 Bonnard, M. *et al.* (2000) Deficiency of T2K leads to apoptotic liver degeneration and impaired NF-kappa B-dependent gene transcription. *EMBO J.* 19, 4976-4985
- 147 Cheong, R. *et al.* (2008) Understanding NF-kappaB signaling via mathematical modeling. *MSB* 4, 192
- 148 Gais, P. *et al.* (2010) TRIF Signaling Stimulates Translation of TNF- α mRNA via Prolonged Activation of MK2. *J Immunol* 184, 5842-5848
- 149 Shen, H. *et al.* (2008) Dual signaling of MyD88 and TRIF is critical for maximal TLR4-induced dendritic cell maturation. *J. Immunol.* 181, 1849-1858
- 150 Yamamoto, M. *et al.* (2002) Cutting Edge: A Novel Toll/IL-1 Receptor Domain-Containing Adapter That Preferentially Activates the IFN- β Promoter in the Toll-Like Receptor Signaling. *J Immunol* 169, 6668-6672
- 151 Mink M *et al.* (2001) A novel human gene (SARM) at chromosome 17q11 encodes a protein with a SAM motif and structural similarity to Armadillo/b-catenin that is conserved in mouse, *Drosophila*, and *Caenorhabditis elegans*. *Genomics* 74, 234-244
- 152 Liberati Nicole T *et al.* (2004) Requirement for a conserved Toll/interleukin-1 resistance domain protein in the *Caenorhabditis elegans* immune response. *Proc. Natl. Acad. Sci. U. S. A.* 101, 6593-6598
- 153 Carty, M. *et al.* (2006) The human adaptor SARM negatively regulates adaptor protein TRIF-dependent Toll-like receptor signaling. *Nature Immunology* 7, 1074-1081
- 154 Kim, Y. *et al.* (2007) MyD88-5 links mitochondria, microtubules and JNK3 in neurons and regulates neuronal survival. *J. Exp. Med.* 204, 2063-2074
- 155 Yamamoto, M. *et al.* (2003) TRAM is specifically involved in the Toll-like receptor 4-mediated MyD88-independent signaling pathway. *Nature Immunology* 4, 1144-1150
- 156 Rowe, D.C. *et al.* (2006) The myristoylation of TRIF-related adaptor molecule is essential for Toll-like receptor 4 signal transduction 103, 6299-6304
- 157 McGettrick, A.F. *et al.* (2006) Trif-related adapter molecule is phosphorylated by PKC ϵ during Toll-like receptor 4 signaling. *Proceedings of the National Academy of Sciences* 103, 9196-9201
- 158 O'Neill, L.A.J. *et al.* (2003) The Toll-IL-1 receptor adaptor family grows to five members. *Trends Immunol* 24, 286-290
- 159 Croston, G.E. *et al.* (1995) Nf-Kappa-B Activation by Interleukin-1 (IL-1) Requires An Il-1 Receptor-Associated Protein-Kinase Activity. *J. Biol. Chem.* 270, 16514-16517

- 160 Slack, J.L. *et al.* (2000) Identification of Two Major Sites in the Type I Interleukin-1 Receptor Cytoplasmic Region Responsible for Coupling to Pro-inflammatory Signaling Pathways. *J. Biol. Chem.* 275, 4670-4678
- 161 Kuno, K. *et al.* (1993) Structure and Function of the Intracellular Portion of the Mouse Interleukin-1 Receptor (Type-I) - Determining the Essential Region for Transducing Signals to Activate the Interleukin-8 Gene. *J. Biol. Chem.* 268, 13510-13518
- 162 Xu, Y.W. *et al.* (2000) Structural basis for signal transduction by the Toll/interleukin-1 receptor domains. *Nature* 408, 111-115
- 163 Khan, J.A. *et al.* (2004) Crystal structure of the Toll/interleukin-1 receptor domain of human IL-1RAPL. *J. Biol. Chem.* 279, 31664-31670
- 164 Tao, X. and Tong, L. (2009) Expression, Purification, and Crystallization of Toll/Interleukin-1 Receptor (TIR) Domains. *Toll-Like Receptors: Methods and Protocols*, 81-88
- 165 Larkin, M.A. *et al.* (2007) Clustal W and Clustal X version 2.0. *Bioinformatics* 23, 2947-2948
- 166 Ginalski, K. *et al.* (2003) 3D-Jury: a simple approach to improve protein structure predictions. *Bioinformatics* 19, 1015-1018
- 167 Nyman, T. *et al.* (2008) The Crystal Structure of the Human Toll-like Receptor 10 Cytoplasmic Domain Reveals a Putative Signaling Dimer. *J. Biol. Chem.* 283, 11861-11865
- 168 Chan, S.L. *et al.* (2009) Molecular mimicry in innate immunity: Crystal structure of a bacterial TIR domain. *J. Biol. Chem.*, C109
- 169 Ohnishi, H. *et al.* (2009) Structural basis for the multiple interactions of the MyD88 TIR domain in TLR4 signaling. *Proc. Natl. Acad. Sci. U. S. A.* 106, 10260-10265
- 170 Tao, X. *et al.* (2002) An extensively associated dimer in the structure of the C713S mutant of the TIR domain of human TLR2. *Biochem. Biophys. Res. Commun.* 299, 216-221
- 171 Farhat, K. *et al.* (2008) Heterodimerization of TLR2 with TLR1 or TLR6 expands the ligand spectrum but does not lead to differential signaling. *J. Leukoc. Biol.* 83, 692-701
- 172 Nunez Miguel, R. *et al.* (2007) A dimer of the Toll-like receptor 4 cytoplasmic domain provides a specific scaffold for the recruitment of signalling adaptor proteins. *PLoS ONE* 2, e788
- 173 Radons, J.R. *et al.* (2003) The interleukin 1 (IL-1) receptor accessory protein Toll/IL-1 receptor domain - Analysis of putative interaction sites by in vitro mutagenesis and molecular modeling. *J. Biol. Chem.* 278, 49145-49153

- 174 Kubarenko, A. *et al.* (2007) Structure-function relationships of Toll-like receptor domains through homology modelling and molecular dynamics. *Biochem. Soc. Trans.* 35, 1515-1518
- 175 Standley, D.M. *et al.* (2008) Structure-based functional annotation of protein sequences guided by comparative models. *Optimization and Systems Biology, Proceedings* 9, 395-403
- 176 Gautam, J.K. *et al.* (2006) Structural and Functional Evidence for the Role of the TLR2 DD Loop in TLR1/TLR2 Heterodimerization and Signaling. *J. Biol. Chem.* 281, 30132-30142
- 177 Jiang, Z. *et al.* (2006) Details of Toll-like receptor:adapter interaction revealed by germ-line mutagenesis. *Proceedings of the National Academy of Sciences* 103, 10961-10966
- 178 Toshchakov, V.U. *et al.* (2005) Differential involvement of BB loops of Toll-IL-1 resistance (TIR) domain-containing adapter proteins in TLR4-versus TLR2-mediated signal transduction. *J. Immunol.* 175, 494-500
- 179 Toshchakov, V. *et al.* (2005) Cell-permeable peptides containing sequences derived from BB-loops of TIR-domain containing adapter proteins inhibit TLR4, but not TLR2 signaling. *FASEB J.* 19, A956
- 180 Toshchakov, V.Y. *et al.* (2007) Cutting edge: Differential inhibition of TLR signaling pathways by cell-permeable peptides representing BB loops of TLRs. *J. Immunol.* 178, 2655-2660
- 181 Toshchakov, V.Y. and Vogel, S.N. (2007) Cell-penetrating TIR BB loop decoy peptides: a novel class of TLR signaling inhibitors and a tool to study topology of TIR-TIR interactions. *Expert Opinion on Biological Therapy* 7, 1035-1049
- 182 Bartfai, T. *et al.* (2003) A low molecular weight mimic of the Toll/IL-1 receptor/resistance domain inhibits IL-1 receptor-mediated responses. *Proc. Natl. Acad. Sci. U. S. A.* 100, 7971-7976
- 183 Loiarro, M. *et al.* (2007) Pivotal Advance: Inhibition of MyD88 dimerization and recruitment of IRAK1 and IRAK4 by a novel peptidomimetic compound. *J. Leukoc. Biol.* 82, 801-810
- 184 Loiarro, M. *et al.* (2005) Peptide-mediated interference of TIR domain dimerization in MyD88 inhibits interleukin-1-dependent activation of NF-kappa B. *J. Biol. Chem.* 280, 15809-15814
- 185 Fanto, N. *et al.* (2008) Design, synthesis, and in vitro activity of peptidomimetic inhibitors of myeloid differentiation factor 88. *J. Med. Chem.* 51, 1189-1202

- 186 Ronni, T. *et al.* (2003) Common interaction surfaces of the toll-like receptor 4 cytoplasmic domain stimulate multiple nuclear targets. *Mol. Cell. Biol.* 23, 2543-2555
- 187 Rhee, S.H. and Hwang, D. (2000) Murine Toll-like Receptor 4 Confers Lipopolysaccharide Responsiveness as Determined by Activation of NF κ B and Expression of the Inducible Cyclooxygenase. *J. Biol. Chem.* 275, 34035-34040
- 188 Hasan, U.A. *et al.* (2004) Differential induction of gene promoter constructs by constitutively active human TLRs. *Biochem. Biophys. Res. Commun.* 321, 124-131
- 189 Laird, M.H.W. *et al.* (2009) TLR4/MyD88/PI3K interactions regulate TLR4 signaling. *J. Leukoc. Biol.*, jlb
- 190 Brown, V. *et al.* (2006) Binding specificity of Toll-like receptor cytoplasmic domains. *Eur. J. Immunol.* 36, 742-753
- 191 Hertz CJ *et al.* (2003) Activation of toll-like receptor2 on human tracheobronchial epithelial cells induces the antimicrobial peptide human beta defensin-2. *J. Immunol.* 171, 6820-6826
- 192 Blander, J.M. and Medzhitov, R. (2004) Regulation of phagosome maturation by signals from Toll-like receptors. *Science* 304, 1014-1018
- 193 Gebbia JA *et al.* (2004) Selective induction of matrix metalloproteinases by *Borrelia burgdorferi* via toll-like receptor 2. *Journal of Infectious Disease* 189, 113-119
- 194 Flo TH *et al.* (2004) Lipocalin 2 mediates an innate immune response to bacterial infection by sequestering iron. *Nature* 432, 917-921
- 195 West MA *et al.* (2004) Enhanced dendritic cell antigen capture via toll-like receptor-induced actin remodelling. *Science* 305, 1153-1157
- 196 Aliprantis AO *et al.* (1999) Cell activation and apoptosis by bacterial lipoproteins through toll-like receptor 2. *Science* 285, 736-739
- 197 Hsu Li-Chung *et al.* (2004) The protein kinase PKR is required for macrophage apoptosis after activation of toll-like receptor 4. *Nature* 428, 341-345
- 198 Pinhal-Enfield, G. *et al.* (2003) An angiogenic switch in macrophages involving synergy between toll-like receptors 2, 4, 7, and 9 and adenosine A(2A) receptors. *Am. J. Pathol.* 163, 711-721
- 199 Iwasaki, A. and Medzhitov, R. (2004) Toll-like receptor control of the adaptive immune responses. *Nature Immunology* 5, 987-995
- 200 Ghosh, S. *et al.* (1998) NF-kappa B and rel proteins: Evolutionarily conserved mediators of immune responses. *Annu. Rev. Immunol.* 16, 225-260

- 201 Caamano, J. and Hunter, C.A. (2002) NF-kappa B family of transcription factors: Central regulators of innate and adaptive immune functions. *Clin. Microbiol. Rev.* 15, 414-429
- 202 Sha, W.C. *et al.* (1995) Targeted disruption of the p50 subunit of NF-kappa B leads to multifocal defects in immune responses. *Cell* 80, 321-330
- 203 Franzoso, G. *et al.* (1998) Mice deficient in nuclear factor (NF)-kappa B/p52 present with defects in humoral responses, germinal center reactions, and splenic microarchitecture. *J exp med* 187, 147-159
- 204 Hoffmann, A. *et al.* (2006) Transcriptional regulation via the NF-kappaB signaling module. *Oncogenes* 25, 6706-6716
- 205 Leung, T.H. *et al.* (2004) One nucleotide in a kappaB site can determine cofactor specificity for NF-kappaB dimers. *Cell* 118, 453-464
- 206 Yamazaki, S. *et al.* (2005) Stimulus-specific induction of a novel nuclear factor-kappaB regulator, IkappaB-zeta, via Toll/Interleukin-1 receptor is mediated by mRNA stabilization. *J Biol Chem* 280, 1678-1687
- 207 Yamazaki, S. *et al.* (2001) A novel IkappaB protein, IkappaB-zeta, induced by proinflammatory stimuli, negatively regulates nuclear factor-kappaB in the nuclei. *J Biol Chem* 276, 27657-27662
- 208 Karin, M. *et al.* (1997) AP-1 function and regulation. *curr opin cell biol* 9, 240-246
- 209 Karin, M. (1995) The regulation of AP-1 activity by mitogen-activated protein kinases. *J Biol Chem* 270, 16483-16486
- 210 Hess, J. *et al.* (2004) AP-1 subunits: quarrel and harmony among siblings. *J cell sci* 117, 5965-5973
- 211 Taniguchi, T. *et al.* (2001) IRF family of transcription factors as regulators of host defense. *annu rev immunol* 19, 623-655
- 212 Negishi, H. *et al.* (2006) Evidence for licensing of IFN-gamma-induced IFN regulatory factor 1 transcription factor by MyD88 in Toll-like receptor-dependent gene induction program. *Proceedings of the National Academy of Sciences* 103, 15136-15141
- 213 Takaoka A *et al.* (2005) Integral role of IRF-5 in the gene induction programme activated by Toll-like receptors. *Nature* 434, 243-249
- 214 Lin, R. *et al.* (2005) A CRM1-dependent nuclear export pathway is involved in the regulation of IRF-5 subcellular localization. *J Biol Chem* 280, 3088-3095

- 215 Kawai Taro *et al.* (2004) Interferon-alpha induction through Toll-like receptors involves a direct interaction of IRF7 with MyD88 and TRAF6. *Nature Immunology* 5, 1061-1068
- 216 Honda, K. *et al.* (2005) IRF-7 is the master regulator of type-I interferon-dependent immune responses. *Nature (London)* 434, 772-777
- 217 Kim, T.K. *et al.* (2000) Chemotherapeutic DNA-damaging drugs activate interferon regulatory factor-7 by the mitogen-activated protein kinase kinase-4-cJun NH2-terminal kinase pathway. *Cancer Res* 60, 1153-1156
- 218 Tsujimura, H. *et al.* (2004) Toll-like receptor 9 signaling activates NF-kappaB through IFN regulatory factor-8/IFN consensus sequence binding protein in dendritic cells. *J Immunol* 172, 6820-6827
- 219 Basak, S. and Hoffmann, A. (2006) Crosstalk via the NF-[kappa]B signaling system. *Cytokine & Growth Factor Reviews* 19, 187-197
- 220 Laudanna, C. *et al.* (2002) Rapid leukocyte integrin activation by chemokines. *Immunol. Rev.* 186, 37-46
- 221 Hessle, C. *et al.* (2000) Gram-Positive Bacteria Are Potent Inducers of Monocytic Interleukin-12 (IL-12) while Gram-Negative Bacteria Preferentially Stimulate IL-10 Production. *Infect. Immun.* 68, 3581-3586
- 222 Jiang, Y. *et al.* (1999) Bacterium-Dependent Induction of Cytokines in Mononuclear Cells and Their Pathologic Consequences In Vivo. *Infect. Immun.* 67, 2125-2130
- 223 Ghosh, T.K. *et al.* (2006) Toll-like receptor (TLR) 2-9 agonists-induced cytokines and chemokines: I. Comparison with T cell receptor-induced responses. *Cell. Immunol.* 243, 48-57
- 224 Der, S.D. *et al.* (1998) Identification of genes differentially regulated by interferon alpha, beta, or gamma using oligonucleotide arrays. *Proc. Natl. Acad. Sci. U. S. A.* 95, 15623-15628
- 225 de Veer, M.J. *et al.* (2001) Functional classification of interferon-stimulated genes identified using microarrays. *J. Leukoc. Biol.* 69, 912-920
- 226 Schaefer, T.M. *et al.* (2004) Toll-like receptor (TLR) expression and TLR-mediated cytokine/chemokine production by human uterine epithelial cells. *IMMUNOL* 112, 428-436
- 227 Heinrich, P.C. *et al.* (2003) Principles of interleukin (IL)-6-type cytokine signalling and its regulation. *Biochem. J.* 374, 1-20
- 228 Liu, Z.G. (2005) Molecular mechanism of TNF signaling and beyond. *Cell Res* 15, 24-27

- 229 Banchereau, J. *et al.* (1998) Dendritic cells and the control of immunity. *Nature (London)* 392, 245-252
- 230 Hertz, C.J. *et al.* (2001) Microbial Lipopeptides Stimulate Dendritic Cell Maturation Via Toll-Like Receptor 2. *J Immunol* 166, 2444-2450
- 231 Hemmi, H. *et al.* (2000) A Toll-like receptor recognizes bacterial DNA. *Nature (London)* 408, 740-745
- 232 Tsuji, S. *et al.* (2000) Maturation of human dendritic cells by cell wall skeleton of *Mycobacterium bovis* bacillus Calmette-Guérin: involvement of toll-like receptors. *Infect Immun* 68, 6883-6890
- 233 Michelsen, K.S. *et al.* (2001) The role of toll-like receptors (TLRs) in bacteria-induced maturation of murine dendritic cells (DCS). Peptidoglycan and lipoteichoic acid are inducers of DC maturation and require TLR2. *J Biol Chem* 276, 25680-25686
- 234 Kaisho, T. *et al.* (2001) Endotoxin-induced maturation of MyD88-deficient dendritic cells. *J Immunol* 166, 5688-5694
- 235 Akira Shizuo *et al.* (2007) Toll-like receptors: critical proteins linking innate and acquired immunity. *Nature Immunology* 2, 675-680
- 236 Reis e Sousa (2004) Toll-like receptors and dendritic cells: for whom the bug tolls. *Sem Immunol* 16, 27-34
- 237 Sallusto, F. *et al.* (2000) Understanding dendritic cell and T-lymphocyte traffic through the analysis of chemokine receptor expression. *Immunol Rev* 177, 134-140
- 238 Dieu, M.C. *et al.* (1998) Selective recruitment of immature and mature dendritic cells by distinct chemokines expressed in different anatomic sites. *J exp med* 188, 373-386
- 239 Gunn, M.D. (2003) Chemokine mediated control of dendritic cell migration and function. *Sem Immunol* 15, 271-276
- 240 Hemmi, H. *et al.* (2003) The roles of Toll-like receptor 9, MyD88, and DNA-dependent protein kinase catalytic subunit in the effects of two distinct CpG DNAs on dendritic cell subsets. *J Immunol* 170, 3059-3064
- 241 Ogata, H. *et al.* (2000) The toll-like receptor protein RP105 regulates lipopolysaccharide signaling in B cells. *J exp med* 192, 23-29
- 242 Gerondakis, S. *et al.* (2007) Regulating B-cell activation and survival in response to TLR signals. *Immunol Cell Biol* 85, 471-475
- 243 Banerjee, A. and Gerondakis, S. (2007) Coordinating TLR-activated signaling pathways in cells of the immune system. *Immunol Cell Biol* 85, 420-424

- 244 Hsia,C.Y. *et al.* (2002) c-Rel regulation of the cell cycle in primary mouse B lymphocytes. *Int Immunol* 14, 905-916
- 245 Gerondakis,S. *et al.* (2003) The role of Rel/NF-kappaB transcription factors in B lymphocyte survival. *Sem Immunol* 15, 159-166
- 246 Grumont,R.J. *et al.* (1998) B lymphocytes differentially use the Rel and nuclear factor kappaB1 (NF-kappaB1) transcription factors to regulate cell cycle progression and apoptosis in quiescent and mitogen-activated cells. *J Exp Med* 187, 663-674
- 247 Grumont,R.J. *et al.* (1999) Rel-dependent induction of A1 transcription is required to protect B cells from antigen receptor ligation-induced apoptosis. *Genes & Dev* 13, 400-411
- 248 Cheng,S. *et al.* (2003) Cyclin E and Bcl-xL cooperatively induce cell cycle progression in c-Rel-/- B cells. *Oncogenes* 22, 8472-8486
- 249 Pulendran,B. *et al.* (2001) Sensing Pathogens and Tuning Immune Responses. *Science* 293, 253-256
- 250 Wagner,H. (2001) Toll meets bacterial CpG-DNA. *Immunity* 14, 499-502
- 251 Wagner,H. (1999) Bacterial CpG DNA activates immune cells to signal infectious danger. *Adv. Immunol.* 73, 329-368
- 252 Redecke,V. *et al.* (2004) Cutting edge: activation of Toll-like receptor 2 induces a Th2 immune response and promotes experimental asthma. *J Immunol* 172, 2739-2743
- 253 Agrawal,S. *et al.* (2003) Cutting edge: different Toll-like receptor agonists instruct dendritic cells to induce distinct Th responses via differential modulation of extracellular signal-regulated kinase-mitogen-activated protein kinase and c-Fos. *J Immunol* 171, 4984-4989
- 254 Yam,K.K. *et al.* (2008) Innate inflammatory responses to the Gram-positive bacterium *Lactococcus lactis*. *Vaccine* 26, 2689-2699
- 255 Thoma-Uszynski,S. *et al.* (2000) Activation of Toll-Like Receptor 2 on Human Dendritic Cells Triggers Induction of IL-12, But Not IL-10. *J Immunol* 165, 3804-3810
- 256 Pulendran,B. *et al.* (2001) Lipopolysaccharides from Distinct Pathogens Induce Different Classes of Immune Responses In Vivo. *J Immunol* 167, 5067-5076
- 257 Schnare,M. *et al.* (2001) Toll-like receptors control activation of adaptive immune responses. *Nat Immunol* 2, 947-950
- 258 Bjorkbacka,H. *et al.* (2004) The induction of macrophage gene expression by LPS predominantly utilizes Myd88-dindependent signaling cascades. *Physiological Genomics* 19, 319-330

- 259 Schnare M *et al.* (2001) Toll-like receptors control activation of adaptive immune responses. *Nature Immunology* 2, 947-950
- 260 Didierlaurent A *et al.* (2004) Flagellin promotes myeloid differentiation factor 88-dependent development of the Th-2-type response. *J. Immunol.* 172, 6922-6930
- 261 Fremont, C.M. *et al.* (2004) Fatal Mycobacterium tuberculosis infection despite adaptive immune response in the absence of MyD88. *J Clin Invest* 114, 1790-1799
- 262 Kaisho, T. *et al.* (2002) Endotoxin can induce MyD88-deficient dendritic cells to support T(h)2 cell differentiation. *Int Immunol* 14, 695-700
- 263 Jankovic, D. *et al.* (2002) In the absence of IL-12, CD4(+) T cell responses to intracellular pathogens fail to default to a Th2 pattern and are host protective in an IL-10(-/-) setting. *Immunity* 16, 429-439
- 264 Fujimoto, C. *et al.* (2004) Polyriboinosinic polyribocytidylic acid [poly(I:C)]/TLR3 signaling allows class I processing of exogenous protein and induction of HIV-specific CD8+ cytotoxic T lymphocytes. *Int. Immunol.* 16, 55-63
- 265 Schulz, O. *et al.* (2005) Toll-like receptor 3 promotes cross-priming to virus-infected cells. *Nature* 433, 887-892
- 266 Caramalho I *et al.* (2007) Regulatory T cells selectively express toll-like receptors and are activated by lipopolysaccharide. *J. Exp. Med.* 197, 403-411
- 267 Yang Y *et al.* (2004) Persistent toll-like receptor signals are required for reversal of regulatory T cell-mediated CD8 tolerance. *Nature Immunology* 5, 515
- 268 Le Bon A *et al.* (2003) Cross-priming of CD8+ T cells stimulated by virus induced type I interferons. *Nature Immunology* 4, 1009-1015
- 269 Pasare C and Medzhitov, R. (2003) Toll pathway-dependent blockade of CD4+CD25+ T cell mediated suppression by dendritic cells. *Science* 299, 1033-1036
- 270 Tzou, P. *et al.* (2002) Constitutive expression of a single antimicrobial peptide can restore wild-type resistance to infection in immunodeficient Drosophila mutants. *Proc Natl Acad Sci* 99, 2152-2157
- 271 Birchler, T. *et al.* (2001) Human Toll-like receptor 2 mediates induction of the antimicrobial peptide human beta-defensin 2 in response to bacterial lipoprotein. *Eur J Immunol* 31, 3131-3137
- 272 Ganz, T. (2003) Defensins: antimicrobial peptides of innate immunity. *Nat Rev Immunol* 3, 710-720
- 273 Kougias, P. *et al.* (2005) Defensins and cathelicidins: neutrophil peptides with roles in inflammation, hyperlipidemia and atherosclerosis. *J Cell Mol Med* 9, 3-10

- 274 Chertov, O. *et al.* (1996) Identification of defensin-1, defensin-2, and CAP37/azurocidin as T-cell chemoattractant proteins released from interleukin-8-stimulated neutrophils. *J Biol Chem* 271, 2935-2940
- 275 Bals, R. (2000) Epithelial antimicrobial peptides in host defense against infection. *Respir Res* 1, 141-150
- 276 Dürr, U.H. *et al.* (2006) LL-37, the only human member of the cathelicidin family of antimicrobial peptides. *Biochem Biophys Acta* 1758, 1408-1425
- 277 Yuk, J.M. *et al.* (2009) Vitamin D3 Induces Autophagy in Human Monocytes/Macrophages via Cathelicidin. *Cell Host & Microbe* 6, 231-243
- 278 Bogdan, C. *et al.* (2000) Reactive oxygen and reactive nitrogen intermediates in innate and specific immunity. *Curr. Opin. Immunol.* 12, 64-76
- 279 Thoma-Uszynski, S. *et al.* (2001) Induction of direct antimicrobial activity through mammalian toll-like receptors. *Sci* 291, 1544-1547
- 280 Martins, P. *et al.* (2008) Expression of cell surface receptors and oxidative metabolism modulation in the clinical continuum of sepsis. *Critical Care* 12, R25
- 281 Flint, D.H. *et al.* (1993) The Inactivation of Dihydroxy-Acid Dehydratase in *Escherichia-Coli* Treated with Hyperbaric-Oxygen Occurs Because of the Destruction of Its Fe-S Cluster, But the Enzyme Remains in the Cell in A Form That Can be Reactivated. *J. Biol. Chem.* 268, 25547-25552
- 282 Gardner, P.R. and Fridovich, I. (1991) Superoxide Sensitivity of the *Escherichia-Coli* 6-Phosphogluconate Dehydratase. *J. Biol. Chem.* 266, 1478-1483
- 283 Gardner, P.R. and Fridovich, I. (1991) Superoxide Sensitivity of the *Escherichia-Coli* Aconitase. *J. Biol. Chem.* 266, 19328-19333
- 284 Miller, R.A. and Britigan, B.E. (1997) Role of oxidants in microbial pathophysiology. *Clin. Microbiol. Rev.* 10, 1-&
- 285 Wink, D.A. and Mitchell, J.B. (1998) Chemical biology of nitric oxide: Insights into regulatory, cytotoxic, and cytoprotective mechanisms of nitric oxide. *Free Radic. Biol. Med.* 25, 434-456
- 286 Kroemer, G. and Levine, B. (2008) Autophagic cell death: the story of a misnomer. *Nat Rev Mol Cell Biol* 9, 1004-1010
- 287 Bortoluci, K. and Medzhitov, R. (2010) Control of infection by pyroptosis and autophagy: role of TLR and NLR. *Cell. Mol. Life Sci.* 67, 1643-1651
- 288 Haase, R. *et al.* (2003) A dominant role of toll-like receptor 4 in the signaling of apoptosis in bacteria-faced macrophages. *J. Immunol.* 171, 4294-4303

- 289 Salaun, B. *et al.* (2007) Toll-like receptors' two-edged sword: when immunity meets apoptosis. *Eur. J. Immunol.* 37, 3311-3318
- 290 Monack, D.M. *et al.* (1997) Yersinia signals macrophages to undergo apoptosis and YopJ is necessary for this cell death. *Proc. Natl. Acad. Sci. U. S. A.* 94, 10385-10390
- 291 Bergsbaken, T. and Cookson, B.T. (2007) Macrophage Activation Redirects *Yersinia*-Infected Host Cell Death from Apoptosis to Caspase-1-Dependent Pyroptosis. *PLoS Pathog* 3, e161
- 292 Shi, C.S. and Kehrl, J.H. (2008) MyD88 and Trif Target Beclin 1 to Trigger Autophagy in Macrophages. *J. Biol. Chem.* 283, 33175-33182
- 293 Sanjuan, M.A. *et al.* (2007) Toll-like receptor signalling in macrophages links the autophagy pathway to phagocytosis. *Nature* 450, 1253-1257
- 294 Lam, E. (2004) Controlled cell death, plant survival and development. *Nat Rev Mol Cell Biol* 5, 305-315
- 295 Karin, M. *et al.* (2002) NF-kappaB at the crossroads of life and death. *Nat Immunol* 3, 221-227
- 296 Liu, H. *et al.* (2002) NF-kappaB inhibition sensitizes hepatocytes to TNF-induced apoptosis through a sustained activation of JNK and c-Jun. *Hepatology* 35, 772-778
- 297 Ruckdeschel, K. *et al.* (2001) Yersinia outer protein P of *Yersinia enterocolitica* simultaneously blocks the nuclear factor-kappa B pathway and exploits lipopolysaccharide signaling to trigger apoptosis in macrophages. *J. Immunol.* 166, 1823-1831
- 298 Zhang, Y. *et al.* (2005) Inhibition of MAPK and NF-kappa B pathways is necessary for rapid apoptosis in macrophages infected with *Yersinia*. *J. Immunol.* 174, 7939-7949
- 299 Kitamura, M. (1999) NF-kappaB-mediated self defense of macrophages faced with bacteria. *Eur J Immunol* 29, 1647-1655
- 300 Aliprantis, A.O. *et al.* (2000) The apoptotic signaling pathway activated by Toll-like receptor 2. *The EMBO Journal* 19, 3325-3326
- 301 Molloy, A. *et al.* (1994) Apoptosis, but not necrosis, of infected monocytes is coupled with killing of intracellular bacillus Calmette-Guérin. *The Journal of Experimental Medicine* 180, 1499-1509
- 302 Aliprantis, A.O. *et al.* (2001) Toll-like receptor-2 transduces signals for NF-kappa B activation, apoptosis and reactive oxygen species production. *J Endotoxin Res* 7, 287-291
- 303 Lopez, M. *et al.* (2003) The 19-kDa Mycobacterium tuberculosis protein induces macrophage apoptosis through Toll-like receptor-2. *J Immunol* 170, 2409-2416

- 304 Ruckdeschel Klaus *et al.* (2007) Signaling of apoptosis through TLRs critically involves Toll/Il-1 receptor domain-containing adapter inducing IFN- β , but not MyD88, in bacteria-infected murine macrophages. *J Immunol* 173, 3320-3328
- 305 Blander,J.M. and Medzhitov,R. (2007) Toll-like receptors and phagosome maturation - Reply. *Nature Immunology* 8, 217-218
- 306 Blander,J.M. (2008) Phagocytosis and antigen presentation: a partnership initiated by Toll-like receptors. *Ann. Rheum. Dis.* 67, 44-49
- 307 Ribes,S. *et al.* (2010) Toll-Like Receptor Stimulation Enhances Phagocytosis and Intracellular Killing of Nonencapsulated and Encapsulated *Streptococcus pneumoniae* by Murine Microglia. *Infect. Immun.* 78, 865-871
- 308 Shen,Y. *et al.* (2010) Toll-Like Receptor 2- and MyD88-Dependent Phosphatidylinositol 3-Kinase and Rac1 Activation Facilitates the Phagocytosis of *Listeria monocytogenes* by Murine Macrophages. *Infect. Immun.* 78, 2857-2867
- 309 Celli,J. *et al.* (2003) *Brucella* evades macrophage killing via VirB-dependent sustained interactions with the endoplasmic reticulum. *J. Exp. Med.* 198, 545-556
- 310 Roy Craig R and Mocarski Edward S (2007) Pathogen subversion of cell-intrinsic innate immunity. *Nature Immunology* 8, 1179-1187
- 311 Raetz,C.R.H. and Whitfield,C. (2002) Lipopolysaccharide endotoxins. *Annu. Rev. Biochem.* 71, 635-700
- 312 Shimazu,R. *et al.* (1999) MD-2, a molecule that confers lipopolysaccharide responsiveness on Toll-like receptor 4. *J. Exp. Med.* 189, 1777-1782
- 313 Wright,S.D. *et al.* (1990) Cd14, A Receptor for Complexes of Lipopolysaccharide (Lps) and Lps Binding-Protein. *Science* 249, 1431-1433
- 314 Miller,S.I. *et al.* (2005) LPS, TLR4 and infectious disease diversity. *Nature Reviews Microbiology* 3, 36-46
- 315 Schromm,A.B. *et al.* (1998) The charge of endotoxin molecules influences their conformation and IL-6-inducing capacity. *J. Immunol.* 161, 5464-5471
- 316 Girard,R. *et al.* (2003) Lipopolysaccharides from *Legionella* and *Rhizobium* stimulate mouse bone marrow granulocytes via Toll-like receptor 2. *J. Cell Sci.* 116, 293-302
- 317 Schromm,A.B. *et al.* (2000) Biological activities of lipopolysaccharides are determined by the shape of their lipid A portion. *Eur. J. Biochem.* 267, 2008-2013
- 318 Moran AP *et al.* (1997) Structural characterization of the lipid A component of *Helicobacter pylori* rough- and smooth-form lipopolysaccharides. *J. Bacteriol.* 179, 6453-6463

- 319 Ernst RK *et al.* (1999) How intracellular bacteria survive: surface modifications that promote resistance to host innate immune responses. *Journal of Infectious Disease* 179, S326-S330
- 320 Kawasaki,K. *et al.* (2004) Deacylation and palmitoylation of lipid A by Salmonellae outer membrane enzymes modulate host signaling through Toll-like receptor 4. *J Endotoxin Res* 10, 439-444
- 321 Kawasaki,K. *et al.* (2004) 3-O-deacylation of lipid A by PagL, a PhoP/PhoQ-regulated deacylase of Salmonella typhimurium, modulates signaling through Toll-like receptor 4. *J Biol Chem* 279, 20044-20048
- 322 Hayashi F (2001) The innate immune response to flagellin is mediated by Toll-like receptor 5. *Nature* 410, 1099-1103
- 323 Smith,K.D. *et al.* (2003) Toll-like receptor 5 recognizes a conserved site on flagellin required for protofilament formation and bacterial motility. *Nature Immunology* 4, 1247-1253
- 324 Andersen-Nissen E (2005) Evasion of Toll-like receptor 5 by flagellated bacteria. *Proceedings of the National Academy of Sciences* 102, 9247-9252
- 325 Wong,C.E. *et al.* (2009) Salmonella exploits Toll-like receptor signaling during the host-pathogen interaction. *Infect. Immun.*, IAI
- 326 Sing,A. *et al.* (2002) Yersinia V-antigen exploits toll-like receptor 2 and CD14 for interleukin 10-mediated immunosuppression. *J. Exp. Med.* 196, 1017-1024
- 327 Giacomini,E. *et al.* (2001) Infection of Human Macrophages and Dendritic Cells with Mycobacterium tuberculosis Induces a Differential Cytokine Gene Expression That Modulates T Cell Response. *J Immunol* 166, 7033-7041
- 328 Higgins,S.C. *et al.* (2003) Toll-Like Receptor 4-Mediated Innate IL-10 Activates Antigen-Specific Regulatory T Cells and Confers Resistance to Bordetella pertussis by Inhibiting Inflammatory Pathology. *J Immunol* 171, 3119-3127
- 329 Kayal,S. *et al.* (1999) Listeriolysin O-dependent activation of endothelial cells during infection with Listeria monocytogenes: activation of NF-kappa B and upregulation of adhesion molecules and chemokines. *Mol. Microbiol.* 31, 1709-1722
- 330 Kayal,S. *et al.* (2002) Listeriolysin O secreted by Listeria monocytogenes induces NF-kappa B signalling by activating the I kappa B kinase complex. *Mol. Microbiol.* 44, 1407-1419
- 331 Graham Stephen C *et al.* (2008) Vaccinia Virus Proteins A52 and B14 Share a Bcl-2-Like Fold but Have Evolved to Inhibit NF-kB rather than Apoptosis. *PLoS Pathog* 4, e1000128

- 332 Maloney,G. *et al.* (2005) Vaccinia virus protein A52R activates p38 mitogen-activated protein kinase and potentiates lipopolysaccharide-induced interleukin-10. *J. Biol. Chem.* 280, 30838-30844
- 333 Hiscott,J. *et al.* (2006) Manipulation of the nuclear factor-kappa B pathway and the innate immune response by viruses. *Oncogene* 25, 6844-6867
- 334 Orth,K. *et al.* (2000) Disruption of signaling by Yersinia effector YopJ, a ubiquitin-like protein protease. *Science* 290, 1594-1597
- 335 Orth Kim *et al.* (1999) Inhibition of the Mitogen-Activated Protein Kinase Kinase Superfamily by a Yersinia Effector. *Science* 285, 1920-1923
- 336 Palmer,L.E. *et al.* (1999) YopJ of Yersinia spp. is sufficient to cause downregulation of multiple mitogen-activated protein kinases in eukaryotic cells. *Infect. Immun.* 67, 708-716
- 337 Collier-Hyams,L.S. *et al.* (2002) Salmonella AvrA effector inhibits the key proinflammatory, anti-apoptotic NF-kappa B pathway. *J. Immunol.* 169, 2846-2850
- 338 Park,J.M. *et al.* (2002) Macrophage apoptosis by anthrax lethal factor through p38 MAP kinase inhibition. *Sci* 297, 2048-2051
- 339 Kim,D.W. *et al.* (2005) The Shigella flexneri effector OspG interferes with innate immune responses by targeting ubiquitin-conjugating enzymes. *Proc Natl Acad Sci* 102, 14046-14051
- 340 Bowie,A. *et al.* (2000) A46R and A52R from vaccinia virus are antagonists of host IL-1 and toll-like receptor signaling. *Proc. Natl. Acad. Sci. U. S. A.* 97, 10162-10167
- 341 Stack,J. *et al.* (2005) Vaccinia virus protein Toll-like-interleukin-1 A46R targets multiple receptor adaptors and contributes to virulence. *J. Exp. Med.* 201, 1007-1018
- 342 Newman,R.M. *et al.* (2006) Identification and characterization of a novel bacterial virulence factor that shares homology with mammalian Toll/interleukin-1 receptor family proteins. *Infect. Immun.* 74, 594-601
- 343 Cirl Christine *et al.* (2008) Subversion of Toll-like receptor signaling by a unique family of bacterial Toll/Interleukin-1 receptor domain-containing proteins. *Nat. Med.*
- 344 Sengupta,D. *et al.* (2010) Subversion of Innate Immune Responses by Brucella through the Targeted Degradation of the TLR Signaling Adapter, MAL. *J. Immunol.* 184, 956-964
- 345 Radhakrishnan,G.K. *et al.* (2009) Brucella TIR Domain-containing Protein Mimics Properties of the Toll-like Receptor Adaptor Protein TIRAP. *J. Biol. Chem.* 284, 9892-9898
- 346 Salcedo,S.P. *et al.* (2008) Brucella Control of Dendritic Cell Maturation Is Dependent on the TIR-Containing Protein Btp1. *PLoS Pathog* 4, e21

- 347 Jayachandran,R. (2002) Anthrax: Biology of *Bacillus anthracis*. *Curr. Sci.* 82, 1220-1226
- 348 Mock,M. *et al.* (2001) Anthrax. *annu rev microbiol* 55, 647-671
- 349 Hanna,P.C. *et al.* (1993) On the role of macrophages in anthrax. *Proc Natl Acad Sci* 90, 10198-10201
- 350 Hanna,P.C. *et al.* (1994) Role of macrophage oxidative burst in the action of anthrax lethal toxin. *Mol Med* 1, 7-18
- 351 Gleiser,C.A. (1967) Pathology of anthrax infection in animal hosts. *Fed Proc* 26, 1518-1521
- 352 Abramova,F.A. *et al.* (1993) Pathology of inhalational anthrax in 42 cases from the Sverdlovsk outbreak of 1979. *Proc Natl Acad Sci* 90, 2291-2294
- 353 Jernigan,J.A. *et al.* (2001) Bioterrorism-related inhalational anthrax: the first 10 cases reported in the United States. *Emerg Infect Dis* 7, 933-944
- 354 Collier,R.J. and Young,J.A.T. (2003) ANTHRAX TOXIN. *Annu. Rev. Cell Dev. Biol.* 19, 45-70
- 355 Pellizzari,R. *et al.* (1999) Anthrax lethal factor cleaves MKK3 in macrophages and inhibits the LPS/IFN gamma-induced release of NO and TNF alpha. *FEBS Lett.* 462, 199-204
- 356 Vitale,G. *et al.* (2000) Susceptibility of mitogen-activated protein kinase kinase family members to proteolysis by anthrax lethal factor. *Biochem. J.* 352, 739-745
- 357 Vitale,G. *et al.* (1998) Anthrax lethal factor cleaves the N-terminus of MAPKKs and induces tyrosine/threonine phosphorylation of MAPKs in cultured macrophages. *Biochem. Biophys. Res. Commun.* 248, 706-711
- 358 Duesbery,N.S. *et al.* (1998) Proteolytic Inactivation of MAP-Kinase-Kinase by Anthrax Lethal Factor. *Science* 280, 734-737
- 359 Popov,S.G. *et al.* (2002) Effect of *Bacillus anthracis* lethal toxin on human peripheral blood mononuclear cells. *febs lett* 527, 211-215
- 360 Popov,S.G. *et al.* (2002) Lethal toxin of *Bacillus anthracis* causes apoptosis of macrophages. *Biochem Biophys Res Commun* 293, 349-355
- 361 Hanna,P.C. *et al.* (1992) Biochemical and physiological changes induced by anthrax lethal toxin in J774 macrophage-like cells. *Mol Biol Cell* 3, 1269-1277

- 362 Pellizzari,R. *et al.* (2000) Lethal factor of *Bacillus anthracis* cleaves the N-terminus of MAPKKs: analysis of the intracellular consequences in macrophages. *Int J Med Microbiol* 290, 421-427
- 363 Tournier,J.N. *et al.* (2005) Anthrax edema toxin cooperates with lethal toxin to impair cytokine secretion during infection of dendritic cells. *J Immunol* 174, 4934-4941
- 364 Lyons,C.R. *et al.* (2004) Murine Model of Pulmonary Anthrax: Kinetics of Dissemination, Histopathology, and Mouse Strain Susceptibility. *Infect. Immun.* 72, 4801-4809
- 365 Chand,H.S. *et al.* (2009) Discriminating Virulence Mechanisms among *Bacillus anthracis* Strains by Using a Murine Subcutaneous Infection Model. *Infect. Immun.* 77, 429-435
- 366 Kirby,J.E. (2004) Anthrax Lethal Toxin Induces Human Endothelial Cell Apoptosis. *Infect. Immun.* 72, 430-439
- 367 Drysdale,M. *et al.* (2007) Murine Innate Immune Response to Virulent Toxigenic and Nontoxigenic *Bacillus anthracis* Strains. *Infect. Immun.* 75, 1757-1764
- 368 Park,J.M. *et al.* (2004) Anthrolysin O and other gram-positive cytolysins are toll-like receptor 4 agonists. *J exp med* 200, 1647-1655
- 369 Weiss,S. *et al.* (2009) Involvement of TLR2 in innate response to *Bacillus anthracis* infection. *Innate Immunity* 15, 43-51
- 370 Sabet,M. *et al.* (2006) Modulation of cytokine production and enhancement of cell viability by TLR7 and TLR9 ligands during anthrax infection of macrophages. *FEMS Immunol. Med. Microbiol.* 47, 369-379
- 371 Hughes,M.A. *et al.* (2005) MyD88-dependent signaling contributes to protection following *Bacillus anthracis* spore challenge of mice: implications for Toll-like receptor signaling. *Infect Immun* 73, 7535-7540
- 372 Haubrich,W.S. (2005) Yersin of *Yersinia* infection. *Gastroenterology* 128, 23
- 373 Pujol,C. and Bliska James B (2003) The Ability To Replicate in Macrophages Is Conserved between *Yersinia pestis* and *Yersinia pseudotuberculosis*. *Infect. Immun.* 71, 5892-5899
- 374 Hinnebusch,B.J. (2005) The Evolution of Flea-borne Transmission in *Yersinia pestis*. *Current Issues in Molecular Biology* 7, 197-212
- 375 Balada-Llasat,J.M. *et al.* (2006) *Yersinia* has a tropism for B and T cell zones of lymph nodes that is independent of the type III secretion system. *PLoS Pathog* 2, e86

- 376 Cornelis C R *et al.* (1998) The virulence plasmid of *Yersinia*, an antihost genome. *Molecular Biology Reviews* 62, 1315-1352
- 377 Cornelis,G.R. and Wolfwatz,H. (1997) The *Yersinia* Yop virulon: A bacterial system for subverting eukaryotic cells. *Mol. Microbiol.* 23, 861-867
- 378 Galan,J.E. and Bliska,J.B. (1996) Cross-talk between bacterial pathogens and their host cells. *Annu. Rev. Cell Dev. Biol.* 12, 221-255
- 379 Straley,S.C. *et al.* (1993) Yops of *Yersinia* Spp Pathogenic for Humans. *Infect. Immun.* 61, 3105-3110
- 380 Viboud,G.I. and Bliska,J.B. (2005) *Yersinia* outer proteins: Role in modulation of host cell signaling responses and pathogenesis. *Annu. Rev. Microbiol.* 59, 69-89
- 381 Mills,S.D. *et al.* (1997) *Yersinia enterocolitica* induces apoptosis in macrophages by a process requiring functional type III secretion and translocation mechanisms and involving YopP, presumably acting as an effector protein. *Proc. Natl. Acad. Sci. U. S. A.* 94, 12638-12643
- 382 Palmer,L.E. *et al.* (1998) YopJ of *Yersinia pseudotuberculosis* is required for the inhibition of macrophage TNF-alpha production and downregulation of the MAP kinases p38 and JNK. *Mol. Microbiol.* 27, 953-965
- 383 Rosqvist,R. *et al.* (1988) Inhibition of Phagocytosis in *Yersinia-Pseudotuberculosis* - A Virulence Plasmid-Encoded Ability Involving the Yop2B Protein. *Infect. Immun.* 56, 2139-2143
- 384 Rosqvist,R. *et al.* (1990) The Cytotoxic Protein Yope of *Yersinia* Obstructs the Primary Host Defense. *Mol. Microbiol.* 4, 657-667
- 385 Mittal,R. *et al.* (2006) Acetylation of MEK2 and I kappa B kinase (IKK) activation loop residues by YopJ inhibits signaling. *Proc. Natl. Acad. Sci. U. S. A.* 103, 18574-18579
- 386 Mukherjee,S. *et al.* (2006) *Yersinia* YopJ acetylates and inhibits kinase activation by blocking phosphorylation. *Science* 312, 1211-1214
- 387 Zhou,H.L. *et al.* (2005) *Yersinia* virulence factor YopJ acts as a deubiquitinase to inhibit NF-kappa B activation. *J. Exp. Med.* 202, 1327-1332
- 388 Ruckdeschel,K. *et al.* (1997) Interaction of *Yersinia enterocolitica* with macrophages leads to macrophage cell death through apoptosis. *Infect. Immun.* 65, 4813-4821
- 389 Boland,A. and Cornelis,G.R. (1998) Role of YopP in suppression of tumor necrosis factor alpha release by macrophages during *Yersinia* infection. *Infect. Immun.* 66, 1878-1884

- 390 Ruckdeschel, K. *et al.* (1997) *Yersinia enterocolitica* promotes deactivation of macrophage mitogen-activated protein kinases extracellular signal-regulated kinase-1/2, p38, and c-jun NH2-terminal kinase - Correlation with its inhibitory effect on tumor necrosis factor-alpha production. *J. Biol. Chem.* 272, 15920-15927
- 391 Beuscher, H.U. *et al.* (1995) Bacterial evasion of host immune defense: *Yersinia enterocolitica* encodes a suppressor for tumor necrosis factor-alpha expression. *Infect. Immun.* 63, 1270-1277
- 392 Nakajima, R. and Brubaker, R.R. (1993) Association Between Virulence of *Yersinia Pestis* and Suppression of Gamma-Interferon and Tumor-Necrosis-Factor-Alpha. *Infect. Immun.* 61, 23-31
- 393 Goure, J. *et al.* (2005) Protective anti-V antibodies inhibit *Pseudomonas* and *Yersinia* translocon assembly within host membranes. *J. Infect. Dis.* 192, 218-225
- 394 Leary, S.E. *et al.* (1995) Active immunization with recombinant V antigen from *Yersinia pestis* protects mice against plague. *Infect Immun* 63, 2854-2858
- 395 Motin, V.L. *et al.* (1994) Passive immunity to yersiniae mediated by anti-recombinant V antigen and protein A-V antigen fusion peptide. *Infect Immun* 62, 4192-4201
- 396 Roggenkamp, A. *et al.* (1997) Passive immunity to infection with *Yersinia* spp. mediated by anti-recombinant V antigen is dependent on polymorphism of V antigen. *Infect Immun* 65, 446-451
- 397 Cheng, A.C. and Currie, B.J. (2005) Melioidosis: Epidemiology, Pathophysiology, and Management. *Clin. Microbiol. Rev.* 18, 383-416
- 398 Dance, D.A. (1991) Melioidosis: the tip of the iceberg? *Clin. Microbiol. Rev.* 4, 52-60
- 399 Ulett, G.C. *et al.* (2001) *Burkholderia pseudomallei* virulence: definition, stability and association with clonality. *Microbes and Infection* 3, 621-631
- 400 Ngauy, V. *et al.* (2005) Cutaneous melioidosis in a man who was taken as a prisoner of war by the Japanese during World War II. *J Clin Microbiol* 43, 970-972
- 401 Vorachit, M. *et al.* (1993) Resistance of *Pseudomonas pseudomallei* growing as a biofilm on silastic discs to ceftazidime and co-trimoxazole. *Antimicrob. Agents Chemother.* 37, 2000-2002
- 402 Matsuura, M. *et al.* (1996) Biological activities of lipopolysaccharide of *Burkholderia (Pseudomonas) pseudomallei*. *FEMS Microbiol Lett* 137, 79-83
- 403 Utaisincharoen, P. *et al.* (2000) Kinetic studies of the production of nitric oxide (NO) and tumour necrosis factor-alpha (TNF-alpha) in macrophages stimulated with *Burkholderia pseudomallei* endotoxin. *Clin Exp Immunol* 122, 324-329

- 404 Reckseidler-Zenteno, S.L. *et al.* (2005) The capsular polysaccharide of *Burkholderia pseudomallei* contributes to survival in serum by reducing complement factor C3b deposition. *Infect Immun* 73, 1106-1115
- 405 Jones, A.L. *et al.* (1996) Intracellular survival of *Burkholderia pseudomallei*. *Infect Immun*. 64, 782-790
- 406 Utaisincharoen, P. *et al.* (2001) *Burkholderia pseudomallei* interferes with inducible nitric oxide synthase (iNOS) production: a possible mechanism of evading macrophage killing. *Microbiol Immunol* 45, 307-313
- 407 Stevens, M.P. *et al.* (2002) An Inv/Mxi-Spa-like type III protein secretion system in *Burkholderia pseudomallei* modulates intracellular behaviour of the pathogen. *Mol Microbiol* 46, 649-659
- 408 Sun, G.W. *et al.* (2005) Caspase-1 dependent macrophage death induced by *Burkholderia pseudomallei*. *Cell Microbiol* 7, 1447-1458
- 409 Kespichayawattana, W. *et al.* (2000) *Burkholderia pseudomallei* induces cell fusion and actin-associated membrane protrusion: a possible mechanism for cell-to-cell spreading. *Infect Immun* 68, 5377-5384
- 410 Breitbach, K. *et al.* (2003) Actin-based motility of *Burkholderia pseudomallei* involves the Arp 2/3 complex, but not N-WASP and Ena/VASP proteins. *Cell Microbiol* 5, 385-393
- 411 Wiersinga, W.J. *et al.* (2007) Toll-Like Receptor 2 Impairs Host Defense in Gram-Negative Sepsis Caused by *Burkholderia pseudomallei* (Meloidosis). *PLoS Med* 4, e248
- 412 West, T.E. *et al.* (2008) Activation of Toll-like receptors by *Burkholderia pseudomallei*. *BMC Immunology* 9
- 413 Jacques, G. *et al.* (2005) From the discovery of the Malta fever's agent to the discovery of a marine mammal reservoir, brucellosis has continuously been a re-emerging zoonosis. *Vet. Res.* 36, 313-326
- 414 Barquero-Calvo Elias *et al.* (2007) *Brucella abortus* uses a stealthy strategy to avoid activation of the innate immune system during the onset of infection. *PLoS ONE* 2, e631
- 415 Kohler, S. *et al.* (2003) What is the nature of the replicative niche of a stealthy bug named *Brucella*? *Trends Microbiol.* 11, 215-219
- 416 Gorvel, J.P. (2008) *Brucella*: a Mr "Hide" converted into Dr Jekyll. *Microbes and Infection* 10, 1010-1013
- 417 Watarai, M. *et al.* (2002) Modulation of *Brucella*-induced macropinocytosis by lipid rafts mediates intracellular replication. *Cellular Microbiology* 4, 341-355

- 418 Köhler, S. *et al.* (2002) The analysis of the intramacrophagic virulome of *Brucella suis* deciphers the environment encountered by the pathogen inside the macrophage host cell. *Proc. Natl. Acad. Sci. U. S. A.* 99, 15711-15716
- 419 Roop, R.M. *et al.* (2009) Survival of the fittest: how *Brucella* strains adapt to their intracellular niche in the host. *Med. Microbiol. Immunol. (Berl)*. 198, 221-238
- 420 He, Y.Q. *et al.* (2006) *Brucella melitensis* triggers time-dependent modulation of apoptosis and down-regulation of mitochondrion-associated gene expression in mouse macrophages. *Infect. Immun.* 74, 5035-5046
- 421 Starr, T. *et al.* (2008) *Brucella* intracellular replication requires trafficking through the late endosomal/lysosomal compartment. *Traffic* 9, 678-694
- 422 Castano, M.J. and Solera, J. (2009) Chronic Brucellosis and Persistence of *Brucella melitensis* DNA. *J. Clin. Microbiol.* 47, 2084-2089
- 423 Rambow-Larsen, A.A. *et al.* (2008) Putative Quorum-Sensing Regulator BlxR of *Brucella melitensis* Regulates Virulence Factors Including the Type IV Secretion System and Flagella. *J. Bacteriol.* 190, 3274-3282
- 424 Delrue, R.M. *et al.* (2001) Identification of *Brucella* spp. genes involved in intracellular trafficking. *Cell Microbiol* 3, 487-497
- 425 de Jong, M.F. *et al.* (2008) Identification of VceA and VceC, two members of the VjbR regulon that are translocated into macrophages by the *Brucella* type IV secretion system. *Mol Microbiol* 70, 1378-1396
- 426 Fretin, D. *et al.* (2005) The sheathed flagellum of *Brucella melitensis* is involved in persistence in a murine model of infection. *Cellular Microbiology* 7, 687-698
- 427 Abdallah, A.I. *et al.* (2003) Type III secretion homologs are present in *Brucella melitensis*, *B. ovis*, and *B. suis* biovars 1, 2, and 3. *Curr. Microbiol.* 46, 241-245
- 428 Larnontagne, J. *et al.* (2009) Intracellular Adaptation of *Brucella abortus*. *Journal of Proteome Research* 8, 1594-1609
- 429 Seleem, M.N. *et al.* (2008) *Brucella*: A pathogen without classic virulence genes. *Vet. Microbiol.* 129, 1-14
- 430 Hallez, R. *et al.* (2007) The asymmetric distribution of the essential histidine kinase PdhS indicates a differentiation event in *Brucella abortus*. *EMBO J.* 26, 1444-1455
- 431 Swartz, T.E. *et al.* (2007) Blue-light-activated histidine kinases: Two-component sensors in bacteria. *Science* 317, 1090-1093
- 432 Lapaque, N. *et al.* (2005) *Brucella* lipopolysaccharide acts as a virulence factor. *Curr. Opin. Microbiol.* 8, 60-66

- 433 Forestier,C. *et al.* (1999) Lysosomal accumulation and recycling of lipopolysaccharide to the cell surface of murine macrophages, an in vitro and in vivo study. *J. Immunol.* 162, 6784-6791
- 434 Forestier,C. *et al.* (2000) Brucella abortus lipopolysaccharide in murine peritoneal macrophages acts as a down-regulator of T cell activation. *J. Immunol.* 165, 5202-5210
- 435 Sun,Y.H. *et al.* (2002) virB-Mediated Survival of Brucella abortus in Mice and Macrophages Is Independent of a Functional Inducible Nitric Oxide Synthase or NADPH Oxidase in Macrophages. *Infect. Immun.* 70, 4826-4832
- 436 Li,W.Z. *et al.* (2000) Saturated BLAST: an automated multiple intermediate sequence search used to detect distant homology. *Bioinformatics* 16, 1105-1110
- 437 Chaudhuri,R.R. *et al.* (2008) xBASE2: a comprehensive resource for comparative bacterial genomics. *Nucleic Acids Res.* 36, D543-D546
- 438 Shi,J. *et al.* (2001) FUGUE: sequence-structure homology recognition using environment-specific substitution tables and structure-dependent gap penalties. *J. Mol. Biol.* 310, 243-257
- 439 Liolios K *et al.* (2006) The Genomes On Line Database (GOLD) v.2: a monitor of genome projects worldwide. *Nucleic Acids Res.* 34, D332-D334
- 440 Cirl,C. *et al.* (2008) Subversion of Toll-like receptor signaling by a unique family of bacterial Toll/interleukin-1 receptor domain-containing proteins. *Nat. Med.* 14, 399-406
- 441 Low,L.Y. *et al.* (2007) Characterization of a TIR-like protein from *Paracoccus denitrificans*. *Biochem. Biophys. Res. Commun.* 356, 481-486
- 442 Novatchkova,M. *et al.* (2003) The STIR-domain superfamily in signal transduction, development and immunity. *Trends Biochem. Sci.* 28, 226-229
- 443 Boyd,E.F. and Brussow,H. (2002) Common themes among bacteriophage-encoded virulence factors and diversity among the bacteriophages involved. *Trends Microbiol.* 10, 521-529
- 444 Brussow,H. *et al.* (2004) Phages and the evolution of bacterial pathogens: From genomic rearrangements to lysogenic conversion. *Microbiol. Mol. Biol. Rev.* 68, 560+
- 445 Spear,A.M. *et al.* (2009) Microbial TIR domains: not necessarily agents of subversion? *Trends Microbiol.* 17, 393-398
- 446 Sikora,S. *et al.* (2005) Convergent evolution as a mechanism for pathogenic adaptation. *Trends Microbiol.* 13, 522-527
- 447 Gough Julian (2005) Convergent evolution of domain architectures (is rare). *Bioinformatics* 21, 1464-1471

- 448 Pallen,M.J. and Wren,B.W. (2007) Bacterial pathogenomics. *Nature* 449, 835-842
- 449 Pallen,M.J. *et al.* (2003) Tetratricopeptide-like repeats in type-III-secretion chaperones and regulators. *FEMS Microbiol. Lett.* 223, 53-60
- 450 Wehenkel,A. *et al.* (2008) Mycobacterial Ser/Thr protein kinases and phosphatases: Physiological roles and therapeutic potential. *Biochimica et Biophysica Acta (BBA) - Proteins & Proteomics* 1784, 193-202
- 451 Hughes Austin L and Piontkivska Helen (2008) Functional diversification of the Toll-like Receptor gene family. *Immunogenetics* 60, 249-256
- 452 Medzhitov R. and Janeway C.A. (1998) An ancient system of host defense. *Curr. Opin. Immunol.* 10, 12-15
- 453 Nürnberger,T. *et al.* (2004) Innate immunity in plants and animals: striking similarities and obvious differences. *Immunol. Rev.* 198, 249-266
- 454 Ausubel Frederick M (2005) Are innate immune signalling pathways in plants and animals conserved? *Nature Immunology* 6, 973-977
- 455 Ulrichs,P. *et al.* (2010) Caspase-1 targets the TLR adaptor Mal at a crucial TIR-domain interaction site. *J. Cell Sci.* 123, 256-265
- 456 Invivogen (2010) TLR expression in HEK293 cells.
http://www.invivogen.com/sscat.php?ID=8&ID_cat=2#table
- 457 Swisher,J.F.A. *et al.* (2010) Annexin A2 tetramer activates human and murine macrophages through TLR4. *Blood* 115, 549-558
- 458 Wiersinga,W.J. *et al.* (2010) Inflammation patterns induced by different *Burkholderia* species in mice. *Cellular Microbiology* 10, 81-87
- 459 Lukaszewski,R.A. *et al.* (2005) Pathogenesis of *Yersinia pestis* Infection in BALB/c Mice: Effects on Host Macrophages and Neutrophils. *Infect. Immun.* 73, 7142-7150
- 460 Sharma,R.K. *et al.* (2005) Involvement of TLR6/1 in rLcrV-mediated immunomodulation of murine peritoneal macrophages in vitro. *Mol. Immunol.* 42, 695-701
- 461 Grabenstein,J.P. *et al.* (2006) Characterization of phagosome trafficking and identification of PhoP-regulated genes important for survival of *Yersinia pestis* in macrophages. *Infect Immun* 74, 3727-3741
- 462 Bi,Y. *et al.* (2009) Reduced Apoptosis of Mouse Macrophages Induced by yscW Mutant of *Yersinia pestis* Results from the Reduced Secretion of YopJ and Relates to Caspase-3 Signal Pathway. *Scand. J. Immunol.* 70, 358-367

- 463 Lemaître, N. *et al.* (2006) *Yersinia pestis* YopJ Suppresses Tumor Necrosis Factor Alpha Induction and Contributes to Apoptosis of Immune Cells in the Lymph Node but Is Not Required for Virulence in a Rat Model of Bubonic Plague. *Infect. Immun.* 74, 5126-5131
- 464 Pollack, C. *et al.* (1986) Probing the phagolysosomal environment of human macrophages with a Ca²⁺ - responsive operon fusion in *Yersinia pestis*. *Nature* 322, 834-836
- 465 Datsenko, K.A. *et al.* (2000) One-step inactivation of chromosomal genes in *Escherichia coli* K-12 using PCR products. *Proc Natl Acad Sci* 97, 6640-6645
- 466 Taylor, V.L. *et al.* (2005) Oral immunization with a dam mutant of *Yersinia pseudotuberculosis* protects against plague. *Microbiology-Sgm* 151, 1919-1926
- 467 Rosenberg, M. (1984) Isolation of pigmented and nonpigmented mutants of *Serratia marcescens* with reduced cell surface hydrophobicity. *J Bacteriol* 160, 480-482
- 468 Beck, G. *et al.* (1988) Effect of growth on surface charge and hydrophobicity of *Staphylococcus aureus*. *Annales de l'Institut Pasteur / Microbiologie* 139, 655-664
- 469 Stubben, C.J. *et al.* (2009) Steps toward broad-spectrum therapeutics: discovering virulence-associated genes present in diverse human pathogens. *BMC Genomics* 10, 501
- 470 Robinson, V.L. *et al.* (2005) A dam mutant of *Yersinia pestis* is attenuated and induces protection against plague. *FEMS Microbiol Lett* 252, 251-256
- 471 Felek, S. *et al.* (2010) Phosphoglucosyltransferase of *Yersinia pestis* Is Required for Autoaggregation and Polymyxin B Resistance. *Infect. Immun.* 78, 1163-1175
- 472 Han, Y. *et al.* (2005) Comparative transcriptome analysis of *Yersinia pestis* in response to hyperosmotic and high-salinity stress. *Res Microbiol* 156, 403-415
- 473 Han, Y. *et al.* (2007) Comparative transcriptomics in *Yersinia pestis*: a global view of environmental modulation of gene expression. *BMC Microbiol* 7, 96
- 474 Sweet, C.R. *et al.* (2007) YopJ targets TRAF proteins to inhibit TLR-mediated NF-kappaB, MAPK and IRF3 signal transduction. *Cellular Microbiology* 9, 2700-2715
- 475 Straley, S.C. *et al.* (1986) Virulence genes regulated at the transcriptional level by Ca²⁺ in *Yersinia pestis* include structural genes for outer membrane proteins. *Infect Immun* 51, 445-454
- 476 Straley, S.C. and Cibull, M.L. (1989) Differential clearance and host pathogen interactions of YopE- and YopK- YopL- *Yersinia pestis* in BALB/c mice. *Infect. Immun.* 57, 1200-1210

- 477 Monack,D.M. *et al.* (1998) *Yersinia*-induced apoptosis *in vivo* aids in the establishment of a systemic infection of mice. *J. Exp. Med.* 188, 2127-2137
- 478 Yoshida,T. *et al.* (2006) Transcription Regulation of ompF and ompC by a Single Transcription Factor, OmpR. *J. Biol. Chem.* 281, 17114-17123
- 479 Dean S.R. and Meola,R.W. (2002) Effect of Diet Composition on Weight Gain, Sperm Transfer and Insemination in the Cat Flea. *J. Med. Entomol.* 39, 370-375
- 480 Zhou,D.S. and Yang,R.F. (2009) Molecular Darwinian Evolution of Virulence in *Yersinia pestis*. *Infect. Immun.* 77, 2242-2250
- 481 Felek,S. *et al.* (2008) The *Yersinia pestis* autotransporter YapC mediates host cell binding, autoaggregation and biofilm formation. *Microbiology* 154, 1802-1812
- 482 Qiu,J. *et al.* (2008) DNA microarray-based global transcriptional profiling of *Yersinia pestis* in multicellularity. *J Microbiol* 46, 557-563
- 483 Kirov,S.M. *et al.* (2007) Biofilm differentiation and dispersal in mucoid *Pseudomonas aeruginosa* isolates from patients with cystic fibrosis. *Microbiology* 153, 3264-3274
- 484 Matthews C.K. (1993) Enzyme organisation in DNA precursor biosynthesis. *Prog. Nucleic Acid Res. Mol. Biol.* 44, 167-203
- 485 Koebnik,R. *et al.* (2000) Structure and function of bacterial outer membrane proteins: barrels in a nutshell. *Mol Microbiol* 37, 239-253
- 486 Kirillina,O. *et al.* (2004) HmsP, a putative phosphodiesterase, and HmsT, a putative diguanylate cyclase, control Hms-dependent biofilm formation in *Yersinia pestis*. *Mol. Microbiol.* 54, 75-88
- 487 Felek,S. *et al.* (2009) Phosphoglucomutase of *Yersinia pestis* is Required for Autoaggregation and Polymyxin B Resistance. *Infect Immun*
- 488 Skurnik,M. *et al.* (1984) Virulence plasmid-associated autoagglutination in *Yersinia* spp. *J Bacteriol* 158, 1033-1036
- 489 Rosqvist,R. *et al.* (1988) Increased virulence of *Yersinia pseudotuberculosis* by two independent mutations. *Nature (London)* 334, 522-524
- 490 Skurnik,M. *et al.* (1989) Analysis of the yopA gene encoding the Yop1 virulence determinants of *Yersinia* spp. *Mol Microbiol* 3, 517-529
- 491 Buchanan,J.T. *et al.* (2005) *Streptococcus iniae* phosphoglucomutase is a virulence factor and a target for vaccine development. *Infect Immun* 73, 6935-6944

- 492 Ugalde, J.E. *et al.* (2000) Identification and characterization of the *Brucella abortus* phosphoglucomutase gene: role of lipopolysaccharide in virulence and intracellular multiplication. *Infect Immun* 68, 5716-5723
- 493 McKay, G.A. *et al.* (2003) Role of phosphoglucomutase of *Stenotrophomonas maltophilia* in lipopolysaccharide biosynthesis, virulence, and antibiotic resistance. *Infect Immun* 71, 3068-3075
- 494 Marchler-Bauer, A. *et al.* (2009) CDD: specific functional annotation with the Conserved Domain Database. *Nucleic Acids Res* 37, D205-D210
- 495 Yomano, L.P. *et al.* (2009) Deletion of methylglyoxal synthase gene (*mgsA*) increased sugar co-metabolism in ethanol-producing *Escherichia coli*. *Biotechnol Lett* 31, 1389-1398
- 496 Eboigbodin, K.E. *et al.* (2007) Investigating the surface properties of *Escherichia coli* under glucose controlled conditions and its effect on aggregation. *Langmuir* 23, 6691-6697
- 497 Fareleira, P. *et al.* (1997) Pathways for Utilization of Carbon Reserves in *Desulfovibrio gigas* under Fermentative and Respiratory Conditions. *J. Bacteriol.* 179, 3972-3980

Appendix A: Amino acid sequences of bacterial TIR domain proteins investigated in this work

BaTdp

MYYHIRINLTTRVQESKFNITFEELEERYLSRYRKGEDFTLN GRVIKINDIQKMSINV
 SENENELDILVDRIEYEDQKSSIVRVGGPSRKWRAAGRLKDVSDDELLEGPPGYMLK
 EAEVAASVEVDNTKVFIVHGHDDNLKQQLEIFLNSIGIKPVVLHREANEGLTVLEK
 FEKHSDVQYAFVLLTPDDIGCSVKERAKSVEEYSFRARQNVIFELGFFIGKLGRAKV
 CTLYKDGVELPNDISGLVYQKVNDNIEDVGYHIMKELRAAGLKVTY

BmTdp

MSKEKQAQSKAHKAQQAISAKSLSTQKSKMSELERATRDGAAIGKKRADIAKKI
 ADKAKQLSSYQAKQFKADEQAVKKVAQEQLSDERTKHEAFIKQSLSSMRTTAS
 ATMEAEEYDFFISHASEDKEAFVQDLVAALRDLGAKIFYDAYTLKVGDSLRRKID
 QGLANSKFGIVVLSEHFFSKQWPARELDGLTAMEIGGQTRILPIWHKVSYDEVRRF
 SPSLADKVALNTSLKSVEEIAKELHSLI

BmTdp2

MNRTHWAVKDVNLPKELHTAKGITLPSWTRQASRAVDITQHDFDVGLSFPGEARG
 LVEQVARELEARVGPNAFYDNNYVSQLARPSLDTLLQDIYRNRCKLIVFVVGDD
 YQRKDRCGVEFRAIREIIMARAEQRIMFVRVDDGAVDGVFRTDGYVDARRFNPSEI
 AQFIAERVALIT

BpTdp

MNHPSVFHPGPAAISPPQRLLLMHEGEWEDFIEECVRQLQKEGNYVEVVALGGSG
 DKGRDVCGYSKEYPAAGTWDLYQAKHYDSPLTPSEFFPELAKFVTCVWREDYTR
 PAKYFICASRDVGTTLFDLLKNPVRLKERLLDDWRKKGGKFGKFKQPLDADLEKFI
 EVFPFDVVKRLPPMELLSIHERDTASYWARFGVLAPRENDPEVPPKPVSSSESTYVT
 ALLRVYAEHAQVKIDDVPDIPPAHGAHFKAQRRLFYSAEGLHRFSRDKLPGAFEAL
 LDEVENGIGAELTFPHESGFVRLHSVLKTANVLQIMNNPLRARLRSGDLQGSCHHL
 ANQGRAQWVESDEADGESV

BthTdp

MASVFFSYTHIDESLRDQLEIHLSLMKREGLITAWHDRRIVAGSDIDDSIDEHLESA
 DIILLV SANFIASEYCFATEMKRAMERHKAGEVRVIPVILRACDWH SAPFGKLNA
 VPTDGRPVT SWPNQDEAFADITKSIRAAVSATASSARARVAAPAREAGAARAVA
 VPAASTQLPRSSNMRVKHQFSDLDRDTFVSETFDFIARFFDGSLQELEKRHGQFQG
 RFTRIDARRFTASIYKDGKSIQCSVSHGGAFGGSSNREITYSSQISTHTNSFNEALTI
 AEDSQTLYLKPMNMARGVSEKLSDTGAAEYLWSMLMEPVQR

YpTdp

MASCIPPKVPGYLQRIREQYKESEPVYKVL SHAKV FVREDYHTDHN YDAVGH DIC
 LFLPMEILIDIHISKQEAYTNLIKNDLNIL TRSVHDEWIGEVALELNSEIDPEYQQAISI
 NEIVNEVLNPDELSIWKPNLIRVFISHRD KYKRE AQELANSLEEYGFSCFVAHETIEP
 LKEWRNEIVNGLKTMEVMLVLLTDDFNDSIWTCQEVGYALGANKPVVTLKVGKV
 DPAGFISHLQAVKGS LDNPTHNAELLNMLLAESIGKASRIQQALISTFIASQSFDEAK
 HRFNRMNKSIKKLTEENLNTVMDGFRRNNQLNQCMYLNNNYNRLKTFIERTTGKS
 AITSGKEIFIETV NKIV

YpTIR

SIWKPNLIRVFISHRD KYKRE AQELANSLEEYGFSCFVAHETIEPLKEWRNEIVNGL
 KTMEVMLVLLTDDFNDSIWTCQEVGYALGANKPVVTLKVGKVD PAGFISHLQAV
 KGSLDNPTHNAELLNMLLAESIGKASRIQQALISTFIASQSFDEA

Appendix B: Full list of PSI-BLAST protein results

Please see Appendix B.xls on CD submitted with this thesis

**Appendix C: DNA sequences of bacterial TIR domain proteins
cloned in this work**

Please see files in “Appendix C” folder on CD submitted with this thesis

Appendix D: Publications

See following pages

Microbial TIR domains: not necessarily agents of subversion?

Abigail M. Spear¹, Nicholas J. Loman², Helen S. Atkins¹ and Mark J. Pallen²

¹ Defence, Science and Technology Laboratory, Porton Down, Salisbury, Wiltshire SP4 0JQ, UK

² Centre for Systems Biology, University of Birmingham, Edgbaston, Birmingham, B15 2TT, UK

The Toll/interleukin-1 receptor (TIR) domain plays a crucial role in the mammalian innate immune response. Recently, proteins containing TIR domains have been described in bacteria and it has been suggested that these bacterial proteins are involved in subversion of the vertebrate immune system. Here we describe the distribution of TIR-domain proteins among bacteria, fungi, archaea and viruses and evaluate the subversion hypothesis in the light of our findings. We suggest that most TIR domains in bacteria have nothing to do with subverting eukaryotic cells; instead, TIR domains function simply as general purpose protein-protein interaction domains put to diverse uses.

The Toll/interleukin-1 receptor (TIR) domain: a versatile signalling module in multicellular organisms

The TIR domain was first recognized as a stretch of sequence homology spanning approximately 200 amino acids, and common to the cytoplasmic domains of the Toll receptor from *Drosophila* and the mammalian interleukin-1 receptor (IL-1R) [1,2]. The Toll receptor was initially identified through its role in dorso-ventral patterning during embryogenesis and was then later implicated in the fly immune response [3,4]. Toll-like receptors (TLRs) were subsequently discovered in the innate immune systems of mammals [5], where they mediate recognition of pathogen-associated molecular patterns (PAMPs), such as lipopolysaccharide (LPS), flagellin or CpG DNA [6,7]. Mice are now known to have 13 TLRs, while the human genome encodes 10 TLRs. Each mammalian TLR is thought to recognize a distinct set of PAMPs or endogenous danger signals characteristic of host tissue damage [8].

The similarity between IL-1R and TLR signalling extends beyond their shared TIR domains: specifically, the downstream signalling components, such as adaptor proteins, kinases and transcription factors, are also often homologous. In fact, the TIR domain occurs not just in the receptors, but also in the cytoplasmic adaptor molecules of these signalling pathways [6]. In this setting, the TIR domain functions as a protein-protein interaction domain, transducing the signal from ligand binding through a signalling cascade that culminates in the activation of transcription factors and production of immune effector molecules.

The contribution of TIR domains to the mammalian immune response has been the focus of intense research

interest, including studies linking sequence, structure and function (Box 1). However, it is important to stress that TIR domains are widespread among multicellular organisms; for example, the sea urchin is predicted to contain an astonishing 222 TLRs and 26 adaptors [9]. One might argue that a specialized immune system is a prerequisite of a multicellular lifestyle. However, plants, animals and fungi are known to have independently evolved multicellularity [10], so one would not anticipate that their pathogen-recognition pathways should be derived from homologous components. In fact, no TIR domains have been described in fungi to date, even though they are closely related to animals, and are classified together as “opisthokonts” [11]. Surprisingly, TIR-domain proteins are involved in disease resistance in plants, where they occur in pathogen-detection proteins from the nucleotide-binding site-leucine-rich repeat (NBS-LRR) family [12]. However, despite these superficially similar functional associations, it is clear that the TIR domains of plants and animals are involved in quite distinct aspects of pathogen recognition and immune signal transduction [12]. These differences, together with the different evolutionary routes to multicellularity in plants and animals, imply that TIR domains have been independently recruited for defensive roles in plants and animals.

Hints at a possible ancestral role for TIR domains in unicellular eukaryotes come from the recent discovery of a TIR-domain protein in the social amoeba *Dictyostelium discoideum* [13]. In times of plenty, these soil organisms feed singly on bacteria, but when starved they aggregate to form a migrating multicellular slug. A TIR-domain protein (TirA) is required both for consumption of bacteria during the vegetative phase and for immune-like functions during the multicellular phase [13]. Thus, it seems plausible that TIR domains represent components of a primordial foraging mechanism in unicellular eukaryotes that has subsequently been adapted to functions in development and defense in some multicellular organisms.

Some TIR-domain proteins and pathways are also implicated in another key feature of multicellular life (programmed cell death [apoptosis]). In 2002, Koonin and Aravind [14] investigated the origins of the metazoan apoptotic machinery by surveying prokaryotic genomes. They found that several protein domains associated with apoptosis in eukaryotes occurred widely in bacteria, sometimes co-occurring in the same bacterial species. Specifically, they found TIR domains in diverse bacterial genera

Corresponding author: Pallen, M.J. (m.pallen@bham.ac.uk).

Box 1. Sequence and structural features of the TIR domain

TIR domains often show relatively low sequence homology both within and between species. In the past, mammalian TIR domains have been categorized according to the presence of three "boxes" of sequence [22,23] (Figure 1a). However, other regions have also been shown to be important [24], and with the discovery of TIR domains in many more settings, it is unclear whether these boxes should continue to be regarded as defining characteristics of TIR domains.

Many of the bacterial proteins identified in our survey have already been annotated as containing TIR domains, but some are annotated as containing either SEFIR or DUF1863 domains. PFAM classifies these domains with TIR domains within the STIR domain superfamily [26]. However, given the co-occurrence of all three domains in our PSI-BLAST results, we question whether classifying them as distinct domains, rather than as merely variants of the TIR domain, is warranted.

Crystal structures of TIR domains have been obtained from TLR1, TLR2, IL-1RAPL (interleukin-1 receptor associated protein-like) and

TLR10 [26–29] (Figure 1b). These structures have been used as templates to create models of other TIR domains [26,29]. Mutagenesis and structural studies have helped to clarify the TIR–TIR interface [26]. Structurally, the TIR domain consists of a central five-stranded parallel β sheet (β A– β E) surrounded by five helices (α A– α E) with connecting loop structures, similar in structure to flavodoxin and the bacterial chemotaxis protein CheY [30]. The loop regions appear to play an important role in mediating the specificity of protein–protein interactions. In particular, much attention has focused on the BB loop. This loop comprises part of sequence box 2 and is characterised by a motif $RDx\phi PG$ (x is any residue and ϕ denotes a hydrophobic residue). The importance of the conserved proline residue in signalling is highlighted by the fact that the mutation to histidine in mice confers hyper-responsivity to lipopolysaccharide [31]. Residues located on other loop portions of the TIR domain have also been shown to play a role in TIR–TIR interactions [24].

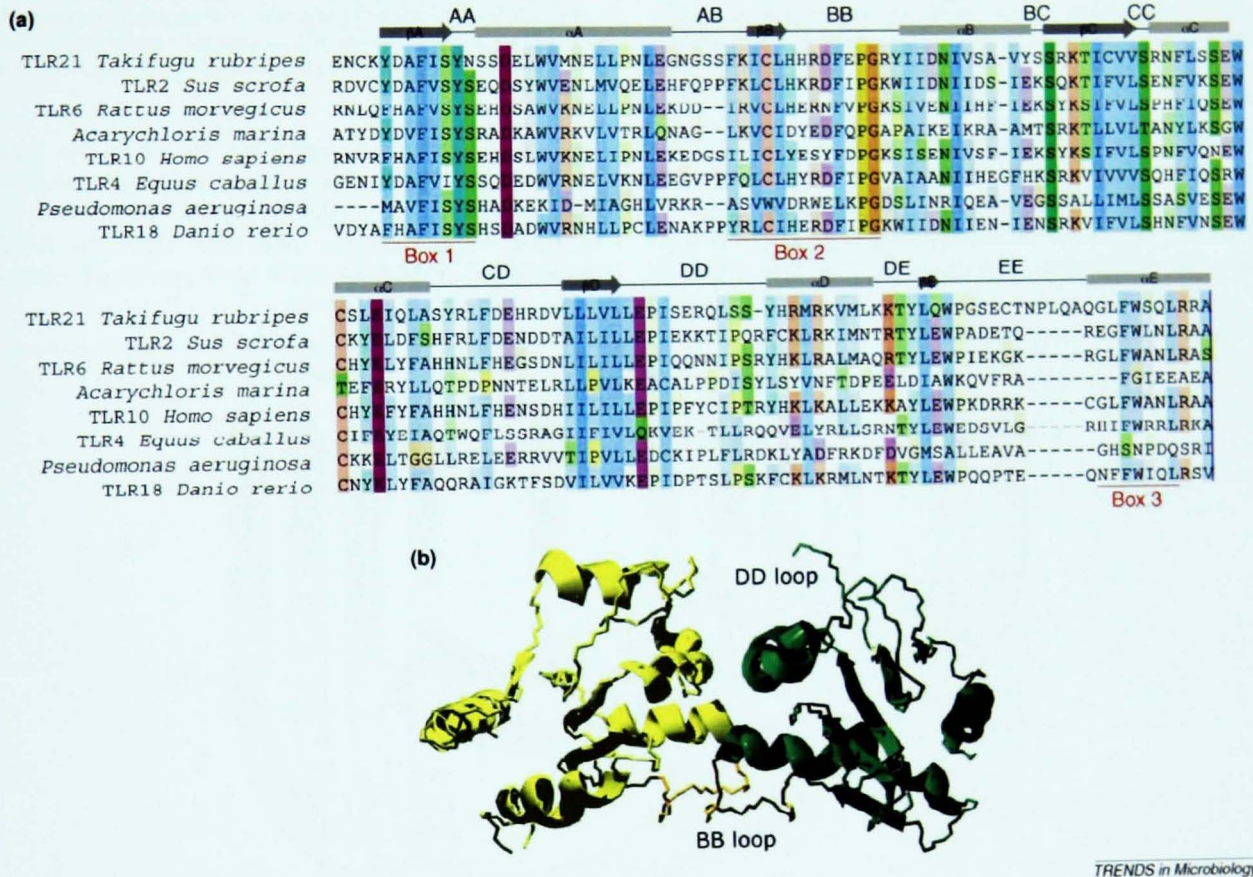


Figure 1. Sequence and structure of TIR domains. (a) Sequence alignment of TIR domains. Alignment performed and edited using Jalview/ClustalW and shaded using ClustalX colour scheme with shading intensity by conservation index. Sequence IDs: NP_001027751 (TLR21, *Takifugu rubripes*), NP_998926 (TLR2, *Sus scrofa*), NP_9987487 (TLR6, *Rattus norvegicus*), YP_001519438 (TPR domain-containing protein, *Acaryochloris marina* MBIC11017), AAQ88667 (TLR10, *Homo sapiens*), NP_001093239 (TLR4, *Equus caballus*), YP_001347742.1 (*Pseudomonas aeruginosa*) and NP_001082819 (TLR18, *Danio rerio*). Structural features added according to TLR10 structure (PDB: 2j67). Grey boxes denote alpha helices, grey arrows denote areas of beta sheet and black lines denote connecting loops. (b) Structure of TLR10 TIR domain (*Homo sapiens*). TLR10 structure downloaded from PDB (www.rcsb.org). Coloured and drawn with Swiss PDB-Viewer and rendered with POV-Ray.

(*Streptomyces*, *Caulobacter*, *Rhizobium*, *Anabaena*, *Synechocystis* and *Bacillus*), and even reported a TIR domain and apoptosis-ATPase domain located in the same bacterial protein (SCO5629 from *Streptomyces*). They suggested that apoptotic effectors and TIR domains were acquired by eukaryotes as a consequence of mitochondrial endosymbiosis and subsequent additional horizontal gene transfer events.

TIR domains in bacteria: a subversive agenda?

In 2006, Newman and colleagues [15] performed a bioinformatics survey to identify TIR domains in bacterial proteins. They found > 200 bacterial TIR domains and then focused their research efforts on a TIR-domain protein (TlpA) from *Salmonella enterica* serovar Enteritidis. They showed that this protein, when expressed in the eukaryotic cytoplasm, impaired TLR- and MyD88-

Opinion

Box 2. How widespread are TIR domains?

We carried out a survey of TIR domains in bacteria, fungi, archaea and viruses using PSI-BLAST and PFAM searches (see Supplementary Methods). As a result, 922 bacterial TIR domain proteins were identified (Supplementary Table 1). When evaluated against the number of completed and ongoing genome sequencing projects using the GOLD database [32], the numbers of TIR proteins in bacterial phyla generally correlated with the proportion of genomes sequenced, with the most notable exception being the Cyanobacteria (accounting for 13.8% of TIR domains and 3.2% of sequencing projects). TIR domain proteins were also found in Bacteroidetes, Chlorobi, Proteobacteria, Firmicutes, Fusobacteria, Nitrospirae, Acidobacteria, Verrucomicrobia, Aquificae, Chloroflexi, Actinobacteria, Planctomycetes, Spirochaetes and Tenericutes (Supplementary Table 2). A single TIR domain protein was found in fungi (hypothetical protein An11g08390 from *Aspergillus niger*). Six archaeal proteins contained the TIR domain (two from *Methanococcoides burtonii*, one from *Methanocarcina barkeri*, one from *Thermofilum pendens* and two from an uncultured archaean). One archaeal protein contained a SEIR domain and three contained DUF1863 domains (Supplemen-

tary Table 3). This is the first published report of the presence of STIR domains in both fungi and archaea.

In elegant studies by Bowie and colleagues [33], and Stack and co-workers [34], the A46R protein from the vaccinia virus was shown to interact with mammalian TIR domain-containing proteins and to disrupt IL-1 and TLR signalling *in vitro*. Disruption of A46R also renders vaccinia virus less virulent *in vivo*. After subjective scrutiny of a multiple alignment, these authors claimed that A46 contained a TIR domain [34]. However, in our survey, we found no evidence for a TIR domain in A46 or any other eukaryotic viral protein using BLAST or PSI-BLAST (homology search methods that allow unbiased searching of sequence libraries and provide an objective statistical evaluation of each alignment) [35]. Searches starting with known TIR domains do not find A46, and searches starting with A46 do not find TIR domains. Instead, both BLAST and PFAM searches reveal homology to other vaccinia proteins of known structure (B14 and A52), which contain a Bcl-2 fold. We conclude that A46 does not contain a TIR domain and the original claim is erroneous.

mediated activation of NF-KappaB. Furthermore, they showed that a *tlpA* deletion mutant was attenuated in cell culture and mouse models of infection. They postulated that TlpA interacts with host proteins via a TIR-TIR interaction; however, they were unable to demonstrate

such an interaction, nor did they provide any evidence that TlpA was translocated into host cells.

Most recently, Cirl and co-workers [16] focused on two bacterial TIR-containing proteins (Tcps), one from *Brucella* (TepB), and the other from a uropathogenic strain of

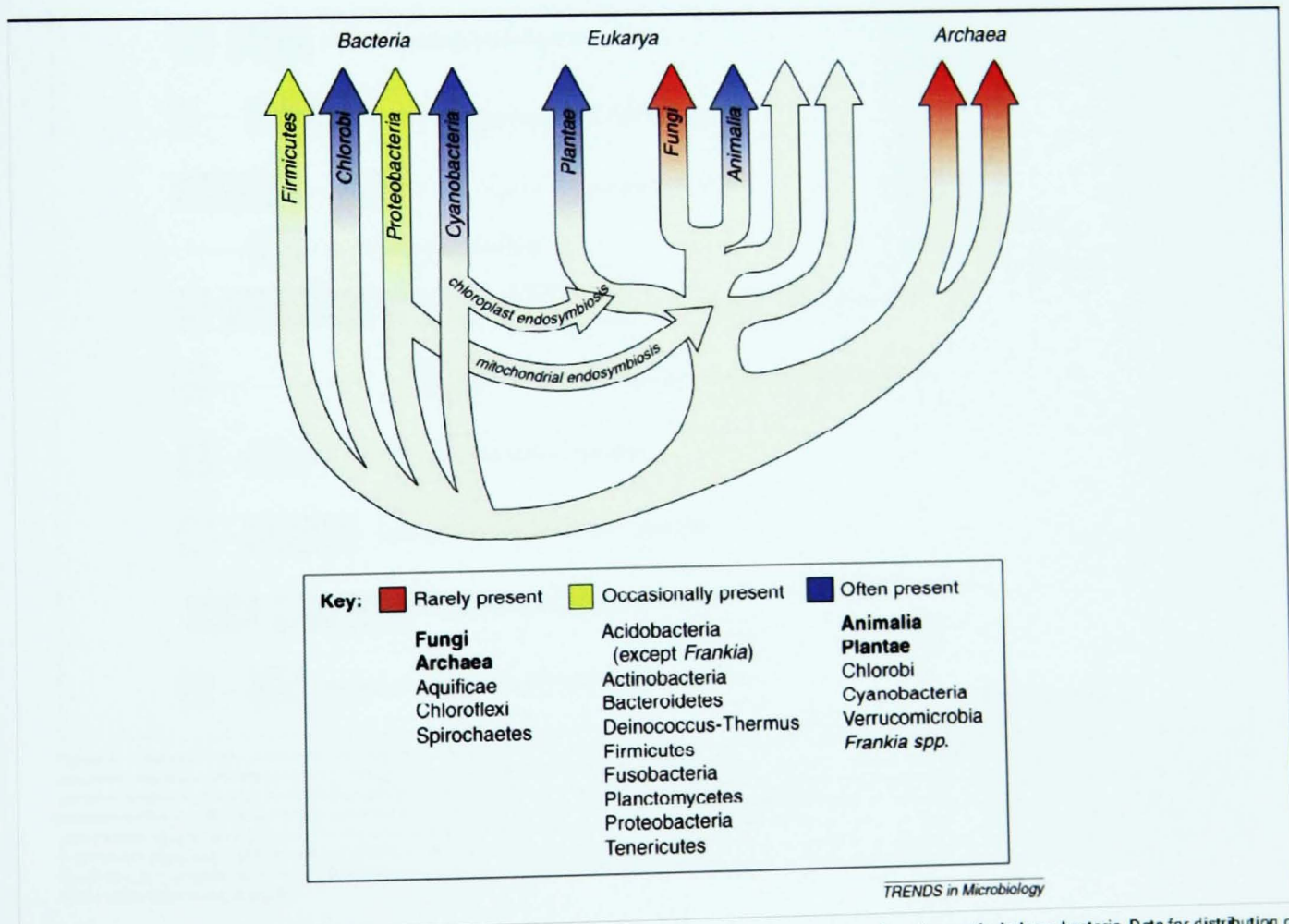


Figure 1. Schematic representation of the Tree of Life to illustrate distribution of TIR domains across Kingdoms, focusing particularly on bacteria. Data for distribution of TIR domains across bacterial phyla can be found in Supplementary Table 3. "Often" indicates TIR domains are found in $\geq 50\%$ of genomes sequenced. "Occasionally" indicates TIR domains are found in $\geq 10\%$ of genomes sequenced (but $< 50\%$) and "Rarely" indicates TIR domains are found in $< 10\%$ genomes sequenced. Information on genome sequencing projects obtained from GOLD. Tree of Life adapted from figure by W. Ford Doolittle [36].

Escherichia coli (TepC). They reported that both proteins impair TLR signalling and interact with MyD88, and showed through deletion mutagenesis that the *tcpB* gene plays a role in pathogenesis in a mouse model of pyelonephritis. They also demonstrated that TepB is secreted by the bacterial cell and that purified recombinant TepB is internalised by human cells.

Keeping an open mind

How do we explain the existence of TIR domains in bacterial proteins? The work mentioned in the previous section [15,16] lead the reader to the "subversion hypothesis"; that is, the primary function of bacterial TIR-domain proteins is to subvert the mammalian immune response by interacting with eukaryotic TIR-mediated signalling. However, an alternative explanation is that most or all TIR domains in bacteria have nothing to do with subverting eukaryotic cells. Instead, TIR domains function simply as general purpose protein-protein interaction domains which are probably put to diverse uses in bacteria. For

example, Iyer *et al.* [17] noted that some bacterial TIR domains are fused to proteins involved in nucleic acid metabolism and proposed that they play a role in nucleic acid binding or as nucleases.

In an attempt to shed more light on this issue, we have performed a fresh bioinformatics survey of TIR domains (Box 2), focusing particularly on the distribution of TIR domain proteins among bacteria, archaea, viruses and fungi. We will now evaluate the evidence for and against the subversion hypothesis.

Problems with subversion

Although one cannot ignore the experimental work on TlpA and TepB, there remain some unresolved issues. Both proteins lack signal peptides and it is unclear whether TlpA is even secreted. In both cases, no well-defined mechanism has been identified for protein export across the bacterial cell envelope. Moreover, experiments on proteins expressed from artificial constructs may not mirror actual physiologic conditions.

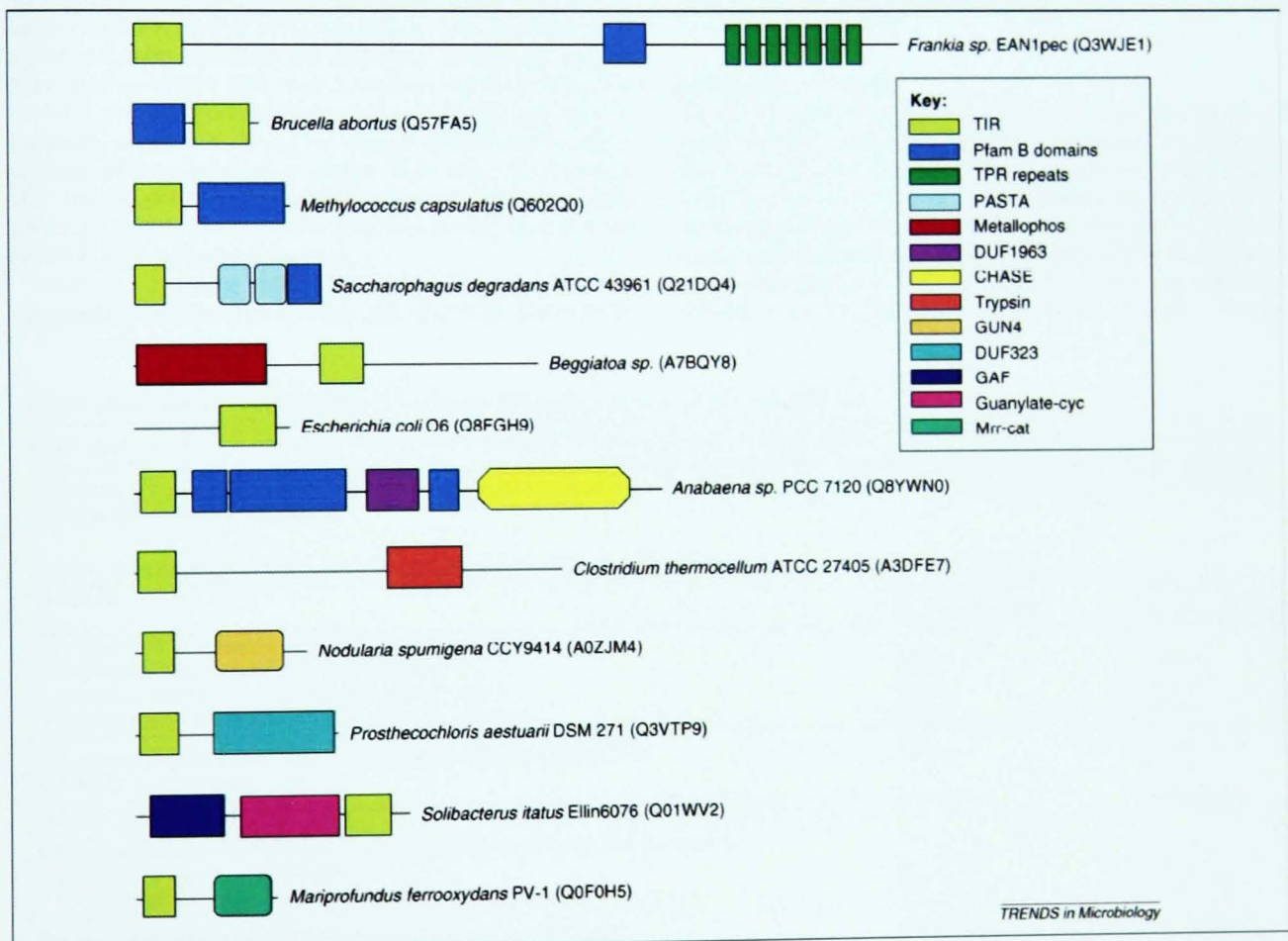


Figure 2. Diverse domain architectures of bacterial proteins containing TIR domains. Explanation for domain names: TIR, Toll/interleukin-1 receptor; PFAM B-domains, miscellaneous automatically annotated domains of unknown function; TPR repeats, tetratricopeptide repeats, a common protein-protein interaction domain; PASTA, small globular domain found at C-terminus of penicillin-binding proteins and bacterial serine/threonine kinases involved in binding to peptidoglycan precursors; Metallophos, a calcineurin-like metallo-phosphoesterase domain found in many proteins involved in phosphorylation; DUF1963, one of many domains of unknown function; CHASE, an extracellular ligand-binding domain from receptor-like proteins; Trypsin, a serine protease domain; GUN4, a domain involved in regulation of chlorophyll synthesis and intracellular signaling in chloroplasts; DUF323, another domain of unknown function; GAF, a domain present in phytochromes and cGMP-specific phosphodiesterases; Guanylate_cyc, catalytic domain of adenylate and guanylate cyclases and Mrr-cat, a type IV restriction endonuclease domain. Figure re-drawn from results displayed by PFAM (<http://pfam.sanger.ac.uk>).

Opinion

The sporadic occurrence of genes encoding bacterial TIR domain proteins might also be viewed as problematic for the subversion hypothesis. The *tlpA* gene occurs in only 5 of > 70 genome-sequenced strains of *S. enterica*, while *tcpB* occurs in only a minority of uropathogenic *E. coli* isolates, so neither gene can be considered an essential conserved component of enteropathogenesis or uropathogenesis, respectively. However, the patchy phylogenetic distribution of TIR-domain genes in bacteria, which seldom if ever follow vertical lines of descent (Figure 1), need not count against the subversion hypothesis, as similar patchiness exists in the genomic distribution of well-established subversion factors, such as type-III secretion effectors [18], which is a hallmark of horizontal gene transfer.

However, two other lines of evidence from bioinformatics surveys suggest that the subversion hypothesis cannot explain all bacterial TIR domain proteins. First, when the broad phylogenetic distribution of bacterial TIR domain proteins is considered, the vast majority of these proteins are encoded within the genomes of environmental organisms not usually thought of as pathogens. While in the eco-evo view of bacterial pathogenomics we cannot rule out a role for bacterial TIR domains in "non-pathogens" as agents of subversion against microbial eukaryotic predators or competitors [19], such a widespread distribution is curious given the over-representation within the cyanobacteria, which seldom if ever engage in subversive interactions with metazoans or plants. It is also worth noting that the closest homologue of the TcpB TIR domain (52% identity) occurs in a marine flavobacterium that has no credible role in human disease.

Second, our survey confirms the association with other apoptosis domains, but also reveals that TIR domains in

bacteria are promiscuous in their co-occurrence with other domains in individual proteins; we found dozens of domain architectures built around TIR domains (Figure 2). This counts against any unified theory that attempts to place all bacterial TIR domain proteins into a single functional category. In fact, these two lines of evidence suggest that the TIR domain is no different from many other "eukaryotic signalling domains," which were first associated with signalling in eukaryotes, but then found to occur widely in bacteria. In almost all such cases, the signalling function occurs in a specific context in eukaryotes that is not shared by bacteria. Instead, the microorganisms adopt and adapt the domains for their own use. For example, tetratricopeptide repeats mediate protein-protein interactions in humans and bacteria, but in different contexts (for example, in eukaryotes as scaffolds for the assembly of multi-protein complexes in the nucleus or peroxisomes, or for binding cargo onto microtubules; and in bacteria as chaperones in type III secretion [20]). Similarly, serine-threonine protein kinases, although prominent in signalling in humans, are also intimately integrated into bacterial signalling pathways (particularly within mycobacteria) [21].

Is the jury still out?

So, do we need to reject the subversion hypothesis for all bacterial TIR domains? No, but we do need to recognize that the subversive role is likely to be the exception rather than the rule. One can draw a parallel with other enzymatic signalling domains common to eukaryotes and bacteria; such domains can engage in "moonlighting," with or without engaging in cellular subversion. For example, the already mentioned serine-threonine protein kinase

Box 3. How could we tell whether a bacterial TIR protein is involved in subversion?

A key question for future research is how many bacterial TIR domains play a role in subverting immune signalling via interactions with eukaryotic TIR domains and what roles are played by other bacterial TIR domains. When assessing the chain of evidence for the subversion hypothesis for any given bacterial TIR domain protein, we propose a number of criteria, which we use to assess two papers published on bacterial TIR domains (see Table I).

Table I. Criteria for evaluating the subversive role of bacterial TIR proteins

Criterion	Newman and co-workers [15]	Cirl and co-workers [16]
Wild type and complemented mutant bacteria are able to: <ul style="list-style-type: none"> influence TLR signalling in mammalian cells produce disease in animal or cell culture model and these activities are absent or decreased in mutants	Shown Shown Shown	Shown Shown Shown
TIR domain protein interferes with TLR signalling when applied to or expressed in mammalian cells	Shown	Shown
and this activity is decreased when predicted mammalian partner is over-expressed	Not shown	Not shown
Interaction between bacterial and mammalian TIR domain proteins detected by: <ul style="list-style-type: none"> <i>in vitro</i> assays (e.g., pull-downs) co-localisation on confocal microscopy 	Not shown Not shown	Shown Not shown
Bacterial-mammalian TIR:TIR interactions shown by mutagenesis, competitive binding assays and structural studies to rely on same sites and mechanisms as mammalian TIR:TIR interactions	Not shown	Not shown
Bacterial TIR protein secreted into supernatant	Not shown	Shown
Bacterial TIR protein taken up by mammalian cells	Not shown	Shown
Secretion and translocation linked to defined sequences within TIR protein	Not shown	Not shown
Secretion linked to well-characterised bacterial secretion system	Not shown	Not shown

domains regulate mycobacterial physiology, but can also act on host cell pathways via secretion into macrophages [21].

In conclusion, as bacterial TIR domains occur in a wide range of domain architectures in a wide range of bacteria, they almost certainly play diverse roles in bacterial physiology. Thus, when contemplating any bacterial TIR domain protein, it is inadvisable to assume a subversive function, but to consider all options. Furthermore, even in cases where there is experimental support for bacteria as agents of subversion, gaps remain in the chain of evidence (Box 3). For now, it seems prudent to maintain a healthy scepticism and keep an open mind. Only time and more experiments will tell how often and to what extent the "subversion hypothesis" fits the facts.

Appendix A. Supplementary data

Supplementary data associated with this article can be found, in the online version, at doi:10.1016/j.tim.2009.06.005.

References

- 1 Cay, N.J. and Keith, F.J. (1991) *Drosophila* Toll and IL-1 receptor. *Nature* 351, 355–356
- 2 Sims, J.E. *et al.* (1988) cDNA expression cloning of the IL-1 receptor, a member of the immunoglobulin superfamily. *Science* 241, 585–589
- 3 Lemaitre, B. *et al.* (1996) The dorsoventral regulatory gene cassette *spätzle/Toll/cactus* controls the potent antifungal response in *Drosophila* adults. *Cell* 86, 973–983
- 4 Anderson, K.V. *et al.* (1985) Establishment of dorsal-ventral polarity in the *Drosophila* embryo: the induction of polarity by the Toll gene product. *Cell* 42, 791–798
- 5 Medzhitov, R. *et al.* (1997) A human homologue of the *Drosophila* Toll protein signals activation of adaptive immunity. *Nature* 388, 394–397
- 6 O'Neill, L.A. and Bowie, A.C. (2007) The family of five: TIR-domain-containing adaptors in Toll-like receptor signalling. *Nat Rev Immunol* 7, 353–364
- 7 Medzhitov, R. and Janeway, C.A.J. (1997) Innate immunity: the virtues of a nonclonal system of recognition. *Cell* 91, 295–298
- 8 Mogensen, T.H. (2009) Pathogen recognition and inflammatory signaling in innate immune defenses. *Clin Microbiol Rev* 22, 240–273 Table of Contents
- 9 Rast, J.P. *et al.* (2006) Genomic insights into the immune system of the sea urchin. *Science* 314, 952–956
- 10 Rokas, A. (2008) The molecular origins of multicellular transitions. *Curr Opin Genet Dev* 18, 472–478
- 11 Steenkamp, E.T. *et al.* (2006) The protistan origins of animals and fungi. *Mol Biol Evol* 23, 93–106
- 12 Burch-Smith, T.M. and Dincă-Kumar, S.P. (2007) The functions of plant TIR domains. *Sci STKE* 2007, pc46
- 13 Chen, C. *et al.* (2007) Immune-like phagocytic activity in the social amoeba. *Science* 317, 678–681
- 14 Koonin, E.V. and Aravind, L. (2002) Origin and evolution of eukaryotic apoptosis: the bacterial connection. *Cell Death Differ* 9, 394–404
- 15 Newman, R.M. *et al.* (2006) Identification and characterization of a novel bacterial virulence factor that shares homology with mammalian Toll/interleukin-1 receptor family proteins. *Infect Immun* 74, 594–601
- 16 Cifri, C. *et al.* (2008) Subversion of Toll-like receptor signaling by a unique family of bacterial Toll/interleukin-1 receptor domain-containing proteins. *Nat Med* 14, 399–406
- 17 Iyer, L.M. *et al.* (2008) MutL homologs in restriction-modification systems and the origin of eukaryotic MORC ATPases. *Biol Direct* 3, 8
- 18 Tobc, T. *et al.* (2006) An extensive repertoire of type III secretion effectors in *Escherichia coli* O157 and the role of lambdaoid phages in their dissemination. *Proc Natl Acad Sci U S A* 103, 14941–14946
- 19 Pallan, M.J. and Wren, B.W. (2007) Bacterial pathogenomics. *Nature* 449, 835–842
- 20 Pallan, M.J. *et al.* (2003) Tetratricopeptide-like repeats in type-III-secretion chaperones and regulators. *FEMS Microbiol Lett* 223, 53–60
- 21 Wehenkel, A. *et al.* (2008) Mycobacterial Ser/Thr protein kinases and phosphatases: physiological roles and therapeutic potential. *Biochim Biophys Acta* 1784, 193–202
- 22 Li, C. *et al.* (2005) Interactive sites in the MyD88 Toll/interleukin (IL) 1 receptor domain responsible for coupling to the IL1beta signaling pathway. *J Biol Chem* 280, 26152–26159
- 23 Slack, J.L. *et al.* (2000) Identification of two major sites in the type I interleukin-1 receptor cytoplasmic region responsible for coupling to pro-inflammatory signaling pathways. *J Biol Chem* 275, 4670–4678
- 24 Gautam, J.K. *et al.* (2006) Structural and functional evidence for the role of the TLR2 DD loop in TLR1/TLR2 heterodimerization and signaling. *J Biol Chem* 281, 30132–30142
- 25 Novatchkova, M. *et al.* (2003) The STIR-domain superfamily in signal transduction, development and immunity. *Trends Biochem Sci* 28, 226–229
- 26 Nunez Miguel, R. *et al.* (2007) A dimer of the Toll-like receptor 4 cytoplasmic domain provides a specific scaffold for the recruitment of signalling adaptor proteins. *PLoS ONE* 2, e788
- 27 Nyman, T. *et al.* (2008) The crystal structure of the human toll-like receptor 10 cytoplasmic domain reveals a putative signaling dimer. *J Biol Chem* 283, 11861–11865
- 28 Khan, J.A. *et al.* (2004) Crystal structure of the Toll/interleukin-1 receptor domain of human IL-1RAPL. *J Biol Chem* 279, 31664–31670
- 29 Xu, Y. *et al.* (2000) Structural basis for signal transduction by the Toll/interleukin-1 receptor domains. *Nature* 406, 111–115
- 30 Rock, F.L. *et al.* (1998) A family of human receptors structurally related to *Drosophila* Toll. *Proc Natl Acad Sci U S A* 95, 588–593
- 31 Poltorak, A. *et al.* (1998) Defective LPS signaling in C3H/HeJ and C57BL/10ScCr mice: mutations in Tlr4 gene. *Science* 282, 2085–2088
- 32 Liolios, K. *et al.* (2008) The Genomes On Line Database (GOLD) in 2007: status of genomic and metagenomic projects and their associated metadata. *Nucleic Acids Res* 36, D475–D479
- 33 Stack, J. *et al.* (2005) Vaccinia virus protein A46R targets multiple Toll-like-interleukin-1 receptor adaptors and contributes to virulence. *J Exp Med* 201, 1007–1018
- 34 Bowie, A. *et al.* (2000) A46R and A52R from vaccinia virus are antagonists of host IL-1 and toll-like receptor signalling. *Proc Natl Acad Sci U S A* 97, 10162–10167
- 35 Altschul, S.F. *et al.* (1997) Gapped BLAST and PSI-BLAST: a new generation of protein database search programs. *Nucleic Acids Res* 25, 3389–3402
- 36 Doolittle, W.F. (1999) Phylogenetic classification and the universal tree. *Science* 284, 2124–2129